Advanced Debonding on Demand Systems for Dental Adhesives

Zur Erlangung des akademischen Grades eines

DOKTORS DER NATURWISSENSCHAFTEN

(Dr. rer. nat.)

Karlsruher Institut für Technologie (KIT)

Fakultät für Chemie und Biowissenschaften

genehmigte

DISSERTATION

von

Dipl.-Chem. Alexander Marc Schenzel

geboren in

Hamburg, Deutschland

Dekan: Prof. Dr. Willem M. Klopper

Referent: Prof. Dr. Christopher Barner-Kowollik

Koreferent: Prof. Dr. Manfred Wilhelm

Tag der mündlichen Prüfung: 25.04.2017

Die vorliegende Arbeit wurde im Zeitraum von Februar 2014 bis März 2017 im Rahmen einer Kollaboration zwischen dem KIT und der Ivoclar Vivadent AG unter der Betreuung von Prof. Dr. Christopher Barner-Kowollik durchgeführt.

In the beginning the Universe was created. This has made a lot of people very angry and been widely regarded as a bad move.

Douglas Adams

Abstract

The present thesis reports a novel approach for the preparation of readily degradable dental adhesives as well as thermally and photochemically triggered debonding on demand (DoD) methods for polymer networks.

At first, a novel dental adhesive is developed that – in contrast to the currently employed adhesives – can be degraded upon thermal exposure within minutes. For this purpose, a stimuli-responsive moiety (SRM) is incorporated into the network. The stimuli response is based on a Hetero-Diels-Alder (HDA) system that can be cleaved in a retro HDA reaction upon heating. As HDA pair a phosphoryl dithioester and a bisclyclopentadiene linker are chosen, as the particular HDA couple features the desired properties of the degradable adhesive, such as a degradation at relatively low temperatures (80 °C), combined with a rapid release within 3 minutes and a facile quantitative analysis of the degradation based on a colour change. The prepared adhesive is investigated in detail by UV/Vis and high-temperature ^{1}H nuclear magnetic resonance spectroscopy (HT-NMR) of the retro HDA reaction and rheologic measurements of the mechanical properties of the formed polymer networks to final pull-off tests determining the adhesion forces. When compared to common methacrylate based systems, similar mechanical properties and adhesion forces are found at ambient temperature, however, significantly lower values are determined for the invented thermodegradable adhesive at elevated temperatures (e.g. 42 N instead of 553 N for the pull-off force) demonstrating the highly significant advance over the current state of the art for DoD adhesives. Thus, the novel system is highly interesting not only for dental adhesives but of critical importance for adhesion systems in general.

Due to the nature of free radically polymerized systems, networks can only be degraded into linear polymeric chains, as the degradable unit can solely by incorporated into the crosslinker. For step-growth polymers that fact does not hold true. Therefore, in a second project, the same HDA pair is employed for the development of thermoreversible bonding/debonding on demand polycarbonate networks, which can be degraded into small molecules as the SRM can be incorporated into the backbone of the polymeric chain. Again, bonding and debonding can readily be seen and quantified due to the self-reporting nature of the HDA moiety. In order to

prove the reversibility of the system, linear polycarbonates (M_w = 4.200 – 20.000 g·mol^{-1}) bearing the reversible moiety in each repeating unit are synthesized and extensively analyzed *via* size exclusion chromatography (SEC), high-temperature ^{1}H NMR spectroscopy and UV/Vis analysis in terms of their debonding and bonding behavior. Next, a new triol linker bearing three HDA moieties is prepared and reacted with dimethyl carbonate to form the desired polycarbonate network. Heating and cooling cycles in the temperature range of 25 to 120 °C demonstrate that the polymer network can be debonded and bonded multiple times within minutes, as the colorless and solid polymer turns into a red liquid upon heating, yet is reformed at ambient temperature. Thus, the present study introduces a new concept that in contrast to networks based on C-C bond formation can be degraded and rebonded completely.

After the extensive study of thermo-responsive moieties, a light responsive system is investigated in the third project of the thesis. Therefore, networks based on disulfone crosslinkers are prepared that can be cured and degraded in a λ-orthogonal fashion. *Via* irradiation with visible light (400 – 520 nm), a methacrylate based monomer mixture containing a germanium based initiator can be cured within 10 minutes, followed by a UVA light (350 – 400 nm) triggered degradation of the polymer network. The degradation is triggered by the decomposition of a photo-generated amine (PGA) that cleaves the present disulfone crosslinks of the polymer network *via* a nucleophilic substitution. In a first step, the degradability of the novel disulfone based crosslinker is evidenced by using 5 eq. of diethylamine, resulting in a fast S-S bond cleavage proven *via* ^{1}H NMR spectroscopy. In order to obtain the λ-orthogonality, a UV-degradable PGA is prepared and its decomposition upon irradiation with UV light as well as its visible light stability is evidenced unambiguously. Next, the ability of the PGA to degrade the disulfone upon UV light irradiation is successfully studied in solution via ^{1}H NMR spectroscopy. In the last step, a swollen network is prepared using the disulfone crosslinker, the germanium based initiator, and the PGA. The polymer network is prepared *via* visible light irradiation and degraded within 4 hours using UVA light, proving the general concept of the invented system. As the PGA can easily be adapted to the desired decomposition wavelength, the invented disulfone based approach can be used as a universal system for wavelength-dependent decomposition, which is a clear advance over the systems known today, where a new linker needs to be synthesized for each wavelength.

Zusammenfassung

Die vorliegende Arbeit befasst sich mit einem neuartigen Ansatz zur Herstellung von thermisch degradierbaren Dentalklebstoffen sowie weiteren thermischen und photochemischen Methoden für gezielt degradierbare Polymernetzwerke.

Zuerst wird ein Dentalklebstoff entwickelt, der im Gegensatz zu den auf dem Markt befindlichen Adhäsiven unter Wärmezufuhr innerhalb weniger Minuten zum Zerfall gebracht werden kann. Zu diesem Zweck wird eine stimuliresponsive Gruppe in das Netzwerk integriert, welche auf einem Hetero-Diels-Alder (HDA) Baustein basiert, der unter Erhitzen in einer retro HDA Reaktion zerfällt und somit das Netzwerk auflöst. Also HDA Paar werden ein Phosphoryldithioester und ein Biscyclopentadien-Linker gewählt, da diese Kombination die gewünschten Eigenschaften des Dentalklebstoffes gewährleisten kann. Neben dem Zerfall bei relativ milden Temperaturen (80 °C) in kürzester Zeit (3 Minuten) ist es mit dem gewählten Paar möglich eine quantitative Analyse des Zerfalls durchzuführen, da der beim Zerfall gebildete Dithioester sich durch eine charakteristische violette Färbung auszeichnet. Die retro HDA Reaktion wird intensiv mittels UV/Vis und Hochtemperatur-Kernresonanz (HT-NMR) Spektroskopie untersucht, sowie die mechanischen Eigenschaften des Klebstoffes mittels Rheologie charakterisiert und Abzugstests zur Bestimmung der Adhäsionskräfte durchgeführt. Vergleicht man die erhaltenen Ergebnisse mit den Werten für herkömmliche methacrylatbasierte Dentalklebstoffe, so zeigt das entwickelte System bei Raumtemperatur ein ähnliches Verhalten. Beim Erhitzen werden jedoch auf Grund der degradierbaren Struktur signifikant kleinere Werte für die Abzugskraft des entwickelten Materials erhalten (42 N anstatt 553 N für die Abzugstests), welche den beträchtlichen Vorteil gegenüber dem Stand der Technik aufzeigen. Das entwickelte System zeigt daher vielversprechende Eigenschaften für die Anwendung als degradierbares Adhäsive, nicht nur für den Dentalbereich.

Auf Grund der Natur von Polymeren die mittels freier radikalischer Polymerisation hergestellt werden können polymere Netzwerke nur bis auf die lineare Polymerebene aufgebrochen werden, da die stimuliresponsive Gruppe nur in den Vernetzer eingebaut werden kann. Für Stufenwachstumspolymere ist dies jedoch nicht der Fall. Daher wird im nächsten Schritt das entwickelte HDA Paar für den Aufbau eines reversibel spaltbaren Polycarbonatnetzwerkes verwendet, welches bis hin zu kleinen Molekülen aufgebrochen werden kann, da es möglich ist

die degradierbare Gruppe in das Rückgrat des Makromoleküls einzubauen. Auch hier lässt sich der Zerfall und die Rückbildung des Netzwerkes auf Grund der Natur des HDA Paares charakterisieren und quantifizieren. Zunächst werden lineare Polycarbonate (M_w = 4.200 – 20.000 g·mol^{-1}) welche den HDA Baustein in jeder Wiederholeinheit tragen synthetisiert und die reversible thermische Spaltung mittels Hochtemperatur NMR Spektroskopie, SEC und UV/Vis Spektroskopie im Detail bewiesen. Anschließend wird ein Trialkohol, welcher drei HDA Bausteine enthält, hergestellt und mit Dimethylcarbonat zur Bildung des gewünschten Polycarbonatnetzwerkes umgesetzt. Durchgeführte Heiz- und Abkühlzyklen beweisen die reversible Natur des entwickelten Systems, da das farblose, feste polymere Netzwerk beim Erhitzen reversibel in eine rote Flüssigkeit zerfällt. Es ist somit gelungen ein neues Konzept für die Herstellung stufenwachstumsbasierter Netzwerke vorzustellen, die sich im Gegensatz zu den herkömmlichen auf C-C-Bindungen basierten Netzwerken durch einen vollkommen reversible Bindungsbildung und Bindungsbruch auszeichnet.

Nach der intensiven Studie thermoresponsiver Systeme, wird im zweiten Teil der Dissertation ein lichtresponsives System entwickelt und im Detail untersucht. Hierzu wird ein Polymernetzwerk basierend auf einem Disulfonvernetzer synthetisiert welches λ-orthogonal hergestellt und aufgebrochen werden kann. Die Wellenlängenorthogonalität wird hierbei durch die Kombination eines im sichtbaren Licht (400 – 520 nm) zerfallenden, Germanium basierten Photoinitiators, welcher für die Aushärtung des Systems verwendet wird, mit einem im UV (350 – 400 nm) degradierbaren Additiv, welches für den Zerfall des Netzwerkes verantwortlich ist, gewährleistet. Das Additiv kann unter Bestrahlung mit UV-Licht (350 – 400 nm) ein primäres Amin freisetzen, welches die S-S Bindung des Disulfonvernetzers in einer nukleophilen Substitution spaltet. In einem ersten Schritt wird die Funktionsweise des Systems mittels NMR Spektroskopie bewiesen indem der zuvor hergestellte neuartige Disulfonvernetzer mit 5 eq. Diethylamine umgesetzt wird. Anschließend wird die UV-labilität des Additivs, sowie dessen Stabilität im sichtbaren Licht untersucht und bewiesen. Mittels ^{1}H NMR Spektroskopie kann gezeigt werden, dass das Additiv unter UV Bestrahlung das Disulfon erfolgreich aufzuspalten vermag. Zuletzt wird ein gequollenes Netzwerk welches den Disulfonvernetzer, den germaniumbasierten Photoinitiator und das Additiv enthält mittels Bestrahlung mit sichtbarem Licht hergestellt und erfolgreich unter UV Bestrahlung in 4 Stunden degradiert, welches das Konzept des Systems beweist.

Publications

Publications Arising from this Thesis

(1) *Reversing Adhesion – A Triggered Release Self-Reporting Adhesive*

A. M. Schenzel, C. Klein, K. Rist, N. Moszner and C. Barner-Kowollik, *Advanced Science* **2016**, *3*, 1500361.

(2) *Self-Reporting Dynamic Covalent Polycarbonate Networks*

A. M. Schenzel, N. Moszner and C. Barner-Kowollik, *Polym. Chem.* **2017**, *8*, 414-420.

(3) *Disulfone Crosslinkers for λ-Orthogonal Photo-Induced Curing and Degradation of Polymeric Networks*

A. M. Schenzel, N. Moszner and C. Barner-Kowollik, *ACS Macro Lett.* **2017**, *6*, 16–20.

Patents Arising from this Thesis

(4) *Polymerizable Compositions Based on Thermally Splittable Thermolabile Compounds for Use in Adhesives, Composites, Stereolithog. Materials etc. in Dental Materials*

A. Schenzel, C. Barner-Kowollik, M. Langer, N. Moszner, I. Lamparth, K. Rist, **WO 2017064042**, April 20th, 2017.

Additional Publications

(5) *Photo-Induced Tetrazole-Based Functionalization of Off-Stoichiometric Clickable Microparticles*

C. Wang, M. M. Zieger, **A. M. Schenzel**, M. Wegener, J. Willenbacher, C. Barner-Kowollik and C. N. Bowman, *Adv. Funct. Mater.* **2017**, in press.

Contents

Abstract i

Zusammenfassung iii

Publications v

1. Introduction 1

2. Theory and Background 5

2.1 Polymer Chemistry 5

2.1.1 History of Polymer Chemistry 6

2.1.2 General Properties of Polymers 7

2.1.3 Chain-Growth Polymerization 9

2.1.4 Step-Growth Polymerization 13

2.1.3 Polymer Networks 19

2.2 Adhesives 31

2.2.1 General Aspects of Adhesion 31

2.2.2 Different Types of Adhesives 32

2.2.3 Dental Adhesives 34

2.3 Thermally Triggered Debonding on Demand 42

2.3.1 Diels-Alder/Hetero-Diels-Alder Systems 42

2.3.2 Other Systems for Thermally Triggered Debonding on Demand 48

2.4 Photochemically Triggered Debonding on Demand 50

2.5. Introduction to Disulfones 53

3. Debonding on Demand for Dental Adhesive 55

3.1 Motivation and Monomer Design 55

3.2 Molecular analysis of the thermodegradability 59

3.3 Mechanical properties of the invented adhesive 63

3.4 Adhesion and Pull-off Tests 66
3.5 Conclusion and Further Remarks 68
4. Dynamic Covalent Polycarbonate Networks 71
4.1 Motivation and Monomer Design 71
4.2 Linear Polycarbonates 75
4.3 Polycarbonate Network 78
5. Disulfone Network for Photoinduced Degradation 81
5.1 Motivation and Monomer Design 81
5.2 Solution studies 84
5.3 Network studies 89
6. Conclusion and Outlook 91
7. Experimental Section 95
7.1 Materials 95
7.2 Instrumentation 96
7.3 Synthetic Protocols 99
7.3.1 Debonding on Demand for Dental Adhesive 99
7.3.2 Dynamic Covalent Polycarbonate Networks 105
7.3.3 Disulfone Network for Photoinduced Degradation 110
Bibliography 115
Appendix 131
List of Figures 151
List of Schemes 157
List of Tables 162
Abbreviations 163
Curriculum Vitae 167
Publications and Conference Contributions 167

Acknowledgements 171

Declaration 173

1

Introduction

The ongoing efforts and advances in science, especially in the field of chemistry and polymer science, enable the design and preparation of new materials with adaptive characteristics.[1, 2] These, so-called smart materials lead to the opportunity of combining properties of different material classes into one system, featuring unique and unprecedented material characteristics. Smart materials usually contain stimuli-responsive moieties, which allow the system to respond on demand to physical or chemical alterations, such as heat, light, pH changes, redox potentials, acid-base reactions, changed solvents and magnetic or electric fields.[3-15] Such responsive materials start to play an increasingly important role for a wide range of applications, such as diagnostics, tissue engineering, smart optical systems, drug delivery, microelectromechanical systems, biosensors, coatings, and textiles.[15]

A frequently employed method for the generation of smart materials is the integration of supramolecular or dynamic covalent bonds in the chemical composition of the respective material.[16-20] Hence, reversible bonding and/or debonding on demand at a molecular level using diverse stimuli is possible. By employing such motives, self-healing, -immolative, –assembling or reformable moieties can be prepared. Especially the field of thermosets, which are usually non-alterable materials that cannot be easily recycled, would benefit significantly if one of those motives is incorporated.[21] For example, the ability to reform a material after damage (self-healing materials) to restore its function, leads to a prolonged lifetime of the material, and is, therefore, beneficial under economic and ecologic aspects. However, also an entire reformation of a thermoset, in order for the polymer to be applicable in a different context is highly desirable as it would give the opportunity to recycle and reuse a thermoset in a facile way.

A different kind of thermosets – at least in their cured form – are adhesives. Adhesives play a vital role in our daily life, due to their broad range of application. Countless products of our everyday life, such as cars, aircraft, and electronic devices would otherwise not be producible, as more than 50% of the goods produced in Germany contain adhesives. In total, almost 1.4 million tons of various adhesives, as well as 1 billion m^2 of adhesive tape and film are produced in Germany today, generating a total turnover of 3.7 billion euros.[22] By definition, an adhesive binds two materials in a permanent manner, when applied to their respective surfaces.[23] The stability of the joint is necessary for a long-term usage of the product. However, for some applications and also for the recyclability of the different parts, an adhesive that can be degraded on demand, in order to ease the separation, is highly desirable. Especially for dental applications such an adhesive would have numerous advantages. Today, removing a dental crown is a difficult and time-consuming task for the dentist. First, the dentist has to drill a hole in the crown, followed by the mechanical breakage of the restorative material into pieces. Finally, the residual adhesive has to be ground of the tooth. If a degradable adhesive would be available, it would ease the removal of dental crowns significantly, as upon the specific trigger, the bond strength would be decreased drastically, allowing the dentist to easily take off the restorative material and simply wipe off the residual adhesive. Surprisingly, such a degradable adhesive is not available on the market today.

The main part of the thesis, therefore, addresses this drawback by the preparation of an advanced debonding on demand system for dental adhesives. As heat can briefly be applied in the oral cavity, it was targeted to prepare a thermo-responsive adhesive. A feasible motive for a fast response to thermal stimulus are Hetero-Diels-Alder (HDA) moieties. Therefore, the present work focuses on the selection of an HDA unit that cleaves in the desired temperature range and a detailed investigation of its applicability for a degradable adhesive. Therefore, the debonding on a molecular level, the effect on the mechanical properties and practical adhesion test under thermal impact have to be carried out and analyzed extensively.

Secondly, the preparation of a reformable thermoset is tackled. Therefore, a polycarbonate network is synthesized, bearing thermo-responsive moieties in each repeating unit. In order to evidence that the material can be reformed multiple times, debonding and bonding of the

polymer network has to take place as a function of the temperature. For a detailed investigation and understanding, studies on linear polycarbonates bearing the thermo-responsive motive, which again is based on an HDA moiety, have to be carried out first, before the polycarbonate-based thermoset is studied for its reversible nature.

In the final part of the thesis, the preparation of a photodegradable polymer network addressed. Today, the crosslinker has to be adapted to the desired decomposition wavelength, resulting in high synthetic efforts. Therefore, in the present work, a universal system for a light-induced and λ-orthogonal formation and degradation of polymer networks based on disulfone chemistry is designed.

The newly established systems are studied in detail in the present thesis, therefore, expanding the ongoing developments in smart material design. The first time preparation of a thermodegradable adhesive gives the unprecedented opportunity to debond joint materials in a facile manner. The responsive material is employed for dental applications, however, could be useful for various adhesion purposes. Next, a smart polycarbonate network is prepared, which can be reformed multiple times upon a thermal stimulus, broadening the range of applicability for polycarbonates. Finally, a universal system for the light triggered degradation of a polymer network is introduced, which in contrast to the previous state of the art can be employed at any wavelength by simply varying the network additive.

2

Theory and Background

Throughout the following chapter, a literature review of the principles necessary for a general understanding of the present dissertation is given. It is designed to provide an overview and background information, however, is not meant to be exhaustive. For in-depth information, the reader is kindly advised to refer to the relevant literature stated in the thesis. The chapter begins with the development of polymer chemistry, which leads to the introduction of common polymerization techniques, where the methods employed in the present thesis (free radical polymerization and polycarbonate formation) are discussed in detail. Subsequently, polymer properties, with a focus on the behavior of polymer networks are outlined, followed by an introduction to adhesives. Different adhesive systems are explained with a focus on dental adhesives in particular, as its development lays the basis for the present work. Finally, debonding on demand systems are highlighted, with an in-depth discussion of the thermodegradable (Hetero-Diels-Alder) and light responsive systems (disulfone with photo-generated amine) employed in the dissertation.

2.1 Polymer Chemistry

The current section outlines the development and importance of polymer chemistry in general and specifically for the present work, by exploring different polymerization techniques and characteristics of macromolecules, especially of polymer networks. As a detailed discussion would exceed the scope of the present work due to the large amount of research that has been carried out in the field of polymer chemistry, the reader is kindly referred to the literature for an in-depth survey.[24-29]

2.1.1 History of Polymer Chemistry

Polymers, such as cellulose, silk, cotton and natural rubber have been utilized by human beings since the time of the Mayan culture (about 2000 b.c.), as it was discovered that the children were fond of playing with balls made from rubber trees.[30] Without the biopolymer deoxyribonucleic acid (DNA) life would not even be possible as we know it today. In the 1800s, the chemical modification of natural polymers increased in importance, in order to enhance and modify their properties. The most prominent example is vulcanized rubber, whose preparation was established by Charles Goodyear in 1839.[31, 32] The modified polymer demonstrated to be much more durable than its natural precursor. Another example is celluloid, which is a nitrocellulose product that was commercialized by John W. Hyatt in 1868.[33] The first fully synthetic plastic, which was named Bakelite by Leo Hendrik Baekeland, is a thermoset made using phenol and formaldehyde. The reaction of the two components was discovered by Adolf v. Baeyer in 1872 and later commercialized in 1909 by Baekeland.[30, 34, 35]

The first time, the term “polymer” was mentioned, can be traced back to Marcelin Berthelot, who published an article in the Bulletin of the Chemical Society of France in 1866, stating that “styrolene (styrene) heated at 200 °C for a few hours, transforms itself into a resinous polymer”.[36] However, until the beginning of the 20th century scientists thought that polymers were colloids, which would crystallize if they were sufficiently purified.[37] It was Hermann Staudinger in 1920, who was the first to propose that polymers consist of a chain-like macromolecular structure, build of covalently linked repeating units.[38] Staudinger fought for his conviction, however, it took additional efforts from other scientists to underpin his theory. Herman Mark, Hans and Werner Kuhn and Wallace Carothers investigated natural polymers using crystallography, found a statistical description for chain molecules and explored the polycondensation reaction for the preparation of nylon and neoprene. Due to their valuable contributions, Staudinger’s hypothesis found greater notice, finally leading to him being awarded the Nobel Prize in 1953.[39] Staudinger was the first of a number of polymer chemist (K. Ziegler and G. Natta 1963, A. J. Heeger, A. G. MacDiarmid and H. Shirakawa 2000, Y. Chauvin, H. Grubbs and R. R. Schrock 2005), who were honored with the Nobel Prize as a tribute to their work, underlining the importance of polymer chemistry.[40-46]

During World War II, a significant change took place in the polymer industry. Prior to the war, natural substances for the production of polymers were readily available. However, during the war, the natural sources for products such as latex, wool, and silk were cut off from Germany,

making the usage of synthetic polymers inevitable. Therefore, fully synthetic materials such as nylon, styrene-butadiene-rubber, and polyethylene were developed. After World War II, the extensive progress in the field of polymer chemistry, combined with worldwide economic growth, led to numerous novel developments and finally enabled mass manufacturing of plastics for convenience products (1.7 million tons in 1950).[47] Since then, the demand for polymeric materials increased steadily, so that nowadays close to 322 million tons are produced each year.[48] Today, the focus of polymer research lies in the preparation of tailor-made materials. Therefore, novel polymerization methods such as reversible-deactivation radical polymerization (RDRP) were developed and combined with advances in organic chemistry to form so-called "smart materials". These materials are able to respond to external stimuli, leading among others to immolative, self-healing, shape memorizing and reversible debonding on demand characteristics, which offer new possibilities for polymer applications.[49-53]

2.1.2 General Properties of Polymers

Polymers exhibit unique properties, which are based on their chain-like macromolecular structure. In order to discuss polymer characteristics, some basic definitions have to be given, first. Typical polymers have a molecular weight ranging from 10^3 – 10^6 g·mol^{-1}. As monomers can vary drastically in their molecular weight (< 100 to > 1000 g·mol^{-1}), the degree of polymerization DP_n is introduced, which denotes the number of repeating units (reacted monomers) in a macromolecule. It can be calculated by dividing the mass of the polymer $M_{polymer}$ by the mass of the monomer $M_{monomer}$ (see Equation 1):

$$\boldsymbol{DP_n = \frac{M_{polymer}}{M_{monomer}}} \qquad \text{Equation 1}$$

Due to the characteristics of the different polymerization techniques (refer to Sections 2.1.3 and 2.1.4) not all polymers have the exact same chain length, but rather exhibit a range of different macromolecular sizes. Hence, upon analysis, an average molecular weight of the polymer sample is determined (e.g. using size exclusion chromatography, viscosimetry, light scattering or end-group analysis). There are four different average molecular weights by which a polymer can be characterized. The number average molecular weight, M_n, and the weight average molecular weight, M_w, are the most commonly determined values (see Equation 2 and Equation 3).

$$\boldsymbol{M_n = \frac{\sum_i n_i M_i}{\sum_i n_i}}$$ Equation 2

$$\boldsymbol{M_w = \frac{\sum_i n_i M_i^2}{\sum_i n_i M_i} = \frac{\sum_i w_i M_i}{\sum_i w_i}}$$ Equation 3

With n_i being the number of molecules of weight M_i and w_i being the weight fraction of molecules with the mass M_i. As can be seen in these equations, molecules with higher masses have a higher weighting in M_w compared to M_n, resulting in a discrimination of small masses in M_w. To quantify the width of the chain length distribution of polymers, the dispersity $Đ$ can be calculated using the ratio of M_w/M_n (see Equation 4):

$$Đ = \boldsymbol{\frac{M_w}{M_n}}$$ Equation 4

One way to categorize polymers is by the number of different monomers that are employed for the polymer formation. If only one type of monomer is used, a homopolymer is formed, that solely includes identical repeating units. So-called copolymers are formed when two or more different monomers are polymerized that can be arranged in various constitutional forms along the polymer chain (random, statistical, alternating, block or graft copolymers).[29, 54-56] Moreover, when the employed monomers bear stereogenic centers, the tacticity of the polymer can vary (iso-, syndio- or atactic polymers). Due to the tacticity, the side-chains are more or less orientated, resulting in drastically different bulk material properties. For example, isotactic polymers usually have a higher degree of crystallinity than atactic polymers, resulting in an increased glass transition temperature (T_g) and therefore to an elevation of the temperature until which the polymer can be applied.[29, 57]

An alternative method to classify polymers is *via* their thermal and mechanical properties. In doing so, three main groups can be identified, which are thermoplastics, elastomers, and thermosets. Thermoplastics are linear or branched non-crosslinked macromolecules that are amorphous or partially crystalline. They soften and flow upon heating and can, therefore, be reshaped and remolded at elevated temperatures. The second and the third group are polymer networks, which are either loosely crosslinked (elastomers) or highly crosslinked (thermosets) polymers.

Elastomers are elastic above their glass-transition temperature T_g and amorphous below the T_g. Thermosets cannot be melted or dissolved once formed and therefore cannot be reshaped or remolded. As polymer networks are the main form of polymers prepared in the present

thesis, they will be discussed in more detail. However, first, common polymerization methods have to be introduced for a better understanding.

2.1.3 Chain-Growth Polymerization

One method to further classify polymers is *via* their mechanisms of synthesis. A common classification thereby is the differentiation between chain-growth and step-growth polymerizations. As both techniques are employed in the thesis, the present and the following sections aim to provide a general introduction to both principles.

In a chain-growth polymerization, a monomer is activated by an initiator. The formed reactive center is able to bind to an additional monomer, upon which the reactive property is transferred to the novel repeating unit and the propagating chain is expanded. As the addition of the monomer species is repeated in the same manner multiple times, a chain molecule with high molecular weight is prepared, which is terminated in a final step. Depending on the polymerization method (radical, cationic or anionic polymerization) the reactive center can be a radical, a cation or an anion.

By far, free radical polymerization (FRP) is the most commonly used technique. Due to its simplicity, FRP is the most industrially applied polymerization method, producing close to 50% of the polymers prepared annually.[58] The monomers employed in FRP contain typically vinylic C=C double bonds, whose π-bond is homolytically cleaved during the reaction. FRP, as well as the other aforementioned chain-growth polymerization techniques, can kinetically be divided into four elementary steps: initiation, propagation, chain transfer, and termination. In the first step of the initiation process, an initiator forms a radical, e.g. upon a heat or light triggered homolytic decomposition. The so formed radical subsequently adds to a monomer in the second step of the process, whereupon the reactive center is transferred to the monomer species (see Scheme 1).

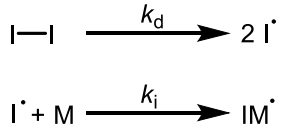

Scheme 1 Steps during the initiation process of a free radical polymerization. After homolytic dissociation of the initiator, a monomer is added to the radical initiation species, whereupon the reactive center is transferred to the monomer.

Typical initiators are azo- and peroxy-type compounds, which either decompose on irradiation or on thermal impact. Today, numerous initiators are readily available, cleaving with almost any desired decomposition rate. A large variety can be found in the *Polymer Handbook*.[59] The rate coefficient for the decomposition of the initiator k_d, depends on the reaction conditions but is typically in the order of 10^{-5} s^{-1}. However, not all radicals, which are formed, initiate a polymerization, as recombination of the initiator radicals can occur. The ability of the initiator to start a polymerization is, therefore, quantified by the initiator efficiency, *f*, which is a dimensionless value between zero and one. If $f = 0$, no initiation takes place, whereas every generated radical initiates the polymerization if $f = 1$. Typically, *f* is between 0.5 and 0.8, depending on the reaction media viscosity and the nature of the formed radicals. It is worth mentioning that an FRP can be initiated by alternative methods, such as redox, ionizing, plasma, electro- and ultrasonic initiation,[60] and that self-initiation can also take place at elevated temperatures (e.g. for styrene), or even at ambient temperature (e.g. for acrylates).[61, 62] However, the methacrylate species employed in the present thesis do not tend to self-initiate.[63] Therefore, an initiator is required to induce macromolecular growth.

The propagation reaction is the subsequent addition of monomer molecules to the species generated during the initiation process (refer to Scheme 2). It is a chemically controlled reaction, which is demonstrated clearly, when the average collision frequency at ambient temperature in the liquid state (10^{12} s^{-1}) is compared to the frequency of a successful propagation (~10^3 s^{-1}), indicating that only one in 10^9 collisions leads to a reaction of a monomer with a macroradical.[58]

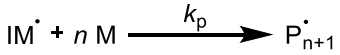

Scheme 2 Propagation reaction. A (macro-)radical reacts with monomer molecules, leading to an increase in the molecular weight of the polymer.

The propagation rate coefficient k_p, as well as its activation parameters E_A and *A*, depend on entropic and electronic factors. While steric effects should have an impact on the pre-exponential factor *A*, E_A is influenced by electronic effects. For example, when comparing methyl methacrylate (MMA) and dimethyl itaconate (DMI), a decrease in *A* by one order of magnitude can be observed, which can be explained with the sterically more demanding nature of the DMI radical. A decrease in E_A is visible when MMA is compared to methyl acrylate (MA), due to the electronic effect of the α-methyl group in MMA.[64, 65] The propagation rate coefficients, as well as the values of E_A and *A* for a selection of monomers, are given in Table 1.

Table 1 E_A, A and k_p values of a selection of vinylic monomers obtained *via* PLP-SEC.[66, 67]

Monomer	E_A [kJ·mol^{-1}]	A [L·mol^{-1}·s^{-1}]	k_p at 60 °C [L·mol^{-1}·s^{-1}]
Methyl methacrylate	22.3	$2.65 \cdot 10^6$	833
Butyl methacrylate	22.9	$3.80 \cdot 10^6$	976
Methyl acrylate	13.9	$3.61 \cdot 10^6$	24000
Butyl acrylate	17.4	$1.8 \cdot 10^7$	33700
Styrene	32.5	$4.27 \cdot 10^7$	341
Dimethyl itaconate	24.9	$2.20 \cdot 10^5$	27

In the termination process, irreversible deactivation of the reactive radical centers takes place. The termination reaction is by far the most complex reaction in an FRP. Depending on the monomer and the reaction conditions, two pathways are possible (refer to Scheme 3). In the first one (combination), two growing chains are combined resulting in an inactive polymer chain with combined molecular weight. The second possibility is disproportionation, which occurs when a hydrogen atom is abstracted from one macroradical and transferred to another one, leading to termination of both chains. Which process dominates largely depends on the nature of the monomer, however, is also influenced by the reaction temperature and pressure, even though to a minor extent. For example, styrene tends to terminate *via re*combination, whereas MMA favors to disproportionate.[68]

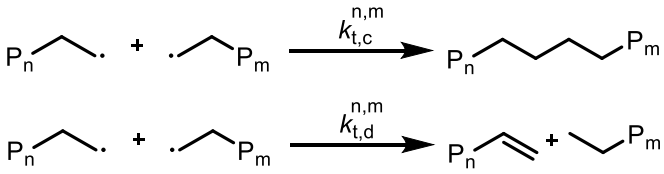

Scheme 3 Possible pathways for a termination reaction in a free radical polymerization (combination and disproportionation)

The termination reaction is diffusion controlled, as the diffusion of the macroradicals towards each other, into a conformation, in which a reaction is possible, is much slower than the chemical reaction of the two radicals itself.[69] At high conversions, the so-called Trommsdorff-Norrish effect can be observed, which is indicated by an autoacceleration of the polymerization due to an increased viscosity.[70]

The termination rate coefficient k_t is influenced by numerous parameters, such as the monomer conversion, the viscosity, the temperature, the pressure and the chain length of the terminating macroradicals.[71] Therefore, it is difficult to provide exact values for k_t. However, average termination rate coefficients have been reported ranging from 50 to 10^9 $L \cdot mol^{-1} \cdot s^{-1}$.[59] Typical examples for monomers with a high k_t ($\approx 10^8$ $L \cdot mol^{-1} \cdot s^{-1}$) are MMA and styrene, whereas low values have been reported for dialkyl fumarates ($k_t \approx 500$ $L \cdot mol^{-1} \cdot s^{-1}$).[72] Due to the statistical nature of the termination process, polymers prepared *via* FRP feature a broad variety of chain length and therefore polydispersity values are commonly between 1.5 and 2.

The measured average molecular weights are often lower than predicted values, taking into account initiation, propagation and termination processes. This is due to the fact that chain transfer reactions can take place (see Scheme 4). A transfer reaction can occur between a propagating chain and the solvent, the monomer, another polymer chain or a transfer agent. In this process, a propagating macroradical abstracts an atom from the reaction partner *via* homolysis, forming a dead chain and a new radical species, which can reinitiate through adding a monomer molecule. If the reaction partner is a polymer chain, polymers bearing side branches are prepared.

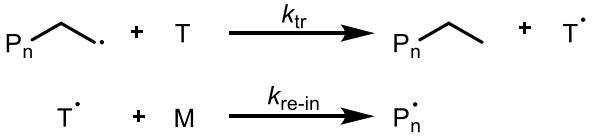

Scheme 4 Chain transfer in free radical polymerization. A macroradical can transfer the reactive center to the solvent, the initiator, the monomer, another polymer chain or a transfer agent (T). The transferred radical can potentially reinitiate the reaction *via* addition to a monomer.

Technically, four different cases can be distinguished: (1) $k_p \gg k_{tr}$ and $k_{re\text{-}in} \approx k_p$, which leads to a conventional chain transfer that decreases M, however, has no effect on the polymerization rate R_p; (2) where $k_p \ll k_{tr}$ and $k_{re\text{-}in} \approx k_p$, which leads to a drastic decrease of M, R_p remains unaffected; (3) $k_p \gg k_{tr}$ and $k_{re\text{-}in} < k_p$, results in a retardation, and a decrease in M and R_p; and (4) $k_p \ll k_{tr}$ and $k_{re\text{-}in} < k_p$, resulting in a degenerative chain transfer, alongside with a drastic decrease in M and R_p. Therefore, it can easily be seen that chain transfer can have a significant effect on the polymer properties in an undesirable or desirable way. E.g. it may be advantageous for the properties of the material to decrease the polymer length during the polymerization.

The chain transfer reactions that cannot be avoided, are the transfer to the initiator and the monomer. Fortunately, the rate coefficients for a transfer to monomer are usually rather low (~10^{-4} L·mol^{-1}·s^{-1}), and the transfer to the initiator can be controlled by the selection of a suitable initiator. Moreover, due to the low concentration of the initiator in the polymerization reaction, the effect of this chain transfer process is negligible.

A non-neglectable transfer process is a transfer to the solvent, as solvents are usually employed in most industrial polymerization processes in high amounts. Typical solvents with comparably small transfer constants C_T are benzene and toluene. Carbon tetrachloride is an example for a solvent, which exhibits transfer to the solvent to a large extent. It can, therefore, also be employed as a chain transfer agent.[59] Other, more effective chain transfer agents are thiols and halogenated compounds, which play an important role for industrial applications. They can be employed to regulate the molecular weight of the polymer, and therefore the viscosity of the system, allowing for a good heat transfer.

The last transfer reaction that can occur during a polymerization, is the transfer to the polymer, which becomes important at high monomer conversions. Additionally, compared to the transfer to the respective monomer, the transfer to polymer is more significant. Transfer to the polymer can either result in a long-chain branching if the transfer reaction occurs intermolecularly, or can lead to short-chain branching due to an intramolecular backbiting process. E.g. polyacrylates tend to backbite *via* a six-membered transition state to a high extend.[73] β-scission of non-terminal radicals might also broaden the molecular weight distribution, as it results in a macromonomer species.

2.1.4 Step-Growth Polymerization

Step-growth polymerization is the second important polymerization method, which yields polymers employed in countless products of everyday life. The most significant difference between the two polymerization methods is that in chain-growth polymerizations single monomer molecules are added to a propagating chain, whereas in step-growth polymerizations all molecules can react with each other in a stepwise manner, independent of their size.[28, 29] An outcome of this different behavior can clearly be seen in the dependence of the molecular weight of the polymer on the monomer conversion. In chain-growth polymerizations, poly-

mers with high molecular weights are already present at small degrees of monomer conversion, with the monomer being present throughout the entire reaction. On the other hand, high-molecular-weight polymers are only obtained at very high monomer conversions (>98%) in step-growth polymerizations and the monomer is consumed in an early stage. In order to achieve these high conversions, the absence of side reactions as well as close to stoichiometric amounts of the different functional groups is necessary. This chapter will outline the basic principles of step-growth polymerizations with a closer look at polycarbonates.

Step-growth polymerizations can be subdivided into condensation and addition reactions. In (poly-)addition reactions, such as the reaction of alcohols and isocyanates to form (poly-)urethanes, no small molecules are formed during the process. In contrast, small molecules are cleaved upon a polymerization, which proceeds *via* a (poly-)condensation mechanism. For instance, water is eliminated upon the reaction of alcohols with carboxylic acids during the formation of polyesters.

Another possibility to subdivide step-growth polymerizations is *via* the nature of the monomers. The first group involves two different bi- and/or polyfunctional monomers, where the monomers contain one kind of functionality (refer to Scheme 5). The second type is monomers, which bear two types of functional groups that can react with each other forming a polymer. Polyamides illustrate an example of a polymer that can be prepared using either of the methods. Polyamides can be obtained *via* the condensation reaction of diamines (A-A) with dicarboxylic acids (B-B) or upon the intermolecular reaction of amino acids (A-B).

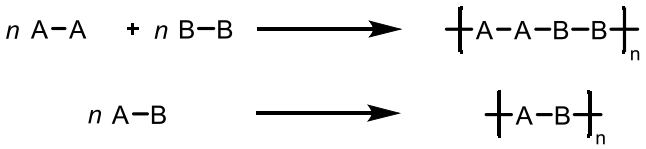

Scheme 5 Schematic display of a step-growth polymerization, either using to different monomers (A-A and B-B), or a monomer bearing two different functional groups, which are capable of reacting with each other (A-B).

In order to understand the basic principles of step-growth polymerizations and their kinetic behavior, the conversion of the reaction p, as well as the degree of polymerization DP_n have to be defined. In a first step, an equimolar amount of the two reaction partners is assumed ($A = B = N$). The conversion p can, therefore, be calculated using the initial amount of monomer N_o at the beginning of the reaction and the number of monomers present after a specific time of polymerization N_t. (see Equation 5)

$$p = \frac{N_o - N_t}{N_o} = 1 - \frac{N_t}{N_o}$$ Equation 5

By definition, the degree of polymerization DP_n is:

$$DP_n = \frac{N_o}{N_t}$$ Equation 6

When both equations are combined, the dependence of the degree of polymerization on the conversion becomes clear in the so-called Carothers equation (Equation 7):[74]

$$DP_n = \frac{1}{1 - p}$$ Equation 7

If one of the monomers is used in stoichiometric excess, the equation has to be adapted, with *r* being the stoichiometric ratio of the reaction partners (r < 1):

$$DP_n = \frac{1 + r}{1 + r - 2rp}$$ Equation 8

In Table 2, the importance of high conversions and a strict equimolar use of the monomers is outlined clearly. For example, if a reaction with *r* = 1 is only conducted until 90% conversion, the average polymer has a length of 10 repeating units. In order to obtain a polymer with a DP_n of 1000, a conversion of 99.9% is required. The effect of an off-stoichiometric use of the reaction partners becomes visible, as even at complete conversion (*p* = 1), only a degree of polymerization of 198 can be achieved if the stoichiometry is off by 1%.

Table 2 Relation between the stoichiometric ratio of the reaction partners *r*, the conversion *p* and the degree of polymerization DP_n in a step-growth polymerization.

r	*p*	DP_n
1	0.5	2
1	0.90	10
1	0.99	100
1	0.999	1000
0.99	1	199
0.95	1	39

It has to be noted that the Carothers equation is only valid if all molecules in the reaction mixture have equal reactivity in all polymerization steps. Upon experimental investigation of the assumption, it was found that the postulation is close to reality. E.g. Ueberreiter and Engel demonstrated that the polyesterification of α,ω-alkane diols with sebacoyl chloride has a constant reaction rate, and hence, is independent of the length of the polymer.[75]

Therefore, kinetic considerations can also be simplified, as one rate coefficient can be used for a specific step-growth polymerization. For a catalyzed reaction of two monomer *A* and *B,* the reaction rate can be specified. As the concentration of the catalyst is close to constant, it can be combined with the rate coefficient (refer to Equation 9).

$$-\frac{\boldsymbol{d}[\boldsymbol{A}]}{\boldsymbol{dt}} = \boldsymbol{k}' \cdot [\boldsymbol{Cat.}] \cdot [\boldsymbol{A}] \cdot [\boldsymbol{B}] = \boldsymbol{k} \cdot [\boldsymbol{A}] \cdot [\boldsymbol{B}] \qquad \text{Equation 9}$$

If the reaction mixture is equimolar in terms of the functional moieties ([A] = [B] = c), Equation 9 can be simplified:

$$-\frac{\boldsymbol{dc}}{\boldsymbol{dt}} = \boldsymbol{k} \cdot \boldsymbol{c}^{\boldsymbol{2}} \qquad \text{Equation 10}$$

In order to derive the dependency of the degree of polymerization DP_n on the reaction time t and the starting concentration c_o, Equation 10 is integrated from $c = c_o - c$ and $t = 0 - t$. When combined with the Carothers equation (Equation 7) and $c_o/c = N_o/N$, the degree of polymerization is given by Equation 11.

$$\boldsymbol{DP_n} = \frac{\boldsymbol{1}}{\boldsymbol{1} - \boldsymbol{p}} = \boldsymbol{k} \cdot \boldsymbol{t} \cdot \boldsymbol{c_o} + \boldsymbol{1} \qquad \text{Equation 11}$$

Therefore, the targeted molecular weight of the polymer can be adjusted for a known rate coefficient by the reaction time and the initial concentration.

By using statistical theories, the weight-average molecular weight M_w and the dispersity $Đ$ can be investigated as well. The dispersity $Đ$ is given by Equation 12.

$$Đ = \frac{\boldsymbol{M_w}}{\boldsymbol{M_n}} = \boldsymbol{1} + \boldsymbol{p} \qquad \text{Equation 12}$$

As the conversion for step-growth polymerizations should be close to 1, the polymers have a theoretical dispersity of about to 2.

A broad variety of polymers is prepared *via* step-growth polymerization, such as polyesters, polyamides, polycarbonates, polyurethanes and polyethers, to mention just a few. As a discussion of all polymer types would exceed the scope of the thesis, only polycarbonates (PCs) are discussed further, as they were employed in the presented work for two reasons. First, PCs can be prepared at ambient temperature, which is crucial for the incorporation of the employed Hetero-Diels-Alder (HDA) moiety, as it starts to decompose at temperatures above 30 °C. Secondly, it is possible to incorporate the HDA moiety into the monomer species, and therefore in every repeating unit of the respective polymer, which allows degradation of the polymer network to the level of small molecules.

Polycarbonates

Polycarbonates are important engineering polymers with a broad variety of optical and technical applications. Today, more than 4.5 million tons of polycarbonates are produced annually.[76]

The most important polycarbonate on the market is based on Bisphenol A (BPA). The polycarbonate poly(oxycarbonyloxy-1,4-phenylenedimethylmethylene-1,4-phenylene) is prepared *via* two different processes (Schotten-Baumann reaction or transesterification), which were developed by Bayer A.G. and General Electric (see Scheme 6).[77, 78] In the Schotten-Baumann reaction, BPA and phosgene are reacted in a base catalyzed interfacial condensation reaction at temperatures between 0 and 50 °C. The BPA is dissolved in basic aqueous media, whereas the phosgene is dissolved in an organic solvent (e.g. tetrahydrofuran, 1,2-dichloroethane or dioxane), which is not miscible with water. The organic solvent hinders the loss of phosgene due to hydrolysis and the precipitation of the polymer before reaching the desired molecular

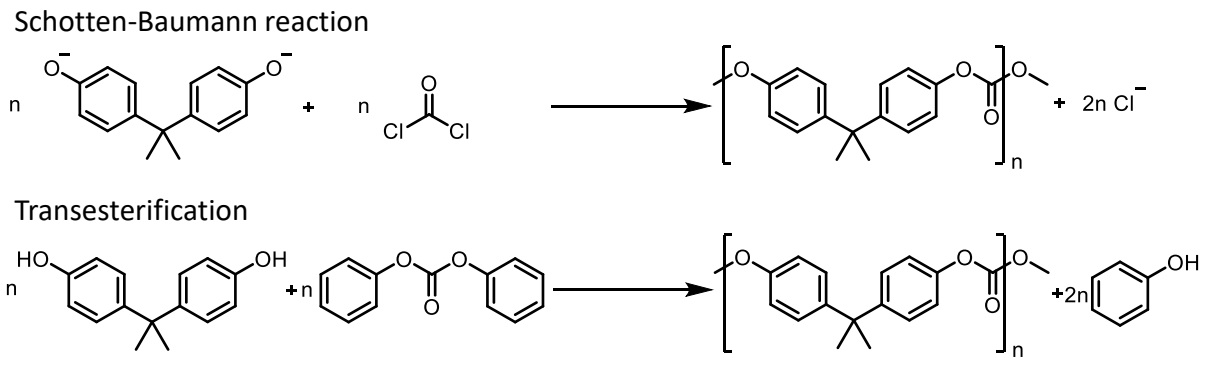

Scheme 6 Schematic display of the two procedures conducted for the preparation of Bisphenol A based polycarbonate: Schotten-Baumann reaction and transesterification.

weight. After oligomers are formed in the first step of the process, tertiary amines are added to catalyze the reaction to high degrees of polymerization.

The transesterification of BPA with a monomeric carbonate (e.g. diphenyl carbonate) is carried out under base catalysis in two steps. First, oligomers are formed at 180 – 220 °C and a pressure of about 400 Pa. Then, the polymer with a DP_n of about 100 is formed in the second step at close to 300 °C and 130 Pa. Overall, the phosgene-based approach is favored due to an easier control of the molecular weight and a more cost-efficient preparation. Moreover, higher degrees of polymerization can be achieved using the Schotten-Baumann process.

An efficient process for the synthesis of cyclic oligomer mixtures is reported in the literature, as well.[79] Herein, the BPA bis(chloroformate) is employed in a hydrolysis and condensation using triethylamine as catalyst, affording a mixture of cyclic oligomers (DP_n = 2 – 12). As the viscosity is 10^5 times lower than that of the polymeric PC, processing techniques can be employed, such as resin transfer molding and pultrusion, which are not possible for PCs prepared using a different method.[80] With cyclic oligomers, it is also possible to prepare hydroquinone-BPA copolymers, which cannot be prepared *via* the Schotten-Baumann and transesterification process.[26]

In 1999, Gross et al. published a study on preparing crystalline instead of amorphous PC.[81] The crystalline PC was synthesized *via* a solid-state polymerization process using supercritical CO_2. With crystalline PC, the heat distortion temperature, as well as the gas permeability and the solvent resistance of the material, can be improved.

BPA based PC is prepared in a broad range of molecular weights, depending on the desired application. With increasing molecular weight, the intrinsic viscosity increases, which leads to an improvement of the mechanical properties of PCs (e.g. impact resistance, flexural and tensile strength). Only slight increases in mechanical properties can be detected after the intrinsic viscosity reaches a value of 0.45 $dL \cdot g^{-1}$.[26]

Polycarbonates are usually amorphous polymers, which exhibit exceptionally high levels of ductility, impact strength, and fire resistance, as well as the possibility for engineering over a wide temperature range. Moreover, they demonstrate good dimensional stability, impact resistance, excellent insulating behavior, low moisture absorption and high light transmission. However, PC has limited chemical and scratch resistance and tends to yellow under long-time exposure to UV light. The properties can be improved *via* copolymerization with specific monomers. For example, PC can be made fire-retardant by using tetrabromobisphenol A as a

comonomer. The flame-retardant behavior can even by increased further, when the PC blend is filled with α-zirconium phosphate on silica gel.[82]

Due to their properties, PCs are employed in a broad variety of applications, including compact disks, automobile parts (e.g. instrument panels, taillight lenses, and bumpers), furniture, machinery housing and telephone parts, to mention just a few. As its impact resistance is 250 times greater than the resistance of glass, PC is the number one choice as window glass substitute. Due to its excellent impact resistance, PCs has an unsurpassed projectile-stopping capability and is therefore employed in bullet-proof materials.

2.1.3 Polymer Networks

As mentioned before, polymer networks are crosslinked polymers. They can be prepared *via* different approaches, such as *via* multifunctional monomers or crosslinking formerly prepared linear polymer chains using a linker. The following chapter aims to give a general introduction and insight into different types of polymer networks.[17, 28, 53, 83-85] As a detailed discussion would exceed the scope of the thesis, the reader is kindly referred to the literature for a deeper insight.

Carothers was the first one to point out that gelation occurs when polymer molecules link, forming a three-dimensional network.[86] According to Flory they are of "infinitely large size" in comparison to the molecules they were built of.[87]

When polymer networks are prepared *via* free radical polymerization, di- or multi-functional vinylic monomers, the so-called crosslinkers, have to be employed to achieve network formation. The properties of the prepared polymer networks vary drastically with the amount and nature of the employed crosslinking monomer. However, also the polymerization conditions, such as the nature and amount of initiator, the employment of a solvent and the temperature have significant impact on the network characteristics.[88-91]

Depending on the crosslinker/(monofunctional) monomer ratio and on the degree of functionality of the crosslinker, more or less dense polymer networks can be prepared, which has a significant effect on the material properties. Fore example, if the amount of crosslinker is low compared to the monofunctional monomer, only loose bonds between the polymer chains are present, resulting in an elastomeric behavior. With increasing amount of crosslinks,

the glass transition temperature and the storage modulus tend to increase, forming materials of higher stiffness.

In order to be able to compare different polymer networks, the extent of crosslinking must be quantified.[88] A measure for a polymer network is the average molecular weight between two crosslinks $\overline{Mc}$, which is defined as the ratio of the density of the network, *ρ*, and the concentration of the crosslinked chains *v*.

$$\overline{\boldsymbol{Mc}} = \frac{\boldsymbol{\rho}}{\boldsymbol{v}} \qquad \text{Equation 13}$$

By using dynamic mechanical analysis (DMA) for the measurement of the storage modulus in the rubbery region, $\overline{Mc}$ can be experimentally determined.[92]

It is also possible – and of scientific interest – to calculate $\overline{Mc}$ theoretically. This can be achieved for an ideal polymer network, when complete conversion and no cyclization is assumed. The concentration of crosslinked chains *v* can then be calculated by the following equation.

$$\boldsymbol{v} = \boldsymbol{ndb}[\boldsymbol{M_{xl}}] \qquad \text{Equation 15}$$

Ndb is defined as the number of double bonds of the crosslinker and $[M_{xl}]$ is its concentration. Hence, theoretically, the same crosslinking density will be obtained when the same number of crosslinking double bonds are present, independently if a di- or trivinyl monomer is employed.

$$\overline{\boldsymbol{Mc}}_{\boldsymbol{theo}} = \frac{\overline{\boldsymbol{Mr}}[\boldsymbol{DB_o}]}{\boldsymbol{ndb}[\boldsymbol{M_{xl,o}}]} \qquad \text{Equation 14}$$

The calculation of the polymer density *ρ* depends on the ratio of the monomer to the crosslinker. For loosely crosslinked systems, the density can be calculated be multiplying the concentration of the monovinylic species with its molecular weight. For highly crosslinked polymer networks, *ρ* is determined by the initial double bond concentration *[DB$_o$]* times $\overline{Mr}$, which is the molecular weight average of one repeating unit on a double bond basis. Therefore, $\overline{Mc}$ can be calculated as:

The molecular weight between crosslinks can also be calculated as a function of conversion *p* and cyclization rate. Therefore, the density, *ρ*, is determined by the concentration of incorporated double bonds at a certain conversion *[DB$_o$]p*. The assumption is most accurate at high conversions. The concentration of crosslinked chains, *v*, depends on the extent of crosslinking

and the conversion. For divinyl monomers, non-cyclized moieties are part of two crosslinked chains. If they cycle or have a pendant double bond, they are not part of a crosslinked chain. Hence, $\overline{Mc}$ can be calculated for a divinyl crosslinker as:

$$\overline{\boldsymbol{Mc}}_{\boldsymbol{Di}} = \frac{\overline{\boldsymbol{Mr}}[\boldsymbol{DB}_{\boldsymbol{o}}]\boldsymbol{p}}{\mathbf{2}[\boldsymbol{Pen}_{\boldsymbol{xl}}]} \qquad \text{Equation 16}$$

With $[Pen_{xl}]$ being the concentration of pendants that take part in a crosslinking reaction. A similar equation can be derived for network formations using trivinylic monomers. For those monomers, three different pathways are possible. All vinyl functionalities are incorporated into the network upon reaction or two of them crosslink and the other one is either unreacted or undergoes cyclization. Therefore, for a trivinyl polymerization, $\overline{Mc}$ reads:

$$\overline{\boldsymbol{Mc}}_{\boldsymbol{Tri}} = \frac{\overline{\boldsymbol{Mr}}[\boldsymbol{DB}_{\boldsymbol{o}}]\boldsymbol{p}}{\mathbf{3}[\boldsymbol{Pen}_{\boldsymbol{xl-xl}}] + \mathbf{2}([\boldsymbol{Pen}_{\boldsymbol{xl}}] + [\boldsymbol{Pen}_{\boldsymbol{xl-cyc}}]} \qquad \text{Equation 17}$$

When comparing dimethacrylate and trimethacrylate based polymer networks experimentally, significant differences are present.[93] For a representative comparison, both monomer mixtures contain the same concentration of crosslinkable double bonds, implying that the concentration of the trivinylic monomer is 2/3 of the divinyl concentration. It was found that the trimethacrylate systems polymerize more rapidly, with smaller molecular weights between the crosslinks, resulting in higher glass transition temperatures and larger storage module. However, the trimethacrylate based polymer demonstrates a significantly higher heterogeneity. As both systems reach close to the same conversion, the lower crosslinking density of the dimethacrylate network can be attributed to a higher degree of primary cycle formation compared to the trimethacrylate system. Primary cycles are formed when the pendant double bond reacts intramolecularly with the reactive center of the propagating radical chain. When a pendant double bond reacts with the propagating active center of another chain, which is already crosslinked, secondary cyclization occurs (refer to Scheme 7).

The tendency to form primary and secondary cycles or crosslinks is dependent on numerous factors, such as the distance of the functional groups and the flexibility of the linker between the vinyl moieties.[94-96] For instance, increasing the length of the linker between the polymerizable moieties and the stiffness of the monomer decreases the amount of primary cycles and increases the amount of the desired secondary cycles and crosslinks.[97] Further, the co-monomer ratio and the solvent concentration affect the extent of primary cylcization.[98-101] High

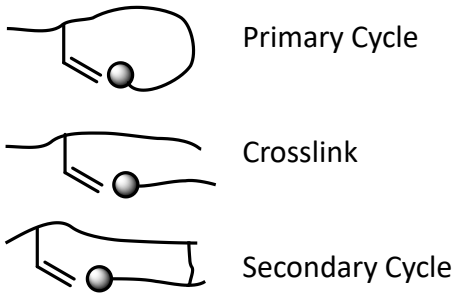

Scheme 7 Possible pathways for the reaction of pendant double bonds. Depending on the reaction partner, the double bond can form a primary or secondary cycle or a crosslink.

crosslinker and/or solvent concentrations increase the probability of primary cycle formation.[102-104]

Primary cycles lead to a heterogeneous material due to the formation of microgels in highly crosslinked networks.[105-107] Microgels are areas within the network with an above average crosslinking density close to a center of initiation. These form because monomeric double bonds have a decreased reactivity compared to pendant double bonds, causing primary cyclization.[94] The enhanced reactivity of the pendant double bonds stems from their significantly higher concentration in the vicinity of the reactive ends of growing radical chains. Microgels are very brittle and therefore act as defects, which reduce the strength of the entire material. The more defects/primary cycles a material has, the more likely premature failure occurs due to the weakening of the structure.

Today, polymer networks are employed in numerous applications, including coatings, dental materials, hydrogels for biomaterials, contact lenses and superabsorbers. For example, contact lenses are made of a copolymer of hydroxyethyl methacrylate (HEMA) and diethylene glycol dimethacrylate and superabsorbent materials are prepared from acrylic acid copolymerized with trimethylolpropane trimethacrylate.[108, 109] All these polymer networks are formed upon irreversible covalent bonding, however, there are also different kinds of polymer networks, such as supramolecular polymer networks (SPNs),[16, 17] interpenetrating polymer networks (IPNs)[84, 110] and covalent adaptable networks (CANs) (see Scheme 8).[19, 20, 111]

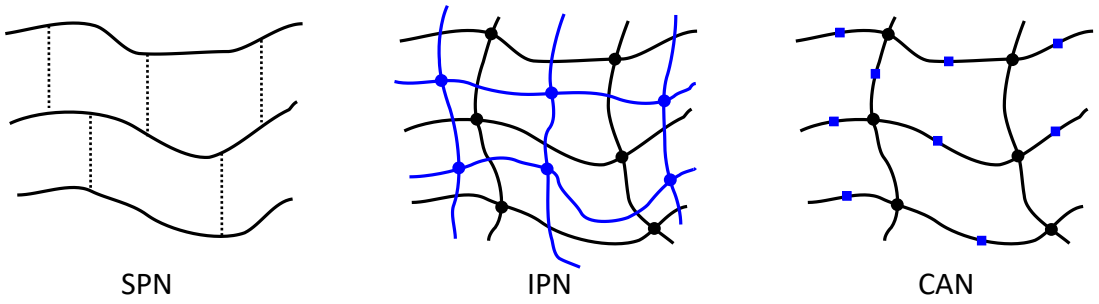

Scheme 8 Different kinds of polymer networks. A supramolecular polymer network (SPN) is (reversibly) crosslinked by noncovalent interactions. A interpenetrating polymer network (IPN) is a combination of two polymer networks, where at least one of the networks is formed in the immediate presence of the other network. A covalent adaptable network (CAN) is reversibly crosslinked by covalent interactions. The reversible moiety can either be the crosslink itself or other motives along the polymer chains.

Supramolecular Polymer Networks

SPNs are materials that are reversibly crosslinked by noncovalent interactions, such as hydrophobic interactions, hydrogen bonding, electrostatic interactions, metal coordination, host-guest interactions or π-π stacking.[17, 53] There are different ways to construct SPNs. The polymer network can be prepared *via* self-organization of low molecular weight species, polymers that bind *via* supramolecular end group motives or polymers with randomly distributed supramolecular crosslinks along the polymer chain. For strong bonding, multiple interactions and sometimes the use of different binding mechanisms are simultaneously necessary.[112] Compared to covalently bonded polymer networks, SPNs have additional fields of application, such as thermoplastic elastomers or as shear-thinning injectable hydrogels employed in biomedicine. SPNs can be subdivided into hydro- or organogels and bulk materials.

Gels are materials that partly consist of water (hydrogel), or a solvent (organogel), which is trapped inside a polymer network. They are usually formed using covalent crosslinking motives, however, can also be prepared using supramolecular interactions. Supramolecular hydrogels are mostly employed as injectable drug carriers,[113] but they can also be used for 3D printing,[114] tissue engineering[115] and oil recovery.[116]

Supramolecular bulk materials are polymer networks made of low molecular weight polymers and oligomers with a T_g below ambient temperature. However, due to the strong, defined supramolecular interactions, the materials behave like a solid. Several recent reviews give an excellent overview of supramolecular materials.[17, 117-119]

Hydrophobic interactions are ideal candidates for the preparation of supramolecular hydrogels. These hydrogels are based on water soluble polymers including non-water soluble monomers, end groups or side chains. The hydrogels are formed at high concentration, whereas at low concentrations, micelles are prepared. E.g. Tsitsilianis and coworkers demonstrated the preparation of hydrogels using polystyrene-*b*-poly(sodium acrylate)-*b*-polystyrene (PSt-*b*-PNaA-*b*-PSt) triblock copolymers with around 3 wt% PSt.[120] Gels were formed at concentrations above 0.4 mol%. It is also possible to prepare thermoresponsive hydrogels, e.g. consisting of poly(*N*-isopropyl acrylamide) (PNIPAM) as thermoresponsive middle block with PSt, poly(2-ethylhexyl acrylate) and poly(*n*-octadecyl acrylate) used as hydrophobic outer blocks.[121] Bio-inspired interactions using the receptor-ligand combination of biotin and avidin are also reported in the literature for hydrogel formation.[122]

Hydrogen bonding is an alternative process that can be employed for the formation of SPNs.[123-125] Usually, several multivalent hydrogen bonding moieties have to be employed for a stable material, e.g. ureidopyrimidinone (UPy) interactions are used in the literature. These can be employed to form self-healing hydrogels using a monomer mixture of 2-(dimethylamino)ethyl methacrylate (DMAEMA) and UPy methacrylate.[126] Sijbesma and coworkers demonstrated that SPNs can also be made of PEG-*b*-bis-urea-*b*-PEG-*b*-bis-urea-*b*-PEG pentablock copolymers.[127] Supramolecular bulk materials can be prepared using hydrogen bonding of UPys and urea as shown by Meijer and his team.[128] The urea-based material demonstrated a higher bulk viscosity, which is attributed to urea forming extended hydrogen bonding alignments phase separated from the polymer, as UPy can only form dimers, which are miscible with the polymer. While all these examples rely on the association of polymer build blocks, SPNs can also be prepared *via* multiple hydrogen bonding of small molecules/oligomers. Leibler and coworkers outlined in their work that urea and fatty acids form oligomers

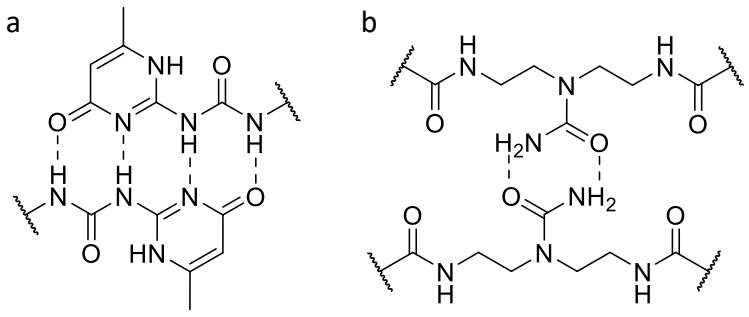

Scheme 9 (a) Ureidopyromidinone and (b) urea hydrogen bonding employed for the preparation of supramolecular polymer networks.

upon reaction, which results in multiple hydrogen bonds, leading to a supramolecular self-healing rubber.[129]

To form SNPs, electrostatic interactions are frequently employed as well.[130, 131] Especially for hydrogels, such interactions are a feasible tool, as charged groups usually demonstrate good water solubility. Electrostatic interactions based hydrogels can be formed using blocks of ionic monomers in combination with non-ionic water soluble building blocks or mixtures of homopolymers including weak polyions. For example, Kramer and Hawker demonstrated that hydrogels form upon mixing ABA triblock copolymers bearing a water soluble middle block and end blocks with cationic and anionic moieties.[132] Further, random copolymerization of anionic and cationic monomers in an equimolar ratio can be employed. Therefore, Gong and coworkers used monomers such as sodium 3-(methacryloylamino)propyl-trimethylammonium chloride (MPTC) and p-styrene sulphonate (NaSS).[133] Several different bulk materials can also be prepared using electrostatic interactions. For instance, when poly(ethylene-*co*-methacrylic acid) is mixed with zinc stearate, a material with self-healing properties upon ballistic impact is formed.[134, 135] As for the hydrogen bonding motives, polymer networks can also be formed directly using small molecules. For example, Grinstaff and coworkers reported SPNs build of phosphonium dications and ethylenediaminetetraacetic acid (EDTA) tetraanions.[136]

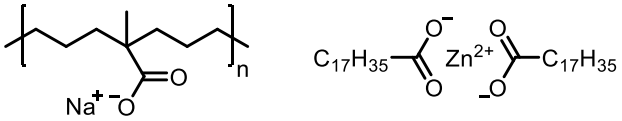

Scheme 10 Poly(ethylene-*co*-methacrylic acid) mixed with zinc stearate for the electrostatic interaction bonding of supramolecular polymer networks.

Metal coordination can also be employed for SPN and hydrogel formation. E.g. Fe^{2+}, Ru^{2+}, Ni^{2+} or Co^{3+} are used to crosslink with poly(2-oxazoline) including bipyridinyl-functionalized side chains.[137, 138] To form thermoreversible gels, Kikuchi and colleagues reported SPNs based on three-armed PEG with terpyridine end groups in combination with Cobalt ions.[139] As frequently, nature serves as an inspiration for synthetically made materials. E.g. mussel-inspired hydrogels can be formed when PEG is end-functionalized using 3,4-dihydroxyphenylalanine (DOPA) and oxidizing agents[140] or metals.[141] Self-healing materials can be designed based on terpyridine complexes. Schubert and co-workers copolymerized terpyridine methacrylate with butyl methacrylate using reversible addition-fragmentation chain transfer polymerization (RAFT).[142] The authors demonstrated that scratched films could be healed at 100 °C. A

metallosupramolecular polymer network with self-healing properties upon irradiation was reported by Rowan and Weder.[143] The self-healing nature is based on 2,6-bis(19-methylbenzimidazolyl)pyridine-Zn^{2+} complexes, which break upon UV light irradiation.

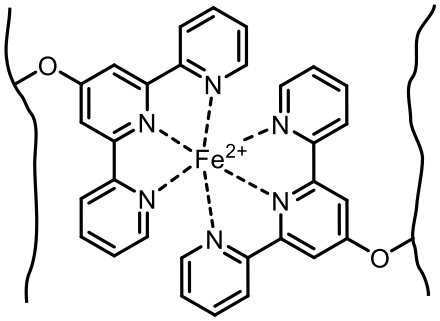

Scheme 11 Self-healing supramolecular polymer network based on metal coordination of Fe^{2+} and terpyridine.[142]

Host-guest interactions have the advantage that besides strong binding motives, they also have a fixed geometry, directionality and often show stimuli-responsive behavior, for example to pH changes.[144, 145] These characteristics make them a feasible tool for biomedical applications including drug delivery. The most widely employed host molecules are cyclodextrins (CD) since they are highly hydrophilic on the outside and hydrophobic on the inside. Moreover, a variety of guest molecules can be trapped. Other used hosts include cucurbituril,[146] crown ether[147] and pillararene.[148] Harada and Kamachi were one of the first to demonstrate that α-CD can form gels *via* a host-guest interaction with PEG.[149] For drug delivery, hydrogels made of PEG-*b*-poly[(R)-3-hydroxybutyrate]-*b*-PEG and α-CD can be employed, as the combination of inclusion complexes between PEG and α-CD with strong hydrophobic interactions between the poly[(R)-3-hydroxybutyrate] motives resulted in a strong SPN.[150] CD can also form other host-guest complexes, e.g. with ferrocene, which can lead to the formation of responsive gels, reversibly switchable *via* an oxidation reaction.[151] Self-healing hydrogels have been demonstrated by Ravoo and coworkers, by employing adamantane modified hydroxyethyl cellulose and β-CD with oligo(ethylene glycol) chains on one side and *n*-dodecyl chains attached on the other side.[152] For bulk materials host-guest interactions are not reported, as the decreased chain mobility in bulk limits the ability of the functional molecules to approach each other, in order to undergo a complexation.

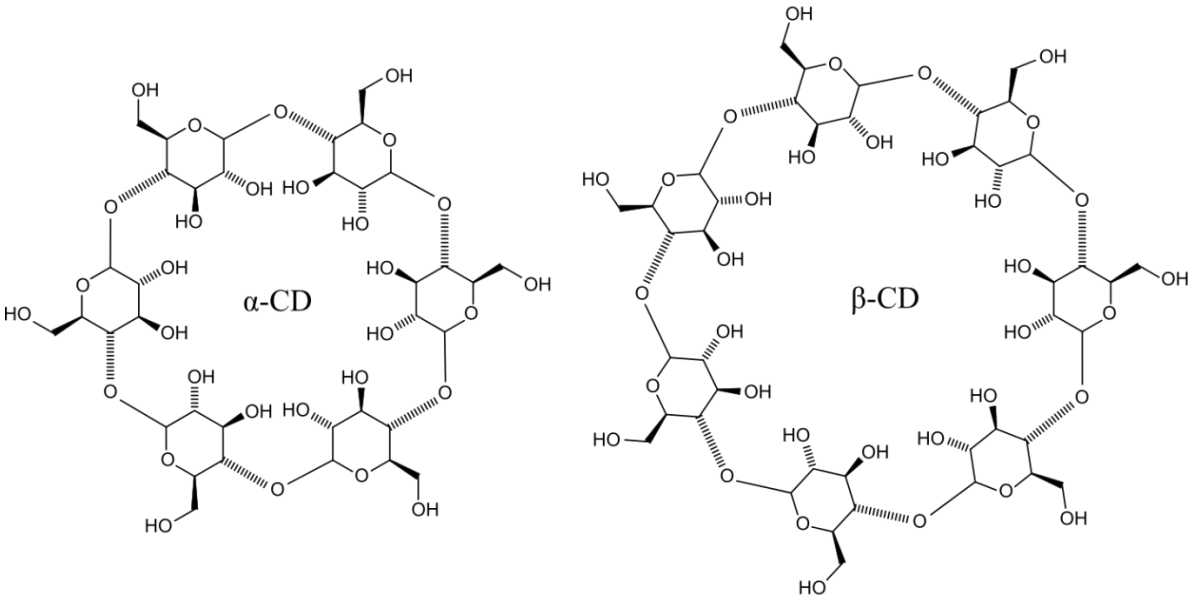

Scheme 12 Stimuli-responsive supramolecular polymer hydrogels can be prepared by employing the host-guest interaction of cyclodextrins (α-CD, β-CD) with various molecules, including poly(ethylene glycol).

Interpenetrating Polymer Networks

Another form of polymer networks are interpenetrating polymer networks (IPNs). By definition, an IPN is a combination of two polymer networks, where at least one of the networks is formed in the immediate presence of the other one.[153, 154] The first record of IPNs goes back to 1914 when Jonas Aylsworth (the chief chemist of Thomas Edison) combined phenol-formaldehyde compositions with Sulphur and natural rubber to make the first rubber-toughened plastic.[155]

IPNs can be divided by the nature of the crosslinks into non-covalent and covalent IPNs. A so-called full-IPN bears two or more independent crosslinked polymer networks, which are at least partially interlocked on a molecular level, however, are not bonded covalently. A semi-IPN is formed, when one or more polymers are crosslinked, and one or more polymers are linear or branched.

Generally, there are three different methods to prepare an IPN (refer to Scheme 13). The first possibility is a polymerization *via* two noninterfering routes, where both networks are formed simultaneously. Secondly, a previously prepared polymer network is synthesized first and then swollen in a monomer mixture of the second polymer network. Upon polymerization, the IPN is formed. The last option is to prepare a polymer network in the presence of a linear polymer chain, which can then selectively be crosslinked in the following step to form the IPN.

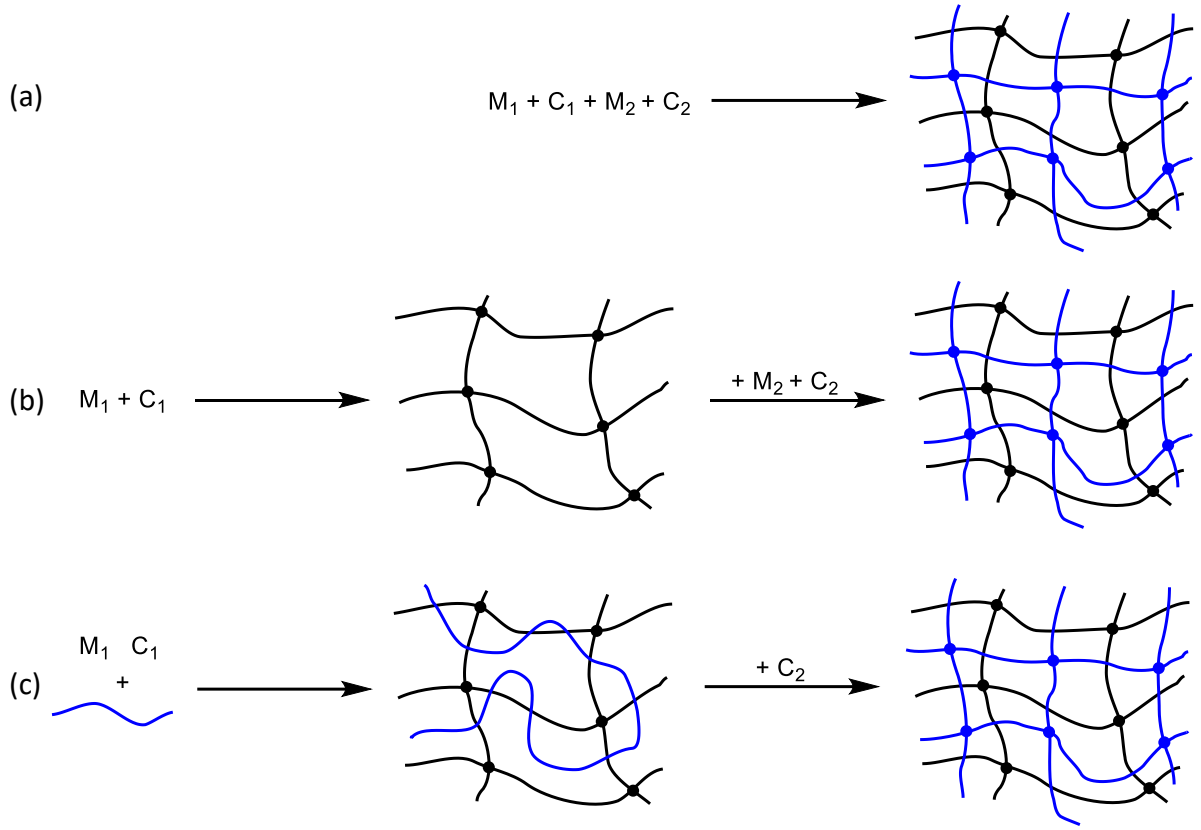

Scheme 13 Schematic presentation of different ways to form an interpenetrating polymer network (IPN). (a) The IPN is prepared by a simultaneous, noninterfering formation of two networks (M: monomer, C: crosslinker). (b) Sequential strategy: One network is prepared first. The network is swollen in the monomer mixture for the second network formation, which is formed in a second step. (c) One polymer network is formed in the presence of a linear polymer, which is subsequently crosslinked in the following step to form the IPN.

IPNs have the capability to form though yet flexible materials. Hence, IPNs are used in various fields of application, such as sound and vibration damping, impact resistant materials and biomedical products.[156, 157] E.g. IPN membranes from polytetrafluoroethylene (PTFE) and polydimethylsiloxane (PDMS) are used for a variety of medical applications, including second-degree burn care. PDMS is able to rapidly transport body fluids away from the side of burning, while PTFE provides mechanical strength and water resistance.[158] IPNs are also used for bone implants, lysozyme adsorption and controlled drug release in the biomedical field.[159]

Another field of application for IPNs is optoelectronics. A major problem of optoelectronics is that electromagnetic energy tends to leak from the fiber. When fibers are coated with a gradient IPN, with the second IPN constituting a polymer of higher refractive index than the first one, this problem can be circumvented.[160]

It is also possible to prepare stimuli-responsive IPNs that are able to respond to changes, such as pH, light, temperature, ionic strength and electromagnetic fields. For example, for drug delivery, hydrogels made of IPNs are advantageous in comparison to conventional hydrogels.

Hydrogels usually bear the disadvantage of low mechanical strength and modulus, due to their swollen nature, alongside with a low loading capacity without significant deformation.[161] As IPNs show improved mechanical properties, they are a feasible tool to improve the properties of hydrogels and, therefore, their ability to be used as drug delivery systems.

For drug release systems, IPN hydrogels that respond to thermal stimulus can be employed.[162-164] Temperature sensitive IPN hydrogels exhibit volume phase transition at a certain temperature, known as the lower critical solution temperature (LCST). Below the LCST, hydrogels absorb water, whereas at temperatures above the LCST hydrogels shrink and release water. E.g. a temperature sensitive IPN hydrogel can be made of poly(vinylic alcohol) (PVA) and poly(*N*-isoproylacrylamide) (PNIPAM).[165] Zang et al. demonstrated the advantages of PNIPAM-IPN hydrogels compared to PNIPAM hydrogels for drug delivery.[166] These authors showed that the IPN based system has an improved mechanical strength, a faster response rate to temperature changes and a better release of the drug. The LCST was about the same for both systems, however, the IPN based system demonstrated a significantly higher T_g.

It is also possible to design pH-sensitive IPN hydrogels. These hydrogels bear the advantage that drugs encapsulated in the system can withstand the conditions of the stomach before they are released into the colon. IPNs based on poly(acrylic acid) (PAA) and gelatin, crosslinked selectively with *N,N*'-methylenebisacrylamide (MBAAm) or glutaraldehyde (GA) were studied for their *in vivo* release of gentamicin sulfate, which is an antibiotic.[167] Analysis demonstrated a significant advance over commonly employed hydrogels. In addition, the mentioned polymers, pH-sensitive IPN hydrogels can be formed using poly(N-vinyl pyrrolidone),[168] chitosan,[169] polyacrylamide and poly(propylene glycol).[170]

IPNs can also be designed to respond to electric-current-stimuli.[171, 172] Materials made of these IPNs are investigated as new actuators, especially for robotics and medical welfare instruments.[173-175] For example, Kim et al. demonstrated that IPNs comprised of PVA and PAA show electrical-sensitive behavior.[173] When the swollen IPN is placed between a pair of electrodes, the material exhibits deformation upon the application of an electric field. Upon removal of the electric stimuli, the IPN returns to its original state. Further, IPNs of a mixture of PAA and poly(propylene glycol)[176] or PVA and polyethyleneimine[177] exhibit electro-responsive behavior.

It is also possible to prepare multi-responsive IPNs.[178] For drug release systems, especially the combination of pH and temperature responsiveness is highly applicable.[179, 180] Zhang et al.

reported the preparation of a dual-responsive IPN, made of pH-sensitive poly(methacrylic acid) (PMAA) and temperature-responsive PNIPAM.[181] Analysis evidenced that the hydrogel showed pH-sensitivity at about a pH value of 5.5, alongside with a thermal response at close to 31 °C. Dual-responsive IPNs can also be prepared using the combination of PAA and polyacrylamide,[182] PMAA and PVA[183] and PNIPAM and silk sericin.[184]

IPNs are also employed in the field of dentistry. Among other applications, they are used in denture base polymers, fiber-reinforcement composites, and artificial teeth.[185-187] For instance, at adhesive interfaces, IPNs provide an improved interfacial adhesion, toughness and mechanical interlocking on a nanometer scale, compared to homo- and copolymers. The strong interlocking of resin adhesives to composites and polymers is crucial for the success of restorative dental treatments. IPNs for dental applications belong to the group of non-covalent semi-IPNs in which only one polymer system is crosslinked. Commonly, the network consists of a dimethacrylate, such as triethylene glycol dimethacrylate, while a monofunctional methacrylate (e.g. MMA) forms the linear polymeric part. After polymerization, different phases can occur, including crosslinked matrices, semi-IPNs, and linear polymers. Hence, the entire polymeric material is not necessarily an IPN, however, there are nano- and microstructured regions of the semi-IPN in the composite or polymer. For a denture base, PMMA beads ($M_w \approx 200000$ g·mol^{-1}, particle size: 50 µm) are dissolved in MMA and 10 wt% ethylene glycol dimethacrylate is employed for the preparation of the IPN. The semi-IPN increases the creep resistance of the denture base polymer.[188, 189] Moreover, the water adsorption is not influenced, but the solvent resistance is increased.[190] Artificial teeth are usually comprised of PMMA beads and color pigments inside a crosslinked polymer matrix. The semi-IPN is employed as a layer between the beads and the matrix. State of the art denture teeth have an uneven distribution of the crosslinking density. For example, the incisal and occlusal area is more highly crosslinked that the gingival ridge-lap area. The semi-IPN in the less crosslinked part of the artificial tooth contributes to a better bonding to the denture base polymer. At higher polymerization temperatures, the bonding strength is increased, as the monomer of the denture base can penetrate deeper into the artificial tooth, prior to curing.[191]

2.2 Adhesives

The following chapter aims at providing an introduction to adhesion and adhesive technology. The field of adhesives is a highly investigated topic due to its significance for industrial applications. For example, more than 50% of the goods produced in Germany today contain adhesives.[22] As a detailed discussion would exceed the scope of the present thesis, the reader is kindly referred to the literature for an in-depth coverage.[192-194] Since a dental adhesive was developed in the presented work, adhesives for dental applications are described in greater detail.

2.2.1 General Aspects of Adhesion

By definition, an adhesive binds two materials in a permanent manner, when applied to their respective surfaces.[23] To understand the concept of adhesion, there are four classical theories (mechanical, adsorption, electrostatic and diffusion theory).[192]

The mechanical theory relies on the interlocking of the adhesive and a rough substrate surface. The liquid adhesive is able to creep into the cracks and cavities of the surface when a good wetting is possible. Upon curing, the adhesive hardens and mechanically interlocks with the substrate surface, generating the adhesion. The surface of the substrate can be pretreated in order to increase the roughness. For example, for dental adhesives, the tooth surface is etched with an acid or an acidic monomer prior to the adhesion step.[195]

The adsorption theory is based on the fact that forces of attraction will occur between an adhesive and the substrate once they are brought into contact. Therefore, as long as a sufficient wetting takes place, the bond (primary: e.g. covalent or secondary: e.g. van der Waals) will be sufficiently strong for adhesion. Covalent bonds occur for example between an organosilane and a glass substrate.[196] The model also takes the surface tension into account. If the surface tension of the adhesive is lower than the surface energy of the substrate, good wetting can take place, resulting in a good adhesion. In contrast to the mechanical theory, no penetration of the substrate surface has to take place for a sufficient bonding.

The electrostatic theory is based on the phenomenon of adhesion to a condenser, where the adhesion is based on the attraction of charges of opposite sign. In the diffusion theory, adhesion is explained *via* the compatibility of polymers. If two polymers are miscible, partial penetration between the two materials can take place, resulting in entanglements of the polymer

chains and therefore bonding between the substrate and the adhesive. The model also suggests a dependency of the adhesion on the molecular weight of the polymer. Due to the higher mobility of shorter polymer chains, they penetrate deeper into the other material than longer chains, forming a strong bond.

2.2.2 Different Types of Adhesives

There are various ways to classify adhesives, as depicted in Table 3.[197] The table is not meant to be exhaustive, yet should give a general insight in adhesive systems.

Physically binding adhesives already contain the polymer, which is responsible for the adhesion. Further, an additive that makes the polymer processable for the desired application is employed. For example, a solvent can be used, such as ethyl acetate or 2-butanone that dissolves the polymer. Upon evaporation of the solvent, the adhesive hardens, causing the desired adhesion. Dispersion-based adhesives contain a dispersion of polymer particles in water. When the water evaporates, the particles get into contact, finally forming the adhesive layer. Hotmels are thermoplastic adhesives that are solid at ambient temperature, however, are reformable when heated. Upon cooling, the adhesion bond is formed.

In chemically binding adhesives, the adhesion is based on a chemical reaction (usually a polymerization). For instance, cyanoacrylate-based adhesives, also known as superglue, harden in an anionic polymerization upon exposure to moisture.[198] Already the humidity of the air is sufficient to start the polymerization. An FRP is responsible for the curing of a methyl methacrylate-based adhesive.[199] The methacrylate is brought into contact with a radical generator (usually a peroxide and a promoter, e.g. an amine). The methacrylate adhesive is a so-called two-component adhesive, as the promoter and the initiator are separated spatially prior to the application. Phenol-formaldehyde adhesives are an example for adhesives that cure *via* a polycondensation reaction.[200] A mixture of a low molecular weight phenol-formaldehyde resin and a formaldehyde source are applied and cured upon heating to about 170 °C, whereupon the water, which is formed during the condensation, evaporates. Epoxy resin adhesives are two-component adhesives, based on monomers or oligomers bearing epoxy end groups and a hardener, which can be a diamine or a dithiol.[201, 202] Upon application, a polyaddition reaction takes place, hardening the adhesive formulation.

Table 3 Different classifications of adhesives and their primary resins.

Main category	***Subcategory***	***Primary resin***
Characteristics	Anaerobic adhesive	Polyester, urethane, epoxy, silicone, acrylate
	Elastic adhesive	Silicone, urethane, polysulfide
	Conductive adhesive	Epoxy, acrylate, polyimide, silicone,
	Flame-retardant adhesive	Polybenzimidazole, polyquinoxazoline, polyimide, bismaleimide
	Damping adhesive	Silicone, polyvinylalcohol
Curing methods	Physical curing	Polyamide, polyacrylate, polyurethane, polychloroprene, poly(vinyl chloride)
	Chain-growth polymerization	Cyanoacrylates, acrylates, methacrylates
	Polycondensation	Silicone, phenol-formaldehyde, polyimide, polysulfide
	Polyaddition	Epoxy, polyurethane, silicone
	No curing	Polyacrylate, polyester, silicone
Applications	Medical adhesive	Fibrin, gelatin, cyanoacrylate, polyurethane
	Structural adhesive	Phenol, epoxy, urethane, acrylate
	Dental adhesive	Methacrylate, acrylamide

There are also adhesive systems where no physical or chemical curing step is required. These solvent-free adhesives are usually made of polyacrylates, styrene-butadiene-styrene block copolymers, polyesters, and silicone. They are applied, for example, as spray adhesives or as adhesive tapes.

All the adhesives mentioned above, are merely few examples of numerous systems, known today. As the development of a dental adhesive was the initial purpose of the present work, dental adhesives are discussed in greater detail in the following section.

2.2.3 Dental Adhesives

Dental adhesives are employed in order to achieve a strong bonding between the tooth substrate (dentin or enamel) and a respective restorative material. A cross section of a human tooth is provided in Figure 1 for a better understanding. Today, the dentist is provided with several methods to adhere a dental restorative to the tooth. All of the methods have in common that in a first step an etching process has to be carried out to enable a strong adhesion, which was first discovered by M. G. Buonocore in 1955, who used phosphoric acid for an improved bonding between the enamel and the resin.[203] In 1979, acid etching of dentin was introduced by Fusayama, leading to an enhanced bonding to dental tissues, finally leading to the total-etch concept introduced by R. L. Bertolotti in 1991.[204]

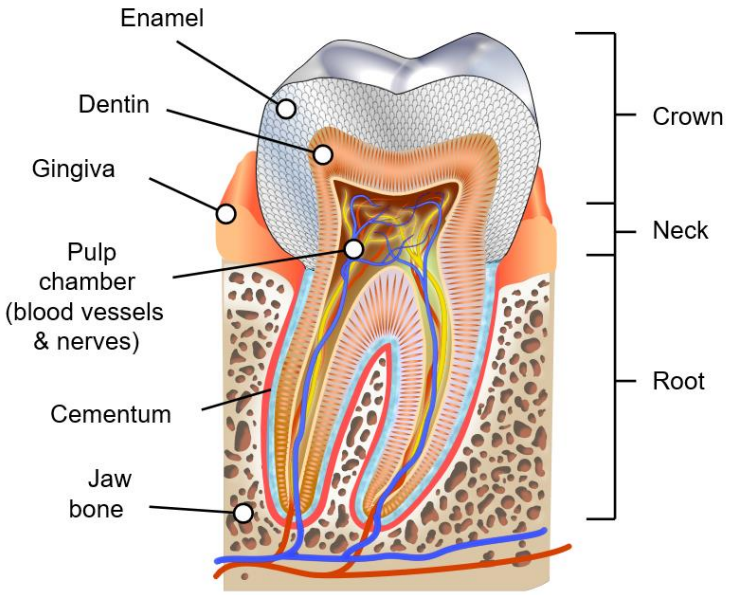

Figure 1 Cross section of a human tooth showing the enamel, cementum, pulp, and dentin, as well as the surrounding tissues (Author: K.D. Schroeder, graphic Human tooth diagram-en.svg from Wikimedia Commons, License: CC-BY-SA 3.0).

The etching leads to a superficial demineralization of the tooth, allowing a replacement by monomers of the resin. Upon application, the adhesive creeps into the cavities. When the resin is cured, it interlocks micromechanically with the created porosities, leading to the desired adhesion. As depicted in Scheme 14, today's adhesion systems can be subdivided by their approach, into etch-and-rinse (E&RA) and self-etching adhesives (SEA). As indicated by Scheme 14, E&RA adhesives require two or three application steps. For both methods, an acid etchant, usually consisting of a phosphoric acid gel (32 – 37 wt%) is employed in a first step. Then, either the primer and the adhesive resin are applied consecutively (three steps) or a

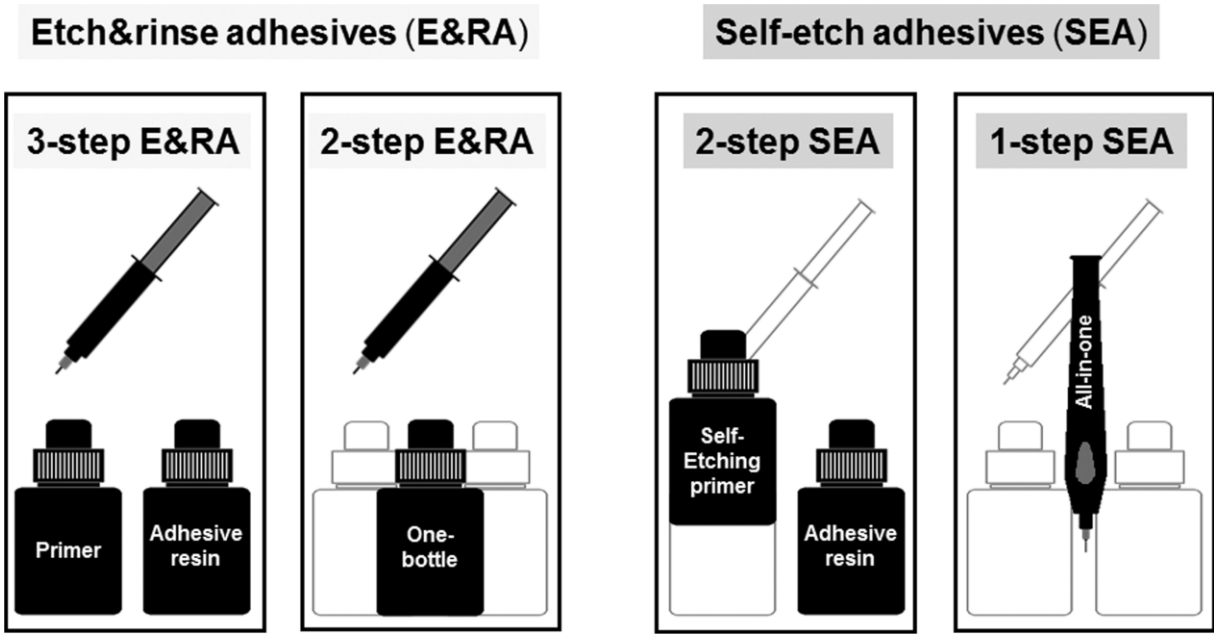

Scheme 14 Classes of current dental adhesives employed for restorative composites. Adapted with permission from John Wiley and Sons.[199] Copyright 2012 Polymer Chemistry.

combination of both is used (two steps). The E&RA approach is the more effective method in order to obtain a strong, efficient and stable bond to enamel, as the acid etching leads to a selective dissolution of the hydroxyapatite crystals (HAP), which are the main component of the enamel. When the dentin is etched using an acid, a microporous network of collagen is exposed. The application of the primer and the adhesive resin then leads to the infiltration of the formed cavities with the monomers. Upon *in situ* curing, so-called resin tags are formed, which are responsible for the adhesion.[205, 206]

SEAs do not require a separate etching step in contrast to the E&RA adhesives. SEAs can further be subdivided into 2-step and 1-step SEAs. 2-step SEAs consist a self-etching primer and an adhesive resin, whereas one-step solutions combine conditioning, priming and the application of the adhesive resin in a single step. Both systems contain so-called nonrinse acid monomers, which condition and prime dentin/enamel simultaneously. The nature as well as the depth of interaction between the adhesive and the tooth highly depends on the structure of the monomers. For example, the interaction depth can be increased from a few hundreds of nanometers, for ultramild SEAs (pH > 2.5), to several micrometers when a strong SEAs (pH ≤ 1) is employed.[199, 207, 208]

To understand the interaction of the monomers with the HAP, the so-called adhesion-decalcification concept (AD-concept) was invented by Yoshida et al. (refer to Scheme 15).[209] In the first step (P1), the acidic monomer, often a phosphonic acid based monomer, leads to the

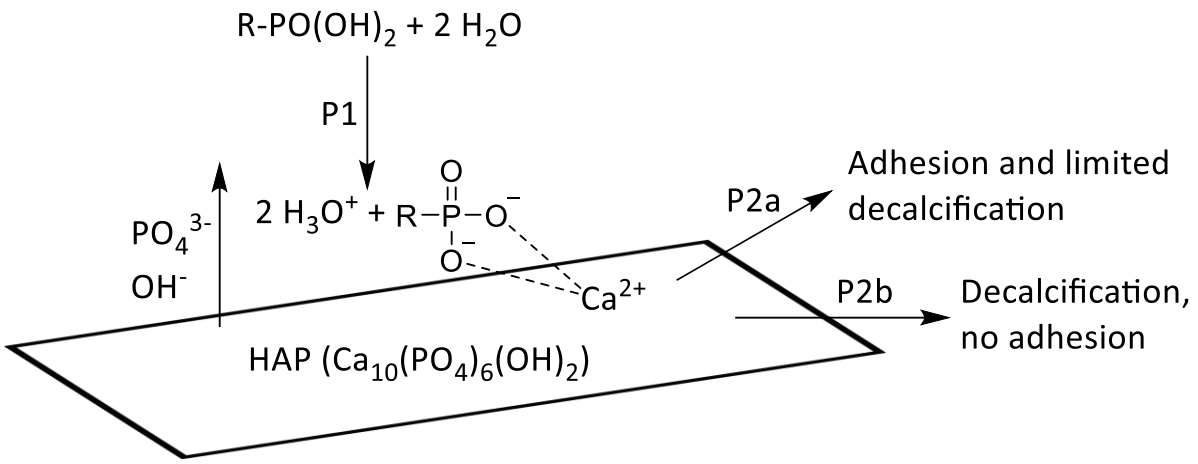

Scheme 15 AD concept, adapted from Yoshida et al.[209] The acidic monomer cleaves phosphate and hydroxyl ions from the tooth surface before it is either bonded or debonded, depending on the strength of the ionic bond.

release of phosphate and hydroxyl ions from the HAP. If the ionic bond between the monomer and the dental tissue is stable, the monomer will remain bonded, resulting in a chemical adhesion to the HAP (P2a). However, if the ionic bond is unstable, the monomer is not bonded to the surface and a complete decalcification takes place (P2b).

Present enamel-dentin-adhesive systems usually consist of various components, such as monomers, initiators, inhibitors, solvents and fillers. The monomers are the integral parts of the mixture, as they are responsible for a strong and durable bond between the tooth, the dental adhesive, and the restorative material. In most cases, a monomer mixture is employed, consisting of non-acidic, acidic, and di- or multi-functionalized monomers. Today, most monomers are based on methacrylates, as they are in contrast to acrylates less toxic, but still demonstrate a sufficient reactivity during FRP. Hydroxyethyl methacrylate (HEMA) is by far the most frequently employed nonacidic monomer, as it is water soluble and improves the miscibility of the other adhesive components alongside with an improved wetting behavior on the dental tissue, which improves the strength of the bond.

As an acidic monomer, a broader variety of monomers can be employed. A selection is displayed in Scheme 16. The monomers range from methacryloyloxydecyl dihydrogen phosphate (MDP), 4-methacryloyloxyethyl trimellitic acid (4-MET) and 11-methacryloyloxy-1,10-undecanedicarboxylic acid (MAC-10), to monomers such as N-tolylglycine glycidyl methacrylate (NTG-GMA). As described in the AD concept, the acidic monomer leads to the etching of the tissue and the consecutive bonding to the tooth structure. In recent years, novel strongly acidic monomers were prepared bearing dihydrogen phosphates and phosphonic acids (PA).

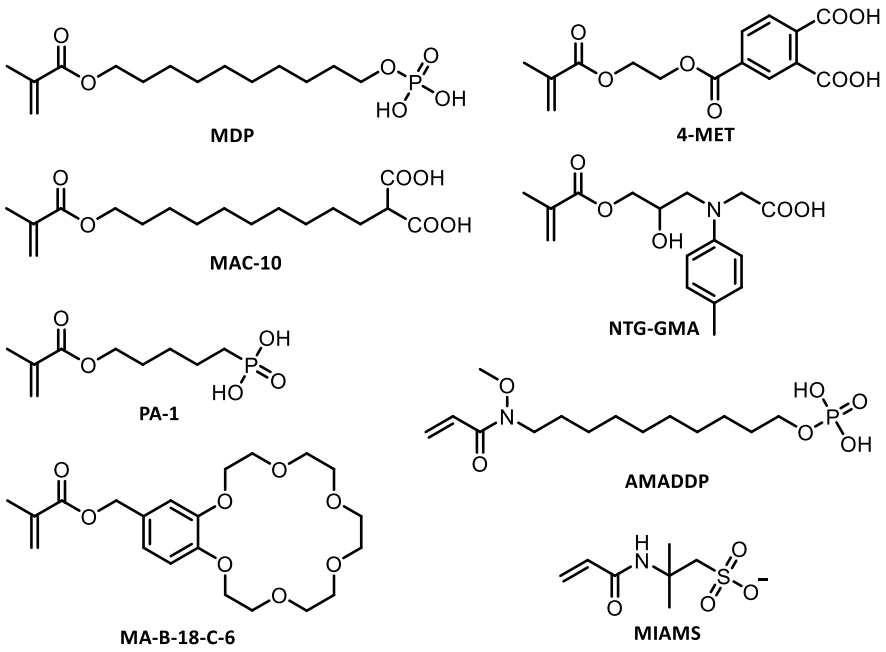

Scheme 16 Examples of acidic monomers employed for adhesive formulations.

The group of Avci prepared a variety of new polymerizable PAs, including (5-(methacryloyloxy)pentyl)phosphonic acid (PA-1) [210, 211] However, as the respective methacrylate derivatives tend to hydrolyse, (meth)acrylamide-based monomers, like *o*-alkylated acrylic acid hydroxyamides (e.g. 10-(*N*-acryloyl-*N*-methoxyamino)-decyl dihydrogen phosphate, AMADDP) were synthesized, which are hydrolytically stable.[212] The monomers demonstrated to be ideally suitable for SEA systems, as they are capable of achieving a strong bond between the restorative material and the dental tissue, due to their hydrolytic stability, high acidity and potential to sufficiently edge enamel.[213, 214] In addition, monomers having the ability to chelate calcium ions bear the potential to improve the bonding performance. For example, it was demonstrated that 4-(methacryloyloxymethyl)-benzo-18-crown-6 (MA-B-18-C-6) significantly increases the dentin shear bond strength when added to an adhesive formulation.[199] The effect can be explained with the optimal cavity size of the specific crown ether (134 – 143 pm) that leads to a strong complexation of Ca^{2+}.[215] Finally, polymerizable ionic liquids, such as 1-butyl-3-methylimidazolium 2-acrylamido-2-methyl-1-propanesulfonate (MIAMS) can be employed to improve the adhesion on dentin and enamel, and, furthermore, can increase the conversion of the polymerization under air.[216]

Di- or higher functionalized methacrylates are employed to prepare a polymer network upon curing (see Scheme 17). The network formation has several positive effects, such as an im-

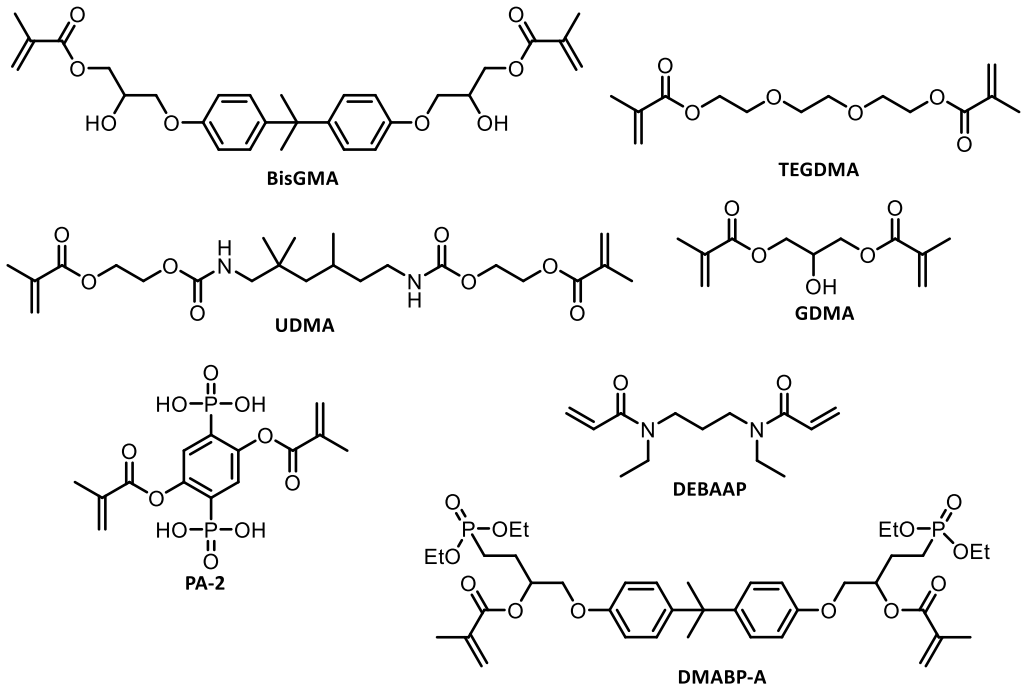

Scheme 17 Examples of crosslinking monomers used for dental adhesives.

provement of the mechanical properties compared to linear polymers, an increased polymerization rate due to the gel effect and a decreased swelling behavior of the adhesive, to mention just a few. Commonly employed dimethacrylates are 2,2-bis[4-(2-hydroxy-3-methacryloyloxypropoxy)-phenyl]propane (BisGMA), triethylene glycol dimethacrylate (TEGDMA), 1,6-bis-[2-methacryloyloxyethoxycarbonylamino]-2,4,4-trimethylhexane (UDMA) and glycerol dimethacrylate (GDMA). Further, difunctional PAs were prepared, which combine the acidity and the crosslinking behavior into one molecule. For example, 2,5-bis(methacryloyloxy)-1,4-phenylenediphosphonic acid (PA-2), whose aqueous solution shows a pH value of 1.65 (1 wt%).[210, 211] However, these dimethacrylates exhibit hydrolysis in aqueous, acidic solutions, which is a drawback for their applicability.[217] To circumvent this problem, Moszner and coworkers prepared novel bisacrylamides, e.g. *N,N*'-diethyl-1,3-bis(acrylamido)propane (DEBAAP), which exhibits an improved stability under acidic conditions, in addition to a good reactivity in FRPs. Furthermore, DEBAAP demonstrates a lower cytotoxicity than the currently employed dimethacrylates.[213, 218, 219] As for the acidic monomers, phosphonate based dimethacrylates were recently prepared, like a bisphenol-A derivative (DMABP-A).[220]

Besides the monomers, the second crucial additive for the adhesive formulation is the initiator, since the initiator has a significant effect on the bonding performance. As dental adhesives are cured *via* FRP, initiators that form radicals upon decomposition are employed. A general

overview on the currently employed initiators is given by Endo and Ikemura.[221] The most commonly employed initiator system is a mixture of camphorquinone (CQ) and a tertiary amine like ethyl 4-dimethlaminobenzoate (EMBO). Upon absorbance of blue light (400 – 500 nm), the CQ is excited and subtracts an electron from the amine, followed by a proton transfer, which forms the initiating species (aminoalkyl radicals) and ketyl radicals that tend to dimerize (see Scheme 18).[222] As the chromophoric group of the CQ is degraded upon reaction, the system demonstrates a good photobleaching effect, which is crucial for an application in dental adhesives.

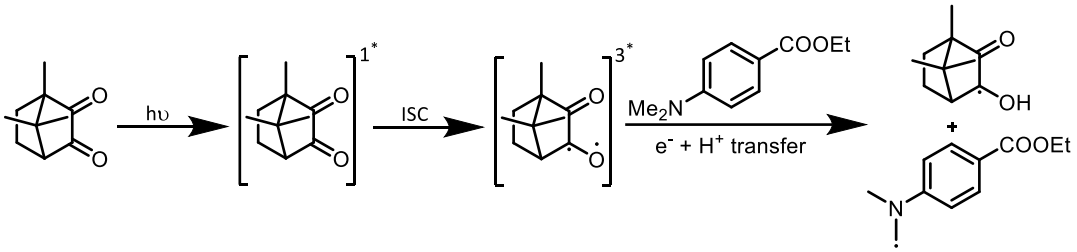

Scheme 18 Radical formation of the camphorquinone/ethyl 4-dimethlaminobenzoate pair upon irradiation with blue light.[222]

However, the CQ-amine system has a number of disadvantages. Firstly, the acid-base reaction between the amine and the acidic monomers decreases the concentration of the initiating species. Moreover, coloration can occur due to an oxidation of the amine.

Hence, alternative photoinitiators, e.g. 2,4,6-trimethylbenzoyldiphenylphosphineoxide (APO) or bis-(2,4,6-trimethylbenzoyl)phenylphosphine oxide (BAPO) are employed, which, however, have to be combined with CQ, as they only strongly absorb in the UV range (refer to Scheme 19). In order to achieve a bathochromic shift, various chromophores, which feature a red shift of the absorption maximum of the crucial n-π* transition, were used as substituents for BAPO. Nevertheless, the substitution did not result in a significant shift of the absorption maximum. In order to achieve a bathochromic shift, Ganster et al. demonstrated in 2007 that organometallic ketones containing germanium can be employed as initiators. For example, benzoyltrimethylgermane (Ge-1) demonstrated a bathochromic shift of the n-π* transition of close to 30 nm, compared to BAPO.[223] Ge-1 undergoes an α-cleavage during irradiation, whereupon benzoyl and germyl radicals are formed, which are able to initiate a polymerization. Upon further investigation, a methoxy-substituted dibenzoyldiethylgermane (Ivocerin®) demonstrated even better performance. The initiator shows, compared to CQ, a significantly stronger absorption in the visible light range, alongside with a high photoinitiation activity (quantum yield

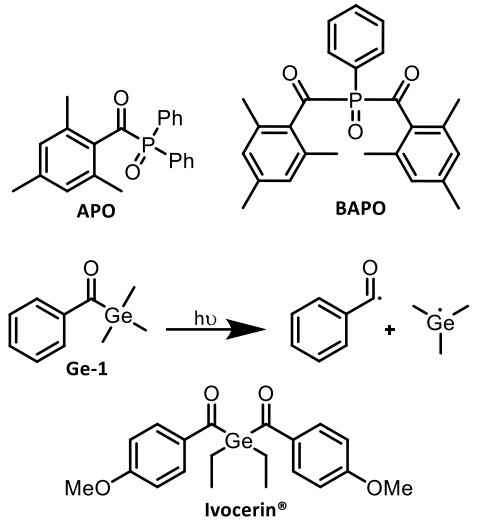

Scheme 19 Selection of employed photoinitiators, as well as the decomposition mechanism of the novel germanium based initiators. Both, the germyl and the benzoyl radicals are capable of initiating a polymerization.

of approximately 0.85 compared to 0.10 for the CQ-amine system) and an excellent photobleaching effect.[224, 225]

For applications in which light cannot be used for the initiation process, redox systems are incorporated in the adhesive.[226] Therefore, an oxidizing agent (e.g. dibenzoyl peroxide (DBPO)) is combined with a reducing agent, such as the tertiary amine *N,N*-diethanol-p-toluidine (DEPT). The reducing agent functions as an accelerator for the homolytic cleavage of the peroxide, whose radicals can initiate a polymerization even at ambient temperature. In addition, boranes and monosubstituted barbituric acids are employed in this context.

Another crucial component of the adhesive system is the solvent that promotes the penetration of the monomer into the dental tissue and increases wetting and flowing behavior. Ethanol, isopropyl alcohol, acetone, and water are most commonly employed as they are available in high purity, have an acceptable scent, good biocompatibility, high volatility, are fairly inexpensive and importantly dissolve most of the other components of the enamel-dentin adhesive.[227, 228]

In order to increase the storage stability, inhibitors are added to the adhesive formulation to prevent premature polymerization (see Scheme 20). Usually, a mixture of an aerobic and an anaerobic inhibitor is used, which can, for example, consist of 100 – 1000 ppm 2,6-di-tert-butyl-4-methylphenol (BHT) and 20 – 100 ppm of phenothiazine (PTZ). However, when used with strongly acidic monomers in single-component SEAs, the phenolic stabilizers are depleted from the system, due to a nonradical reaction with an acrylic double bond.[229] As aerobic in-

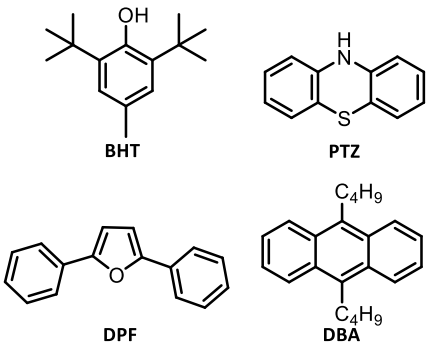

Scheme 20 Selection of commonly employed inhibitors for dental formulations.

hibitor 2,5-diphenylfuran (DPF) and 9,10-dibutylanthracene (DBA) that undergo a [4+2] cycloaddition reaction with singlet oxygen can be employed to enhance the storage stability and the polymerization behavior.[230]

Moreover, nanofillers, such as colloidal or pyrogenic silica, are added to improve the flow properties of the system. Antimicrobial agents, fluoride-releasing components, and dyes can also be part of the formulation.[199]

2.3 Thermally Triggered Debonding on Demand

The term “debonding on demand” is meant to be understood in terms of a debonding of a covalent bond upon application of a certain trigger. In general, triggers such as heat,[231, 232] light,[5, 233] pH changes,[9] an acid/base reaction[10, 12, 234], redox potentials, changed solvents and magnetic or electric fields can be employed to alter polymeric structures. The following chapter gives a deeper insight into various debonding on demand systems based on thermal stimulus.

In general, all bimolecular addition reactions are – at least to some extent – reversible due to the temperature dependence of the equilibrium constant. However, most reactions can in practice be considered as irreversible due to several temperature dependent constraints. The temperature for the system to undergo a cleavage can simply be too high, or side reactions can be induced at high temperatures. Moreover, the time for the debonding to take place is crucial, as debonding times of hours or days are not desirable and not applicable time scales. Especially for the desired application in the field of dental adhesives, degradation times of seconds or minutes are necessary in order for the system to be applicable. Therefore, only systems that degrade at relatively low temperatures (< 130°C) in a fast manner (minutes) are discussed.

2.3.1 Diels-Alder/Hetero-Diels-Alder Systems

Diels-Alder (DA)/Hetero-Diels-Alder (HDA) systems are the first ones to be discussed in detail, as they offer great potential in terms of a fast debonding in a reasonable temperature range.

In 1928, Otto Diels and Kurt Alder described the structure of the product of a reaction between quinone and cyclopentadiene (Cp).[235] They assumed the formation of a [4+2] cycloaddition product of the double bond units of the quinone and the diene moiety of the Cp, analogous to a previous study of Diels, concerning the reaction of an azo diester with Cp.[236] Diels and Alder undertook comprehensive studies on the [4+2] cycloaddition reaction of various dienes and dienophiles, drawing the attention of the scientific society to this feasible synthetic tool.[237-240] Among others, they analyzed Cp, furan, maleic anhydride, anthracene, and pyrrole. Due to their significant contribution to the scientific field of cycloadditions, the reaction was finally named after them and they were awarded the Nobel Price in 1950.

Until today, the Diels-Alder (DA) reaction has become a frequently used tool in chemical synthesis, which can be attributed to the advantageous characteristics of the reaction:

1. No by-products
2. Simple work up
3. High yields
4. Orthogonality
5. Robustness
6. Reversibility

During cycloaddition reactions, no by-products are formed, which facilitates the work up significantly. Moreover, reactions can usually be conducted with high yields. The orthogonality stems from the fact that the cycloaddition reaction provides high functional group tolerance, due to the fact that the diene and the dienophile react selectively with each other. As the reaction can usually be employed in various solvents and under air, it is also a highly robust reaction. Moreover, as all thermally allowed cycloaddition reactions, the DA reaction is reversible, as it undergoes a so-called retro-DA reaction or cycloreversion upon heating, reforming the starting materials.

The Hetero-Diels-Alder (HDA) reaction is a special form of the DA reaction, in which a heteroatom is part of the diene and/or dienophile. The HDA reaction was first seen as a curiosity, and researcher focused more on the DA reaction and the substitution of the starting materials. However, finally, groups like imines and carbonyls were used as dienophiles, and dienes such as α,β-unsaturated carbonyls were employed.[241] In contrast to carbonyl moieties, thiocarbonyl reactants were less studied, even though it was found that they react rapidly with a broad range of dienes at low temperatures.[242] A drawback of most thiocarbonyl based HDA products is that they are not stable under atmospheric conditions. Nevertheless, thioaldehydes,[243] thioketones[244] and dithioesters[245] were successfully used as dienophiles in HDA reactions. In the following, mechanistic characteristics of DA reactions are discussed. All findings for the DA reaction also apply for the HDA reaction.

Multiple studies were conducted to understand the mechanism underpinning the DA reaction and to predict the behavior of the reactants prior to the reaction. The cycloaddition reaction

follows a pericyclic mechanism,[246] with only special cases indicating a diionic or diradical character.[247] As a result of the pericyclic behavior, the conformation of the starting materials is transferred to the DA product. However, if two diastereomers are possible, usually a mixture of both will be present in the product, with the *exo*-product being the thermodynamically favored and the *endo*-product the kinetically favored one (see Scheme 21).

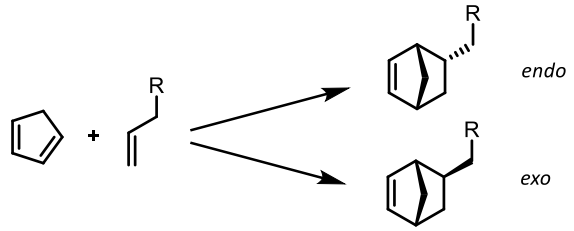

Scheme 21 Possible diastereomers obtained during a Diels-Alder reaction (*exo*- and *endo*-product).

By studying differently substituted dienes and dienophiles it was discovered that electron-donating motives on the diene in combination with electron-withdrawing groups on the dienophile lead to faster cycloaddition reactions. The observation can be explained using the frontier-molecular-orbital (FMO) theory. The theory neglects all molecular orbitals, except the frontier molecular orbitals, e.g. the lowest unoccupied molecular orbital (LUMO) and the highest occupied molecular orbital (HOMO). The DA reaction proceeds *via* the overlap of the LUMO and HOMO of the starting materials in a six-membered transition state. For a positive overlap to occur – which forms the new σ-bond – the wave functions of the overlapping molecular orbitals have to be in phase. A suprafacial overlap, which is the more common case, is present when both changes occur on the same face. If different faces are involved, the overlap is antarafacial. For a DA reaction with normal electron demand, the transition state involves the $LUMO_{dienophile}$ and $HOMO_{diene}$. To reduce the HOMO-LUMO gap, which leads to a faster reaction, the dienophile can be modified with electron-withdrawing groups, while the diene is substituted using electron-donating motives. However, when an electron-rich dienophile and an electron-poor diene is employed, a reaction between the $HOMO_{dienophile}$ and $LUMO_{diene}$ can also be conducted (refer to Scheme 22). Therefore, by using the FMO theory it can be explained why some diene/dienophile pairs react in a DA reaction and why some reactions do not proceed.

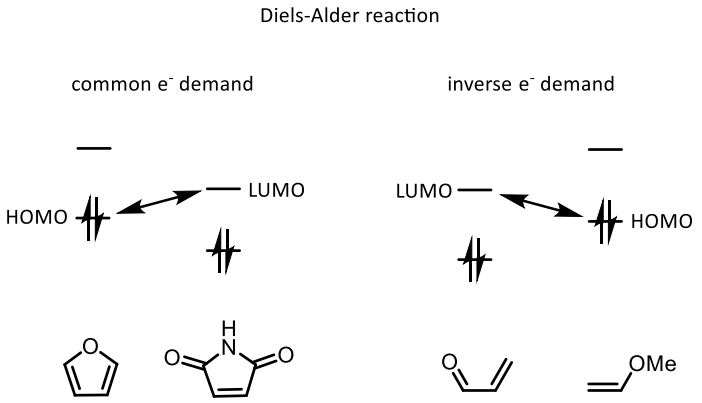

Scheme 22 HOMO-LUMO display of Diels-Alder reactions with common and inverse electron demand, including an example for both cases.

Next, the reversible nature of the DA reaction will be discussed. The DA reaction is based on an equilibrium between the diene and dienophile, and the cycloaddition product. As the equilibrium is dynamic in nature, constant bonding and debonding take place. Since a dynamic equilibrium follows Le Chatelier principle,[248] the state of the equilibrium can be altered by varying concentration, temperature or pressure. The reverse reaction to the diene and dienophile is called retro Diels-Alder (rDA) reaction. The possibility to reversibly form and break covalent bonds by simply varying the temperature makes the DA chemistry a powerful tool for the preparation of smart materials. It is for example employed for macromolecular architectures,[249] adaptable networks[232] and as a protection group.[250] However, despite the numerous available DA and HDA pairs, only a few examples can be reversibly debonded in a reasonable temperature range and time frame. Those DA/HDA pairs are presented in the following part.

The furan/*N*-maleimide couple is by far the most examined system among the DA pairs (see Scheme 23). According to literature, the equilibrium is completely shifted to the DA product at temperatures below 65 °C, whereas above 110 °C, the diene and the dienophile are the predominant species.[251] As side reactions and thermal degradation are negligible, the DA pair is a feasible tool for smart material design, including self-healing materials[252, 253] and thermally cleavable surfactants.[254] For example, Picchioni and coworkers developed a thermally self-healing material using polyketones alternatingly functionalized with furan and maleimide.[255] The reaction to the DA moiety proceeds very slowly (days) if conducted at ambient temperature.[256] Therefore, usually temperatures of about 60 °C are employed, reducing the reaction

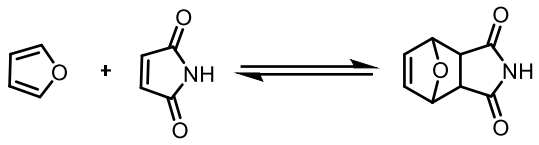

Scheme 23 The equilibrium of the Diels-Alder reaction between furan and *N*-maleimide. Below 65 °C, only the starting materials are present, whereas at temperatures above 110 °C the product dominates.

time to hours. Sometimes, even temperatures of 80 °C are used to further accelerate the reaction.[257] At 80 °C the equilibrium is already slightly shifted to the side of the starting materials, however, upon cooling, the DA product is formed almost exclusively.

Another possibility for a thermoreversible DA pair is the dimerization of Cp, as Cp can simultaneously act as diene and dienophile (see Scheme 24). The driving force for the reaction is the reduction of the ring strain of the Cp units upon cycloaddition. The retro-DA reaction can be induced at temperatures above 170 °C in small molecule form and at 120 °C when incorporated into a network. Cp motives can, therefore, be employed for thermally reversible polymers[258] and polymer networks.[259] To form the polymer network Wudl and co-workers employed a dicyclopentadiene diacid, which was reacted with a diol to form a cyclic diester. Upon heating to 120 °C, the DA product opens, leading to the formation of a linear polymer or/and the formation of a polymer network upon trimerization of a dicyclopentadiene unit with an exposed Cp group. The Cp dimer bears two C=C double bonds, which can react as dienophile for the network formation, the cyclopentene bond and the norbornene bond. Studies revealed that the norbornene bond is the reactant for unsubstituted cyclopentadienes,[260] whereas, for the carboxy-substituted motive, the cyclopentene moiety reacts.

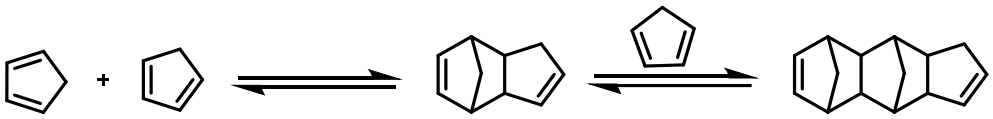

Scheme 24 Equilibrium of the Diels-Alder reaction of cyclopentadiene. Dimers and trimers can be formed upon the cycloaddition. Depending on the substitution, the retro-DA reaction is induced at temperatures between 120 and 170 °C.

It should be noted that also the anthracene/*N*-maleimide pair is employed as DA pair as well, however, as temperatures between 250 and 300 °C are required to trigger the retro-DA reaction, the pair is not discussed further in the present work.[261]

The most prominent example for an HDA pair that can undergo cleavage at relatively mild temperatures is the dithioester/Cp pair. Different dithioesters can be found in the literature that were explored for their retro HDA behavior in combination with Cp. For example, a

cyanodithioester/Cp HDA adduct starts to cleave at close to 70 °C, which can be observed *via* ^{1}H NMR spectroscopy. At 130 °C, 19 mol% of the starting material is present.[262] The substituent attached to the dithioester is crucial for its reactivity in an HDA reaction. Strong electron-withdrawing motives including carbonyl,[263] sulfonyl[264] and cyano[265] groups decrease the electron density of the C=S double bond and, therefore, activate the dithioester, resulting in a fast reaction. However, the moieties show a higher vulnerability towards hydrolysis and oxidation. When electron-donating groups, like thiols and alcohols or aromatic units, are attached, the electron density of the C=S double bond is increased, leading to a deactivation for an HDA reaction with common electron demand. In order to achieve a compromise between an activation for the cycloaddition and a decreased tendency for degradation, pyridinyl and phosphoryl dithioesters can be employed (see Scheme 25). These functional groups do not activate the C=S double bond significantly, reducing the tendency for oxidation and hydrolysis. However, the electron poor character, and therefore the affinity to undergo an HDA reaction, can be increased by the addition of a catalyst. Trifluoroacetic acid (TFA) and the Lewis acid $ZnCl_2$ are frequently employed in this context. The necessity of a catalyst, in order for the HDA reaction to take place, offers the possibility for a more or less permanent debonding upon heating. When the catalyst is removed after the HDA adduct formation, the rebonding after the retro HDA reaction took place is not possible or at least highly hindered. As both dithioesters can also act as a chain transfer agent in reversible addition fragmentation chain transfer (RAFT) polymerizations, telechelic polymers bearing end groups for an HDA post-modification can be prepared.[266] For example, Langer et al. synthesized amphiphilic block copolymers bearing reversible HDA motives based on the phosphoryl dithioester/Cp pair.[231] They demonstrated that the polymer blocks can be reversibly cleaved multiple times during heating and cooling cycles. The pyridinyl dithioester was employed by our team to reversibly crosslink functional polymers.[267] These authors prepared a linker bearing three pyridinyl dithioester motives, which was used to reversibly crosslink PMMA polymers bearing Cp end groups.

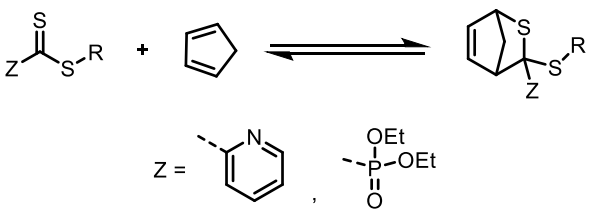

Scheme 25 Equilibrium of the Hetero-Diels-Alder reaction of dithioesters with cyclopentadiene. Depending on the Z and R group, the onset of the debonding can vary between 20 and 40 °C.

However, not only the structure of the employed diene and dienophile is responsible for the retro HDA temperature. As demonstrated by Barner-Kowollik and coworkers, also the position of the HDA linkage within the macromolecule as well as the chain length and the persistence length significantly influence the debonding temperature, which is attributed to entropic effects. [268-270]

2.3.2 Other Systems for Thermally Triggered Debonding on Demand

An alternative motive that can be employed for temperature dependent debonding on demand are alkoxyamines. Zhang and co-workers demonstrated that a homolytic bond cleavage of the C-ON bond occurs at about 125 °C. Upon cooling, the bond is reformed, making the system applicable for reversible alterations.[271] Beside the stable, non-propagating radical (e.g. 2,2,6,6-tetramethylpiperidinyl-1-oxy (TEMPO)) another more reactive radical is formed upon degradation. This radical can undergo side reactions, making the debonding irreversible.

Further, nitroso dimers can be debonded *via* a thermal trigger. Pazo and colleagues demonstrated that the dimers cleave at temperatures between 110 and 150 °C.[272] The reaction is also reversible upon cooling, however, upon cycling, steady degradation of the nitroso functionality takes place resulting finally in a loss of the reversibility.

The reaction between isocyanates and imidazole can also be employed as a thermodegradable motive. The reaction product entails a urea linkage, which cleaves upon heating. Han and coworkers demonstrated *via* ^{1}H NMR analysis that at 30 °C, the equilibrium is on the side of the urea motive (81% urea), while at 80 °C the urea bond is cleaved completely.[273] The new equilibrium state was reached rapidly, as the NMR spectrum was recorded directly after the temperature was reached, and additional measurements demonstrated no change of the peak area ratio within an hour. However, the intolerance of isocyanates to moisture limits the applicability of the system drastically.

Carbene dimers are another candidate for a thermally triggered debonding. Bielawski and coworkers employed the dimerization for the preparation of polymers.[18] At ambient temperature, the equilibrium is almost completely shifted to the dimer side, whereas at 90 °C, approximately 30% is cleaved. The reaction can be cycled, however, carbenes are highly reactive species and not stable under atmospheric conditions. Exposure to oxygen leads to an irreversible formation of a cyclic urea moiety.

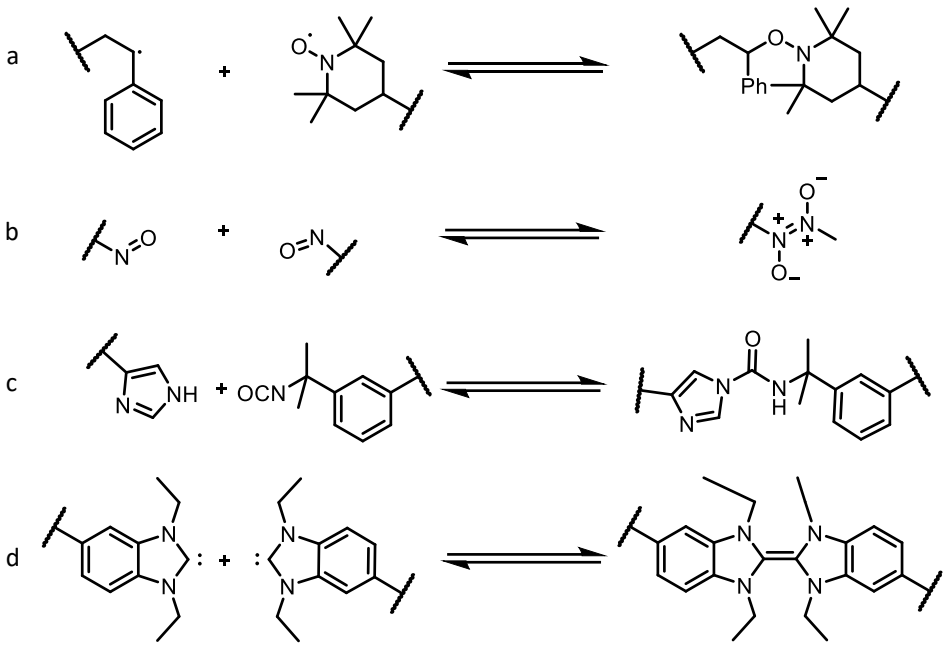

Scheme 26 Selection of thermodegradable moieties. (a) Alkoxyamines, (b) nitroso dimers, (c) reaction of isocyanates with imidazoles and (d) carbene dimerization.

2.4 Photochemically Triggered Debonding on Demand

A different method to induce debonding on demand is *via* a photochemical stimulus. A broad variety of moieties are reported in the literature today that undergo a cleavage when irradiated at a specific wavelength. As a detailed discussion would exceed the scope of the present thesis, the reader is kindly referred to the literature for in-depth information.[233, 274]

The photo-degradable motives can be subdivided by their structure into arylcarbonylmethyl,[275, 276] nitroaryl,[277] coumarin,[278] arylmethyl[279] and metal-containing[280] moieties. Within those classes, *o*-nitrobenzyl, *p*-hydroxyphenacyl and coumarin-4-yl-methyl motives are the most frequently employed groups.

O-nitrobenzyl (*o*-NB) based systems were employed as a photodegradable motive for the first time in 1970.[281] The mechanism of the decomposition is depicted in Scheme 27. Upon UV irradiation the photoisomerization of *o*-NB esters yields the corresponding *o*-nitrosobenzaldehyde and a carboxylic acid. If a carbamate instead of an esters functionality is present, the molecule further decomposes into the amine under release of CO_2.

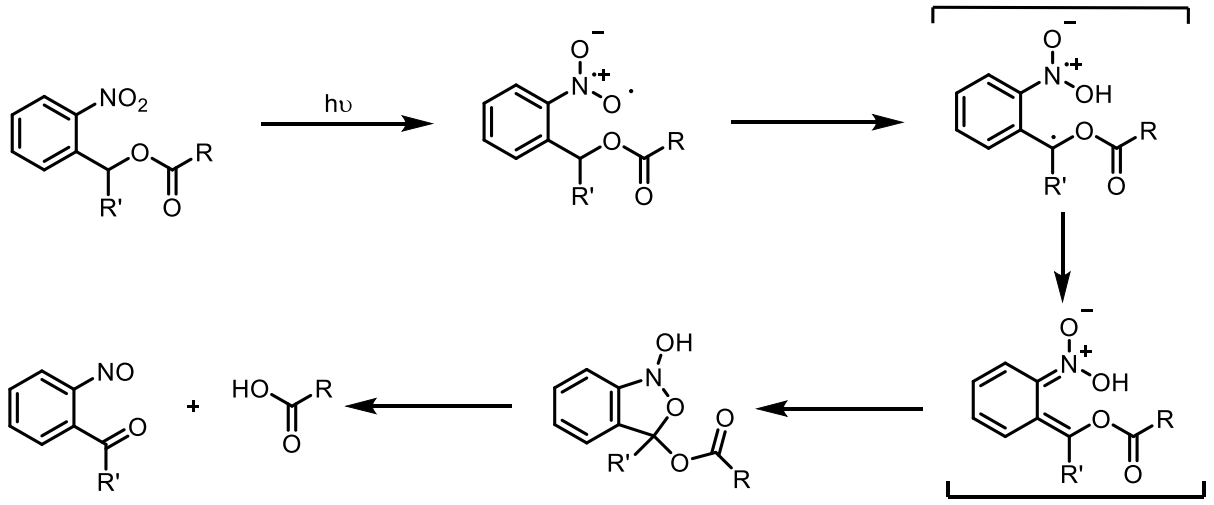

Scheme 27 Mechanism of the photo-triggered decomposition of *o*-nitrobenzyl moieties.

Among other applications, *o*-NBs were employed for the preparation of photodegradable polymer networks based on epoxides.[282] In their study, Radl et al. prepared bifunctional epoxy-based monomers including *o*-NB ester groups. After a thermally induced polymerization, the material was irradiated with UV light, whereupon the polymer degrades. Moreover, the moiety has been utilized for the wavelength-dependent degradation of hydrogels for the release of dyes, proteins, or other bioactive molecules.[283, 284]

P-hydroxyphenacyl (*p*-HP) units are promising alternatives to the *o*-NBs, as a straightforward synthetic route from readily available *p*-hydroxyacetophenone can be employed to prepare the protected compounds. The derivatives are usually soluble in aqueous media which is beneficial for biological applications. The main by-product, *p*-hydroxyphenylacetic acid, is water-soluble and non-toxic in contrast to the products formed by the photodegradation of nitrobenzyl derivatives. Moreover, the UV absorption of p-hydroxyphenyl acetic acid is blue-shifted in comparison to that of the precursor. Therefore, if the irradiation wavelength is properly chosen, the product of the irradiation does not interfere with light absorption, allowing quantitative conversion. The mechanism of the photodegradation as suggested by Wirz and co-workers is depicted in Scheme 28.

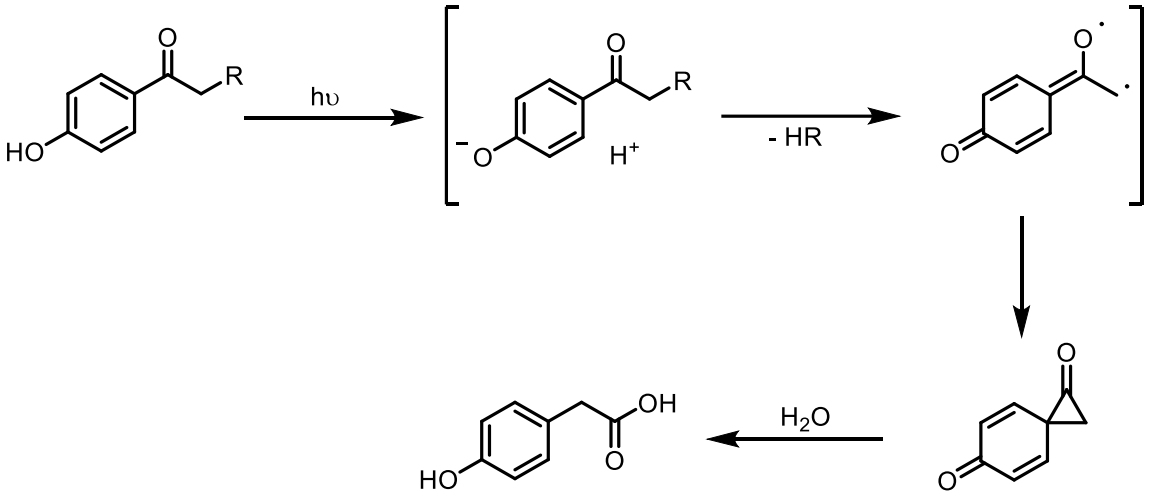

Scheme 28 Proposed mechanism for the photocleavage of *p*-hydroxyphenacyl moieties.

Due to its good water solubility, the *p*-HP group is employed to release bioactive molecules, like ATP,[285] phosphate[286] and glutamate.[287] A drawback of the *p*-HP moiety is its low absorption coefficient at wavelengths above 320 nm.

Coumarin-4-yl-methyl (CM) motives were employed for the first time as a photoactivatable phosphate-releasing group by Givens et al.[288] Cleavage can also be induced in the visible region, and can be shifted further by the addition of certain substituents.[289] Substituents are also employed to regulate the hydrophilicity of the molecule and to enhance the quantum yield of the reaction.[290]

CM moieties can, for example, be employed to prepare photodegradable hydrogels.[291] Anseth and co-workers achieved hydrogel formation under aqueous conditions using a 4-armed PEG azide substituted tetra-coumarin for copper-catalyzed click chemistry with alkyne motives.

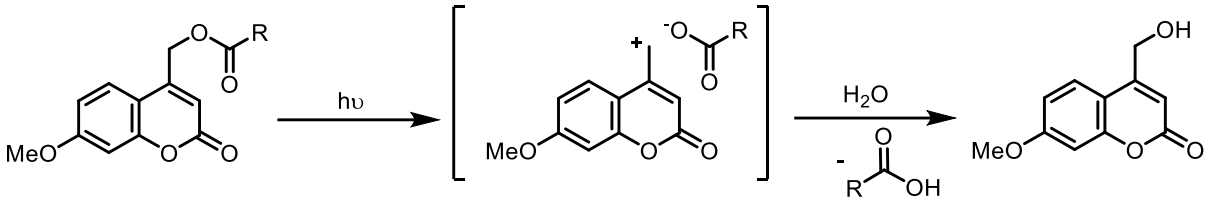

Scheme 29 Mechanism of the photo-triggered decomposition of coumarin-4-yl-methyl motives.

Rapid photodecomposition of the gels, to the point of reverse gelation, was detected at irradiation with 365 and 405 nm. The approach can be employed for biological applications, as the by-products are biologically inert. Photodegradable amphiphilic block copolymer nanocarriers based on CM moieties were prepared by Babin et al.[292] The nanocarrier was composed of poly(ethylene oxide) as hydrophilic and a poly-([7-(diethylamino)coumarin-4-yl]methyl methacrylate) as hydrophobic block. The degradation of the micelles was achieved under irradiation *via* a one-photon UV or two-photon NIR based process, which leads to the release of coumarin molecules and preloaded nil red from the hydrophobic micelle core.

2.5. Introduction to Disulfones

Disulfones can be seen as the completely oxidized form of disulfides, where both sulfur atoms bear two oxygen atoms. Their first mentioning in the literature goes back to 1899 when disulfones were prepared by Kohler and MacDonald.[293] Today, disulfones are used in several applications, such as electrolytes for batteries,[294] epoxy resins[295] and gas generation suppression.[296]

Disulfones can be prepared *via* different routes. One way is to use a sulfonyl chloride and sodium sulfinate.[297] Yields are usually low and protic, aqueous media are required for the reaction to take place. Other possibilities are the reduction of sulfonyl chloride using alkali metals,[298] copper,[299] or iodine.[300] However, side products are prepared in high quantities and only symmetric disulfones can be obtained. In addition, the oxidation of sulphinic acid with permanganate,[301] thallium(III),[302] *N*-chlorosuccinimide[303] or cobalt(III)[304] leads to the formation of disulfones. It is also possible to oxidize starting materials, already including the S-S bond, using hydrogen peroxide[305] or peroxy acids.[306] However, all these methods produce disulfones in poor yields.

One way to obtain high degrees of conversion and also asymmetrical disulfones is the reaction of *N,N*'-disulfonyl hydrazines with nitric acid.[307] The starting material can be prepared using a stepwise conversion of hydrazine with two sulfonyl chlorides in good yields (refer to Scheme 30). Due to the harsh reaction conditions (nitric acid), not many functional groups can be employed in the disulfone, which impedes a post-modification.

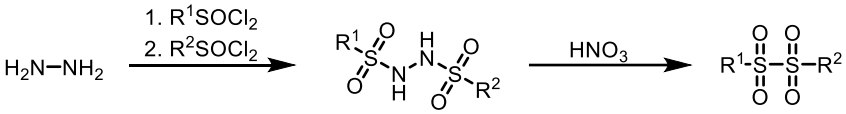

Scheme 30 Preparation of asymmetrical disulfones using hydrazine and nitric acid.

A facile way to prepare disulfones bearing various functional groups was found by Liu und Zhang.[308] The authors employed samarium metal for a selective reduction of arene sulfonyl chlorides to disulfones, thiosulfonates are disulfides under temperature control. Depending on the reaction temperature and the amount of samarium, diaryl disulfones, diaryl thiosulfonates or diaryl disulfides can be prepared (see Scheme 31). The substituents on the arene sulfonyl chloride influence the reaction. It was found that electron-withdrawing groups induce the reduction to a higher extent than electron donating groups. For example, when a nitro substituent is employed, which is a strong electron-withdrawing group, the reduction

cannot be stopped at the disulfone stage. Hence, only the thiosulfonates and the disulfide can be obtained with a nitro substituent on the arene sulfonyl chloride.

Disulfones are highly reactive towards nucleophilic substitution. As demonstrated by Kice and coworkers, various nucleophiles, like primary or secondary amines, azids, acetate and hydroxide ions can be employed to cleave the S-S bond of the disulfone *via* a nucleophilic substitution reaction.[309, 310] As studies revealed, nucleophilic substituents using primary and secondary amines have the highest reaction rates.[311, 312]

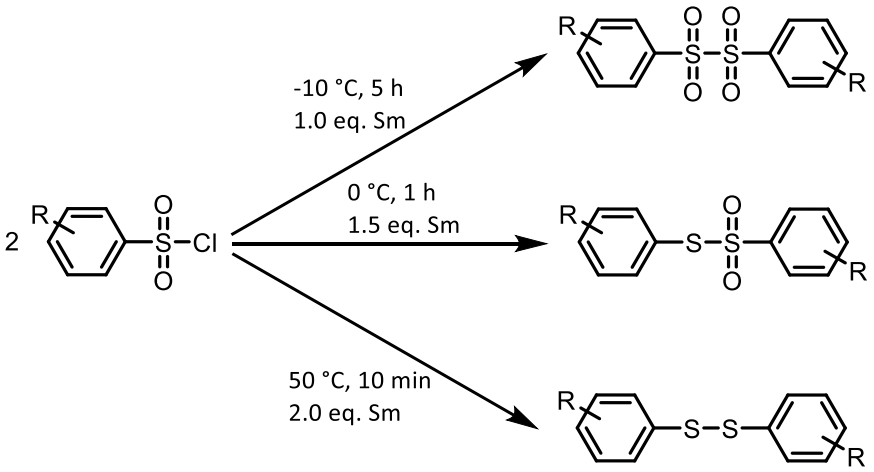

Scheme 31 Schematic display of the selective preparation of diaryl disulfones, diaryl thiosulfonates or diaryl disulfides from sulfonyl chlorides, depending on the reaction temperature and the amount of samarium.

3

Debonding on Demand for Dental Adhesive

3.1 Motivation and Monomer Design

As stated in the theoretical part of the thesis (see Section 2.2.3), dental adhesives usually consist – among other components - of a methacrylate-based monomer system, which is cured *via* a light-induced FRP (refer to Section 2.1.3 for more information). Since the human joint is able to generate high forces, a strong and permanent adhesion can only be achieved by a covalent bonding motive. A major drawback of covalent bonding is its commonly irreversible nature. Hence, if the removal of the dental material becomes necessary, high forces are required to break the adhesion mechanically, resulting in a time-consuming work for the dentist and an increased risk of damage to the teeth. For example, nowadays, dentists remove artificial dental crowns by drilling a hole in the crown, followed by a subsequent mechanic destruction of the material. Afterward, the residual adhesive has to be ground off the teeth.

Therefore, the overall aim of the current work was to overcome this major drawback by developing an adhesive that shows strong adhesion, however, can easily be removed when a certain external stimulus is applied.[*] As human teeth are known to be poor heat conductors, heat can temporarily be applied in the oral cavity.[313] Therefore, heat was selected as the trigger of choice. In order for the system to be applicable in the desired context, several criteria have to be fulfilled that are listed in Figure 2.

[*] Parts from the current chapter are reproduced or adapted from **A. M. Schenzel**, C. Klein, K. Rist, N. Moszner and C. Barner-Kowollik, *Advanced Science* **2016**, *3*, 1500361, with permission from John Wiley and Sons. C. Klein helped with the rheological measurements. K. Rist carried out the pull-off tests. N. Moszner and C. Barner-Kowollik motivated and supervised the project as well as contributed to the scientific discussions.

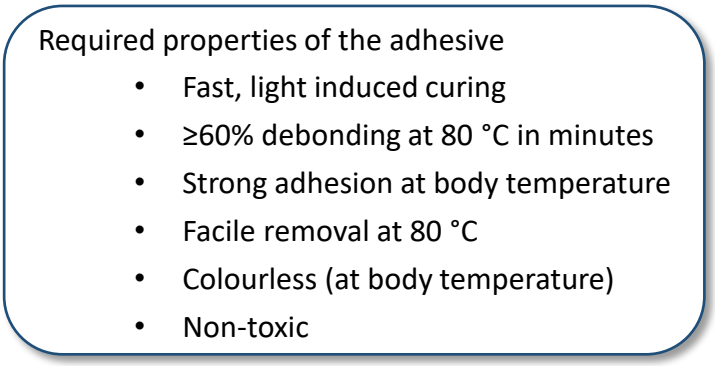

Figure 2 Required properties of the adhesive, in order to be applicable in the desired context.

For a fast and light-induced curing, the system has to contain a photoinitiator and a divinylic monomer, as crosslinking is required for the network formation. Usually, for a fast polymerization, a monomer system based on an acrylate is preferable. However, acrylates are toxic for the human body and can therefore not be employed in the desired context. As methacrylates are less toxic and can be polymerized in the required, short time interval, a monomer based on a dimethacrylate is synthesized. As a free radical polymerization lacks the possibility to incorporate a functional group into the backbone of the macromolecule, the thermodegradable moiety has to be included in the crosslinker. As thermodegradable group, a Hetero-Diels-Alder (HDA) moiety was selected. HDA systems are based on a temperature dependent equilibrium between a closed (HDA moiety) and an open (diene and dienophile) form (for a detailed explanation refer to Section 2.3.1). During the cycloaddition, covalent bonds are formed as is required for a strong adhesion. Since the temperature at which the system starts to decompose can be tuned by varying the diene and the dienophile, an HDA pair can be chosen that cleaves in the desired temperature range. Moreover, a system requiring a catalyst for the HDA reaction is necessary as the debonding should be irreversible or at least highly hindered in order to allow the dentist to remove the dental material in a facile fashion. In a catalyzed system, the reformation of the covalent bonds can be suppressed by removing the catalyst after the initial formation of the HDA moiety. The HDA pair of choice was a phosphoryl dithioester and a cyclopentadiene (Cp) moiety, which requires a Lewis acid (*e.g.* $ZnCl_2$) as a catalyst in order to undergo the cycloaddition reaction. To enhance the debonding probability at elevated temperature, two HDA moieties were incorporated in one dimethacrylate crosslinker, as the cleavage of one moiety would already lead to the breakage of the specific crosslink. In addition, the formation of the highly colored dithioester upon heating leads to a simple visual inspection system for the release of the adhesive. Scheme 32 summarizes the general concept.

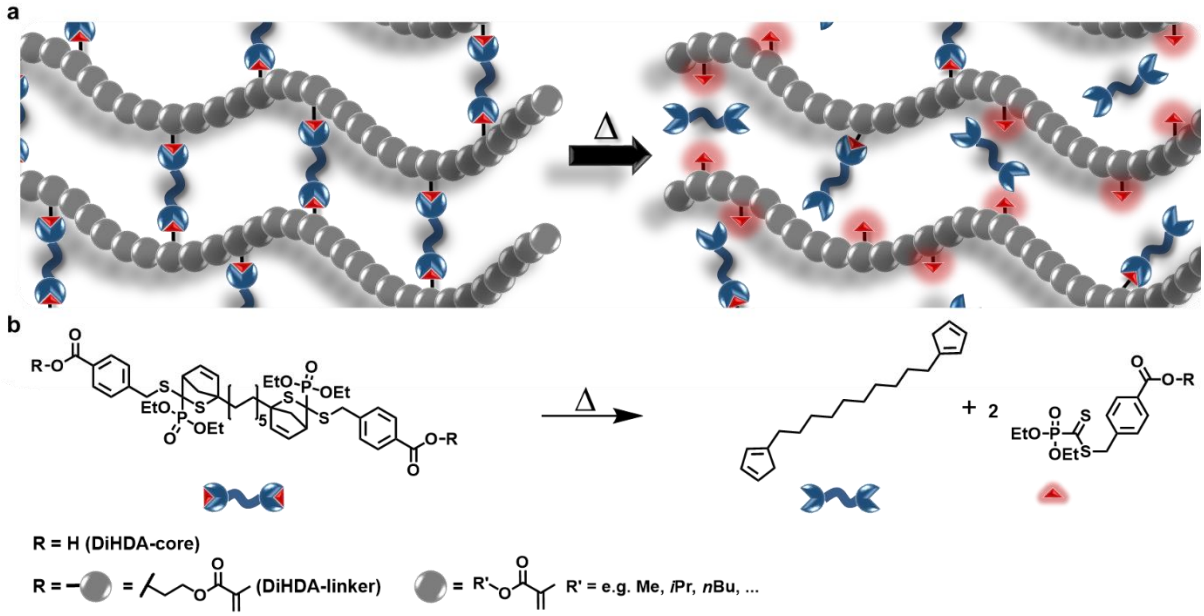

Scheme 32 (a) Schematic display of the degradation of the cured adhesive. (b) Display of the retro HDA reaction occurring upon thermal impact, as well as the structures of the monomer (DiHDA-linker) and a monomer-free system (DiHDA-core) used for the molecular analysis in order to avoid any self-initiation. Any methacrylate can be used as co-monomer if necessary.[314]

Therefore, the first task was the preparation of the thermodegradable monomer (DiHDA-linker). The synthetic procedure is depicted in Scheme 33. For a detailed description of the preparation, the reader is kindly referred to Section 7.3.1. In an initial step, the dithioester species (PDT) was prepared *via* a literature known protocol,[315] followed by a Steglich esterification with HEMA to yield a methacrylate containing phosphoryl dithioester moiety (MA-PDT). As cyclopentadiene is known to dimerize due to a Diels-Alder reaction (described in detail in Section 2.3.1), it was expected that a short DiCp-linker could not be prepared in sufficient purity and could not be stored over a long period of time. However, the first-time preparation of short a DiCp-linker could be achieved by a nucleophilic substitution reaction of 1,10-dibromodecane using NaCp. The critical parameter to prevent dimerization during reaction and purification is the temperature, which should not exceed 25 °C. Tests on the stability towards dimerization showed that even slightly elevated temperatures of 35 °C led to a partial dimerization. In a concentrated form, a slow dimerization is also detected at temperatures below 25 °C, which impedes storages. However, the prepared DiCp-linker crystallizes at temperatures below 0 °C and can, therefore, be stored in the freezer for months as no dimerization could be observed in the solid state during that period of time.

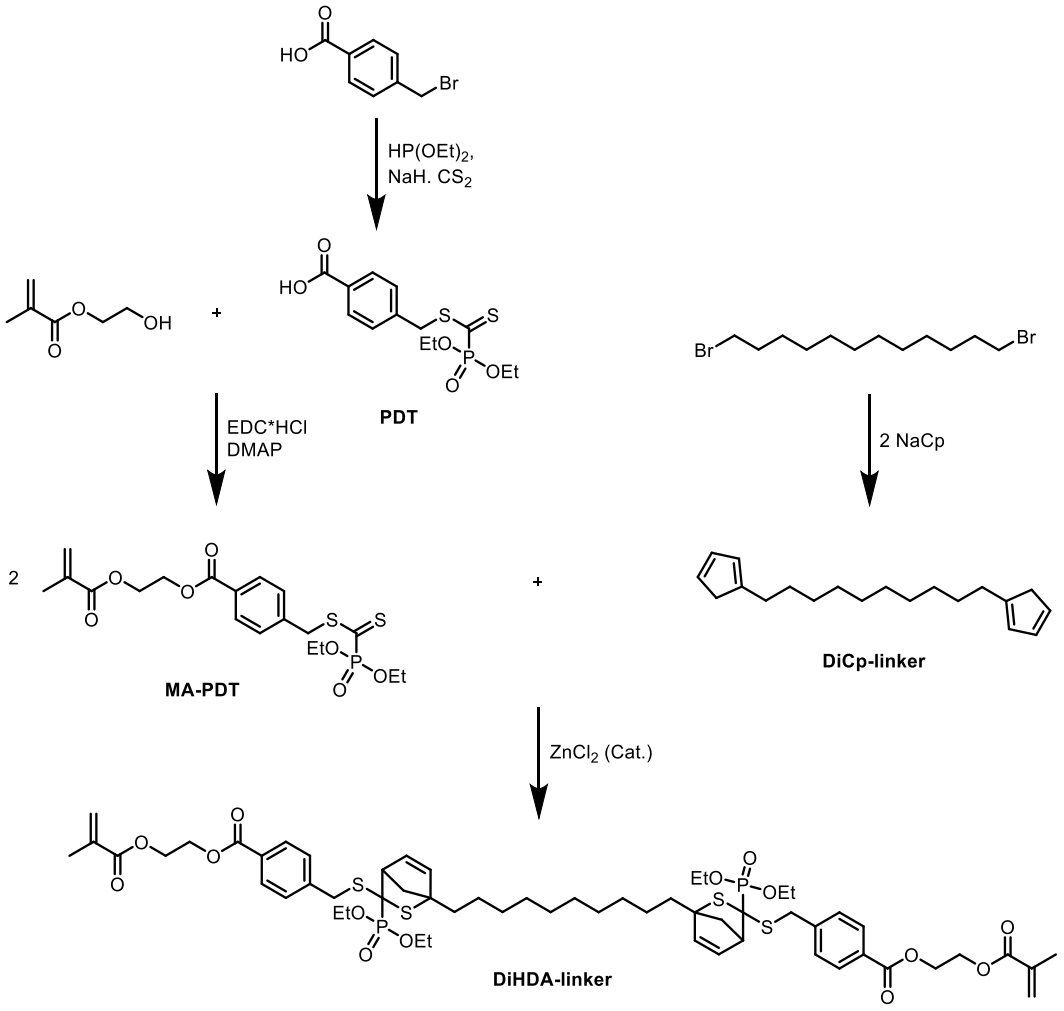

Scheme 33 Synthetic protocol for the preparation of the DiHDA-linker. The prepared phosphoryl dithioester (PDT) is reacted with HEMA to yield the methacrylate containing PDT (MA-PDT). MA-PDT and a previously prepared DiCp-linker are employed to synthesize the desired crosslinker containing two HDA moieties (DiHDA-linker).

In a final step, the MA-PDT and the DiCp-linker were reacted in an HDA reaction to obtain the desired monomer species bearing two HDA motives (DiHDA-linker). Quantitative conversion (99%) was achieved within 30 minutes. In order to remove the catalyst ($ZnCl_2$), the reaction mixture was washed with water. Analytic evidence for the synthesis of the DiHDA-linker can be found in Figure 3. A non-polymerizable species (DiHDA-core) was synthesized as well for solution studies in order to prevent self-initiation at elevated temperatures. Therefore, PDT was directly reacted with the DiCp-linker without the previous incorporation of the methacrylate species. ^{1}H NMR analysis and the date obtained by ESI-MS for the DiHDA-core are depicted in Figure 4. After the successful preparation of the DiHDA-linker and DiHDA-core, the molecular properties were extensively studied, which is subject to the next section.

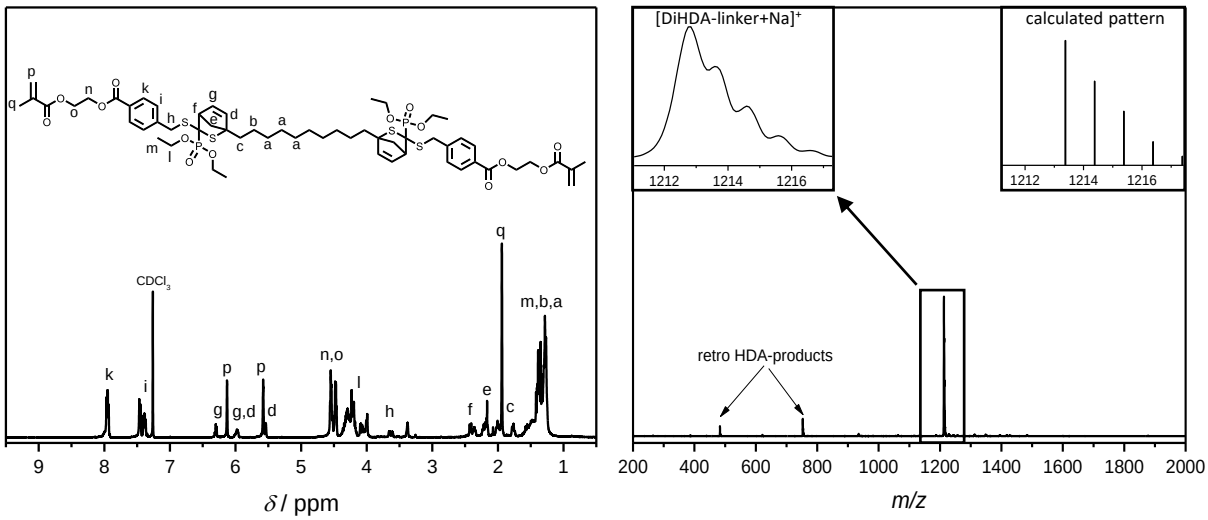

Figure 3 ^{1}H NMR and ESI-MS analysis of the DiHDA-linker. The retro HDA products are formed during the ionization process due to high temperatures (320 °C).

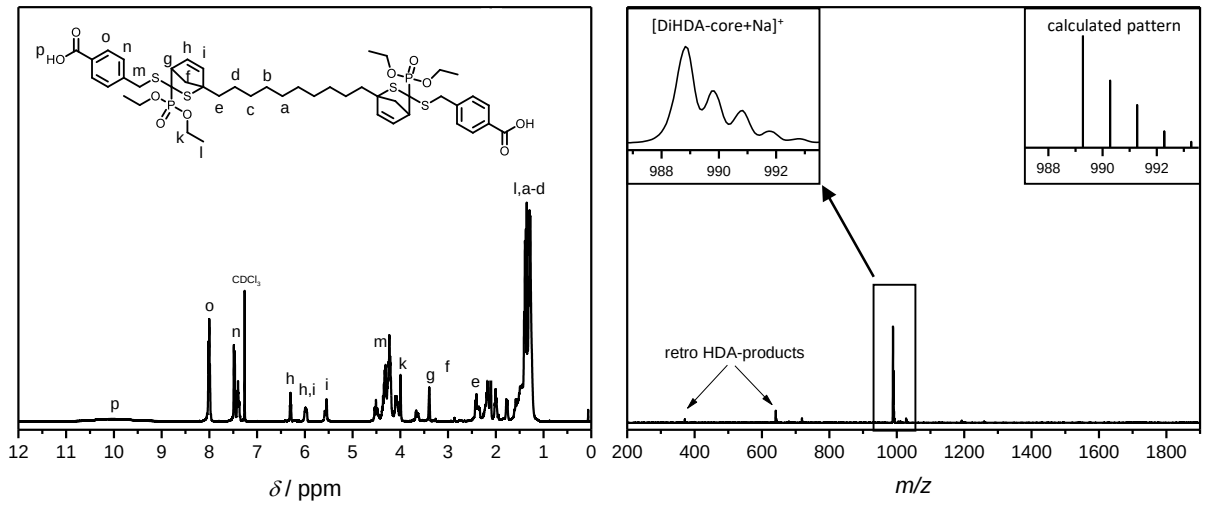

Figure 4 ^{1}H NMR and ESI-MS analysis of the DiHDA-core. The retro HDA products are formed during the ionization process due to high temperatures (320 °C).

3.2 Molecular analysis of the thermodegradability

Prior to the investigation of the mechanical properties of the adhesive, the HDA moiety had to be characterized in detail in order to unambiguously prove and quantify the debonding of the molecular system. In order to avoid any self-initiation, a monomer-free system (DiHDA-core, see Scheme 32) was used for the molecular analysis in solution and analyzed *via* (HT)-NMR and UV/Vis spectroscopy. The DiHDA-core should show the same behavior as the DiHDA-linker since the substitution in proximity to the HDA moiety is identical.

At first, ^{1}H NMR studies were carried out at different temperatures to demonstrate the cleavage of the HDA moiety. As depicted in Figure 5, the equilibrium is completely shifted to the side of the closed form (HDA-moiety) at temperatures below 25°C. When elevating the temperature, the concentration of the open form (PDT and DiCp-linker) steadily increases, until at 120 °C, the proton resonance for the HDA-moiety is undetectable, indicating a complete cleavage of the thermodegradable system.

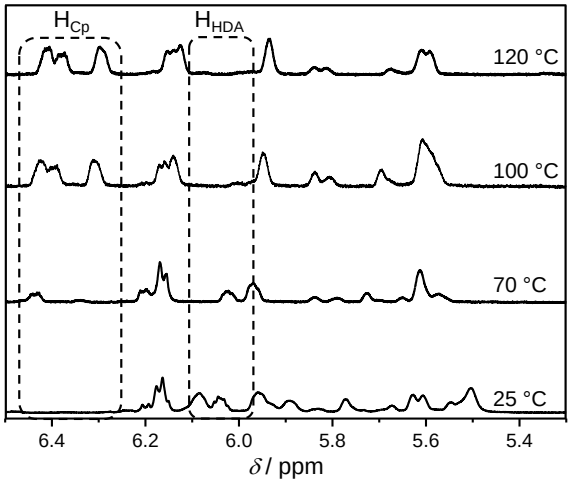

Figure 5 HT-NMR spectroscopic measurements of the DiHDA-core at 25, 700, 100, 120 °C (in toluene-d_8). At 25 °C only the proton resonances that can be assigned to the HDA moiety (H_{HDA}) are present, whereas at 120 °C only the proton resonances of the retro-HDA product (H_{Cp}) can be detected.

In order to further prove the debonding capacity of the molecular system UV/Vis spectroscopic analysis was carried out additionally. UV/Vis spectroscopy can readily be employed to visualize the bonding state of the system, since the dithioester (PDT) that is formed upon heating has a reddish color, due to the formed C=S double bond, which absorbs in the UV (330 nm) and the visible light range (535 nm). As shown in Figure 6a, the color change can readily be detected by the naked eye, demonstrating the self-reporting nature. Moreover, it makes the system highly interesting for a range of applications, since it gives a facile visible inspection possibility for the degree of debonding.

When UV/Vis spectra of a solution of the DiHDA-core are recorded at temperatures between 25 and 140 °C, the expected increase in absorption at 330 nm is clearly visible, which proves the debonding on demand behavior of the invented system (see Figure 6b). The absorbance at 535 nm increases as well, however, due to poor solubility of the DiHDA-core, the difference in absorption is lacking in significance. In order to evidence that the same behavior is present in a cured network, a network based on the DiHDA-linker is formed inside a UV/Vis cuvette.

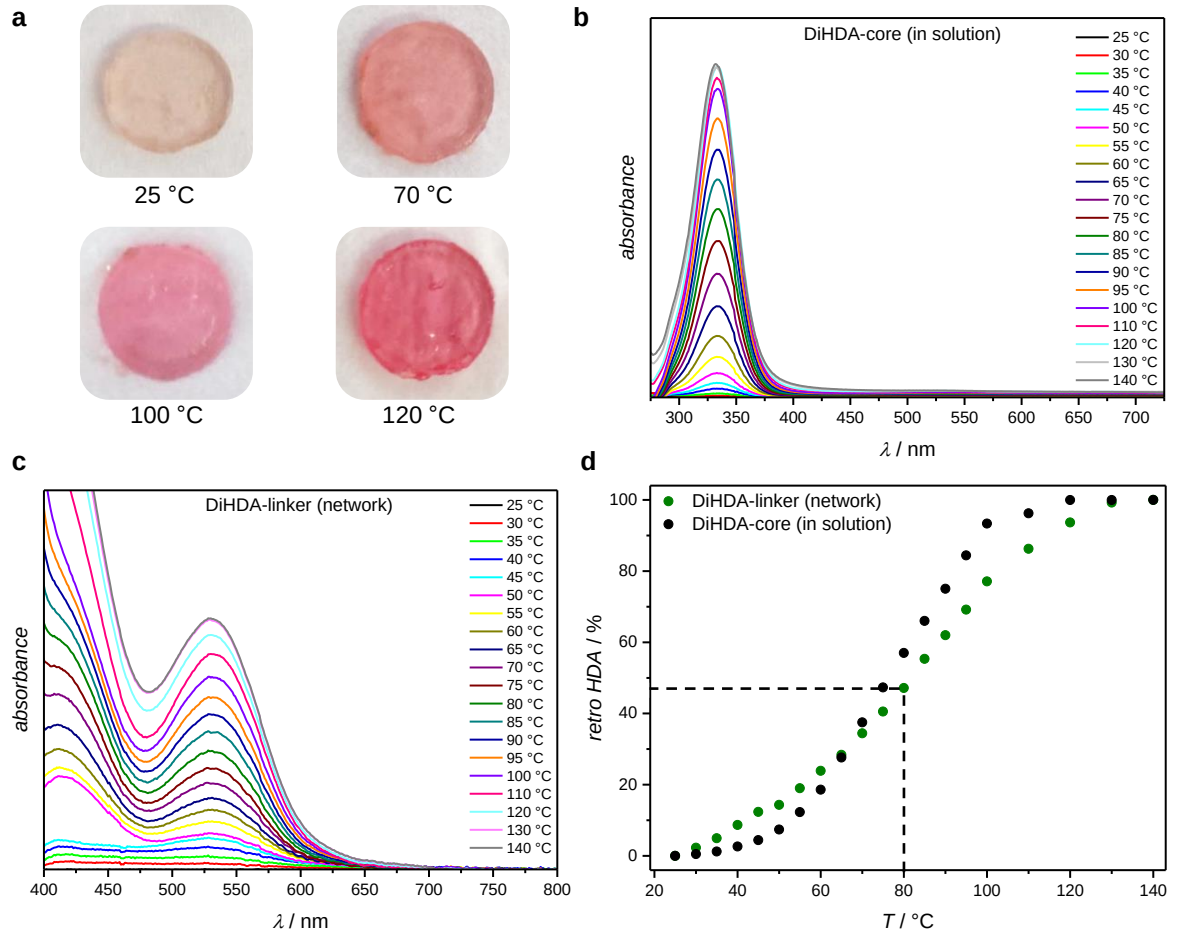

Figure 6 (a) Visible proof of the change in color upon heating to 25 (0%*), 70 (34%*), 100 (93%*) and 120 °C (99.9%*). (b) UV/Vis spectroscopic measurements of the DiHDA-core in DMSO (c = 10 mg·mL^{-1}, l = 10 mm).** (c) UV/Vis spectroscopic analysis of a cured polymer network of the DiHDA-linker (99.8 wt.% DiHDA-linker, 0.2 wt.% Ivocerin, l = 2 mm).** (d) Correlation of the intensities of the maxima at 330 nm (a) and 535 nm (b) at a given temperature to the degree of the retro HDA reaction. The absorption at 330 nm was chosen for the DiHDA-core, as the absorption at 535 nm was difficult to quantify, due to poor solubility. * Amount of retro HDA product. ** Between 25 and 140 °C.

Again, UV/Vis spectra are recorded at different temperatures between, 25 and 140 °C, demonstrating an increase in absorption in the designated area of the spectrum (535 nm, see Figure 6c), indicating that the retro HDA reaction also occurs inside a polymer network. Hence, the cleavage of the HDA-moieties and therefore the degradation of the crosslinks inside the cured adhesive could be proven on a molecular level.

As the start- (no absorption, 99.9% HDA moiety) and end-temperature (maximum absorption, 0% HDA moiety) of the debonding reaction could be determined *via* NMR and UV/Vis spectroscopy, the degree of retro HDA reaction can be calculated directly at any given temperature. To meet the criteria for the intended dental adhesive more than 60% debonding has to be present at 80 °C. As can be seen in Figure 6d, about 48% of the HDA moieties inside the polymer network are cleaved at 80 °C. However, since two HDA moieties are present in each

crosslinker, and the cleavage of one unit is sufficient for the breakage of the crosslink, the likelihood for a crosslink to break is higher. The probability can be determined by calculating the amount of crosslinks that are not debonded at 80 °C. That chance is 27% (0.52^2). Therefore, the probability of the breakage of a crosslink is not 48, but 73%, which fulfills the criteria for the intended thermodegradable adhesive.

When comparing the behaviors of the DiHDA-core in solution and the cured network of the DiHDA-linker during the UV/Vis spectroscopic analysis both system show similar performance (see Figure 6d). However, for temperatures below 65 °C, a higher degree of debonding is visible for the network system, which can be explained by a higher entropy release *via* a detachment within a network, compared to a debonding in a molecule in solution. The entropic effect on the temperature dependent cleaving behavior of macromolecular systems is subject to a series of previous studies carried out by our research group.[268-270]

Since the kinetics of the degradation of the system is a crucial factor for the application as dental adhesive, the time required for the debonding was determined as well. Most reported systems require several hours or days to fully degrade, limiting their applicability.[10-12] In contrast, the retro HDA reaction is known to be quite rapid. Therefore, this limit should be overcome with the present system. To demonstrate fast debonding kinetics, a cured network of the DiHDA-linker was mounted into the UV/Vis spectroscope that was preheated to 100 °C (upper limit of the instrument), and the time needed for the retro HDA reaction was determined. As can be seen in Figure 7, the debonding reaction takes place in less than three minutes, demonstrating that the chosen system can be applied in the context of dental adhesives.

The rapid debonding on demand of the HDA system could, therefore, be evidenced unambiguously on a molecular scale. In a next step, the effect of the degradation on the mechanical properties of the cured adhesive upon heating had to be investigated in detail.

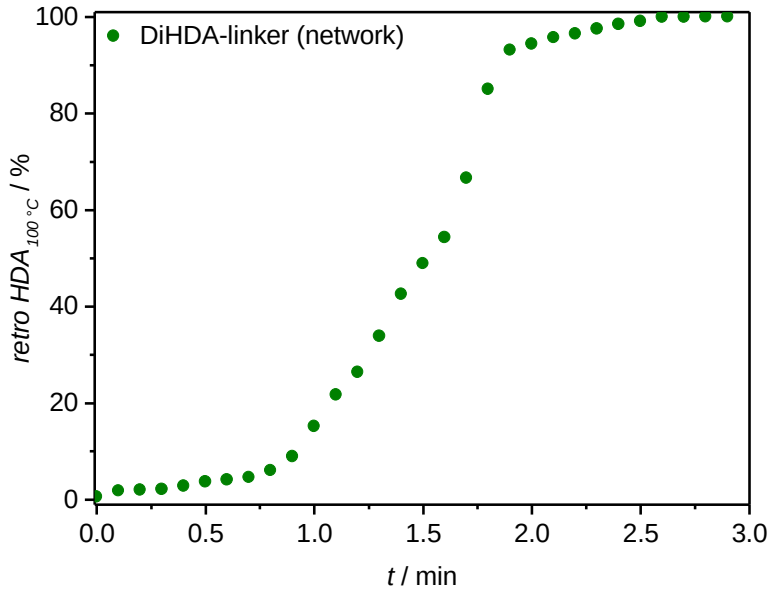

Figure 7 Kinetic investigation of the debonding reaction of a cured network of the DiHDA-linker (99.8% DiHDA-linker + 0.2% Ivocerin) at 100 °C (Absorption at 535 nm, l = 2 mm).

3.3 Mechanical properties of the invented adhesive

A successful degradation on the molecular scale of a polymer network has to lead to a clear decrease in mechanical stability. At the same time, the same effect should be absent in a reference system including a non-cleavable linker.

Therefore, rheology was applied to investigate the mechanical behavior of a DiHDA-linker network. A detailed description of the employed rheometer can be found in the experimental section of the present thesis (Section 7.2). For the measurements, rectangular specimen, so-called “bones” were prepared by curing the monomer mixture inside a metal molding (see Figure 8). A bone (length: 25 mm, width: 5 mm, diameter: 1 mm) was then mounted into the rheometer and an axial force of 0.3 N, an excitation frequency of 1 Hz and a deformation of 0.1% in a temperature range of 25 to 130 °C (heating rate: 1.5 $K \cdot min^{-1}$) were applied. When comparing the mechanical properties of a bone made of 99.8 wt.% DiHDA-linker + 0.2 wt.% Ivocerin® with a bone comprised of a typical, non-degradable polymer network (99.8 wt.% urethane dimethacrylate (UDMA) + 0.2 wt.% Ivocerin®) the differences in mechanical stability are clearly visible. Figure 9a and b show the results of the rheological measurements of the two networks. The storage modulus (G’) is, by definition, the elastic contribution of the stress response of the sample and therefore correlated to the stability of the sample, meaning if G’ decreases the sample loses its stability. The loss modulus (G’’) is defined as a measure of the

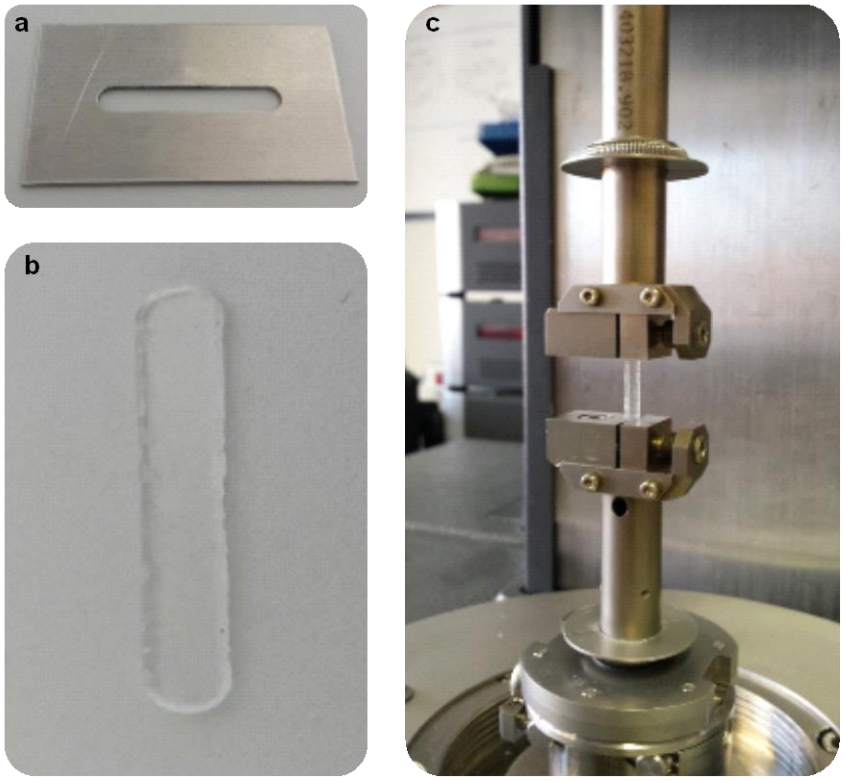

Figure 8 (a) Used setup for the preparation of the bones employed in the rheological measurements. (b) Display of a cured bone of 99.8 wt.% DiHDA-linker and 0.2 wt% Ivocerin® (length: 25 mm, width: 5 mm, diameter: 1 mm). (c) Instrumental setup. The specimen is mounted into the rheometer and an axial force is applied at temperatures between 25 and 130 °C).

energy dissipated in a material in which a deformation has been imposed. Moreover, tanδ is calculated by G''/G'. The maximum of tanδ indicates the glass transition temperature (T_G) of the tested specimen at low frequencies. As can be seen in Figure 9c, the storage modulus of the non-degradable reference network (UDMA) is only slightly affected by a temperature change ($1.1 \cdot 10^9$ Pa at 25 °C to $3.8 \cdot 10^8$ Pa at 120 °C). In contrast, a drastic loss in G' by over two orders of magnitude is determined for the DiHDA-linker network ($8.5 \cdot 10^8$ Pa at 25 °C to $5.5 \cdot 10^6$ Pa at 120 °C). Hence, the DiHDA-linker network shows a substantial loss in the mechanical stability of the network, demonstrating that the invented system can be employed as a thermodegradable adhesive as significant degradation takes place upon heating.

The HDA system, however, offers an additional advantage as the temperature at which G' starts to decrease drastically can be fine-tuned by employing a co-monomer. Therefore, the system can be adapted to various applicational requirements in a facile fashion. In the example shown in Figure 9d, the DiHDA-linker is copolymerized with isobornyl methacrylate (iBoMA), which has a T_G of 110 °C as a homopolymer.[316] A copolymerization should, therefore, lead to an increase of the T_G for the copolymer network.

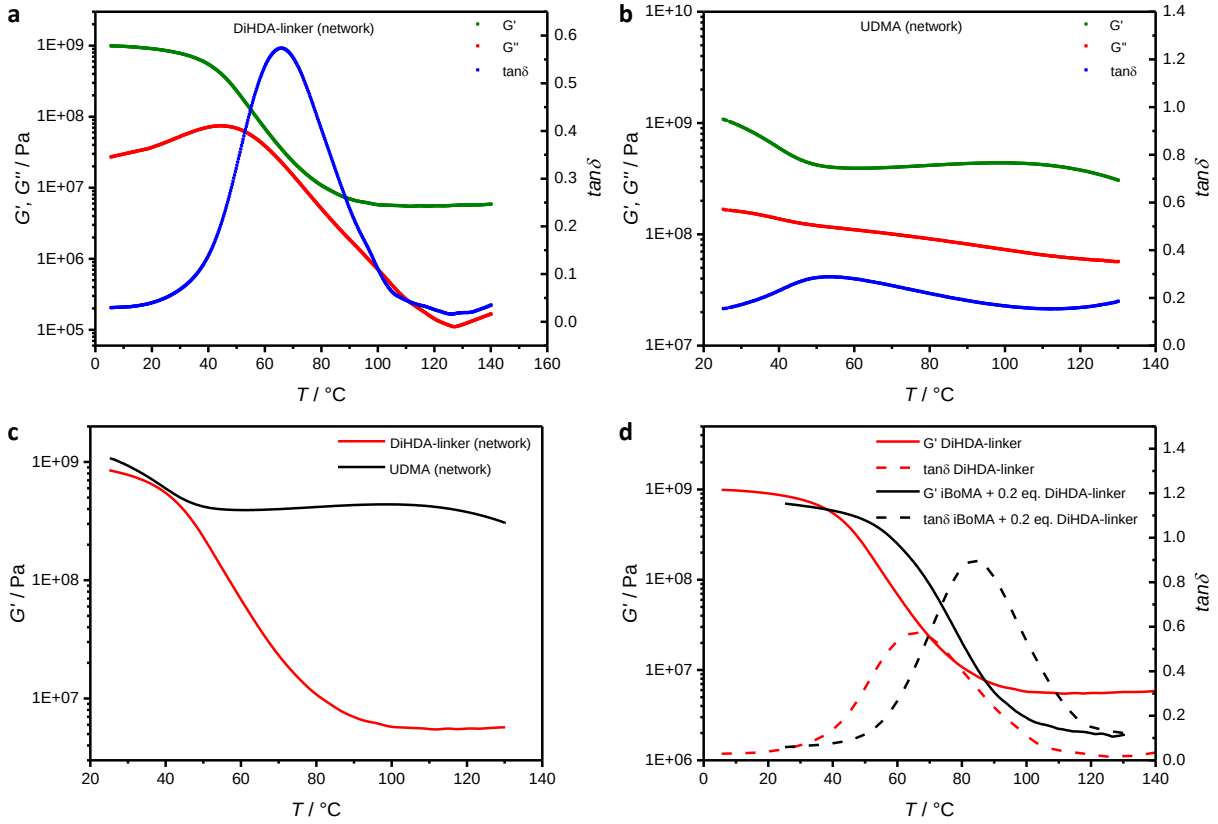

Figure 9 (a) Rheological analysis of a pure HDA linker network. Displayed are the storage modulus (G'), the loss modulus (G'') and tanδ (G''/G'). (b) Rheological analysis of a network based on a non-degradable dimethacrylate (pure UDMA). Displayed are G', G'' and tanδ. (c) Comparison of the storage moduli (G') of (a) and (b) for the temperature range of 25 °C to 130 °C. (d) Comparison of G' and tanδ of a degradable network based on the pure DiHDA-linker with a degradable co-polymer network (iBoMA + 0.2 eq. DiHDA-linker) for the temperature range of 20 to 130 °C. A detailed rheological analysis of the co-polymer network can be found in the Appendix (Figure 24 and Figure 25). Measurements are conducted using the following conditions: axial force = 0.3 N, frequency = 1.0 Hz and deformation = 0.1%.

As expected, the glass transition temperature increases from 67 °C for the pure DiHDA-linker network to 85 °C for the copolymer network (iBoMA + 0.2 eq. DiHDA-linker).

The substantial loss in mechanic stability can also be detected by the naked eye. As displayed in Figure 10, the thermodegradable network is rigid and colorless at ambient temperature. However, when the network is heated to 100 °C, the sample becomes highly colored and can easily be bend or cut in half.

Figure 10 Display of a degradable network based on 99.8 wt.% DiHDA-linker + 0.2 wt.% Ivocerin®. At 25 °C, the network is rigid and not bendable (i). At 100 °C, the network can easily be bend by using tweezers (ii) and cut into pieces (iii).

As the thermodegradability of the invented system was proven without a doubt on a molecular level and *via* mechanical studies, final adhesion test were conducted to evidence the practical applicability.

3.4 Adhesion and Pull-off Tests

To demonstrate the applicability as dental adhesive implant abutments were cemented to artificial dental crowns and the pull-off forces were measured at 23 and 80 °C. The employed dental parts, as well as the experimental setup for the pull-off tests, are displayed in Figure 11. A more detailed description of the test system, the cementation as well as the experimental setup and procedure can be found in the experimental section of the thesis (Section 7.2).

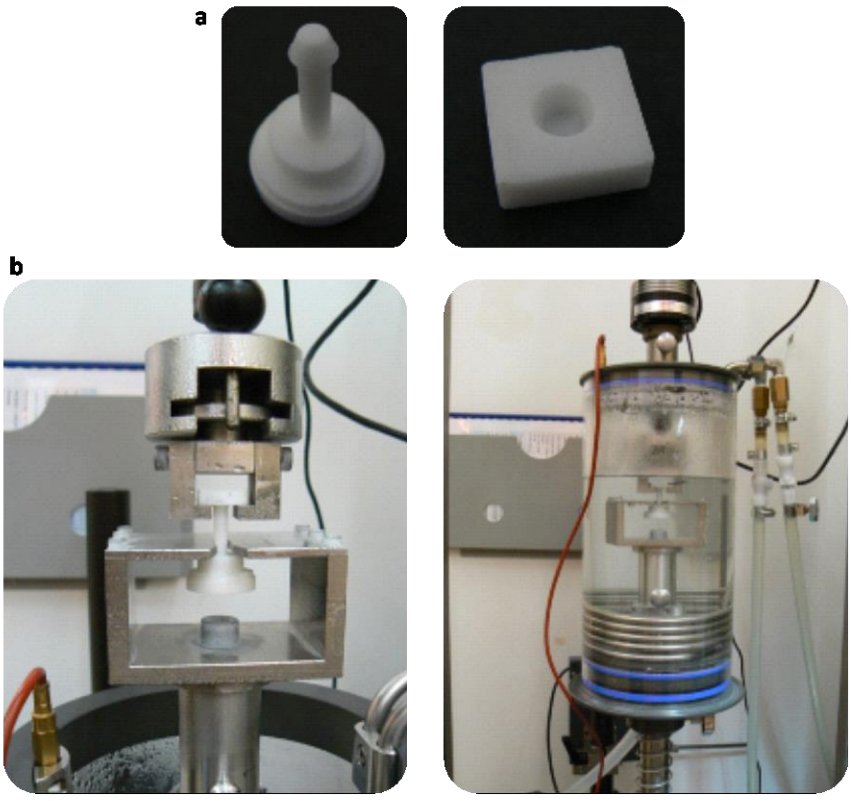

Figure 11 (a) Display of the test abutment and artificial dental crown employed in the pull-off tests. (b) Display of the employed tensile testing machine (Zwick-Roell Z010). A heatable water bath was used in order to ensure the temperature control.

In summary, two different adhesives, one containing a non-degradable dimethacrylate crosslinker (0.2 eq. bisGMA), and one including 0.2 eq. of the DiHDA-linker were used for the cementation of the dental parts. Afterwards, the test specimens were stored at 23 °C for 3 days to ensure complete curing. The samples were randomly divided into two groups and

mounted into the tensile testing device. Subsequently, measurements were conducted either at 23 or at 80 °C. To ensure a defined temperature, the setup was tempered using a water bath. In Figure 12a, the force-elongation graphs of the four different groups are displayed that were obtained when the crowns were pulled off the abutments.

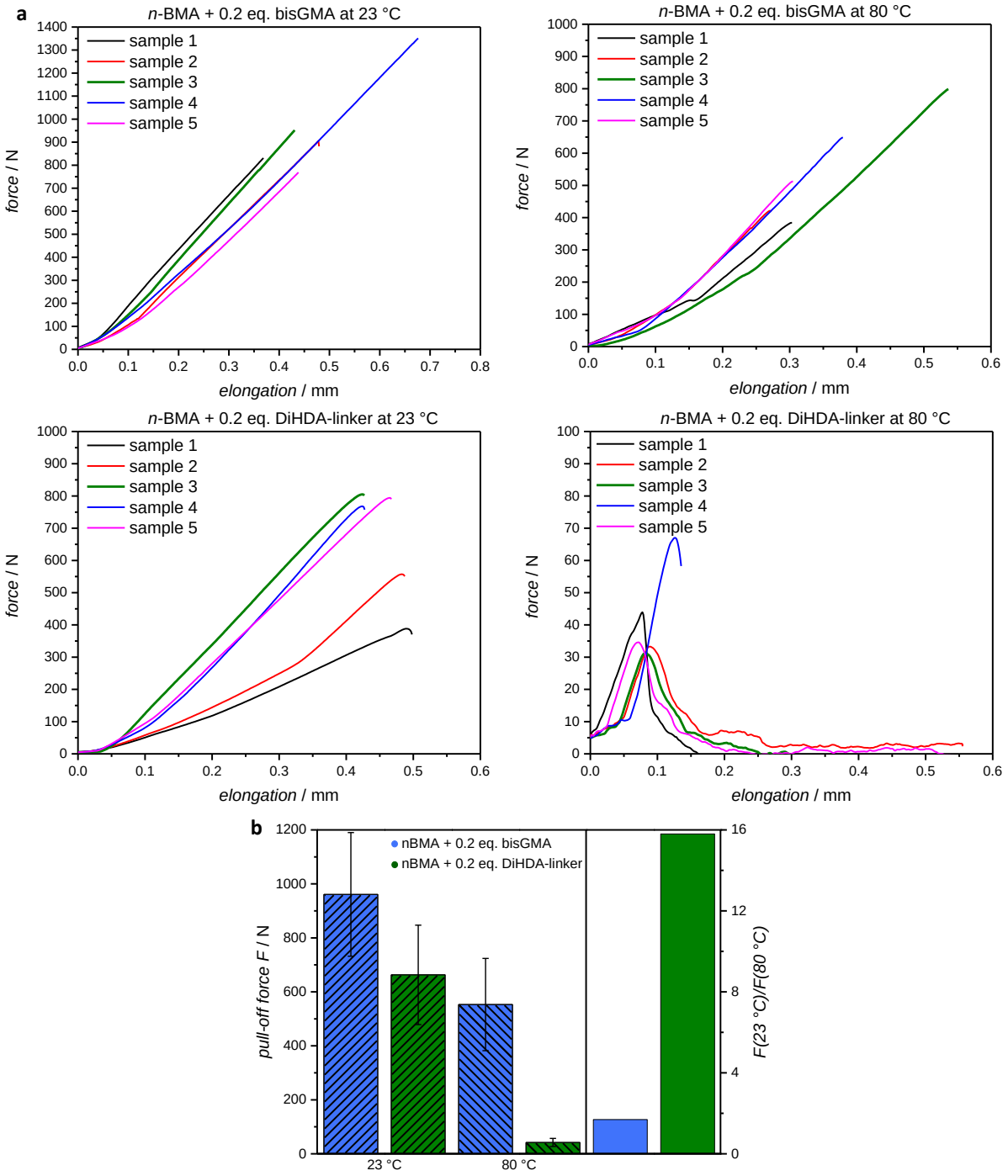

Figure 12 (a) Force-elongation graphs of the performed pull-off tests of a dental model adhesive co-monomer system (*n*BMA + 0.2 eq. bisGMA*) and a mixture including the designed DiHDA-linker (*n*BMA + 0.2 eq. DiHDA-linker) at 23 °C and 80 °C. (b) Summary of the obtained values including the calculated differences between the ratios of the pull-off forces at 23 °C and 80 °C for both systems. * Bisphenol-A-glycidyl methacrylate. A table summarizing the obtained values can be found in the Appendix (Table 4).

Both systems show strong adhesion at 23 °C (pull-off forces: on average 962 N for the bisGMA system and 663 N for the DiHDA-linker adhesive). However, a significant difference in the pull-off forces is visible upon heating to 80 °C. As expected, the non-degradable adhesive shows only a slight decrease in the pull-off force to 553 N, which is equivalent to a loss of 42%. On the other hand, the adhesive based on the thermodegradable DiHDA-linker demonstrates a drastic loss in adhesion strength from 663 N to 42 N, which results in a loss of 94% for the adhesion stability. To clarify the drastic difference between the two systems, the ratios of the pull-off forces at 23 and 80 °C can be compared (see right-hand side of Figure12b). The thermodegradable adhesive thus shows the desired effect, making it an interesting system for the application as a dental adhesive.

3.5 Conclusion and Further Remarks

The presented thermodegradable adhesive is – to the best of our knowledge – a major improvement over the current state of the art, since it is the only adhesive known that combines a ready removability at slightly elevated temperatures with a strong adhesion at ambient temperature.

The properties of the DiHDA-linker as well as the adhesion were carefully analyzed from molecular studies of the HDA system to the investigation of the mechanical properties and final adhesion and pull-off tests, clearly demonstrating the thermodegradability. In summary, the invented adhesive meets (most of) the criteria introduced in the motivational section (see Section 3.1). The system can be cured *via* a light-induced reaction, as Ivocerin® decomposes rapidly under blue light irradiation. Moreover, the curing takes place in a fast manner, since a methacrylate based monomer (DiHDA-linker) is employed. Furthermore, the UV/Vis spectroscopic investigations demonstrate that the degradation takes place in less than three minutes and that 75% of the crosslinks are debonded at 80 °C, which also meets the criteria for the intended dental adhesive. Adhesion and pull-off tests additionally demonstrate the required strong adhesion at ambient temperature, combined with a drastic loss in adhesion stability at 80 °C (663 N at 23 °C compared to 42 N at 80 °C).

In terms of coloration, the thermodegradable adhesive is colorless at ambient temperature, as it is displayed in Figure 10. However, it has to be noted that it shows a slight reddish color at body temperature, which is the actual temperature of use. Hence, the HDA system had to be modified in order to be completely closed until 40 °C. The most facile way is to modify the

dithioester species in order to increase the temperature of decomposition. Therefore, two systems were prepared and tested for their degradation temperatures (see Scheme 34).

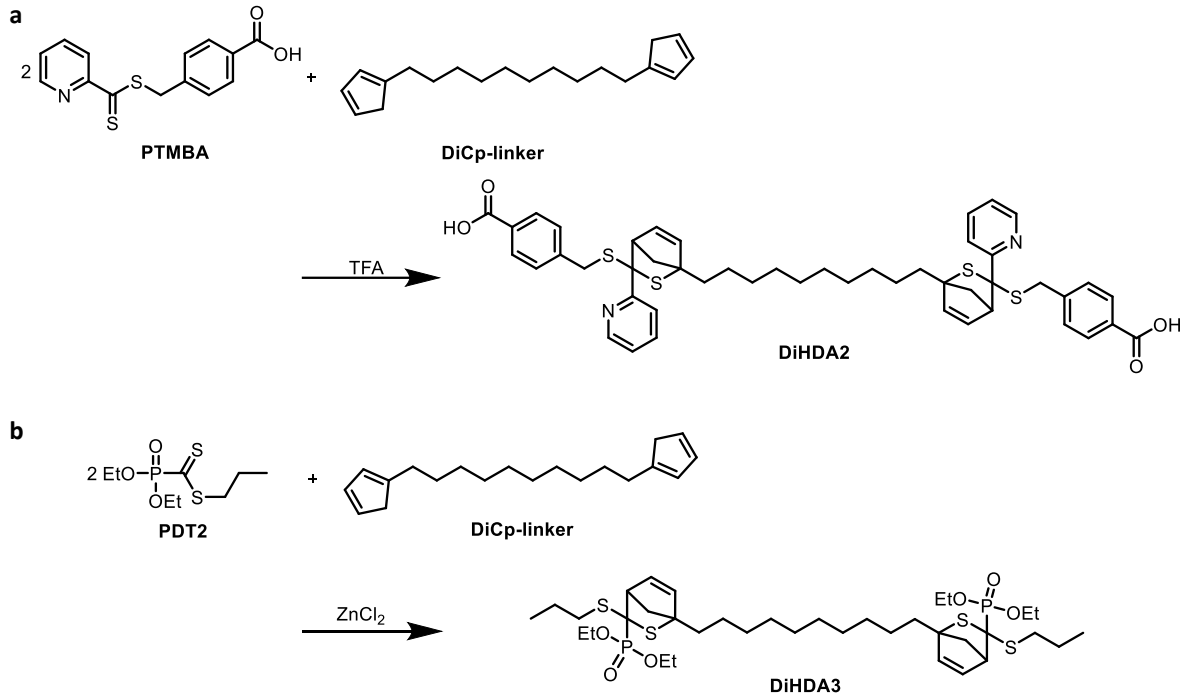

Scheme 34 Display of the additional HDA systems tested for their degradation temperatures. (a) Dithioester based on a pyridinyl moiety (DiHDA2). The HDA reaction is catalyzed by a strong acid (e.g. TFA). (b) Dithioester based on a phosphoryl moiety bearing an alkyl chain instead of the benzoic acid functionality (DiHDA3). The HDA reaction is catalyzed using $ZnCl_2$.

DiHDA2 is based on a pyridinyl moiety (PTMBA). For the HDA reaction with the DiCp-linker a strong acid (*e.g.* TFA) is required as catalyst (for the synthetic protocol see Section 7.3.1). Therefore, DiHDA2 could also be applied in the desired context. In order to assess at which temperature the system starts to open, UV/Vis spectroscopic measurements were carried out. As can be seen in Figure 13, DiHDA2 starts to debond at temperatures of about 30 °C according to the UV/Vis spectroscopic measurements, which is still 10 °C too low for the desired application. Moreover, the system tends to degrade under storage, even at 0 °C ruling out the application as a dental adhesive.

DiHDA3 is similar to the DiHDA-linker. It is also based on a phosphoryl dithioester. However, the benzoic acid moiety is replaced by an alkyl chain, which changes the electron density at the C=S double bond (refer to Section 7.3.1 for the detailed preparation procedure). A change in the electron density has an effect on the debonding temperature of the retro HDA reaction. As indicated in Figure 13, the onset of the retro reaction is shifted to higher temperatures. Until 40 °C, no decomposition can be observed, which meets with the intended colorlessness

at body temperature. In order to prepare a methacrylate based species, 2-bromoethyl methacrylate instead of 1-iodopropane could be used for the preparation of the dithioester. As the behavior of DiHDA3 should be very similar to the properties of the DiHDA-linker, a system based on DiHDA3 should meet all criteria required for the thermodegradable adhesive.

Once an adhesive based on the DiHDA3 motive is developed, the toxicity of the formulation has to be studied in detail. Unfortunately, those tests were not conducted until the day of the submission of the present thesis. Therefore, no statement can be made regarding the toxicity of the adhesive.

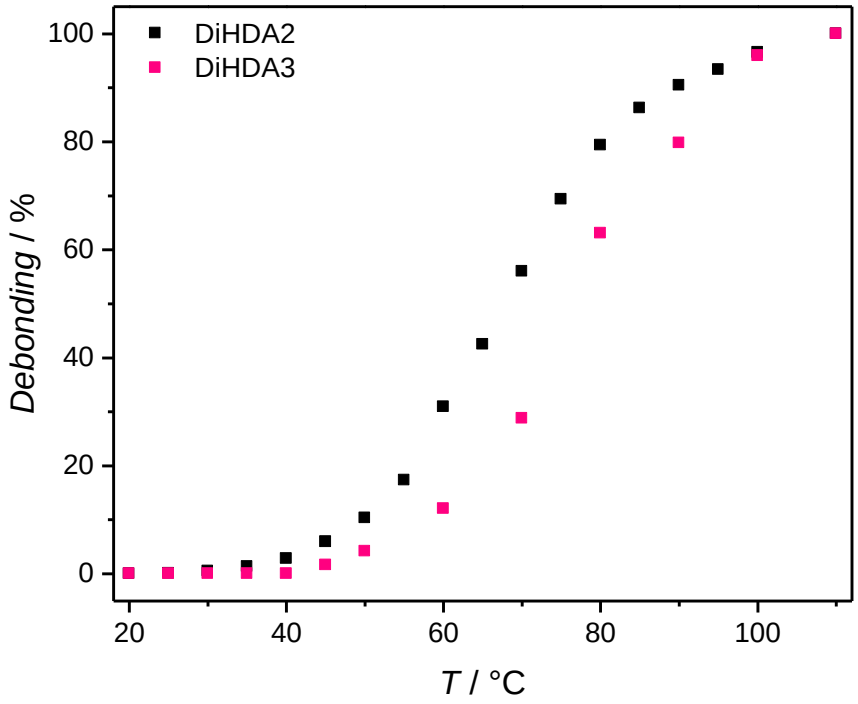

Figure 13 Correlation of the intensities of the absorption maxima (535 nm) of DiHDA2 and DiHDA3 at a given temperature to the extent of debonding.

4

Dynamic Covalent Polycarbonate Networks

4.1 Motivation and Monomer Design

The DoD system in the previous section of the present thesis demonstrates that thermodegradable polymer networks can be designed on the basis of HDA moieties. However, the degradability of the dental adhesive is limited due to the nature of the network formation, as only the crosslinks of a network prepared *via* free radical polymerization can be debonded using HDA systems. Thus, the smallest possible structure is a linear polymeric chain.

The effect of the smallest possible unit upon degradation on the mechanical properties of a polymer network can be seen when the results of the rheological measurements obtained for the degradable adhesive are compared to a previous work from our group.[317] In the study of Oehlenschlaeger et al., the polymer network was based on short chain motives linked *via* HDA moieties. Upon heating, the network degraded into small molecules, resulting in a loss of G' by over 4 orders of magnitude compared to only 2 order of magnitude obtained for the FRP based system of the dental adhesive, where the smallest possible unit is a linear polymer chain. To increase the degradability, a system based on a different polymerization method had to be developed. Step-growth polymerizations offer the possibility to incorporate a functional group in every repeating unit. Therefore, an incorporation of an HDA moiety in a monomer polymerizable *via* a step-growth process would offer the possibility to further degrade a prepared network into small molecules, resulting in a more drastic difference in mechanical stability compared to the FRP based network.

The class of step-growth polymerizations can be subdivided into addition and condensation polymerizations. During condensation polymerizations, small molecules are formed as by-products, which interfere with the network formation. As no side-products are formed *via* an addition polymerization, a system based on this technique was developed. Additionally, the selected monomer system had to be polymerizable at ambient temperature as elevated temperatures would lead to cleavage of the HDA moieties during the network formation. Therefore, polycarbonates were selected as system of choice, since the reaction between an alcohol and phosgene (or a phosgene derivative) can be conducted at ambient temperature. In order to obtain a polymer network a triol or a multi-ol species is required. For more information about step-growth polymerizations and polycarbonates in particular, the reader is kindly referred to Section 2.1.4 of the Theory and Background.

For the thermodegradable dental adhesive, an irreversible system was needed, to allow the dentist to easily remove the dental material in a facile fashion. However, for a DoD polycarbonate network, the reversible nature of the HDA moieties seemed to be more desirable as it allows for continuous reformation and remolding of the polymer network (see Scheme 35). The HDA moiety employed in the dental adhesive demonstrated its applicability for DoD networks and, moreover, it can also be employed in a reversible manner, if the catalyst is incorporated into the polymer network. Therefore, the same HDA pair (phosphoryl dithioester and cyclopentadiene) was employed for the thermodegradable polycarbonate network. As the HDA unit demonstrated bonding/debonding properties at temperatures between 25 and 130 °C within minutes - and common polycarbonates based on Bisphenol A can only be degraded above 480 °C in an irreversible fashion[318] – developing the desired material would represent a highly significant advance over the current state of the art.[†]

As a triol, or higher functionalized alcohol, is required for network formation, a triol bearing three HDA moieties (HDA-triol) was prepared. The synthetic strategy is depicted in Scheme 35 (for a detailed preparation procedure refer to part 7.3.2 of the experimental section).

[†] Parts from the current chapter are reproduced or adapted from **A. M. Schenzel**, N. Moszner and C. Barner-Kowollik, *Polym. Chem.* **2017**, *8*, 414-420, with permission from John Wiley and Sons. N. Moszner and C. Barner-Kowollik motivated and supervised the project as well as contributed to the scientific discussions.

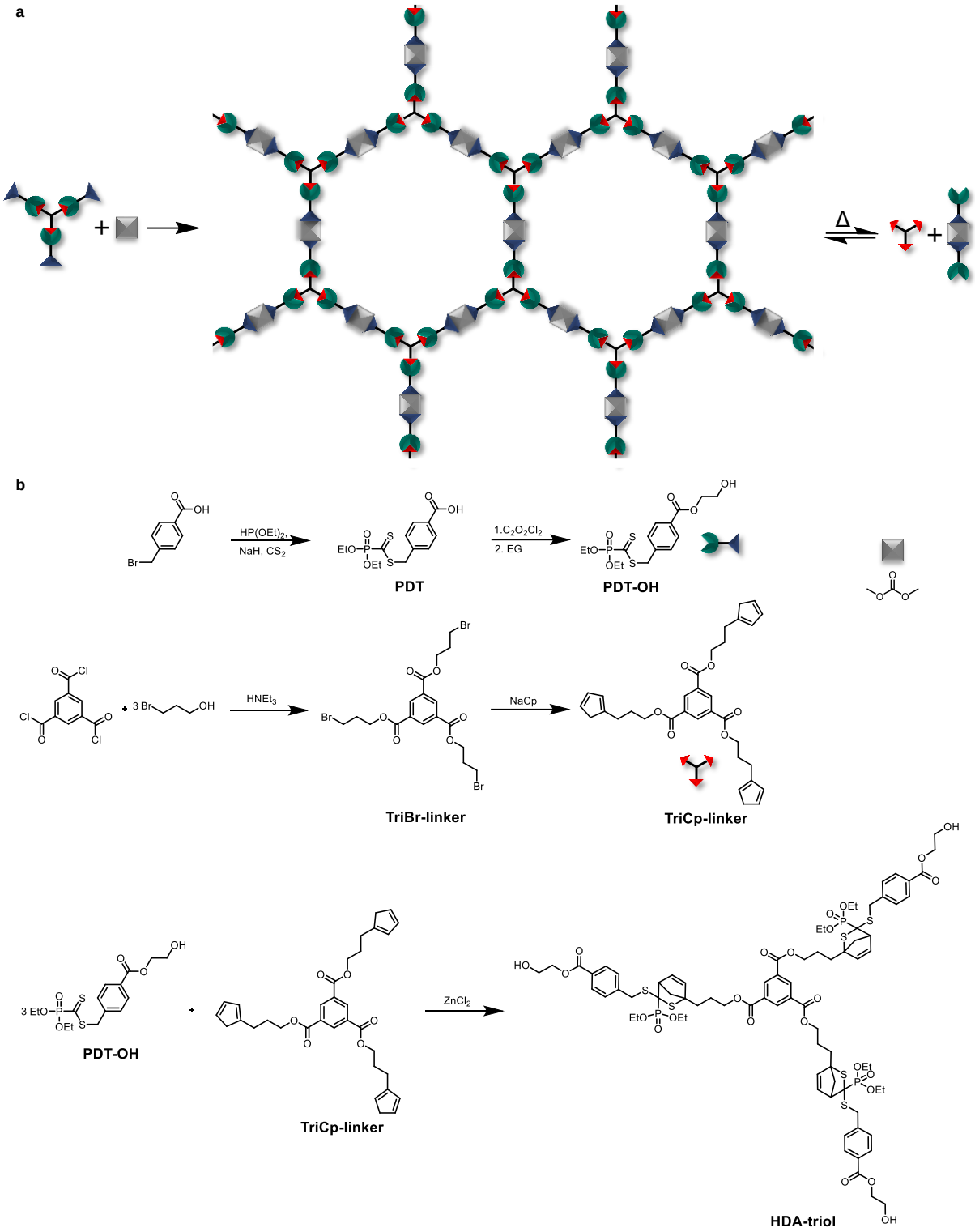

Scheme 35 (a) Schematic display of the bonding/debonding on demand polycarbonate network. The polymer network is prepared *via* the reaction of a triol (HDA-triol) with dimethylcarbonate using catalytic amounts of triazabicyclodecene (TBD). The polycarbonate can then be debonded and rebonded multiple times within minutes depending on the applied temperature, based on the HDA units. (b) Synthetic pathway for the preparation of the HDA triol.[319]

Initially, the phosphoryl dithioester PDT, which was prepared according to a procedure introduced earlier for the dental adhesion system, had to be functionalized in order to bear an OH-group. Therefore, PDT was reacted with oxalyl chloride to form an acid chloride, which could be employed in an esterification reaction with ethylene glycol to form an OH functionalized PDT species (PDT-OH) at slightly elevated temperatures. Next, a linker bearing three Cp moieties had to be synthesized. Hence, 1,3,5-benzenetricarbonyl trichloride was esterified with 3-bromo-1-propanol to form a linker bearing three bromine end-functionalities (TriBr-linker). Next, the TriBr-linker was reacted with NaCp, similar to the DiCp-linker formation, to form a linker bearing three Cp moieties (TriCp-linker). As tests revealed that the pure TriCp-linker starts to form dimers and higher oligomers in a couple of hours, the TriCp-linker was directly reacted with the PDT-OH in an HDA reaction, building up a triol bearing three HDA moieties (HDA-triol). Analytic evidence for the synthesis of the HDA-triol can be found in Figure 14.
To better understand the reversible nature of the HDA system, linear polycarbonate equivalents were prepared. Therefore, a diol species was synthesized by reaction of the PDT-OH with the formerly employed DiHDA-linker (see Figure 15). For a detailed description of the experimental procedure for the HDA-triol and -diol, the reader is kindly referred to the Experimental Section 7.3.2 of the present thesis.

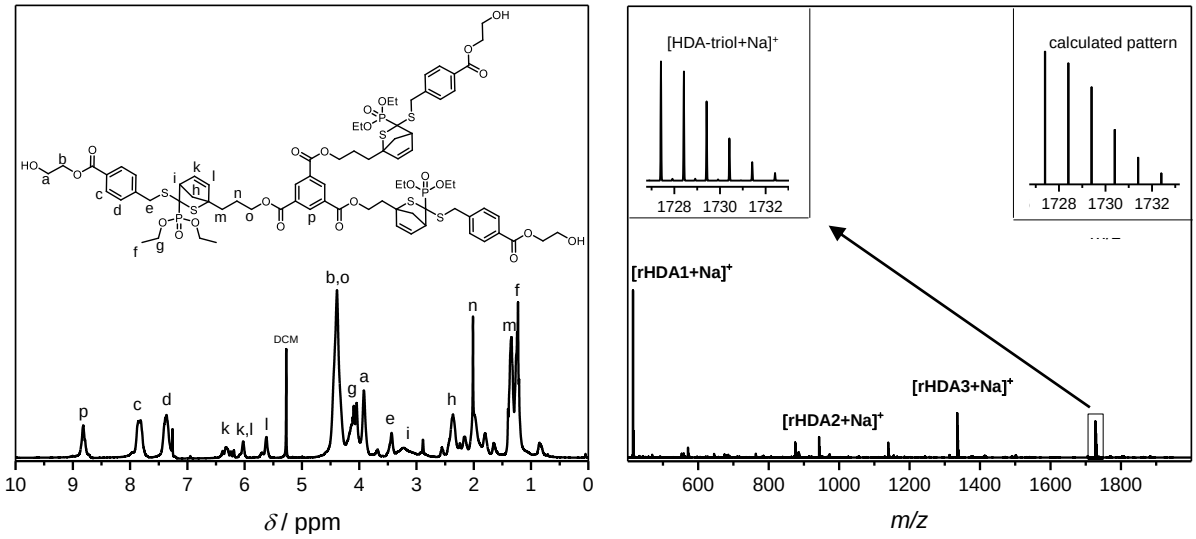

Figure 14 ^{1}H NMR and ESI-MS analysis of the HDA-triol. The retro HDA products are visible due to the high temperatures (320 °C) present at the ionization process. A table summarizing the exact values of the ESI-MS analysis can be found in the Appendix (Table 5).

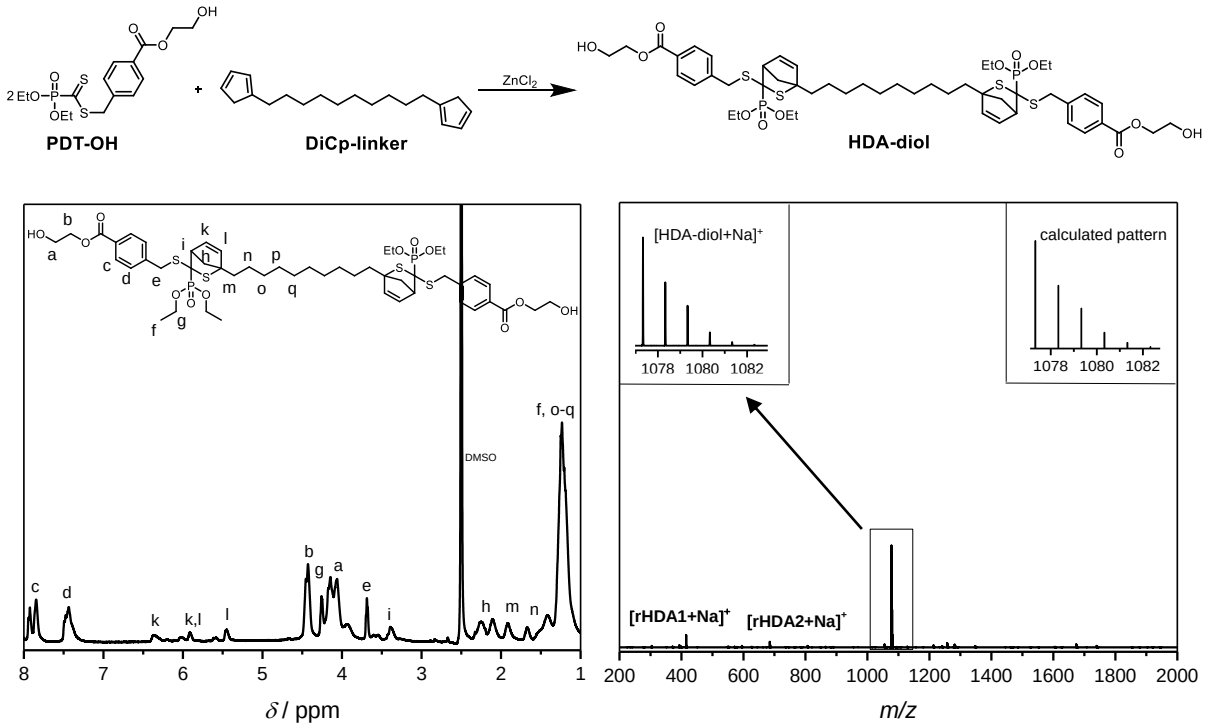

Figure 15 Synthetic protocol for the preparation of the HDA-diol as well as analytical evidence (^{1}H NMR and ESI-MS analysis) for the successful synthesis. The retro HDA products are visible due to the high temperatures (320 °C) present duringt the ionization process. A table summarizing the exact values of the ESI-MS analysis can be found in the Appendix (Table 6).

4.2 Linear Polycarbonates

The linear polycarbonates (HDA-PCs) were prepared using the HDA-diol, a phosgene solution, and pyridine as catalyst (see Figure 16a). The formed polymers were precipitated in hexane for further purification. By varying the monomer mixture composition (ratios between 1.00:1.00 for P4, to 1.00:0.90 for P1), different weight-average molecular weights (M_w) of the HDA-PCs could be obtained ranging from 4200 – 20000 g·mol^{-1} (see Figure 16b). As expected for step-growth polymerizations, the average molecular weight increased with closer to stoichiometric amounts of the reaction partners. A detailed description of the polymer preparation can be found in section 7.3.2. of the experimental part.

First, the degradability of the HDA-PCs was investigated *via* SEC analysis. Hence, P4 was heated to 25, 60, 100 and 140 °C, using dimethylformamide (DMF) as the solvent. After stirring for three minutes at the specific temperature, the solvent was evaporated and the residue was dissolved in THF and employed for SEC analysis. As clearly indicated by Figure 16c, P4 degrades upon heating, as the molecular weight (M_w) decreases from 20000 g·mol^{-1} at 25 °C to only 590 g·mol^{-1} at 140 °C, forming the retro HDA products rHDA1 and rHDA2.

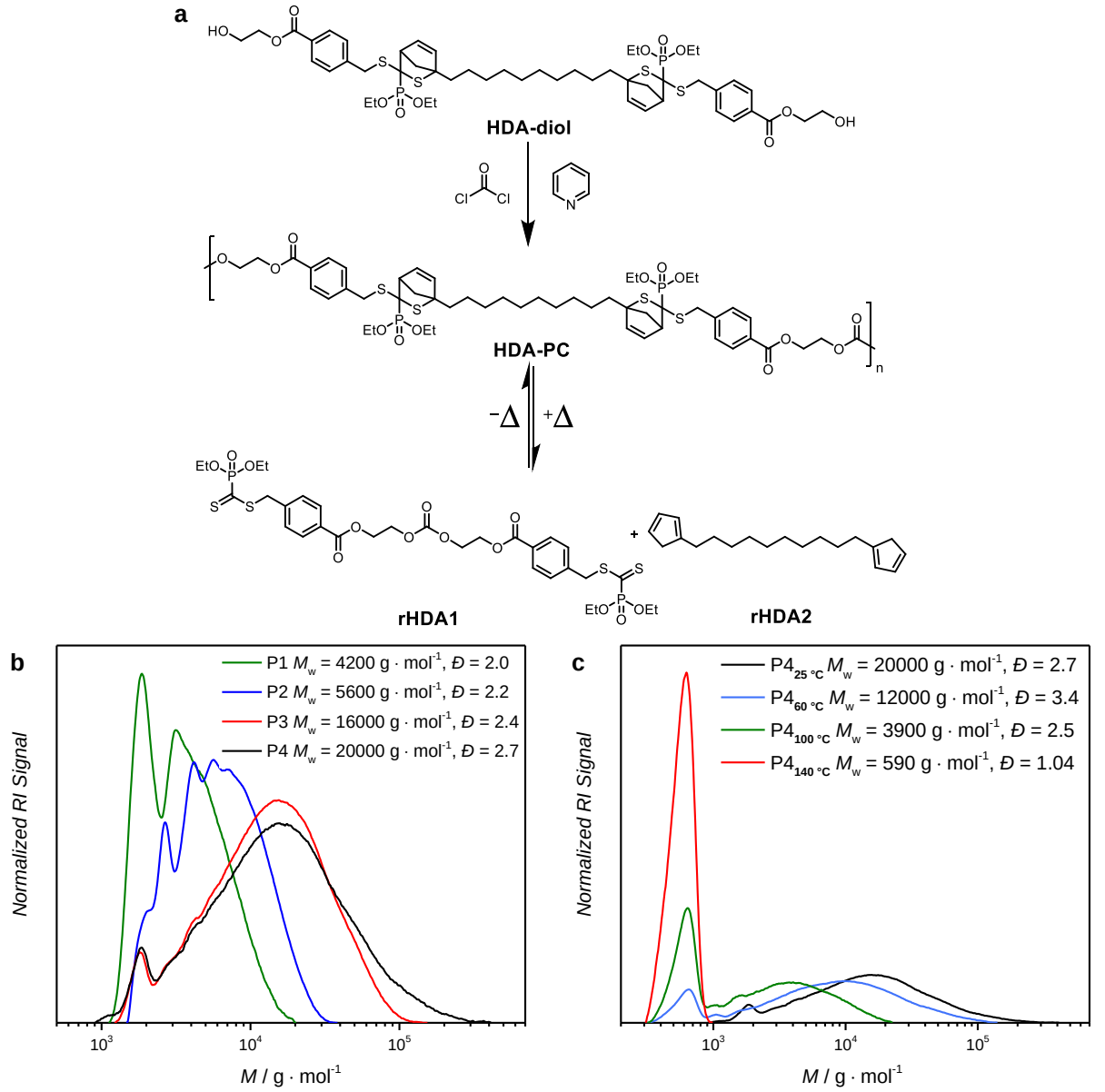

Figure 16 (a) Synthetic protocol for the linear polycarbonates, bearing HDA units in the backbone and the products of the retro HDA reaction upon heating (rHDA1 and rHDA2). (b) SEC analysis in THF of the polycarbonates P1 – P4 with varying degrees of polymerization. (c) SEC analysis in THF of P4 at 25, 60, 100 and 140 °C. M_w decreases due to the decomposition of the polymer based on the retro HDA reaction. Tables summarizing the obtained data of the SEC analysis can be found in the Appendix (Table 7 and Table 8).

In a final step, the reversibility was investigated in detail. Hence, P4 was subjected to SEC, UV/Vis and HT-NMR analysis to unambiguously prove the bonding7debonding behavior. For SEC analysis, P4 was dissolved in DMF and heated to 120 °C for 5 minutes. A sample was taken, and the remaining solution was cooled to 20 °C. In Figure 17a, the SEC traces of the different samples are depicted. As can clearly be seen, the degradation is fully reversible, since the same weight-average molecular weight was obtained for the reformed polymer ($P4_{ref.}$) as for the original polymer ($P4_{or.}$).

In addition, UV/Vis spectroscopic measurements were carried out to prove the reversibility. Therefore, P4 was dissolved in DMF and employed in three heating/cooling cycles in the temperature range of 20 to 100 °C (upper limit of the instrument) using a heating/cooling rate of 5 °C·min^{-1}. The measurement was conducted at 530 nm, as the formed dithioester (rHDA1) shows strong absorption in this range, indicated by its reddish color. As depicted in Figure 17b, it is possible to cleave and rebond the polymer several times upon a thermal stimulus, since the intensity of the absorption reversibly increases when the polymer solution is heated.

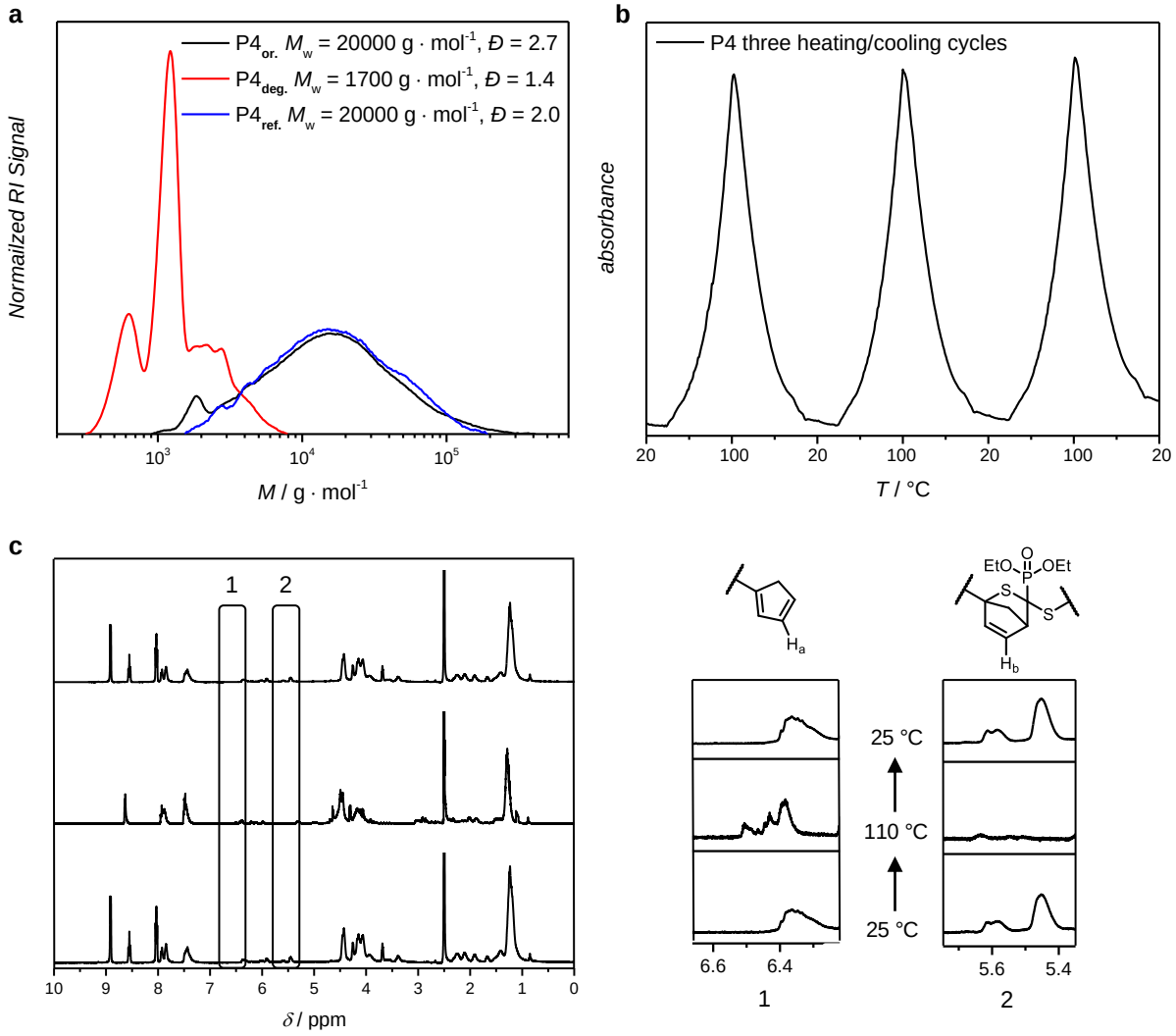

Figure 17 Investigation of the reversibility of the HDA-PC P4. (a) SEC analysis in THF of the bonding/debonding of P4. $P4_{or.}$ Is the original polymer P4, the degraded polymer at 120 °C is termed $P4_{deg.}$and the reformed polymer upon cooling is $P4_{ref.}$. A table summarizing the obtained values of the SEC analysis can be found in the Appendix (Table 9). (b) UV/Vis analysis of the reversibility of P4 at 530 nm in the temperature range of 20 – 100 °C. (c) HT-NMR spectroscopy of the bonding/debonding behavior in DMSO-d_6. H_a is a resonance of the Cp moiety depicted in zoom 1 (6.5 – 6.4 ppm). H_b is a resonance associated with the HDA unit (5.85 – 5.6 ppm, zoom 2). P4 is cleaved at 110 °C, however, is reformed instantly upon cooling to 25 °C.

Finally, HT-NMR spectroscopic analysis was carried out to demonstrate the bonding/debonding behavior on a molecular scale. Therefore, a solution of P4 in DMSO-d_6 was reversibly heated to 110 °C and spectra were recorded at different temperatures (see Figure 17c). At 25 °C, a resonance at 5.45 ppm is visible that can be assigned to a proton (H_b) of the HDA moiety. When heated to 110 °C, a resonance (H_a) appears between 6.35 and 6.50 ppm, indicating the formation of the DiCp-linker. Moreover, H_b is not detectable anymore, proving the debonding of the HDA moieties upon heating. When the solution is cooled to 25 °C again, the resonance of H_a vanishes alongside with the reappearance of the resonance assigned to H_b, demonstrating the reformation of the HDA moiety and, therefore, the bonding/deboning on demand behavior of the employed system on a molecular scale. As the reversibility of the HDA system could be unambiguously evidenced using linear polycarbonates, a polycarbonate network containing HDA units was prepared in a final step to demonstrate the fully reversible nature of the polycarbonate network system.

4.3 Polycarbonate Network

Initially, the attempt was made to prepare the polycarbonate networks *via* a similar reaction procedure as was employed for the synthesis of the linear polycarbonates. However, the pathway was unsuitable for network preparation, as the usage of a phosgene solution and the excess of pyridine required for the reaction impeded the network formation. Moreover, the pyridinium salt would have been incorporated into the network. Hence, a different strategy was pursued for the synthesis of a viable polymer network.

Upon a close inspection of the literature, dimethyl carbonate (DMC) appeared to be a suitable reactant, as the polycarbonate formation can by catalyzed with catalytic amounts of TBD (0.02 eq.) and only methanol is formed as side product that can be readily removed *via* evaporation. Additionally, DMC is a green and ecologically benign replacement for the highly toxic phosgene. Therefore, a polycarbonate network was prepared using the prepared HDA-triol, DMC, and TBD. After removal of the solvent and the formed methanol, a solid network was obtained, as depicted in Figure 18a. Next, the bonding/debonding on demand behavior of the polymer network was studied *via* heating and cooling cycles. As Figure 18b demonstrates, the solid polycarbonate network turns into a red liquid upon heating to 120 °C indicating the formation of the dithioester species (rHDA1) and proving the degradability of the polymer network. Upon cooling, the sample loses its color and the network is reformed within minutes.

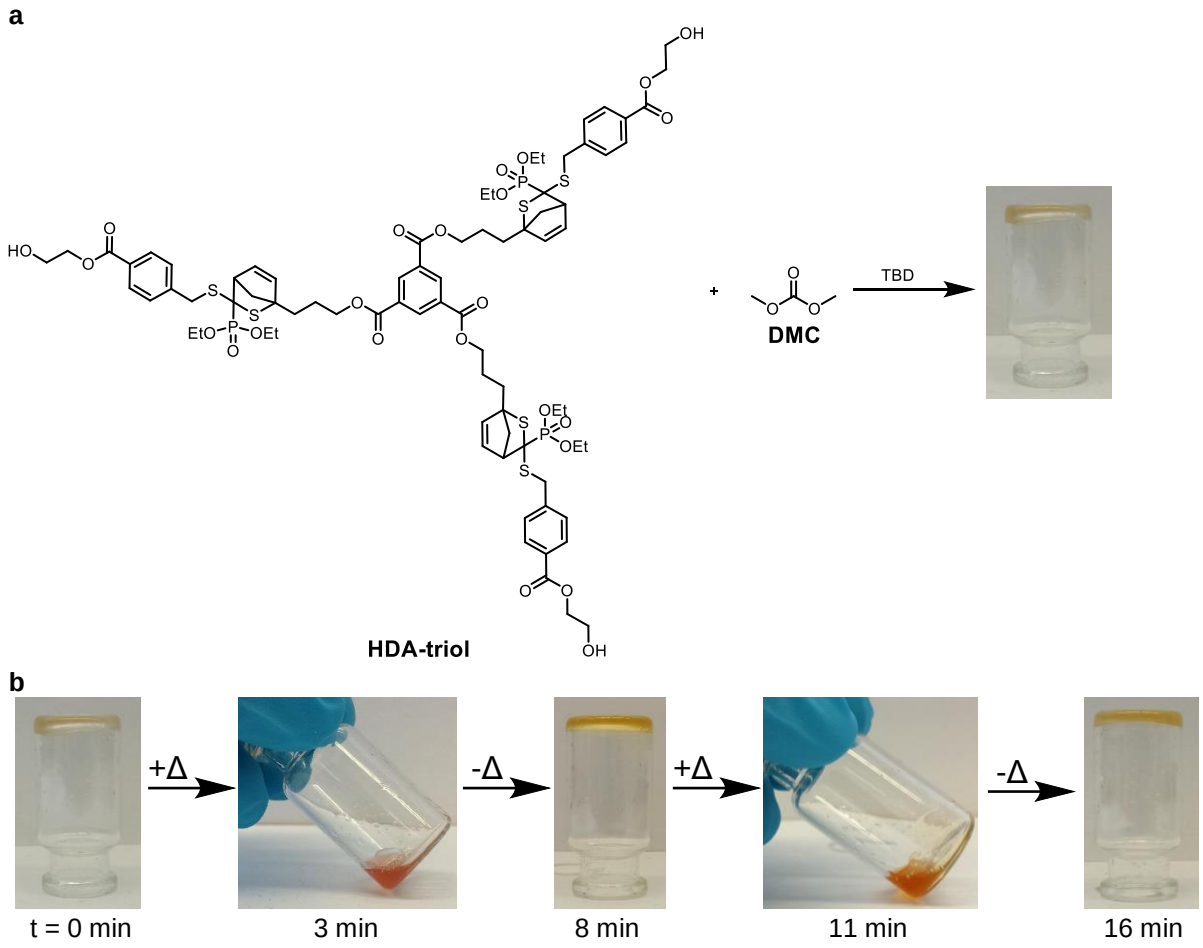

Figure 18 Polycarbonate network. (a) Synthetic protocol for the synthesis of the HDA-containing polycarbonate networks. (b) Pictures of the bonding/debonding behavior of the polymer networks (+Δ: heating to 120 °C, -Δ: cooling to 25 °C). For the heating procedure, a pre-heated oil bath was employed and a water bath was used for cooling. The red color stems from the formation of the dithioester moiety (rHDA1) upon heating.

The sample can be cycled multiple times within minutes, evidencing the fast and complete reversibility of the system and, therefore, the desired bonding/debonding on demand behavior of the polycarbonate network.

The developed polycarbonate network system, therefore, shows the intended improved degradability compared to the polymer network introduced in the previous section, which is based on a free radical polymerization, as the network can be debonded into small molecules instead of linear polymeric chains. Moreover, the polycarbonate network can be reversibly bonded and debonded multiple times as the catalyst for the HDA reaction is incorporated into the network. The bonding/debonding on demand behavior was demonstrated without a doubt *via* a detailed analysis of linear polycarbonates containing the HDA units using SEC, HT-NMR and UV/Vis spectroscopy. Finally, a polycarbonate network bearing the HDA moieties

was prepared and successfully bonded and debonded multiple times within minutes. Therefore, the novel system offers a critical advance over the current state of the art for polycarbonate networks as it can reversibly be degraded under relatively mild conditions.

5

Disulfone Network for Photoinduced Degradation

5.1 Motivation and Monomer Design

After the detailed investigation of thermodegradable polymer systems, network degradation upon photochemical stimuli was investigated in the third part of the present thesis.

As outlined in the theoretical section, light responsive moieties offer great potential for DoD polymer networks. In contrast to thermoresponsive systems, light induced processes can be carried out in an orthogonal fashion when moieties are engaged that react at different wavelengths. E.g. *p*-hydroxyphenacyl,[320] coumarin[321] and *o*-nitrobenzyl[282, 322] units have previously been used for λ-orthogonal alterations of polymer networks. Usually, the polymer networks are based on a free radical polymerization, with the light responsive unit being incorporated into the crosslinks. A clear disadvantage of this approach is that a novel crosslinker must be synthesized for each wavelength regime in order to adapt the system to the specific wavelength required for the intended application. Therefore, the presented work aims to prepare a novel, universal system for a wavelength dependent decomposition at any desired wavelength, giving the new DoD network a clear advantage over the current state of the art.

For a universal system, a different concept for the degradation mechanism has to be pursued. The crosslinker itself cannot be the light responsive unit, as a moiety degrading at various different wavelength is not possible to prepare. Instead, a crosslinker has to be employed that can cleave upon reaction with a molecule that is released by the irradiation of an additive, which is caged within the polymer network. The wavelength at which the network degrades can then be fine-tuned for the targeted application in a facile fashion by selecting an additive

that decomposes at the desired wavelength. In order to trap the additive in the polymer network, it is simply added to the monomer mixture prior to curing.

Upon a thorough investigation of the literature, the class of disulfones seemed to be an interesting and applicable tool for the crosslinker moieties. Disulfones are applied in various fields of application, e.g. in electrolytes for batteries,[323] epoxy resins,[295] organic solar cells[324] and gas generation suppression.[296] However, disulfones have never been employed in the context of degradable polymeric systems before. Moreover, due to the mild conditions at which disulfones are formed, a vast number of functional groups (e.g. a vinylic group) can be incorporated into the disulfone molecule, allowing the incorporation into a network based on FRP, and giving the system various post-modification possibilities. As described in detail in the theoretical part of the present thesis, α-disulfones can be cleaved *via* a nucleophilic substitution reaction in a facile fashion using hydroxides, acetates, or primary or secondary amines just to mention a few examples. Therefore, caging a photo-protected nucleophile in the polymer network should enable network degradation upon irradiation. When having a close look at the literature, the class of photo-generated amines (PGAs) seemed to be an applicable tool as they are able to release primary or secondary amines upon irradiation. Interestingly, they have never been used to degrade disulfones before. As there are various different PGAs known today, which cleave in different wavelength regimes, the wavelength for the network degradation can readily be tuned to the desired application by selecting a PGA that decomposes at the intended wavelength. Moreover, the different PGAs can usually be prepared in a facile fashion *via* single step reactions using well-known literature protocols.[233] Additionally, if an initiator is employed for the polymer network formation, which decomposes at a different wavelength than the used PGA, bonding and debonding of the network can be carried out in a λ-orthogonal fashion.[‡]

Therefore, the combination of α-disulfone crosslinks with a UV-degradable PGA additive and a blue-light decomposable photoinitiator was employed as a universal tool for λ-orthogonal photo-induced curing and degradation of a polymer network. The general concept is summarized in Scheme 36.

[‡] Parts from the current chapter are reproduced or adapted from **A. M. Schenzel**, N. Moszner and C. Barner-Kowollik, *ACS Macro Lett.* **2017**, *6*, 16–20, with permission from the American Chemical Society. N. Moszner and C. Barner-Kowollik motivated and supervised the project as well as contributed to the scientific discussions.

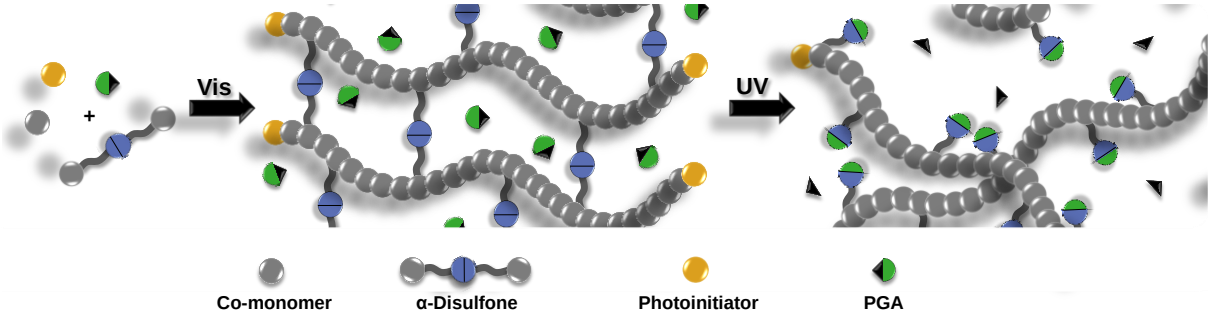

Scheme 36 General concept of the polymer network, curable and degradable in a λ-orthogonal fashion. After a free radical polymerization using a visible light decomposable photoinitiator, the degradation of the network is realized *via* a UV light induced substitution reaction of the disulfone crosslinks with a photo-generated amine.[325]

At first, the disulfone crosslinker had to be prepared. In order to incorporate the linker in a polymer network based on an FRP, a dimethacrylate crosslinker containing the disulfone moiety needed to be synthesized. As outlined in Section 2.5, there are multiple ways to prepare disulfones. First, the oxidation of disulfides was conducted, however, the yields were low and the separation of the different oxidation products was challenging. Therefore, a different pathway was investigated. Well-known precursors for disulfones are sulfonyl chlorides. Therefore, a sulfonyl chloride containing a methacrylate species (MA-$SOCl_2$) was prepared in a two-step reaction. First, the methacrylate was incorporated into the molecule *via* an esterification reaction using methacryloyl chloride, 2-phenoxy ethanol, and triethylamine, followed by the formation of the sulfonyl chloride using chlorosulfonic acid (refer to Scheme 37).

An aryl disulfone can then be synthesized by using hydrazine to prepare an N,N'-disulfonyl hydrazine intermediate, which is oxidized to the disulfone species using nitric acid. However, as tests indicated, the methacrylate moiety is cleaved off upon utilization of the nitric acid. As it is possible to prepare disulfones in good yields *via* the oxidation with nitric acid, it was attempted to introduce the methacrylate species after the disulfone formation. According to the literature,[307] aryl disulfones bearing chloride, bromide or methoxy functionalities were prepared in good yields. Multiple pathways for the post-modification to prepare the dimethacrylate containing disulfone were conducted, however, the synthesis could not be achieved.

Hence, a different pathway was identified and pursued for the preparation of the disulfone containing dimethacrylate (DiMA-$DiSO_2$). The synthetic protocol is depicted in Scheme 37. Samarium powder offers the possibility to reduce the sulfonyl chloride to the disulfone under extremely mild conditions, tolerating various functional groups. The reaction temperature is thereby essential, as arylsulfonyl chlorides can selectively be reduced to disulfides,

thiosulfonates, and disulfones depending on the temperature.[308] To prepare the desired disulfone species (DiMA-DiSO$_2$), the reduction with samarium was conducted at -10 °C. Analytical evidence for the successful preparation of DiMA-DiSO$_2$ is given in Figure 19 (for a detailed description of the experimental procedure, refer to part 7.3.3 of the experimental section).

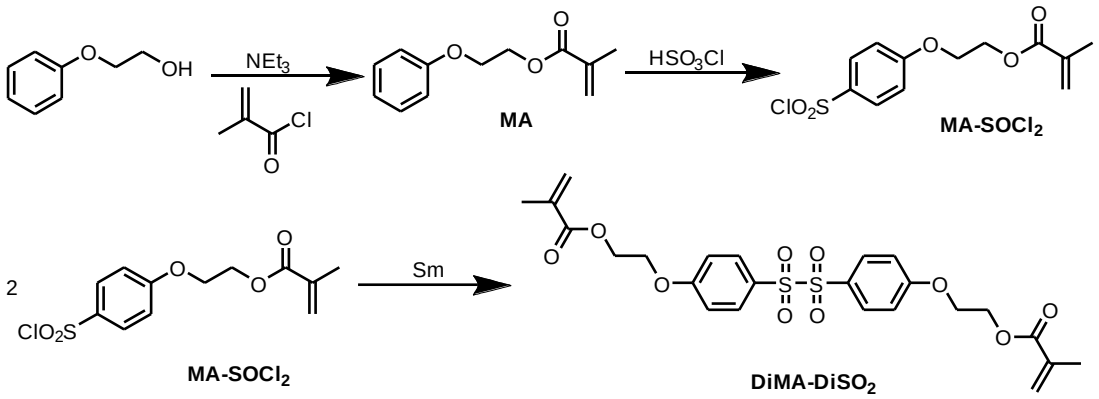

Scheme 37 Synthetic procedure for the preparation of the dimethacrylate crosslinker containing the disulfone species (DiMA-DiSO$_2$).

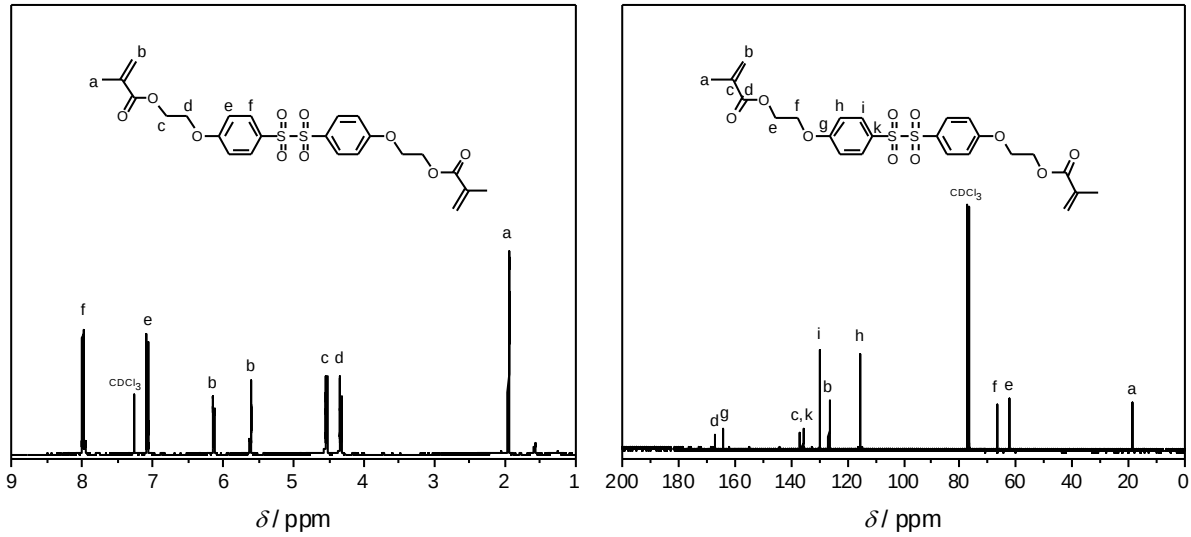

Figure 19 ^{1}H and ^{13}C NMR spectra of the prepared disulfone containing dimethacrylate (DiMA-DiSO$_2$) in CDCl$_3$.

5.2 Solution studies

For a proof of concept, the prepared DiMA-DiSO$_2$ was reacted with variable amounts of diethylamine in a nucleophilic substitution reaction. As indicated by ^{1}H NMR spectroscopy, the S-S bond of the disulfone can be cleaved using a nucleophile, as resonances belonging to the DiMA-DiSO$_2$ (a: 7.1 ppm, b: 8.0 ppm) disappear and resonances of the substitution product S1

(a': 6.9 ppm, b': 7.7 ppm and c': 1.1 ppm) intensify with increasing amount of diethylamine (see Figure 20). The NMR spectra were recorded immediately after the addition of the nucleophile, indicating that the reaction rapidly takes place. The disulfone species could, therefore, be debonded efficiently within minutes using 5 eq. of diethylamine, proving the general concept of the targeted DoD polymer network.

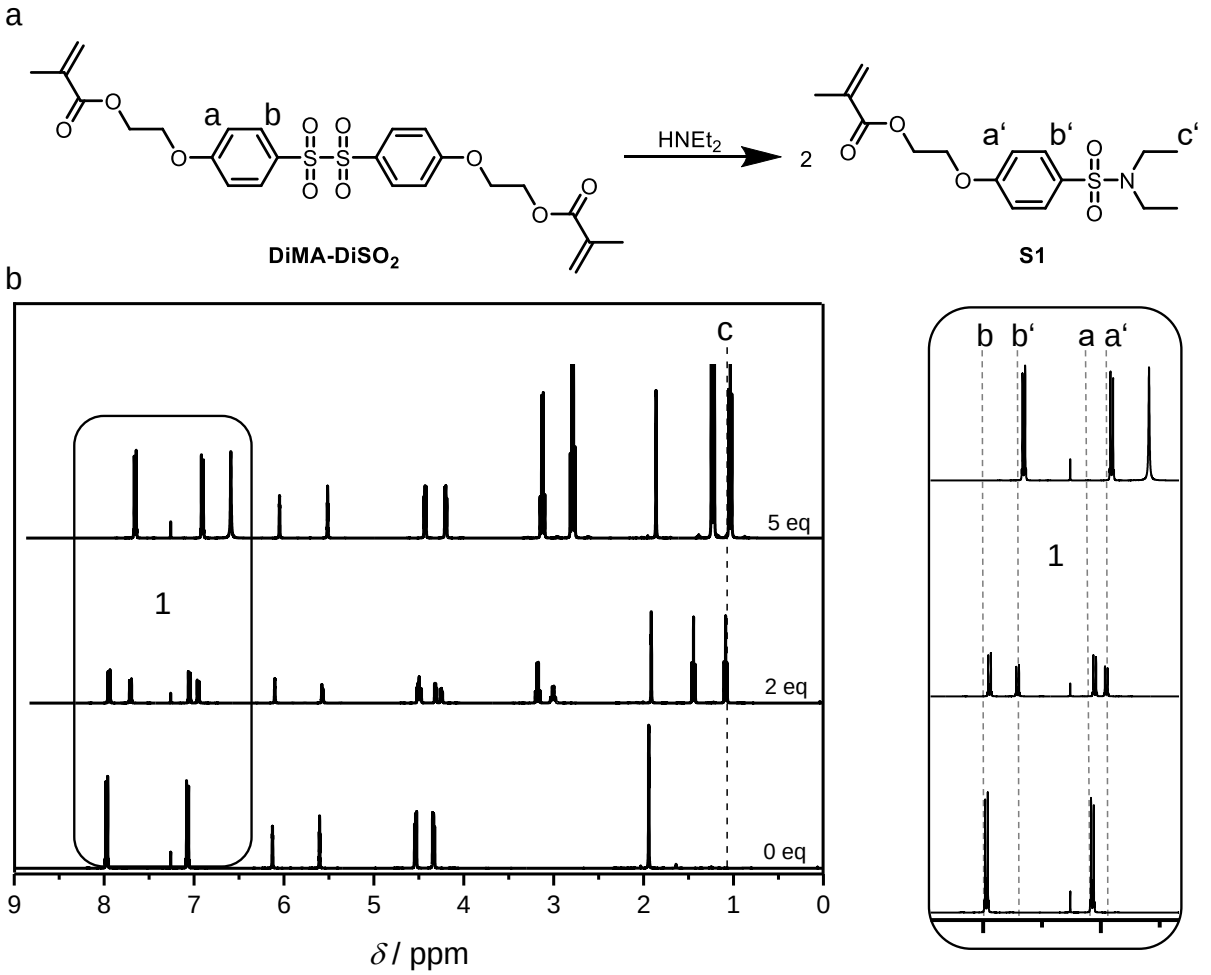

Figure 20 (a) Nucleophilic substitution reaction of DiMA-$DiSO_2$ with diethylamine. (b) ^{1}H NMR spectroscopic evidence of the reaction with 2 and 5 eq. of diethylamine. Resonance a and b belong to the DiMA-$DiSO_2$, whereas resonances a', b' and c' correspond to the substitution product S1.

Subsequently, a PGA had to be selected that is able to cleave upon UV irradiation, releasing a primary or secondary amine, yet is stable in the visible light range. When inspecting the literature, a broad range of possible PGAs can potentially be employed. However, some PGAs, as coumarin-based PGAs, require a catalyst (such as water) to generate the specific amine.[321] Since the decomposition of the PGA has to take place within the network, a catalyst-free system is required. In Scheme 38, three different PGAs are displayed that were tested for their degradability upon UV and visible light irradiation. PGA1 could be cleaved using UV light (355 – 390 nm) as desired, however, it also showed degradation under visible light irradiation (400

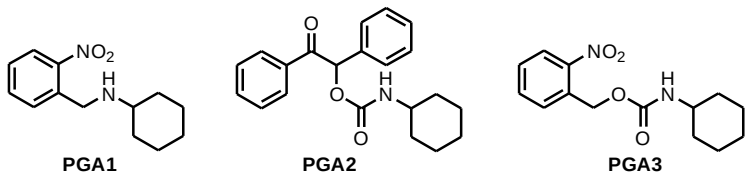

Scheme 38 Three different PGAs, which were analyzed in terms of their degradation behavior upon irradiation with visible and UV light.

– 520 nm) making it unsuitable for the desired application. Next, PGA2 was assessed using different irradiation wavelength, from 280 to 600 nm. Interestingly, no deprotection of the amine was observed at any irradiation wavelength. Last, the cleavage of PGA3 upon irradiation was investigated. Intensive studies revealed that PGA3 combines the desired UV light degradability, alongside with visible light stability.

In Figure 21, the decomposition reaction of PGA3, as well as the analytical evidence for the degradation upon irradiation with UVA light (355 – 390 nm, 500 mW·cm^{-2}) is given. When PGA3 decomposes, 2-nitroso benzaldehyde and CO_2 are formed alongside with the release of cyclohexylamine. The decomposition of PGA3, as well as the formation of the amine, can be analyzed *via* ^{1}H NMR spectroscopy. Upon irradiation with UVA light, the resonances a

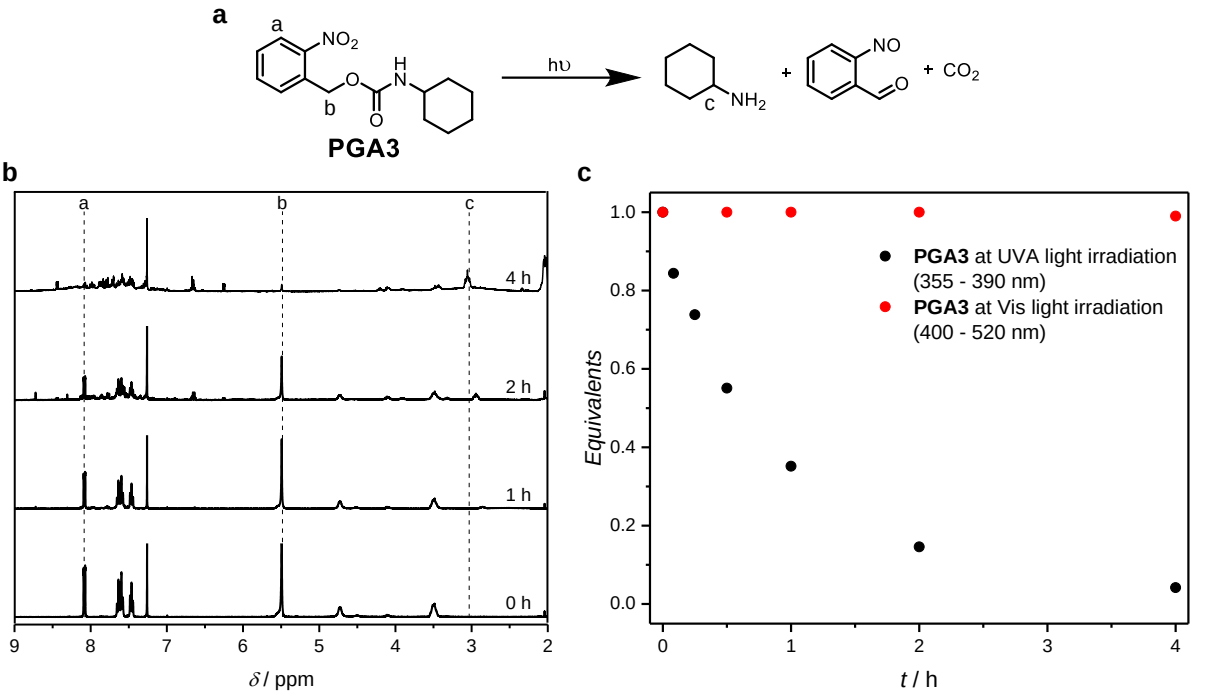

Figure 21 (a) Decomposition reaction of PGA3 upon irradiation with UV light. (b) ^{1}H NMR spectra of the degradation of PGA3 during irradiation with UVA light (355 – 390 nm, 500 mW·cm^{-2}) in $CDCl_3$. The measurements were conducted after 0, 1, 2 and 4 h of irradiation. (c) Decomposition of PGA3 upon UVA and visible light irradiation, determined *via* the decreasing intensity of resonance b. No degradation can be detected under visible light irradiation (400 – 520 nm, 100 mW·cm^{-2}). The emission spectra of the employed light sources can be found in the Appendix (see Figure 26).

(8.1 ppm) and b (5.5 ppm) belonging to PGA3 decrease, whereas a resonance (c, 3.0 ppm) that can be assigned to the cyclohexylamine increases in intensity. When a solution of PGA3 in $CDCl_3$ is irradiated with visible light (400 – 520 nm, 100 mW·cm^{-2}) for up to 4 h, no degradation can be detected using ^{1}H NMR spectroscopy, proving the stability of the PGA at exposure to visible light. When the intensity of resonance (b) is plotted against the irradiation time, the decomposition of PGA3 under UV light irradiation, as well as its visible light stability are clearly apparent (see Figure 21c). After 1 h of exposure to UVA light (355 – 390 nm, 500 mW·cm^{-2}), 65% of the PGA3 is decomposed. Therefore, a suitable PGA could be identified to achieve the desired λ-orthogonality.

In order to evidence that the disulfone itself does not decompose upon light exposure, a solution of DiMA-$DiSO_2$ in $CDCl_3$ was irradiated with UVA and visible light for 24 h. As NMR analysis revealed, no degradation is detectable, proving the light stability of the employed disulfone.

Next, the ability of the chosen PGA to cleave the S-S bond of the disulfone upon irradiation had to be unambiguously proven. In Figure 22a, the molecular structures of the two starting materials (DiMA-$DiSO_2$ and PGA3), as well as the product structure of the substitution reaction (S2) are depicted. To investigate the reaction, 5 eq. of PGA3 and 1 eq. of DiMA-$DiSO_2$ were dissolved in $CDCl_3$, irradiated with UVA light (355 – 390 nm, 500 mW·cm^{-2}) and analyzed *via* ^{1}H NMR spectroscopy after different irradiation time intervals. If the nucleophilic substitution reaction between the photocleaved cyclohexylamine and the disulfone occurs, a new resonance should be detectable associated with the substitution product, alongside with a decrease in the resonances belonging to PGA3 and the DiMA-$DiSO_2$. As can clearly be seen in the zoom in on the ^{1}H NMR spectra (Figure 22c), the resonances belonging to an aromatic proton of the disulfone (resonance a, 7.0 ppm) and the methylene group of the PGA (resonance b, 5.4 ppm) decrease in intensity. Moreover, a new resonance appears and increases in intensity during the irradiation process, which can be assigned to an aromatic proton of the substitution product S2 (resonance c, 6.9 ppm). For further quantification, the integrals of the resonances a, b and c were determined and the equivalents of the respective molecules were calculated. Then, the various equivalents of the reactants and the product were plotted *vs.* the irradiation time, demonstrating the steady degradation of DiMA-$DiSO_2$ and PGA3, as well as the increase in S2, unambiguously (see Figure 22d). The proceeding of the reaction can also be detected by

the naked eye, as the decomposition of PGA3 leads to the formation of 2-nitroso benzaldehyde, which has a yellow color. Upon irradiation, the yellow color intensifies, as depicted in Figure 22e.

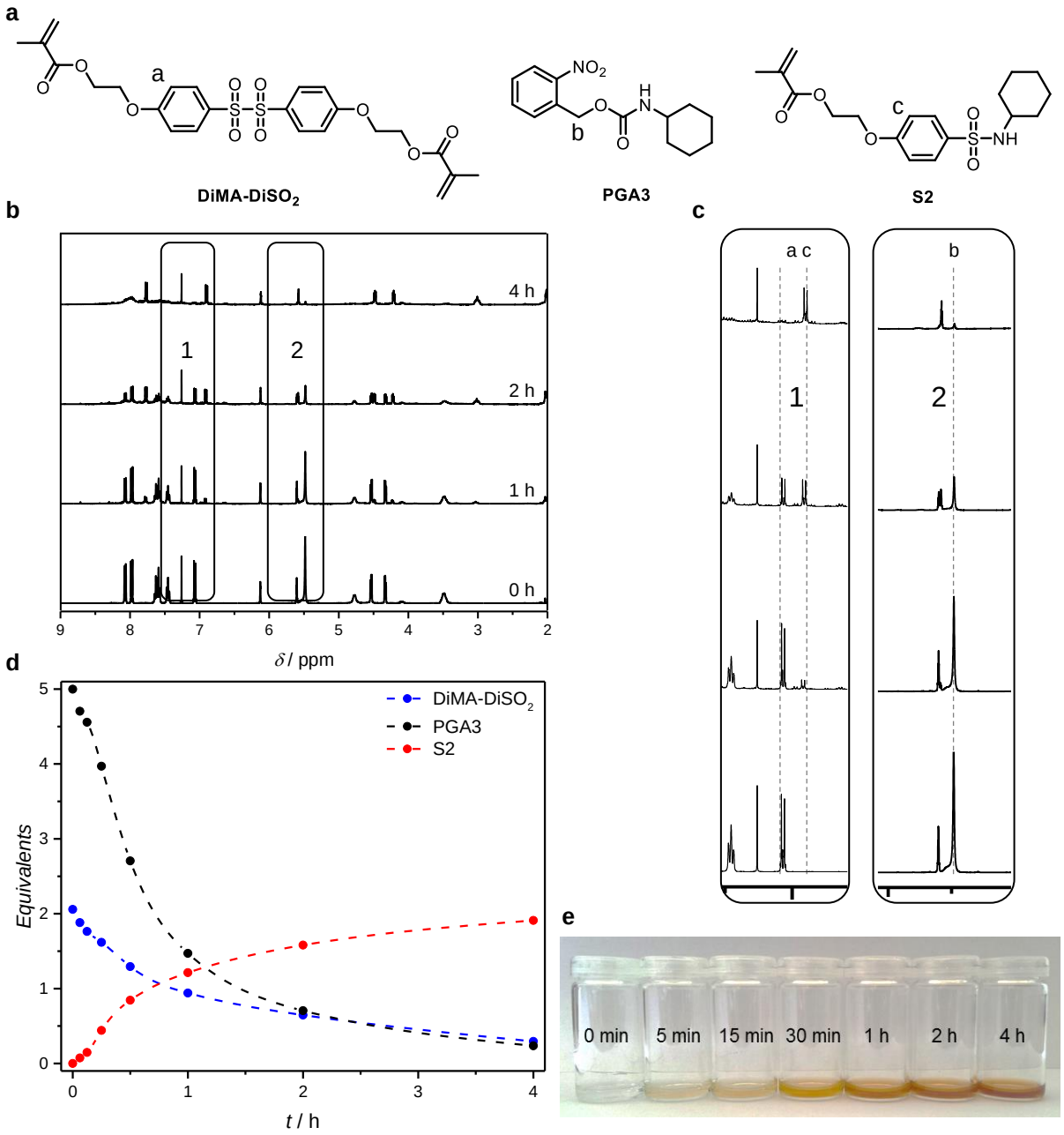

Figure 22 (a) Molecular structures of DiMA-DiSO$_2$, PGA3 and S2. (b) ^{1}H NMR spectroscopy of the reaction of DiMA-DiSO$_2$ and PGA3 in CDCl$_3$ upon irradiation with UVA light (355 – 390 nm, 500 mW·cm^{-2}) after 0, 1, 2 and 4 h. (c) Enlargement of the ^{1}H NMR spectrum between 6.7 – 7.5 ppm (1) and 5.1 – 6.0 ppm (2). Resonance a corresponds to DiMA-DiSO$_2$, resonance b to PGA3 and resonance c to S2. (d) Comparison between the decrease of PGA3 and DiMA-DiSO$_2$ with the increase of S2, by determining the equivalents used/formed during the substitution reaction calculated *via* the integrals of the specific resonance. (e) Observable color change during the reaction between 0 and 4 h. The coloration stems from the formation of 2-nitroso benzaldehyde.

5.3 Network studies

As the cleavage of the S-S bond of the disulfone *via* a photo-induced reaction with an amine formed upon decomposition of a PGA was shown to function in solution, a network using the DiMA-DiSO$_2$ and the PGA3 was prepared in a final step and investigated in terms of its degradability. To achieve the desired λ-orthogonality, a photoinitiator that decomposes at exposure to visible light had to be selected. The photoinitiator of choice was Ivocerin® (bis-(4-methoxybenzoyl)diethylgermane, λ_{max} = 408), which is a Norrish Type-I initiator, combining an excellent curing depth with a high reactivity upon blue light irradiation. Additionally, Ivocerin® shows a photobleaching effect that leads to the disappearance of the yellow color of the initiator and therefore, to the formation of a colorless network.[326] Hence, a monomer mixture in toluene was prepared, employing *n*-butyl methacrylate, 10 mol% of DiMA-DiSO$_2$, 50 mol% of PGA3 and 0.2 wt% Ivocerin® (see Scheme 39).

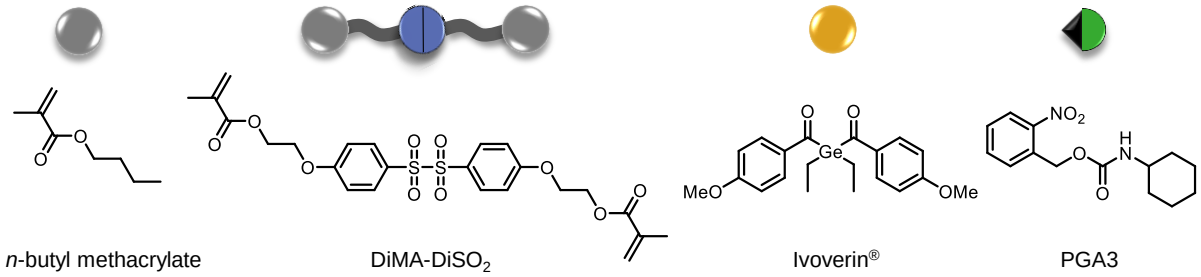

Scheme 39 Summary of the monomer mixture, employing *n*-butyl methacrylate, 10 mol% of DiMA-DiSO2, 50 mol% of PGA3 and 0.2 wt% Ivocerin®.

The solution was degassed using nitrogen and irradiated with blue light (400 – 520 nm, 100 mW·cm^{-2}) for 10 minutes, to form a colorless polymer network. As depicted in Figure 23, the formation of the polymer network could be demonstrated *via* a tube inversion test. Next, the solid network was irradiated with UVA light (355 – 390 nm, 500 mW·cm^{-2}) to induce the degradation. If the reaction of the released cyclohexylamine with the disulfone crosslinks takes place within the network, a clear decrease in mechanic stability, combined with a color change, has to be detectable upon irradiation. As can be seen in Figure 23, the solid and colorless polymer network turns into a yellow liquid during an irradiation time of 4 h, proving the degradability of the polymer network. A control experiment was conducted to evidence the necessity of the PGA to be caged inside the polymer network. Therefore, a reaction was car

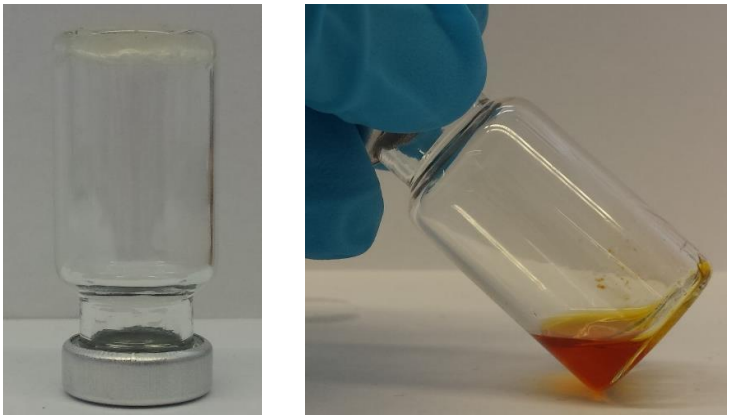

Figure 23 Analysis of the stiffness of the polymer network before and after irradiation with UV light (400 – 520 nm, 100 mW·cm^{-2}) *via* a tube inversion test.

ried out using the same monomer mixture, but excluding PGA3. The solid and colorless network neither showed a color change, nor a sol/gel transition demonstrating the need for the PGA.

In summary, a new and advanced concept for a λ-orthogonal photo-induced curing and decomposition of a polymer network was demonstrated. The λ-orthogonality relies on the combination of a visible light Norrish Type-I photoinitiator (Ivocerin®) with a UVA degradable PGA (PGA3). To prepare a degradable network, a novel disulfone containing dimethacrylate (DiMA-DiSO$_2$) was synthesized. Then, a PGA was selected that was able to release an amine (cyclohexylamine) upon irradiation with UVA light, yet was persistent under exposure to visible light. ^{1}H NMR spectroscopy in solution evidenced the decomposition of the PGA upon irradiation, as well as the nucleophilic substitution reaction between the released amine and the disulfone. In a final step, a polymer network cured using blue light was degraded into a colored liquid upon irradiation with UVA light, proving the overall concept of the λ-orthogonal formation and degradation of the disulfone containing polymer network.

6

Conclusion and Outlook

The constant advances in chemistry, and particularly in the field of polymer chemistry, lead to the development of new, so-called smart materials with unprecedented properties. The unique properties are based on stimuli-responsive moieties that are incorporated in the polymeric material. Upon application of a certain stimulus, the material characteristics alter drastically, constituting a highly useful property for a range of applications, such as self-healing materials, drug release systems and reshapeable polymer networks.

One class of materials, which has not benefitted from these advances yet, are adhesives, even though an adhesive that could be degraded on demand, easing the separation of the bonded parts, would have a significant impact, as more than 50% of the goods produced today contain adhesives. Especially, a dental adhesives with debonding on demand properties is of substantial interest, as it would ease the removal of dental materials, such as crowns and brackets to a great extent.

Consequently, the overall aim of the present thesis was the development of a dental adhesive that can be debonded, when a certain stimulus is applied. Since teeth are known to be poor heat conductors, a thermal stimulus can be employed for the alteration of the polymeric structure. As adhesion in dental systems is commonly achieved *via* free radical polymerization of dimethacrylates, which constitutes a polymer network, a dimethacrylate containing the heat degradable moiety was developed. The temperature response is based on an HDA system that undergoes a retro HDA reaction upon heating, resulting in the cleavage of covalent bonds and, therefore, in the degradation of the polymer network crosslinks. As a consequence of the degradation, the adhesive material will lose its mechanical stability resulting in a facile removal of the dental composite and the residual adhesive.

Chapter 3 describes the development and thorough analysis of the novel dental adhesive with debonding on demand properties. First of all, Section 3.1 addresses the preparation of a dimethacrylate species, containing two HDA moieties (DiHDA-linker) and a non-polymerizable analogue (DiHDA-core) that was employed for solution studies.

Next, debonding upon heating was investigated in detail using HT-NMR and UV/Vis spectroscopy (see Section 3.2). At 80 °C, which is the desired application temperature for the debonding of the dental material, 75% of the crosslinks are degraded. As the retro HDA reaction demonstrates to reach the equilibrium state at 100 °C in less than three minutes, the system is suitable for an application as dental adhesive. The system also has a self-reporting nature, as the intensity of the reddish color of the material, stemming from the formed dithioester can be directly linked to the degree of debonding.

As indicated by rheological measurements in Section 3.3, a drastic loss in mechanical stability upon heating (loss in G' by over two orders of magnitude) is present for the DiHDA-linker based network, with the same effect not observable for the reference polymer network. In Addition, it was demonstrated that the temperature at which the material starts to lose its stability can be tuned by adding a comonomer.

In Section 3.4, final adhesion and pull-off tests were conducted. For the analysis, dental crowns were cemented to an implant abutment, either using an adhesive mixture containing the DiHDA-linker or a non-degradable dimethacrylate. As results clearly demonstrate, both systems are strong adhesives at 25 °C, however, only the HDA-based adhesive shows a drastic loss of adhesion stability at 80 °C. Hence, the applicability of the invented material as easily degradable adhesive was unambiguously shown, demonstrating a significant improvement over the current state of the art for adhesives, as only non-degradable systems were known, before.

For the desired application as dental adhesive, the onset temperature of the retro HDA reaction of the employed system of close to 25 °C is not feasible, as the crosslinks need to be completely closed also at slightly elevated body temperature (40 °C). The increase of the onset temperature by close to 15 °C was realized by substituting the benzoyl unit of the phosphoryl dithioester with an alkyl functionality (DiHDA3). Therefore, the overall aim of the present thesis could be achieved by preparing a novel, degradable dental adhesive that can be degraded upon thermal stimulus, which drastically eases the removal of dental materials.

In Chapter 4, a dynamic covalent polycarbonate network with self-reporting properties is developed and studied in detail that in contrast to the polymer network in Chapter 3, can be degraded to small molecules, as the cleavable motive can be employed in each repeating unit. The dynamic nature is based on the HDA moiety that was also employed for the dental adhesive. As the catalyst of the HDA reaction is added for the polymer network preparation, the system is able to cleave and bond reversibly, depending on the temperature.

Section 4.1 outlines the preparation of di- and triol species containing two and three HDA motives, respectively. In order to enable a detailed investigation of the reversibility, linear polycarbonates (PCs) were prepared and studied extensively in Section 4.2. The degradability as well as the reversibility could be demonstrated using SEC, HT-NMR and UV/Vis spectroscopy.

Finally, polycarbonate networks were prepared and testes for their temperature-based reversible nature (refer to Section 4.3). Dimethyl carbonate was employed for the network formation, which in addition is a more environmentally friendly substitute for phosgene. The polycarbonate networks demonstrated the desired reversible behavior, as they turned into a highly colored liquid when heated to 120 °C, yet reformation of the colorless network took place upon cooling to ambient temperature. Therefore, the first time preparation of a reversibly cleavable polycarbonate network could be achieved, demonstrating a significant advance over the state of the art.

In Chapter 5, a photochemical trigger instead of a thermal stimulus was employed, to achieve a λ-orthogonal curing and degradation of a polymer network. First, the preparation and analysis of the disulfone containing dimethacrylate (DiMA-$DiSO_2$) is outlined in Section 5.1. The DiMA-$DiSO_2$ is thereby prepared *via* a temperature dependent reaction of the respective sulfonyl chloride under Sm catalysis.

The degradability of the disulfone species in solution was demonstrated in Section 5.2 *via* ^{1}H NMR spectroscopy. A complete degradation of DiMA-$DiSO_2$ can be accomplished with 5 eq. of diethylamine within minutes. Next, a suitable PGA that releases a primary amine at UV irradiation, yet is persistent when irradiated with visible light, was identified. The ability of PGA3 to cleave the S-S bond of the disulfone motive in solution after variable irradiation times was demonstrated, as 5 eq. of PGA3 can completely substitute the DiMA-$DiSO_2$ within 4 hours at an irradiation intensity of 500 $mW \cdot cm^{-2}$ using UVA light.

Finally, a polymer network employing *n*-butyl methacrylate, DiMA-DiSO$_2$ and PGA3 was cured under blue light irradiation using Ivocerin® as photoinitiator (refer to Section 5.3). The colorless, rigid network turned into a highly colored liquid upon irradiation with UVA light, demonstrating the desired λ-orthogonal formation and degradation of a polymer network based on disulfone crosslinks.

In summary, the present thesis provides substantial advances in the fields of adhesives and (reversible) debonding on demand polymer networks. As a future perspective, the novel dental adhesive has to be tested in terms of its toxicity. If the system proves to be not harmful to health, final application tests can be carried out with probands to demonstrate the feasibility. Moreover, the thermodegradable adhesive can be tested for numerous other applications, including construction work. The adhesive could for example be employed as chemical anchor for the construction of buildings. Chemical anchors are employed for the reinforcement of concrete and brickwork. Using the thermodegradable adhesive would result in a facile separation when the building is deconstructed, easing the work of the construction workers and, more importantly, making it possible to reuse certain parts. Especially the possibility of recycling/reusing the joint parts, seems to be a significant advance of the invented system over state of the art adhesives. Therefore, future work also has to focus on reducing the production costs, in order to make a large scale application economically conceivable.

Scientifically, the effect of the substitution of the dithioester needs to be studied in greater detail in order to be able to provide a suitable HDA pair for each temperature regime, which would not only be advantageous for adhesives but also for thermosets based on the HDA system. The ability to post-modify the shape of a thermoset *via* heating is a highly useful tool, as typically thermosets are not alterable once they are formed. Hence, future applications could stem from the possibility to reshape the material at any given time, with the material providing thermoset characteristics at ambient temperature. Also in terms of recyclability, such a thermoset is advantageous, as usually thermosets cannot be recycled easily. Therefore, the HDA concept is an environmentally friendly alternative.

For the universal tool for a photochemically degradable polymer network, the broad applicability of the disulfone-based system needs be outlined in detail by employing various network additives, which release the nucleophile at different wavelength, ranging from the visible to the UV spectra of light.

7

Experimental Section

7.1 Materials

1,3,5-Benzenetricarbonyl trichloride (98%, Sigma Aldrich), 1,5,7-triazabicyclo[4.4.0]dec-5-ene (TBD, 98%, Alfa Aesar), 1,10-dibromodecane (97%, Acros), 1-ethyl-3-(3-dimethylaminopropyl)carbodiimide hydrochloride (EDC*HCl, ≥99%, Roth), 1-iodopropane (99%, Sigma Aldrich), 2-hydroxyethyl methacrylate (HEMA, 97%, stabilized with MEHQ, Acros), 2-nitrobenzyl alcohol (97%, Sigma Aldrich), 2-phenoxy ethanol (≥ 99%, Sigma Aldrich), 2-nitrobenzyl bromide (98%, Sigma Aldrich), 3-bromo-1-propanol (97%, Alfa Aesar), 4-bromobutyryl chloride (97%, Alfa Aesar), 4-bromomethylbenzoic acid (>95.0%, TCI chemicals), 4-(dimethylamino)pyridine (DMAP, ≥99%, Sigma Aldrich), benzoin (98%, Sigma Aldrich), benzyl methacrylate (BzMA, 96%, stabilized with MEHQ, Sigma Aldrich), n-butyl methacrylate (nBMA, 99%, stabilized with MEHQ, Sigma Aldrich), carbon disulfide (99.9%, VWR), chloroform (99.9%, Acros Organics), chlorosulfonic acid (97%, Acros Organics), cyclohexyl isocyanate (98%, Sigma Aldrich), cyclopentadienylsodium (NaCp, 2.0M in THF, Sigma Aldrich), dichloromethane (DCM, 99.8 %, dry, Acros), diethylamine (≥99%, Sigma Aldrich), diethyl phosphite (>95.0%, Fluka), dimethyl carbonate (DMC, 99%, Sigma Aldrich), dimethyl sulfoxide (DMSO, ≥99%, Sigma Aldrich), ethyl acetate (EA, 98%, VWR), ethylene glycol (99%, Sigma Aldrich), isobornyl methacrylate (iBoMA, 85-90%, stabilized with MEHQ, Acros), isopropyl methacrylate (iPrMA, >98.0%, stabilized with MEHQ, TCI chemicals), methacryloyl chloride (97%, Sigma Aldrich), N,N-dimethylformamide (DMF, 99%, Merck), n-butyl methacrylate (99%, tci), n-hexane (98%, VWR), oxalyl chloride (98%, Sigma Aldrich), phosgene (15wt.% solution in toluene, Sigma Aldrich), potassium carbonate (99%, Sigma Aldrich), pyridine (anhydrous, 99.8%, Sigma Aldrich), samarium (99.9%, abcr), sodium hydride (95%, Sigma Aldrich), tetrahydrofuran (THF, 99.5%, Acros), toluene

(99.9%, Acros Organics) triethylamine (≥99%, Sigma Aldrich), trifluoroacetic acid (TFA, 99%, Sigma Aldrich) and zinc chloride (≥98%, Sigma Aldrich) were used as received. 1,10-decanediol dimethacrylate (D_3MA), urethane dimethacrylate (UDMA), bisphenole -A- glycidyl methacrylate (bisGMA) and Ivocerin® were kindly provided by Ivoclar Vivadent AG. PTMBA was kindly provided by Evonic Industries.

7.2 Instrumentation

NMR spectroscopy

The structures of the synthesized compounds were characterized *via* ^{1}H and ^{13}C NMR spectroscopy using a Bruker Avance III 400 MHz spectrometer for hydrogen nuclei and 100 MHz for carbon nuclei. Standard measurements were carried out in $CDCl_3$ or DMSO-d_6 and measured with 16 scans. For the linear polycarbonates, measurements were conducted in DMSO-d_6 with 128 scans.

High-temperature measurements were carried out using toluene-d_8. The temperatures were kept constant by continuous heating with a thermal element (20% heating power), while cooling was performed with a compressed air stream (400 L·h^{-1}).

Electrospray-Ionisation-Mass-Spectrometry (ESI-MS)

High-resolution mass spectra (HRMS) were obtained via electron spray ionization mass spectrometry using a Q Exactive (Orbitrap) mass spectrometer (Thermo Fisher Scientific, San Jose, CA, USA) equipped with an HESI II probe. The instrument calibration was carried out in the m/z range 74 - 1822 using calibration solutions from Thermo Scientific. A constant spray voltage of 4.7 kV and a dimensionless sheath gas of 5 were applied. The capillary temperature and the S-lens RF level were set to 320 °C and 62.0. The samples were dissolved in a THF:MeOH mixture (3:2 volume ratio) containing 100 µmol of sodium triflate and injected with a flow of 5 µL min^{-1}.

UV/Vis spectroscopy

UV-visible spectroscopy was performed using a Cary 300 Bio spectrophotometer (Varian) featuring a thermostatted sample cell holder. Absorption spectra of the samples were recorded with a resolution of 1 nm and a slit width of 2 nm in a quartz glass cuvette (VWR, quartz glass

SUPRASIL®). The absorption spectra of the DiHDA-core were measured in DMSO (concentration: 10 mg·mL^{-1}) from 200 nm to 800 nm at temperatures ranging from 25 °C to 140 °C. For the debonding measurements of the networks, the polymerization was performed in the quartz glass cuvettes, ensuring a defined network thickness of 1 mm. The absorption spectra of the networks were recorded from 400 nm to 800 nm at temperatures ranging from 25 °C to 140 °C. From 25 °C to 100 °C the internal heating block of the UV-Vis spectrophotometer was used to temper the samples. To achieve temperatures above 100 °C an external oil bath was used. Afterwards, the samples were placed in the UV-Vis spectrophotometer for analysis. As the catalyst required for the HDA reaction is removed prior to the studies, the back reaction to the HDA product is disabled, resulting in a constant absorption.

For the linear polycarbonates measurements were carried out in DMF (concentration: 10 mg mL^{-1}) in a temperature range between 20 and 100 °C, with a heating/cooling rate of 5 °C min^{-1}.

Rheology

Instrumental setup

The rheology experimental setup is a TA-Instruments Advanced Rheometric Expansion System Generation 2 (ARES G2), which is a strain controlled rotational rheometer using a separate motor and transducer technology. The motor is an air bearing supported, brushless DC motor, where position and rate are measured with an optical encoder including a position feedback loop. The rheometer consists of a Force Rebalance Transducer (FRT), which is suitable for measuring torques between 50 nN·m and 200 mN·m as specified by the manufacturer. The installed brushless DC motor with jeweled air bearings is capable of applying rotational angular velocities from 10^{-6} rad/s to 300 rad/s and deformation amplitudes of 1 µrad to an unlimited maximum. The applied oscillation frequency can be varied between 10^{-7} rad/s and 628 rad/s. For temperature control, a force convection oven (FCO) with nitrogen supply was employed.

The temperature dependent measurements were carried out with rectangular specimen (length: 25 mm, width: 5 mm, diameter: 1 mm) employing an axial force of 0.3 N, an excitation frequency of 1 Hz and a deformation of 0.1% in a temperature range of 25 °C to 130 °C (heating rate: 1.5 K/min).

Sample preparation

The networks were prepared via photochemically induced free radical polymerization using 0.2 wt.% Ivocerin® as an initiator. The samples were irradiated with 3 Osram Dulux Blue lamps (3 x 18 W, 250 mW/cm^2) for 30 min.

Size exclusion chromatography (SEC)

SEC measurements were performed on a Polymer Laboratories (Varian) PL-GPC 50 Plus Integrated System, comprising an autosampler, a PLgel 5 mm bead- size guard column (50 x 7.5 mm), one PLgel 5 mm Mixed E column (300 x 7.5 mm), three PLgel 5 mm Mixed C columns (300 x 7.5 mm) and a differential refractive index detector using THF as the eluent at 35 °C with a flow rate of 1 mL min^{-1}. The GPC system was calibrated using linear poly(styrene) standards ranging from 476 to 2.5·10^6 g mol^{-1} and linear poly(methyl methacrylate) standards ranging from 700 to 2·10^6 g mol^{-1}. The resulting molar mass distributions were determined by universal calibration using Mark-Houwink parameters for PMMA (K = 0.000128 dL g^{-1}, α = 0.69).[327]

Pull-off Tests

Preparation of test abutments and crowns

Test abutments (geometry of a truncated cone, diameter top area 4 mm, diameter bottom area 6 mm, height 3 mm) and corresponding test crowns were milled from zirconium oxide. Construction of the crown was done so that placing it on the test abutment resulted in a cement gap of 0.2 mm. Crowns and abutments were sandblasted (110 µm Al_2O_3, 1 bar), cleaned with ultrasonic sound in deionized water for 2 min, dried and prepared for cementation priming with Monobond Plus® (Ivoclar Vivadent AG, handling according to instructions for use: application, wait for 60 s, drying with oil-free air).

Cementation

For cementation, two different self-curing two-component mixtures (mixing ratio 1:1 wt./wt.) with 20 mol% of either the DiHDA-linker (1) or a non-degradable dimethacrylate (bisGMA, 2) were prepared. The first mixture of 1 contained 25.06% nBMA, 0.01% 2,6-di-tert-butyl-p-cresol (BHT), 60.35% DiHDA-linker and 14.58% BP-50-FT (United Initiators). The second mixture

of 1 contained 33.33% nBMA, 63.67% DiHDA-linker and 3.00% 3,5-di-tert-butyl-N,N-diethyl-aniline (DABA). The first mixture of 2 contained 47.90% nBMA, 47.10% bisGMA and 5.00% BP-50-FT (United Initiators). The second mixture of 2 contained 54.30% nBMA, 42.70% bisGMA and 3.00% DABA (declaration in wt.%). The amounts of BP-50-FT and DABA were chosen to obtain a gel time of 1 min to 5 min. 2 drops of a mixture were thoroughly mixed and applied to the inner face of a primed crown and a primed abutment was put on top. After applying a static load of 2 kg, the excess was removed. After 10 min. the weight was removed, and the test specimens were stored at 23 +/- 2 °C for 3 days. Overall 10 test specimens were prepared from each mixture.

Pull-off tests

For the determination of the pull-off forces, the test specimens of each mixture were randomly divided into 2 groups and mounted to a tensile testing machine (Zwick-Roell Z010). The test specimens of the first group were tempered in a water bath at 23 °C for 1 min. prior to the measurement. For the second group, the water bath was heated to 80 °C. The crowns were pulled-off the abutments in the water bath, with a constant crosshead speed of 1.0 mm/min and the maximum force was determined.

7.3 Synthetic Protocols

7.3.1 Debonding on Demand for Dental Adhesive

Synthesis of 4-((((Diethoxyphosphoryl)carbonothioyl)thio)methyl)-benzoic acid (PDT)

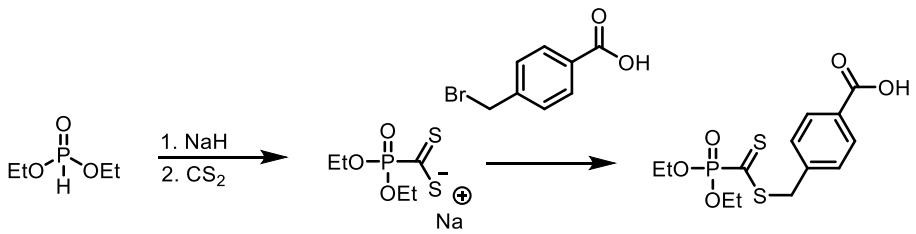

Scheme 40 Preparation of PDT.

A solution of 5.3 mL diethyl phosphite (1.0 eq., 41 mmol, 5.7 g) in 40 mL dry THF was added to a stirred suspension of 1.5 g NaH (1.5 eq., 62 mmol) in 20 mL dry THF at ambient temperature. After completion of the H_2 formation, the reaction mixture was heated to reflux for

15 min. Subsequently, the solution was cooled to -90 °C and 12.3 mL CS_2 (5.0 eq., 205 mmol, 15.6 g) were added dropwise. The reaction mixture was stirred for 2 h. After the addition of 750 mL THF, to facilitate the stirring, a solution of 10.0 g 4-bromomethylbenzoic acid (1.1 eq., 46 mmol) in 75 ml THF was added dropwise at ambient temperature. After stirring for 16 h, the solvent was removed from the purple reaction mixture. DCM and H_2O are added in a ratio of 1:1 until all residue was dissolved. The water phase is washed with DCM and the combined organic layers are dried over Na_2SO_4. After removal of the solvent, the crude product was purified via column chromatography (cyclohexane/EA/acetic acid = 1/1/0.01) to give a purple solid of PDT (yield: 30%, 4.3 g, 12.3 mmol).

^{1}H NMR (400 MHz, $CDCl_3$, δ, ppm): 1.37 (t, 6H, OCH_2CH_3), 4.22 - 4.34 (m, 4H, OCH_2CH_3), 4.54 (s, 2H, SCH_2), 7.41 (d, 2H, ArH), 8.05 (d, 2H, ArH), 10.50 (bs, 1H, COOH). ^{13}C NMR (101 MHz, $CDCl_3$, δ, ppm): 16.40 (OCH_2CH_3), 40.00 (SCH_2), 65.14 (OCH_2CH_3), 129.34 (C_{ar}), 129.53 (C_{ar}), 130.79 (C_{ar}), 140.04 (C_{ar}), 170.73 (COOH), 226.92 (PC=S), 228.66 (PC=S) (see Figure 27 and 28).

Synthesis of 1,10-dicyclopentadienyl decane (DiCp-linker)

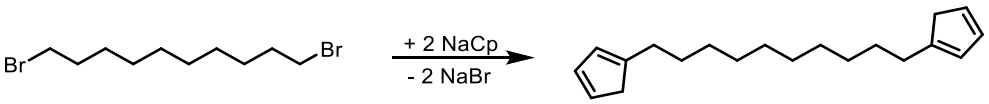

Scheme 41 Synthesis of DiCp-linker.

To a cooled solution of 6.0 g 1,10-dibromodecane (1.0 eq., 20 mmol) in 30 mL dry THF, 20 mL of a 2M solution of NaCp in THF (2.0 eq., 40 mmol) were added at -5 °C. After stirring for 1 h at -5 °C, the reaction mixture was allowed to warm to ambient temperature and stirred over-night. Subsequently, the suspension was filtered over silica gel using 300 mL EA. The solvent was removed and the residue was taken up with n-hexane. The solution was filtered over silica gel using 1.5 L n-hexane. After removal of the solvent, a clear and viscous liquid of the DiCp-linker was obtained (yield: 87%, 4.7 g, 17.4 mmol).

^{1}H NMR (400 MHz, $CDCl_3$, δ, ppm): 1.29 - 1.45 (m, 12H, $(CH_2)_3CH_2CH_2Cp$), 1.50 - 1.65 (m, 4H, $(CH_2)_3CH_2CH_2Cp$), 2.40 - 2.50 (m, 4H, $(CH_2)_3CH_2CH_2Cp$), 2.97 (d, 4H, $CH_{2,Cp}$), 6.05 - 6.53 (m, 6H, CpH). ^{13}C NMR (101 MHz, $CDCl_3$, δ, ppm): 29.02 (CH_2), 29.62 (CH_2), 29.68 (CH_2), 29.77 (CH_2), 29.91 (CH_2), 30.01 (CH_2), 30.87 (CH_2**C**H_2Cp), 41.27 (C_{Cp}), 43.42 (C_{Cp}), 125.72 (C_{Cp}), 126.26 (C_{Cp}),

130.36 (C_{Cp}), 132.56 (C_{Cp}), 133.58 (C_{Cp}), 134.95 (C_{Cp}), 147.49 ($CH_2CH_2\mathbf{C}_{Cp}$), 150.21 ($CH_2CH_2\mathbf{C}_{Cp}$) (see Figure 31 and 32).

Synthesis of 2-(methacryloyloxy)ethyl 4-((((diethoxyphosphoryl)carbonothioyl)thio)methyl)benzoat (MA-PDT))

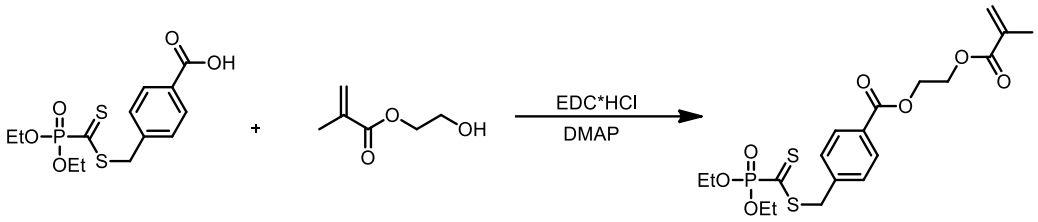

Scheme 42 Synthesis of MA-PDTMBA.

To a solution of 2.0 g PDT (1.0 eq., 5.74 mmol) and 1.05 mL HEMA (1.5 eq., 8.61 mmol, 1.12 g) in dry DCM, a solution of 2.2 g ECD*HCl (2.0 eq., 11.5 mmol) and 0.14 g DMAP (0.2 eq., 1.15 mmol) in dry DCM was added at ambient temperature. After stirring for 20 h, the solution was washed with $NaHCO_3$ solution and brine. The organic layer was dried over Na_2SO_4 and the solvent was removed. The crude product was purified via column chromatography (cyclohecane/EA = 1/1) to yield a purple liquid of MA-PDT (yield: 70%, 1.85 g, 3.90 mmol).

^{1}H NMR (400 MHz, $CDCl_3$, δ, ppm): 1.37 (t, 6H, OCH_2CH_3), 1.90 (s, 3H, CH_3C_{MA}), 4.22 - 4.34 (m, 4H, OCH_2CH_3), 4.42 - 4.58 (m, 4H, OCH_2CH_2O), 4.52 (s, 2H, SCH_2), 5.55 (d, 1H, $CCH_{2,trans}$), 6.10 (d, 1H, $CCH_{2,cis}$), 7.37 (d, 2H, ArH), 7.98 (d, 2H, ArH). ^{13}C NMR (101 MHz, $CDCl_3$, δ, ppm): 16.40 ($OCH_2\mathbf{C}H_3$), 18.40 ($C_{MA}\mathbf{C}H_3$), 40.00 (SCH_2), 62.60 ($O\mathbf{C}H_2\mathbf{C}H_2O$), 65.14 ($O\mathbf{C}H_2CH_3$), 126.27 ($\mathbf{C}H_2C_{MA}$), 129.48 ($C_{ar}$), 129.65 ($C_{ar}$), 130.28 ($C_{ar}$), 136.03 ($C_{MA}$), 139.50 ($C_{ar}$), 165.90 ($C_{ar}\mathbf{C}$=O), 167.26 ($C_{MA}\mathbf{C}$=O), 227.18 (PC=S), 228.93 (PC=S) (see Figure 29 and 30).

Synthesis of the DiHDA-core

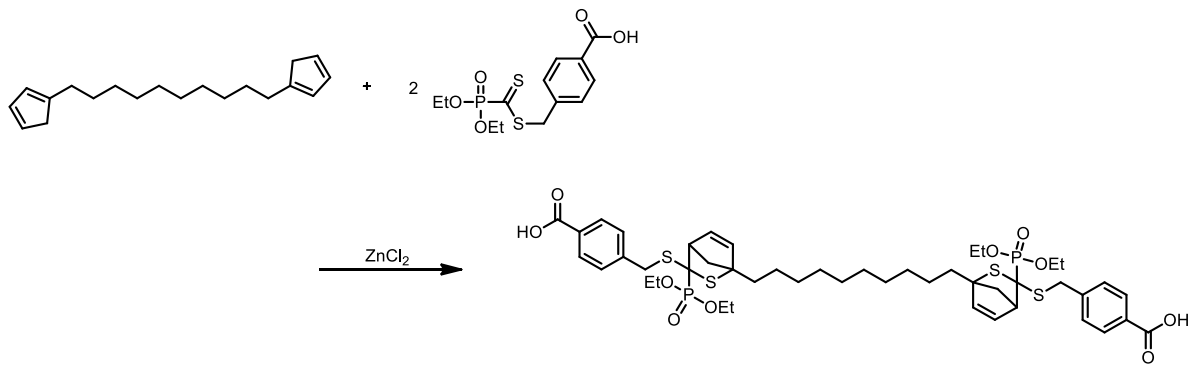

Scheme 43 Synthesis of the DiHDA-core.

3.0 g PDT (2.00 eq., 8.61 mmol), 1.16 g 1,10-DiCp-decane (1.00 eq., 4.31 mmol) and 63 mg $ZnCl_2$ (0.10 eq., 0.46 mmol) were dissolved in EA and stirred at ambient temperature for 30 min. Subsequently, the organic layer was washed with water. After removal of the solvent a white solid of the DiHDA-core was obtained (yield: 99%, 4.13 g, 4.30 mmol).

^{1}H NMR (400 MHz, $CDCl_3$, δ, ppm): 1.25 - 1.65 (m, 28H, OCH_2CH_3, $C_{HDA}CH_2(CH_2)_4$), 1.95 - 2.18 (m, 4H, $CH_{2,HDA\text{-}Brücke}$), 2.18 - 2.50 (m, 4H, $C_{HDA}CH_2(CH_2)_4$), 3.35 - 3.68 (m, 2H, CH_{HDA}), 4.00 - 4.25 (m, 8H, OCH_2CH_3), 4.26 - 4.44 (m, 4H, SCH_2C_{ar}), 5.52 - 5.60 (m, 1H, $CH_{HDA\text{-}Db.}$), 5.95 - 6.03 (2H, $CH_{HDA\text{-}Db.}$), 6.28 - 6.33 (m, 1H, $CH_{HDA\text{-}Db.}$), 7.42 (d, 4H, ArH), 7.95 (d, 4H, ArH), 10.10 (bs, 2H, COOH). ESI-MS: *m/z* calculated 966.29, found 966.29 (see Figure 33 and 34).

Synthesis of the DiHDA-linker

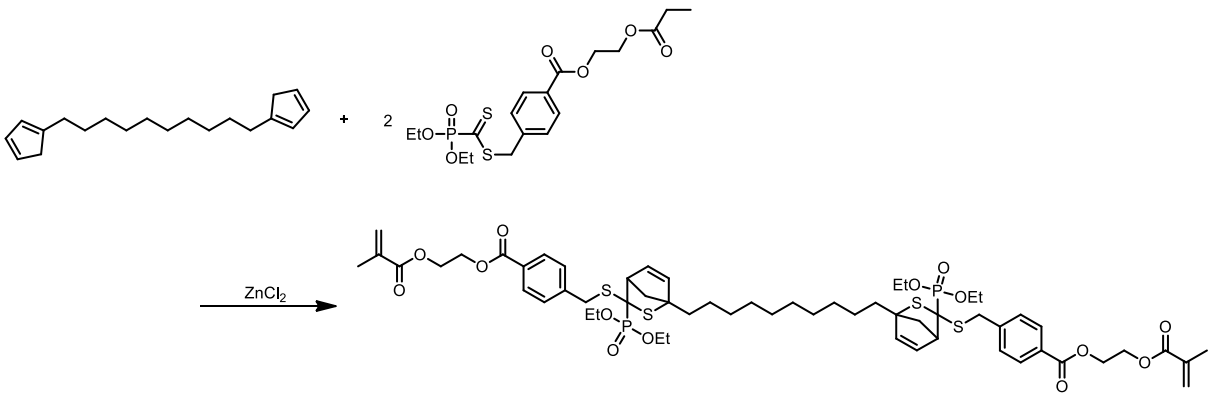

Scheme 44 Synthesis of the DiHDA-linker.

0.59 g 1,10-DiCp-decane (1.0 eq., 2.17 mmol), 2.0 g MA-PDT (2.0 eq., 4.34 mmol) and 30 mg $ZnCl_2$ (0.1 eq., 0.22 mmol) were dissolved in EA and stirred at ambient temperature for 30 min. Subsequently, the organic layer was washed with water. After removal of the solvent, the DiHDA-linker was obtained as a highly viscous liquid (yield: 99%, 2.56 g, 2.16 mmol).

^{1}H NMR (400 MHz, $CDCl_3$, δ, ppm): 1.25 - 1.65 (m, 28H, OCH_2CH_3, $C_{HDA}CH_2(CH_2)_4$), 1.94 (s, 6H, CH_3C_{MA}), 1.95 - 2.18 (m, 4H, $CH_{2,HDA\text{-}Brücke}$), 2.18 - 2.50 (m, 4H, $C_{HDA}CH_2(CH_2)_4$), 3.35 - 3.68 (m, 2H, CH_{HDA}), 4.00 - 4.25 (m, 8H, OCH_2CH_3), 4.26 - 4.44 (m, 4H, SCH_2C_{ar}), 4.45 – 4.58 (m, 8H, OCH_2CH_2O), 5.52 - 5.60 (m, 1H, $CH_{HDA\text{-}Db.}$), 5.58 (d, 2H, $CCH_{2,trans}$), 5.95 - 6.03 (2H, $CH_{HDA\text{-}Db.}$), 6.13 (d, 2H, $CCH_{2,cis}$), 6.28 - 6.33 (m, 1H, $CH_{HDA\text{-}Db.}$), 7.42 (d, 4H, ArH), 7.95 (d, 4H, ArH). ESI-MS: *m/*z calculated 1190.39, found 1190.37 (see Figure 35 and 36).

Synthesis of DiHDA2

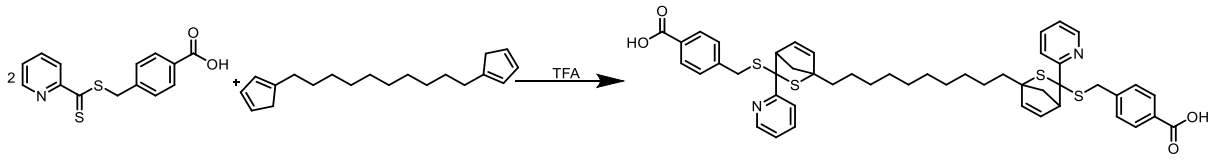

Scheme 45 Synthesis of DiHDA2.

1.00 g 1,10-DiCp-decane (1.0 eq., 3.70 mmol), 2.14 g MA-PDT (2.0 eq., 7.40 mmol) were dissolved in EA. 0.84 g TFA (2.0 eq., 7.40 mmol) were added dropwise and the solution was stirred at ambient temperature for 30 min. Subsequently, the organic layer was washed with water. After removal of the solvent, DiHDA2 was obtained as a highly viscous liquid (yield: 99%, 3.12 g, 3.68 mmol).

^{1}H NMR (400 MHz, DMSO-d_6, δ, ppm): 0.89 – 1.39 (m, 16H, $C_{HDA}CH_2(C\mathbf{H}_2)_4$), 1.39 – 1.55 (m, 4H, $C_{HDA}C\mathbf{H}_2(CH_2)_4$), 1.85 – 2.09 (m, 4H, $CH_{2,HDA\text{-}bridge}$), 3.41 – 3.60 (m, 2H, CH_{HDA}), 3.84 – 4.12 (m, 4H, SCH_2C_{ar}), 5.58 -6.46 (m, 4H, $CH_{HDA\text{-}Db.}$), 7.15 (d, 4H, $H_{Ar(Bz)}$), 7.21 – 7.50 (m, 4H, $H_{Ar(Py)}$), 7.70 – 7.85 (m, 6H, $H_{Ar(Bz)}$, $H_{Ar(Py)}$), 8.45 – 8.59 (m, 2H, $H_{Ar(Py)}$), 11.5 – 13.0 (COOH). ESI-MS (+H^+): *m/*z calculated 849.2883, found 849.2549 (see Figure 37).

Synthesis of propyl (diethoxyphosphoryl)methanedithioate (PDT2)

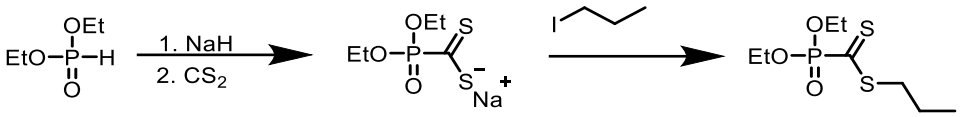

Scheme 46 Synthesis of PDT2.

A solution of 4.4 mL diethyl phosphite (1.0 eq. 33.8 mmol, 4.7 g) in 30 mL dry THF is added to a stirred suspension of 2.0 g NaH (60 % in Öl, 1.5 eq., 50.6 mmol) in 30 mL dry THF at ambient temperature. After completion of the H_2 formation, the reaction mixture is heated to reflux for 15 min. Subsequently, the solution is cooled to -90 °C and 10.2 mL CS_2 (5.0 eq., 170 mmol, 12.9 g) are added dropwise. It is stirred for 4 h, whereat the reaction mixture turns brown. A solution of 10.0 mL 1-Iodopropan (1.0 eq. 33.8 mmol, 17.4 g) in 30 mL dry THF is added dropwise at ambient temperature. The reaction mixture is heated to 40 °C for 48 h. Afterwards, the precipitate is filtered off and the solvent is evaporated. DCM and H_2O are added in a ratio of 1:1 until all residue is dissolved. The water phase is washed with DCM and the combined organic layers are dried over Na_2SO_4. After removal of the solvent, the crude product is purified via column chromatography (cyclohexane : EA = 2:1) to give a purple liquid of PDT2 (2.6 g, 10.1 mmol, 30% yield). ^{1}H NMR (400 MHz, $CDCl_3$, δ, ppm): 0.96 (t, 3H, $SCH_2CH_2C\mathbf{H}_3$), 1.29 (t, 6H, $OCH_2C\mathbf{H}_3$), 1.66 (sx, 2H, $SCH_2C\mathbf{H}_2CH_3$), 3.19 (t, 2H, $SC\mathbf{H}_2CH_2CH_3$), 4.09 – 4.25 (m, 4H, $OC\mathbf{H}_2CH_3$). ^{13}C NMR (101 MHz, $CDCl_3$, δ, ppm): 13.56 ($SCH_2CH_2\mathbf{C}H_3$), 16.20 ($OCH_2\mathbf{C}H_3$), 20.23 ($SCH_2\mathbf{C}H_2CH_3$), 37.47 ($S\mathbf{C}H_2CH_2CH_3$), 64.57 ($O\mathbf{C}H_2CH_3$), 228.16 (PCS), 229.91 (PCS) (see Figure 38 and 39).

Synthesis of DiHDA3

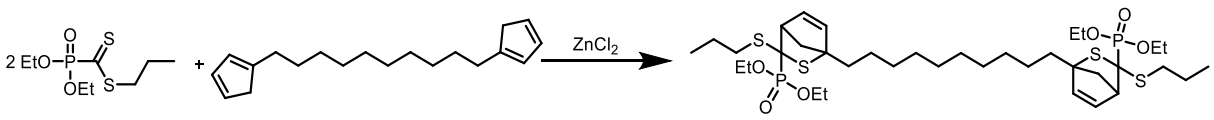

Scheme 47 Synthesis of DiHDA3.

1.00 g 1,10-DiCp-decane (1.0 eq., 3.70 mmol), 1.90 g PDT2 (2.0 eq., 7.40 mmol) and 50 mg $ZnCl_2$ (0.1 eq., 0.37 mmol) were dissolved in EA and stirred at ambient temperature for 30 min. Subsequently, the organic layer was washed with water. After removal of the solvent, DiHDA3 was obtained as a highly viscous liquid (yield: 99%, 2.88 g, 3.68 mmol).

^{1}H NMR (400 MHz, DMSO-d_6, δ, ppm): 1.00 (t, 6H, $SCH_2CH_2C\mathbf{H}_3$), 1.19 – 1.41 (m, 28H, $C_{HDA}CH_2(C\mathbf{H}_2)_4$, $OCH_2C\mathbf{H}_3$), 1.62 (sx, 4H, $SCH_2C\mathbf{H}_2CH_3$), 1.72 – 2.04 (m, 4H, $C_{HDA}C\mathbf{H}_2(CH_2)_4$), 2.10 -2.45 (m, 4H, $CH_{2,HDA\text{-}bridge}$), 2.85 – 3.51 (m, 4H, $SC\mathbf{H}_2CH_2CH_3$), 3.92 – 4.00 (m, 2H, CH_{HDA}), 4.10 – 4.51 (m, 8H, $OC\mathbf{H}_2CH_3$), 5.55 – 6.45 (m, 4H, $CH_{HDA\text{-}Db.}$) (see Figure 40).

7.3.2 Dynamic Covalent Polycarbonate Networks

Synthesis of 2-hydroxyethyl 4-((((diethoxyphosphoryl)carbonothioyl)thio)methyl)benzoate (PDT-OH)

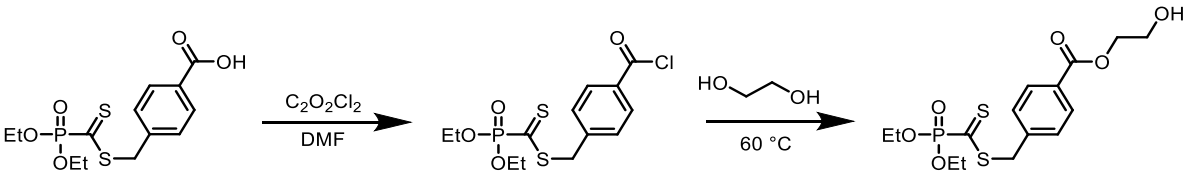

Scheme 48 Synthesis of PDT-OH.

1.0 g of PDT (1.0 eq., 2.87 mmol) was dissolved in 20 ml of dry DCM. After the addition of 0.1 mL dry DMF, 0.27 mL of oxalyl chloride (1.1 eq., 3.16 mmol, 400 mg) were added dropwise and the reaction mixture was stirred for 2 h at ambient temperature. After removal of the solvent, 20 mL ethylene glycol were added and the solution was heated to 60 °C for 16 h. DCM was added and the organic phase was washed with water, $NaHCO_3$ solution and brine. The solvent was removed and the crude product was purified via column chromatography (cyclohexane/EA 1/1) to yield a purple liquid of PDT-OH (yield: 70%, 740 mg, 2.01 mmol).

^{1}H NMR (400 MHz, $CDCl_3$, δ, ppm): 1.34 (t, 6H, OCH_2CH_3), 3.88 – 3.95 (m, 2H, OCH_2CH_2OH), 4.17 - 4.32 (m, 4H, OCH_2CH_3), 4.38 - 4.45 (m, 2H, OCH_2CH_2OH), 4.48 (s, 2H, SCH_2), 7.35 (d, 2H, ArH), 7.98 (d, 2H, ArH). ESI-MS (+Na^+): *m/z* calculated 415.0409, found 415.0410 (see Figure 41).

Synthesis of the DiHDA-diol

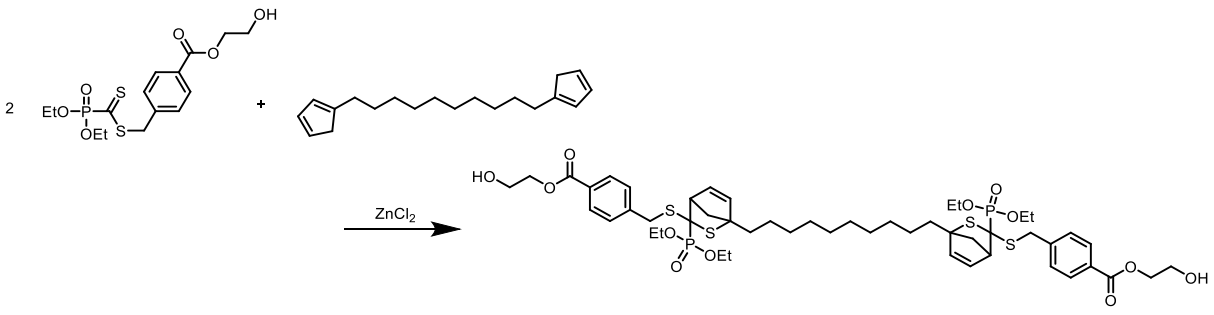

Scheme 49 Synthesis of the DiHDA-diol.

1,0 g of PDT-OH (2.0 eq., 2.66 mmol), 360 mg of DiCp-linker (1.0 eq., 1.33 mmol) and 20 mg $ZnCl_2$ (0.1 eq., 0.13 mmol) were dissolved in 20 mL EA and stirred for 20 minutes. After washing with water, the solvent was removed to yield the DiHDA-diol as a colorless and highly viscous liquid (yield: 99%, 1.35 g, 2.65 mmol).

^{1}H NMR (400 MHz, DMSO-*d6*, *δ*, ppm): 1.12 - 1.35 (m, 24H, OCH_2CH_3, $C_{HDA}CH_2CH_2(CH_2)_3$), 1.37 – 1.58 (m, 4H, $C_{HDA}CH_2CH_2(CH_2)_3$ 1.65 – 1.99 (m, 4H, $C_{HDA}CH_2CH_2(CH_2)_3$), 2.09 - 2.41 (m, 4H, $CH_{2,HDA\text{-}bridge}$), 3.32 –3.43 (m, 2H, CH_{HDA}), 3.65 – 3.73 (m, 4H, SCH_2C_{ar}), 4.02 - 4.23 (m, 4H, OCH_2CH_2OH), 4.24 - 4.33 (m, 8H, OCH_2CH_3), 4.39 – 4.50 (m, 4H, OCH_2CH_2OH), 5.43 – 6.42 (m, 4H, $CH_{HDA\text{-}Db.}$), 7.50 (d, 4H, ArH), 7.93 (d, 4H, ArH). ESI-MS (+Na^+): *m/*z calculated 1077.3274, found 1077.3289 (see Figure 42 and 43).

Synthesis of the HDA containing linear polycarbonates (DiHDA-PC)

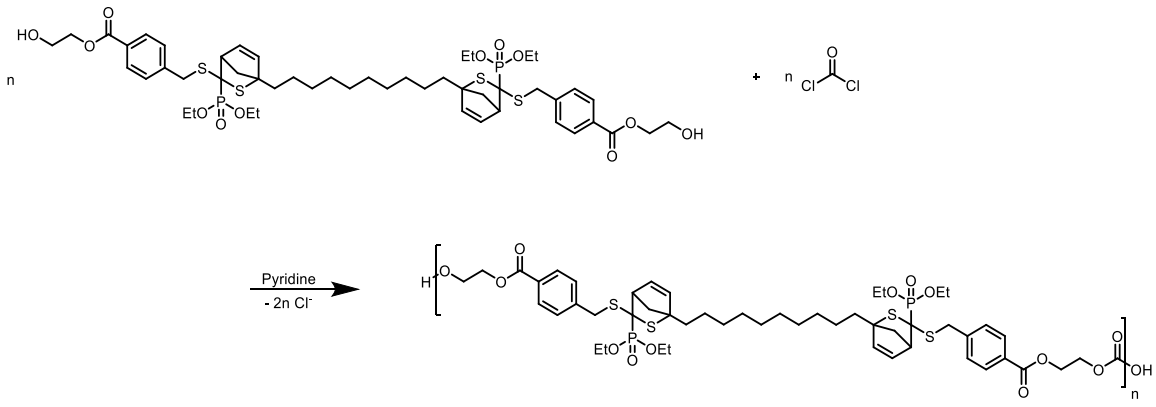

Scheme 50 Synthesis of the DiHDA-PCs.

Different ratios of the HDA-diol and phosgene (15 wt.% in toluene, ratios between 1.00:1.00 for P4, to 1.00:0.90 for P1) were dissolved in dry DCM. Dry pyridine (2.0 eq. compared to diol) was added and the reaction mixture was stirred at ambient temperature for 6 h. Subsequently, the polymer was precipitated in n-hexane and dried under reduced pressure (yield: 90 – 98%) ^{1}H NMR (400 MHz, DMSO-*d6*, δ, ppm): 1.10 - 1.38 (m, OCH_2CH_3, $C_{HDA}CH_2CH_2(CH_2)_3$), 1.38 – 1.60 (m, $C_{HDA}CH_2CH_2(CH_2)_3$ 1.70 - 2.00 (m, $C_{HDA}CH_2CH_2(CH_2)_3$), 2.08 - 2.38 (m, $CH_{2,HDA\text{-}bridge}$), 3.38 –3.45 (m, CH_{HDA}), 3.65 – 3.75 (m, SCH_2C_{ar}), 3.88 – 4.01 (m, OCH_2CH_2OH), 4.02 - 4.23 (m, OCH_2CH_3), 4.32 - 4.33 (m, $OCH_2CH_2OC(O)$), 4.40 – 4.50 (m, OCH_2CH_2OH), 4.92 (t, $OCH_2CH_2OC(O)$) 5.43 – 6.42 (m, $CH_{HDA\text{-}Db.}$), 7.50 (d, ArH), 7.93 (d, ArH) (see Table 7 and Figure 44).

Synthesis of tris(3-bromopropyl) benzene-1,3,5-tricarboxylate (TriBr-linker)

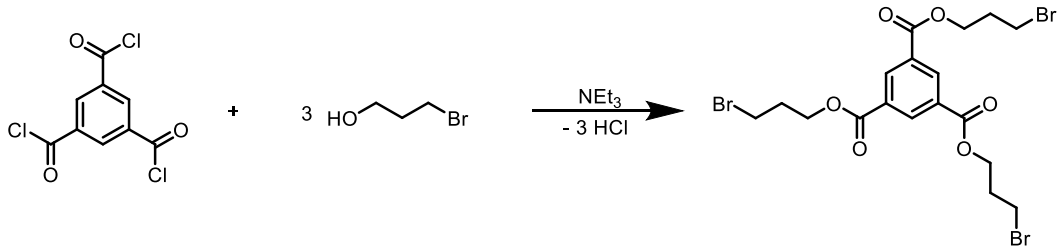

Scheme 51 Synthesis of the TriBr-linker.

6.5 mL 3-bromo-1-propanol (4 eq, 72 mmol, 10 g) were dissolved in dry DCM at 0 °C. 10 ml triethylamine (4 eq, 72 mmol, 7.2 g) were added and the solution was stirred at 0 °C for 30 minutes. Next, a solution of 4.8 g 1,3,5-benzenetricarbonyl trichloride (1.0 eq, 18 mmol) in 20 mL dry DCM were added dropwise. The solution was stirred at 0 °C for 2 h and subsequently at ambient temperature for 16 h. The white precipitant was filtered off and the solution was washed with $NaHCO_3$ solution and brine. After removing the solvent, the crude product was purified via column chromatography (cyclohexane/EA 3/1) to yield the TriBr-linker as a white solid (6.3 g, 62% yield).

^{1}H NMR (400 MHz, $CDCl_3$, δ, ppm): 2.37 (dt, 6H, $CH_2BrCH_2CH_2O$), 3.56 (t, 6H, $CH_2BrCH_2CH_2O$), 4.54 (t, 6H, $CH_2BrCH_2CH_2O$), 8.84 (s, 3H, H_{ar}). ^{13}C NMR (101 MHz, $CDCl_3$, δ, ppm): 29.33

($CH_2BrCH_2CH_2O$), 31.76($CH_2BrCH_2CH_2O$), 63.72($CH_2BrCH_2CH_2O$), 131.34 (C_{Ar}), 134.80 (C_{Ar}), 164.84 (CO) (see Figure 45 and 46).

Synthesis of tris(3-cyclopentadienylpropyl) benzene-1,3,5-tricarboxylate (TriCp-linker)

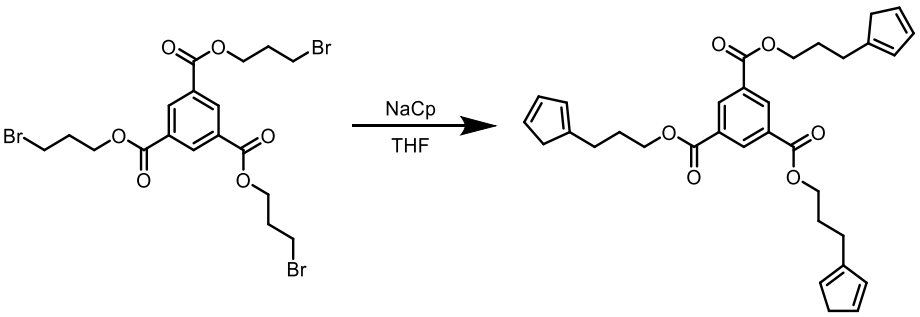

Scheme 52 Synthesis of the TriCp-linker.

To a solution of 10.5 mL of a 2 M NaCp solution in THF (6.0 eq, 21 mmol) in 30 mL dry THF, a solution of 2.0 g TriBr-linker (1.0 eq, 3.5 mmol) in 30 mL dry THF was added dropwise at 0 °C. After stirring for 1 h at 0 °C, the reaction mixture was filtered over silica gel using 200 mL EA. After removal of the solvent the crude product was purified via column chromatography (cyclohexane/EA 6/1) to yield the TriCp-linker as a yellow liquid (yield: 25%, 430 mg, 0.88 mmol). ^{1}H NMR (400 MHz, $CDCl_3$, δ, ppm): 2.08 (dt, 6H, $CH_2BrCH_2CH_2O$), 2.55 (t, 6H, $CH_2BrCH_2CH_2O$), 2.96 (d, 6H, CH_{2Cp}), 4.42 (t, 6H, $CH_2BrCH_2CH_2O$), 6.05 – 6.46 (m, 9H, CH_{Cp}), 8.84 (s, 3H, $H_{ar.}$). ^{13}C NMR (101 MHz, $CDCl_3$, δ, ppm): 26.38 ($CH_2CpCH_2CH_2O$), 27.07 ($CH_2CpCH_2CH_2O$), 27.90 ($CH_2CpCH_2CH_2O$), 28.70 ($CH_2CpCH_2CH_2O$), 41.50 ($CH_2CpCH_2CH_2O$), 43.42 ($CH_2CpCH_2CH_2O$), 65.49($CH_2CpCH_2CH_2O$), 126.78 (C_{Cp}) , 127.25(C_{Cp}), 131.04(C_{Cp}), 131.59(C_{Cp}), 132.54(C_{Cp}), 134.33(C_{Cp}), 134.47(C_{Cp}), 134.60(C_{Cp}), 145.72(C_{Cp}), 148.04(C_{Cp}), 165.19 (CO) (see Figure 47 and 48).

Synthesis of the HDA-triol

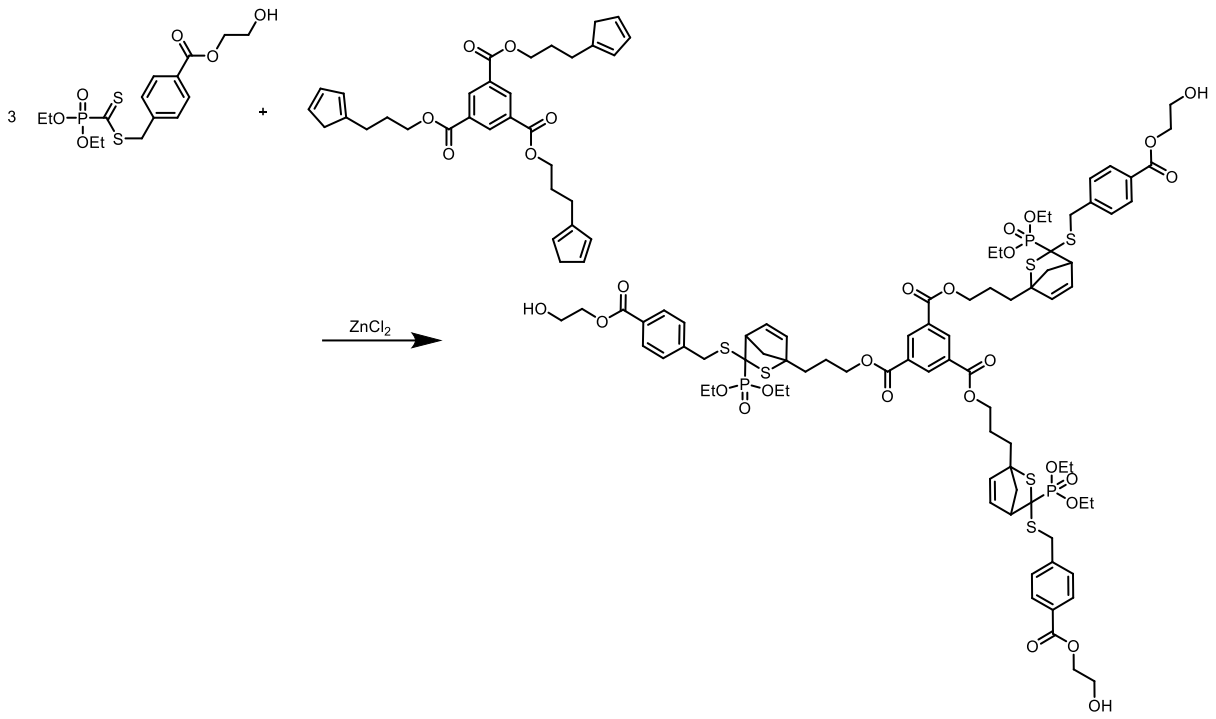

Scheme 53 Synthesis of the HDA-triol.

430 mg TriCp-linker (1.0 eq., 0.8 mmol) were directly added to a solution of 950 mg PDT-OH (3.0 eq., 2.4 mmol) and 2 mg $ZnCl_2$ (0.1 eq., 0.08 mmol) in DCM to prevent dimerization of the Cp moieties. The solution was stirred for 20 minutes at ambient temperature. After washing with water the solvent was removed to yield the HDA-triol as a white solid (yield: 99%, 1.36 g, 0.8 mmol).

^{1}H NMR (400 MHz, $CDCl_3$, δ, ppm): 1.15 – 1.43 (m, 18H, OCH_2CH_3), 1.60 – 1.89 (m, 6H, $C_{HDA}CH_2CH_2CH_2O$), 1.90 - 2.11 (m, 6H, $C_{HDA}CH_2CH_2CH_2O$), 2.15 – 2.45 (m, 6H, $CH_{2,HDA\text{-}bridge}$), 3.01 – 3.34 (m, 3H, CH_{HDA}), 3.35 –3.52 (m, 6H, SCH_2C_{ar}), 3.85 – 4.00 (m, 6H, OCH_2CH_2OH), 4.01 - 4.25 (m, 12H, OCH_2CH_3), 4.26 - 4.54 (m, 12H, OCH_2CH_2OH, $C_{HDA}CH_2CH_2CH_2O$), 5.56 – 6.46 (m, 6H, $CH_{HDA\text{-}Db.}$) 7.50 (d, 6H, H_{Ar}), 7.93 (d, 6H, ArH), 8.84 (s, 3H, $H_{ar.}$). ESI-MS (+Na^+): *m/*z calculated 1727.3956, found 1727.4114 (see Figure 49 and 50).

Synthesis of the HDA-containing polycarbonate network (TriHDA-PC)

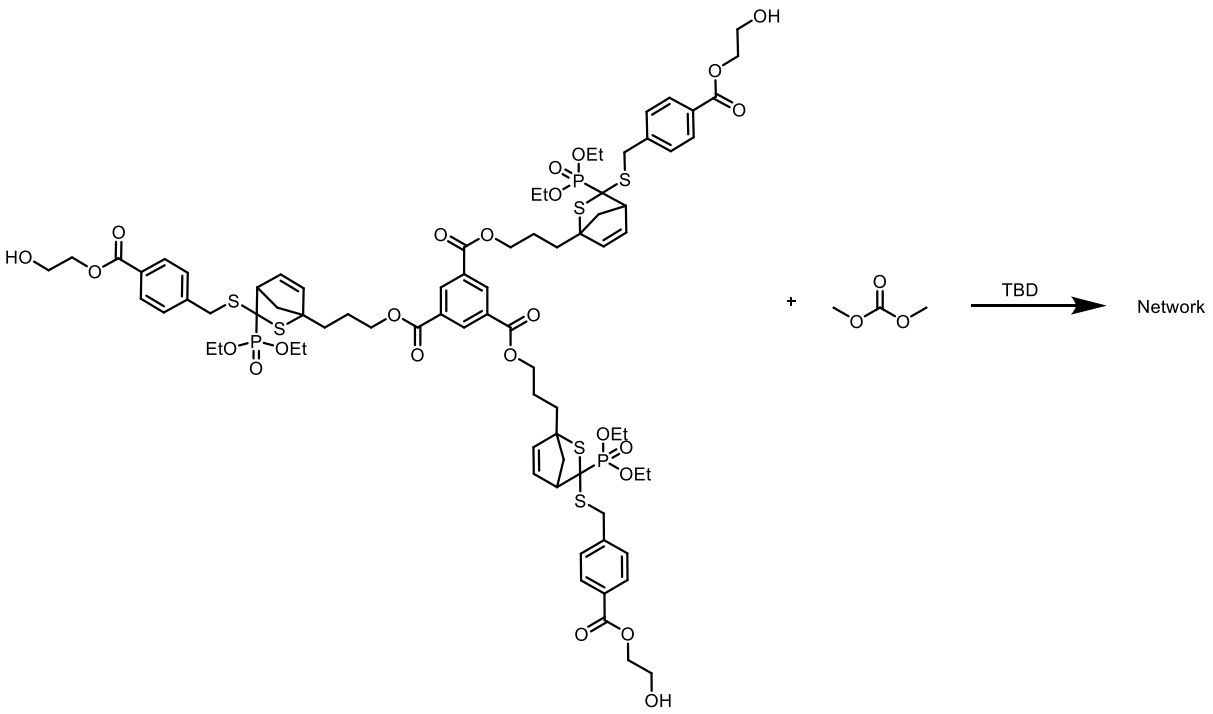

Scheme 54 Synthesis of the TriHDA-PC.

2.0 g HDA-triol (2.0 eq., 1.2 mmol) and 0.15 mL dimethyl carbonate (3.0 eq., 1.8 mmol, 160 mg) were dissolved in 2 mL of DCM. 1.5 mg TBD (0.02 eq., 0.01 mmol) was added and the reaction mixture was heated to 35 °C for 24 h. The formed network was dried under reduced pressure.

7.3.3 Disulfone Network for Photoinduced Degradation

Synthesis of 2-phenoxyethyl methacrylate

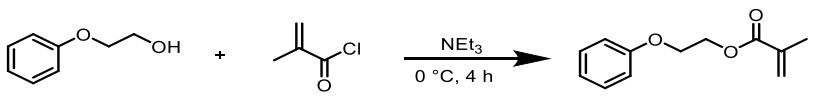

Scheme 55 Synthesis of 2-phenoxyethyl methacrylate.

20 g of 2-phenoxy ethanol (1.0 eq., 145 mmol) were dissolved in 100 ml of dry DCM. After the addition of 40 mL of triethylamine (2.0 eq., 290 mmol), the reaction mixture was cooled to

0 °C and a solution of 17 mL of methacryloyl chloride (1.2 eq., 174 mmol, 18.1 g) in 20 mL of dry DCM was added dropwise. After stirring for 4 h at 0 °C, the white precipitate was filtered off and the solution was washed with water, sodium carbonate solution, 0.1 M HCl, and brine. The crude product was purified via column chromatography (cyclohexane/EA 9/1) to yield 2-phenoxyethyl methacrylate as a colorless oil (yield: 40%, 12 g, 58 mmol).

^{1}H NMR (400 MHz, $CDCl_3$, δ, ppm): 1.98 (s, 3H, CH_3), 4.23 (t, 2H, $COCH_2CH_2OC(O)$), 4.51 (t, 2H, $COCH_2CH_2OC(O)$), 5.60 (s, 1H, $CH_{2,Db}$), 6.16 (s, 1H, $CH_{2,Db}$), 6.93 (d, 2H, H_{Ar}), 6.98 (t, 1H, H_{Ar}), 7.31 (t, 2H, H_{Ar}). ^{13}C NMR (101 MHz, CDCl3, δ, ppm): 18.34 (CH_3), 63.17 ($COCH_2CH_2OC(O)$), 65.92 ($COCH_2CH_2OC(O)$), 114.74 (C_{Ar}), 121.20 (C_{Ar}), 126.05 ($CH_{2,Db}$), 129.57 (C_{Ar}), 136.07 ($CCH_{2,Db}$), 158.63 ($C_{Ar}O$), 167.34 (OC(O)) (see Figure 51 and 52).

Synthesis of 2-(4-(chlorosulfonyl)phenoxy)ethyl methacrylate

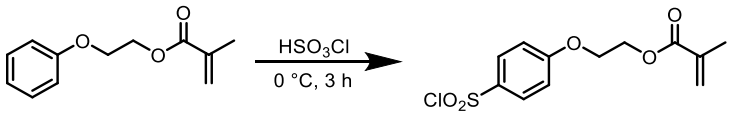

Scheme 56 Synthesis of 2-(4-(chlorosulfonyl)phenoxy)ethyl methacrylate.

12 g of 2-phenoxyethyl methacrylate (1.0 eq., 58 mmol) were dissolved in 100 mL of dry chloroform and cooled to 0 °C. 19.4 mL of chlorosulfonic acid (5.0 eq., 290 mmol, 33.8 g) were added dropwise and the solution was stirred at 0 °C for 3 h. The solution was poured onto ice and extracted three times with chloroform. After removal of the solvent 2-(4-(chlorosulfonyl)phenoxy)ethyl methacrylate was obtained as a white solid (yield: 78%, 13.7 g, 44.9 mmol).

^{1}H NMR (400 MHz, $CDCl_3$, δ, ppm): 1.94 (s, 3H, CH_3), 4.33 (t, 2H, $COCH_2CH_2OC(O)$), 4.53 (t, 2H, $COCH_2CH_2OC(O)$), 5.60 (s, 1H, $CH_{2,Db}$), 6.12 (s, 1H, $CH_{2,Db}$), 7.08 (d, 2H, H_{Ar}), 7.96 (d, 2H, H_{Ar}). ^{13}C NMR (101 MHz, CDCl3, δ, ppm): 18.38 (CH_3), 62.52 ($COCH_2CH_2OC(O)$), 66.76 ($COCH_2CH_2OC(O)$), 115.37 (C_{Ar}), 126.51 ($CH_{2,Db}$), 129.71 (C_{Ar}), 135.87 ($C_{Ar}SOCl_2$), 136.64 ($CCH_{2,Db}$), 163.91 ($C_{Ar}O$), 167.25 (OC(O)) (see Figure 53 and 54).

Synthesis of the disulfone containing dimethacrylate (DS-DMA)

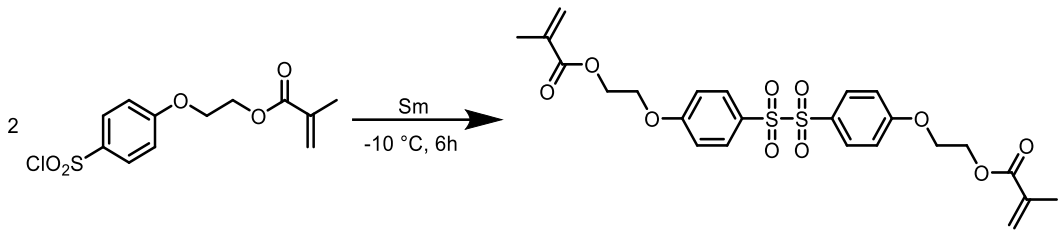

Scheme 57 Synthesis of DS-DMA.

6.75 g of samarium (1.0 eq., 45 mmol) were dissolved in 100 mL of dry DMF and cooled to -15 °C. A solution of 13.7 g of 2-(4-(chlorosulfonyl)phenoxy)ethyl methacrylate (1.0 eq., 45 mmol) in 80 mL of dry DMF was cooled to -15 °C and added dropwise to the suspension of Sm. After stirring for 6 h at -10 °C, the reaction mixture was quenched with 0.1 M HCl and extracted three times with diethyl ether. The combined organic layers were washed with water and brine. The crude product was purified via column chromatography (cyclohexane/EA 2/1) to yield the disulfone containing dimethacrylate DS-DMA as a white solid (yield: 40%, 9.7 g, 18 mmol).

^{1}H NMR (400 MHz, $CDCl_3$, δ, ppm): 1.95 (s, 3H, CH_3), 4.34 (t, 2H, $COCH_2CH_2OC(O)$), 4.54 (t, 2H, $COCH_2CH_2OC(O)$), 5.61 (s, 1H, $CH_{2,Db}$), 6.13 (s, 1H, $CH_{2,Db}$), 7.09 (d, 2H, H_{Ar}), 7.97 (d, 2H, H_{Ar}). ^{13}C NMR (101 MHz, CDCl3, δ, ppm): 18.41 (CH_3), 62.54 ($COCH_2CH_2OC(O)$), 66.78 ($COCH_2CH_2OC(O)$), 115.39 (C_{Ar}), 126.55 ($CH_{2,Db}$), 129.75 (C_{Ar}), 135.90 ($C_{Ar}SOCl_2$), 136.74 ($CCH_{2,Db}$), 163.92 ($C_{Ar}O$), 167.30 (OC(O)). ESI-MS (+Na^+): *m/z* calculated 561.0860 found 561.0869 (see Figure 55 and 56).

Synthesis of N-ethyl-N-(2-nitrobenzyl)ethanamine (PGA1)

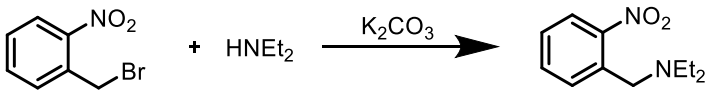

Scheme 58 Synthesis of PGA1.

1.5 g 2-nitrobenzyl bromide (1.0 eq., 7.0 mmol) and 1.0 g K_2CO_3 (1.1 eq., 7.3 mmol) were dissolved in 100 mL acetonitrile. Afterwards, 0.51 g diethylamine (1.0 eq., 7.0 mmol) dissolved in

10 mL acetonitrile were added dropwise and the reaction mixture was stirred for 8 h at ambient temperature. The precipitant was filtered off and the solvent was removed under reduced pressure. The crude product was purified via column chromatography (cyclohexane/EA 20/1) to yield N-ethyl-N-(2-nitrobenzyl)ethanamine (PGA1) as a yellow liquid (yield: 48%, 0.7 g, 3.4 mmol).

^{1}H NMR (400 MHz, $CDCl_3$, δ, ppm): 0.98 (t, 6H, CH_2CH_3), 2.48 (q, 4H, CH_2CH_3), 3.84 (s, 2H, CH_2), 7.35 (t, 1H, H_{Ar}), 7.53 (t, 1H, H_{Ar}), 7.72 (d, 1H, H_{Ar}), 7.78 (d, 1H, H_{Ar}) (see Figure 57).

Synthesis of 2-oxo-1,2-diphenylethyl cyclohexylcarbamate (PGA2)

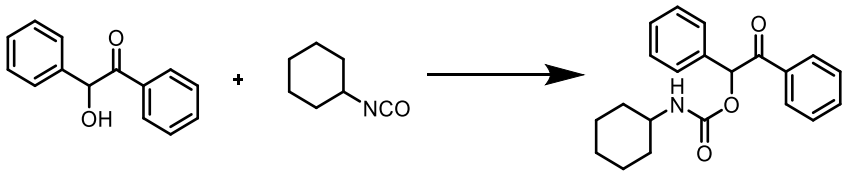

Scheme 59 Synthesis of PGA2.

6.6 mL cyclohexyl isocyanate (1.1 eq., 51.8 mmol, 6.5 g) were added dropwise to a solution of 10 g benzoin in 100 mL dry toluene. The solution was refluxed for 48 h. Afterwards, the white precipitant was filtered off and washed with cold diethyl ether to yield 2-oxo-1,2-diphenylethyl cyclohexylcarbamate (PGA2) as a white solid (yield: 90%, 14.3 g, 42.4 mmol).

^{1}H NMR (400 MHz, DMSO-d6, δ, ppm): 0.85 – 1.15 (m, 4H, CH_2), 1.41 – 2.11 (m, 6H, CH_2), 2.60 – 2.72 (m, 1H, CH), 5.49 (s, 1H, NH), 6.49 (s, 1H, CH(O)), 7.00 – 7.12 (m, 4H, H_{Ar}), 7.30 (t, 2H, H_{Ar}), 7.40 – 7.49 (m, 3H, H_{Ar}), 7.52 – 7.57 (m, 2H, H_{Ar}) (see Figure 58).

Synthesis of 2-nitrobenzyl cyclohexylcarbamate (PGA3)

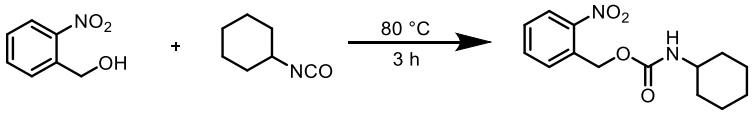

Scheme 60 Synthesis of PGA3.

To a solution of 3.0 g of 2-nitrobenzyl alcohol (1.0 eq, 19.6 mmol) in 30 mL of dry toluene, 2.8 mL of cyclohexyl isocyanate (1.1 eq, 21.5 mmol, 2.7 g) were added dropwise. After heating

to 80 °C for 3 h, the solvent was evaporated and the crude product was purified via column chromatography (cyclohexane/EA 2/1) to yield 2-nitrobenzyl cyclohexylcarbamate (PGA3) as a white solid (yield: 92%, 5.0 g, 18 mmol).

^{1}H NMR (400 MHz, CDCl3, δ, ppm): 1.09 – 1.25 (m, 3H, CH_2), 1.26 – 1.40 (m, 2H, CH_2), 1.55 – 1.75 (m, 3H, CH_2), 1.90 – 1.99 (m, 2H, CH_2), 3.42 – 3.55 (m, 1H, CH), 5.49 (2H, OCH_2), 7.46 (t, 1H, H_{Ar}), 7.56 – 7.67 (m, 2H, H_{Ar}), 8.09 (d, 1H, H_{Ar}). ^{13}C NMR (101 MHz, CDCl3, δ, ppm): 24.90 (CH_2), 25.58 (CH_2), 33.48 (CH_2), 50.18 (CH), 63.12 OCH_2), 125.04, 128.60 (CH_{Ar}), 128.99 (CH_{Ar}), 133.49 (C_{Ar}), 133.77 (CH_{Ar}), 147.61 ($C_{Ar}NO_2$), 155.05 (OC(O)) (see Figure 59 and 60).

Synthesis of the disulfone and PGA3 containing polymer network

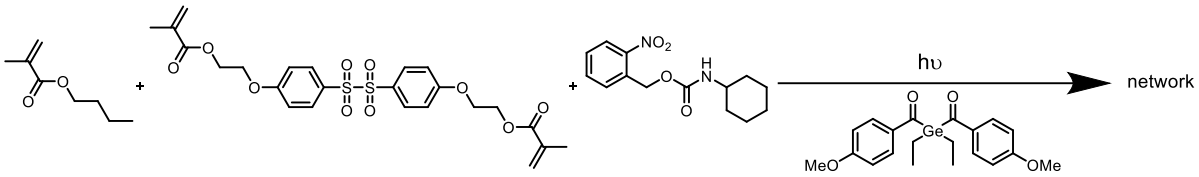

Scheme 61 Synthesis of the disulfone and PGA3 containing polymer network.

A highly concentrated solution of 0.224 mL *n*-butyl methacrylate (1.0 eq, 1.4 mmol, 200 mg), 75 mg of DiMA-$DiSO_2$ (0.1 eq, 0.14 mmol), 195 mg of PGA3 (0.5 eq, 0.70 mmol) and 1 mg Ivocerin® (0.2 wt%) in toluene was degassed and irradiated with blue light (1x 18 W, 400 – 520 nm) for 10 min.

Bibliography

1. Roy, N.; Bruchmann, B.; Lehn, J.-M. *Chem. Soc. Rev.* **2015,** 44, (11), 3786-3807.
2. Schöne, A.-C.; Schulz, B.; Lendlein, A. *Macromol. Rapid Commun.* **2016,** 37, (23), 1856-1859.
3. Sumaru, K.; Kameda, M.; Kanamori, T.; Shinbo, T. *Macromolecules* **2004,** 37, (13), 4949-4955.
4. Cabane, E.; Malinova, V.; Meier, W. *Macromol. Chem. Phys.* **2010,** 211, (17), 1847-1856.
5. Yan, Q.; Han, D.; Zhao, Y. *Polym. Chem.* **2013,** 4, (19), 5026-5037.
6. Oehlenschlaeger, K. K.; Mueller, J. O.; Heine, N. B.; Glassner, M.; Guimard, N. K.; Delaittre, G.; Schmidt, F. G.; Barner-Kowollik, C. *Angew. Chem. Int. Ed.* **2013,** 52, (2), 762-766.
7. Hirschbiel, A. F.; Schmidt, B. V. K. J.; Krolla-Sidenstein, P.; Blinco, J. P.; Barner-Kowollik, C. *Macromolecules* **2015,** 48, (13), 4410-4420.
8. Stumpel, J. E.; Gil, E. R.; Spoelstra, A. B.; Bastiaansen, C. W. M.; Broer, D. J.; Schenning, A. P. H. J. *Adv. Funct. Mater.* **2015,** 25, (22), 3314-3320.
9. Park, I.-K.; Singha, K.; Arote, R. B.; Choi, Y.-J.; Kim, W. J.; Cho, C.-S. *Macromol. Rapid Commun.* **2010,** 31, (13), 1122-1133.
10. Gallagher, J. J.; Hillmyer, M. A.; Reineke, T. M. *Macromolecules* **2014,** 47, (2), 498-505.
11. Themistou, E.; Patrickios, C. S. *Macromolecules* **2007,** 40, (14), 5231-5234.
12. De Clercq, R. R.; Goethals, E. J. *Macromolecules* **1992,** 25, (3), 1109-1113.
13. Meng, H.; Jinlian Hu. *J. Intell. Mater. Syst. Struct.* **2010,** 21, (9), 859-885.
14. Fiore, G. L.; Rowan, S. J.; Weder, C. *Chem. Soc. Rev.* **2013,** 42, (17), 7278-7288.
15. Stuart, M. A. C.; Huck, W. T. S.; Genzer, J.; Muller, M.; Ober, C.; Stamm, M.; Sukhorukov, G. B.; Szleifer, I.; Tsukruk, V. V.; Urban, M.; Winnik, F.; Zauscher, S.; Luzinov, I.; Minko, S. *Nat. Mater.* **2010,** 9, (2), 101-113.
16. Seiffert, S.; Kumacheva, E.; Okay, O.; Anthamatten, M.; Chau, M.; Dankers, P. Y.; Greenland, B. W.; Hayes, W.; Li, P.; Liu, R., *Supramolecular Polymer Networks and Gels*. Springer: **2015**; Vol. 268.
17. Voorhaar, L.; Hoogenboom, R. *Chem. Soc. Rev.* **2016,** 45, (14), 4013-4031.

18. Kamplain, J. W.; Bielawski, C. W. *Chem. Commun.* **2006**, (16), 1727-1729.
19. Kloxin, C. J.; Scott, T. F.; Adzima, B. J.; Bowman, C. N. *Macromolecules* **2010,** 43, (6), 2643-2653.
20. Kloxin, C. J.; Bowman, C. N. *Chem. Soc. Rev.* **2013,** 42, (17), 7161-7173.
21. Pickering, S. *Composites Part A: Applied Science and Manufacturing* **2006,** 37, (8), 1206-1215.
22. http://www.klebstoffe.com/die-welt-des-klebens/konjunkturdaten.html (accessed 25.01.2017),
23. Kinloch, A. J., *Adhesion and Adhesives: Science and Technology* Springer: London, **1987**; p 442.
24. Odian, G., Radical Chain Polymerization. In *Principles of Polymerization*, John Wiley & Sons, Inc.: **2004**; pp 198-349.
25. Odian, G., Step Polymerization. In *Principles of Polymerization*, John Wiley & Sons, Inc.: **2004**; pp 39-197.
26. Mark, H. F., *Encyclopedia of Polymer Science and Technology*. WILEY: **2014**; Vol. 15.
27. Kricheldorf, H. R.; Nuyken, O.; Swift, G., *Handbook of Polymer Synthesis*. 2. ed.; Taylor & Francis Ltd.: **2004**.
28. Odian, G., *Principles of Polymerization*. 4th ed.; John Wiley and Sons: Hoboken, **2004**.
29. Young, R. J.; Lovell, P. A., *Introduction to Polymers*. CRC Press: Boca Raton, **2011**; Vol. 3rd edn.
30. Patterson, G., *A Prehistory of Polymer Science*. Springer: Heidelberg, **2012**.
31. Goodyear, C. *Polytechnisches Journal* **1838,** 69, 382-384.
32. Guise-Richardson, C. *Technol. Cult.* **2010,** 51, (2), 357-387.
33. Reilly, J. A. *J. Am. Inst. Conserv.* **1991,** 30, (2), 145-162.
34. Baeyer, A. v. *Ber. Dtsch. Chem. Ges.* **1872,** 5, 1094-1100.
35. Baekeland, L. H. *Ind. Eng. Chem.* **1909,** 1, (3), 149-161.
36. Kauffman, G. B. *J. Chem. Educ.* **1988,** 65, (11), A301.
37. Graham, T. *Philos. Trans. R. Soc. London* **1861,** 151, 183-224.
38. Staudinger, H. *Ber. Dtsch. Chem. Ges. B: Abhandlungen* **1920,** 53B, 1073-1085.
39. Mülhaupt, R. *Angew. Chem. Int. Ed.* **2004,** 43, (9), 1054-1063.
40. Ziegler, K.; Holzkamp, E.; Breil, H.; Martin, H. *Angew. Chem.* **1955,** 67, (19-20), 541-547.
41. Natta, G. *Angew. Chem.* **1964,** 76, (13), 553-566.

42. Heeger, A. J. *Angew. Chem. Int. Ed.* **2001,** 40, (14), 2591-2611.
43. MacDiarmid, A. G. *Reviews of Modern Physics* **2001,** 73, (3), 701-712.
44. Chauvin, Y. *Angew. Chem. Int. Ed.* **2006,** 45, (23), 3740-3747.
45. Bielawski, C. W.; Grubbs, R. H. *Angew. Chem. Int. Ed.* **2000,** 39, (16), 2903-2906.
46. Schrock, R. R. *Angew. Chem. Int. Ed.* **2006,** 45, (23), 3748-3759.
47. http://www.theglobalist.com/the-rise-of-plastic/ (accessed 31.01.2017),
48. *Plastics - the Facts 2016*. PlasticsEurope: Brussels, 2016.
49. Matyjaszewski, K.; Spanswick, J. *Mater. Today* **2005,** 8, (3), 26-33.
50. Fan, B.; Gillies, E. R., Self-Immolative Polymers. In *Encyclopedia of Polymer Science and Technology*, John Wiley & Sons, Inc.: 2002.
51. Hia, I. L.; Vahedi, V.; Pasbakhsh, P. *Polym. Rev.* **2016,** 56, (2), 225-261.
52. Cheikh, C.; Wael, Z.; Tarak Ben, Z. *Smart Mater. Struct.* **2016,** 25, (10), 103001.
53. Heinzmann, C.; Weder, C.; de Espinosa, L. M. *Chem. Soc. Rev.* **2016,** 45, (2), 342-358.
54. Matyjaszewski, K. *Prog. Polym. Sci.* **2005,** 30, (8–9), 858-875.
55. Ambade, A. V.; Yang, S. K.; Weck, M. *Angew. Chem. Int. Ed.* **2009,** 48, (16), 2894-2898.
56. Sprafke, J. K.; Spruell, J. M.; Mattson, K. M.; Montarnal, D.; McGrath, A. J.; Pötzsch, R.; Miyajima, D.; Hu, J.; Latimer, A. A.; Voit, B. I.; Aida, T.; Hawker, C. J. *J. Polym. Sci., Part A: Polym. Chem.* **2015,** 53, (2), 319-326.
57. Chang, L.; Woo, E. M. *Polym. Chem.* **2010,** 1, (2), 198-202.
58. Matyjaszewski, K.; Davis, T. P., *Handbook of Radical Polymerization*. WILEY: Weinheim, **2002**.
59. Brandrup, J.; Immergut, E. H., *Polymer Handbook*. WILEY: New York, 2003.
60. Braun, D. *Int. J. Polym. Sci.* **2009,** 2009.
61. Olaj, O. F.; Kauffmann, H. F.; Breitenbach, J. W. *Makromol. Chem.* **1977,** 178, (9), 2707-2717.
62. Olaj, O. F.; Kauffmann, H. F.; Breitenbach, J. W.; Bieringer, H. *J. Polym. Sci. Pol. Lett. Edition* **1977,** 15, (4), 229-233.
63. Lehrle, R. S.; Shortland, A. *Eur. Polym. J.* **1988,** 24, (5), 425-429.
64. Heuts, J. P. A.; Gilbert, R. G.; Radom, L. *J. Phys. Chem.* **1996,** 100, (49), 18997-19006.
65. Heuts, J. P. A.; Gilbert, R. G. *Macromol. Symp.* **1996,** 111, 147-157.
66. Van Herk, A. M. *Macromol. Theory Simul.* **2000,** 9, (8), 433-441.

67. Yee, L. H.; Coote, M. L.; Chaplin, R. P.; Davis, T. P. *J. Polym. Sci., Part A: Polym. Chem.* **2000,** 38, (12), 2192-2200.
68. Solomon D. H., M. G. *Macromol. Symp.* **1987,** 10, 109125.
69. Benson, S. W.; North, A. M. *J. Am. Chem. Soc.* **1962,** 84, (6), 935-940.
70. Tulig, T. J.; Tirrell, M. *Macromolecules* **1981,** 14, (5), 1501-1511.
71. Barner-Kowollik, C.; Buback, M.; Egorov, M.; Fukuda, T.; Goto, A.; Olaj, O. F.; Russell, G. T.; Vana, P.; Yamada, B.; Zetterlund, P. B. *Prog. Polym. Sci.* **2005,** 30, (6), 605-643.
72. Matsumoto, A.; Otsu, T. *Macromol. Symp.* **1995,** 98, (1), 139-152.
73. Nikitin, A. N.; Hutchinson, R. A. *Macromolecules* **2005,** 38, (5), 1581-1590.
74. Carothers, W. H. *T. Faraday Soc.* **1936,** 32, (0), 39-49.
75. Ueberreiter, K.; Engel, M. *Makromol. Chem.* **1977,** 178, (8), 2257-2260.
76. www.mcgroup.co.uk (accessed: 06.01.2017),
77. Tagle, L. H.; Diaz, F. R. *Eur. Polym. J.* **1987,** 23, (2), 109-112.
78. Schell, H., *Chemistry and Physics of Polycarbonates*. Wiley: New York, **1964**.
79. Brunelle, D. J. *Makromol. Chem. Macromol. Symp.* **1992,** 64, (1), 65-74.
80. Carlone, P.; Palazzo, G. S.; Pasquino, R. *Computers & Mathematics with Applications* **2007,** 53, (9), 1464-1471.
81. Gross, S. M.; Flowers, D.; Roberts, G.; Kiserow, D. J.; DeSimone, J. M. *Macromolecules* **1999,** 32, (9), 3167-3169.
82. Xu, L.; Lei, C.; Xu, R.; Zhang, X.; Zhang, F. *J. Appl. Polym. Sci.* **2017**, 44829.
83. Broedersz, C. P.; MacKintosh, F. C. *Rev. Mod. Phys.* **2014,** 86, (3), 995.
84. Dragan, E. S. *Pure Appl. Chem.* **2014,** 86, (11), 1707-1721.
85. Sperling, L. H., *Interpenetrating polymer networks and related materials*. Springer Science & Business Media: **2012**.
86. Carothers, W. H. *Chem. Rev.* **1931,** 8, (3), 353-426.
87. Flory, P. J. *J. Am. Chem. Soc.* **1941,** 63, (11), 3083-3090.
88. Elliott, J. E.; Bowman, C. N. *Macromolecules* **2001,** 34, (13), 4642-4649.
89. Elliott, J. E.; Bowman, C. N. *Macromolecules* **1999,** 32, (25), 8621-8628.
90. Ye, S.; Cramer, N. B.; Bowman, C. N. *Macromolecules* **2011,** 44, (3), 490-494.
91. Elliott, J. E.; Bowman, C. N. *Polym. React. Eng.* **2002,** 10, (1-2), 1-19.
92. Hill, L. W., *Structure/property relationships of thermoset coatings*. Federation of Societies for Coatings Technology: Blue Bell, USA, **1992**; Vol. 64.

93. Young, J. S.; Kannurpatti, A. R.; Bowman, C. N. *Macromol. Chem. Phys.* **1998,** 199, (6), 1043-1049.

94. Kloosterboer, J. G., Network formation by chain crosslinking photopolymerization and its applications in electronics. In *Electronic Applications*, Springer Berlin Heidelberg: Berlin, Heidelberg, **1988**; pp 1-61.

95. Soper, B.; Haward, R. N.; White, E. F. T. *J. Polym. Sci., Part A: Polym. Chem.* **1972,** 10, (9), 2545-2564.

96. Ishizu, K.; Kuwabara, S.; Chen, H.; Mizuno, H.; Fukutomi, T. *J. Polym. Sci., Part A: Polym. Chem.* **1986,** 24, (8), 1735-1746.

97. Bowman, C. N.; Anseth, K. S. *Macromol. Symp.* **1995,** 93, (1), 269-276.

98. Kannurpatti, A. R.; Anseth, J. W.; Bowman, C. N. *Polymer* **1998,** 39, (12), 2507-2513.

99. Landin, D.; Macosko, C. *Macromolecules* **1988,** 21, (3), 846-851.

100. Matsumoto, A.; Nishi, E.; Oiwa, M.; Ikeda, J.-I. *Eur. Polym. J.* **1991,** 27, (12), 1417-1420.

101. Okay, O.; Kurz, M.; Lutz, K.; Funke, W. *Macromolecules* **1995,** 28, (8), 2728-2737.

102. Elliott, J. E.; Lovell, L. G.; Bowman, C. N. *Dent. Mater.* **2001,** 17, (3), 221-229.

103. Funke, W. *Chimia* **1968,** 22, (3), 111-116.

104. Kast, H.; Funke, W. *Macromol. Chem. Phys.* **1979,** 180, (5), 1335-1338.

105. Allen, P.; Simon, G.; Williams, D.; Williams, E. *Macromolecules* **1989,** 22, (2), 809-816.

106. Simon, G.; Allen, P.; Bennett, D.; Williams, D.; Williams, E. *Macromolecules* **1989,** 22, (9), 3555-3561.

107. Simon, G. P.; Allen, P. E. M.; Williams, D. R. G. *Polym. Eng. Sci.* **1991,** 31, (20), 1483-1492.

108. Young, G. A.; Moore, D. R.; Cook, J. T. *Absorbent structures containing superabsorbent material and web of wetlaid stiffened fibers*. US Patent 5217445, **1993**.

109. Tanaka, K.; Takahashi, K.; Kanada, M.; Kanome, S.; Nakajima, T. *Copolymer for soft contact lens, its preparation and soft contact lens made thereof*. US4139513, **1979**.

110. Shivashankar, M.; Mandal, B. K. *Int. J. Phram. Phram. Sci* **2012,** 4, (5), 1-7.

111. Bowman, C. N.; Kloxin, C. J. *Angew. Chem. Int. Ed.* **2012,** 51, (18), 4272-4274.

112. Wei, P.; Yan, X.; Huang, F. *Chem. Soc. Rev.* **2015,** 44, (3), 815-832.

113. Yu, L.; Ding, J. *Chem. Soc. Rev.* **2008,** 37, (8), 1473-1481.

114. Tsai, Y.-C.; Li, S.; Hu, S.-G.; Chang, W.-C.; Jeng, U.-S.; Hsu, S.-h. *ACS Appl. Mater. Inter.* **2015,** 7, (50), 27613-27623.

115. Boekhoven, J.; Stupp, S. I. *Adv. Mater.* **2014,** 26, (11), 1642-1659.

116. Liu, H.; Xiong, C.; Tao, Z.; Fan, Y.; Tang, X.; Yang, H. *RSC Adv.* **2015,** 5, (42), 33083-33088.

117. de Espinosa, L. M.; Fiore, G. L.; Weder, C.; Foster, E. J.; Simon, Y. C. *Prog. Polym. Sci.* **2015,** 49, 60-78.

118. Hart, L. R.; Harries, J. L.; Greenland, B. W.; Colquhoun, H. M.; Hayes, W. *Polym. Chem.* **2013,** 4, (18), 4860-4870.

119. Herbst, F.; Döhler, D.; Michael, P.; Binder, W. H. *Macromol. Rapid Commun.* **2013,** 34, (3), 203-220.

120. Tsitsilianis, C.; Iliopoulos, I.; Ducouret, G. *Macromolecules* **2000,** 33, (8), 2936-2943.

121. Bivigou-Koumba, A. M.; Görnitz, E.; Laschewsky, A.; Müller-Buschbaum, P.; Papadakis, C. M. *Colloid. Polym. Sci.* **2010,** 288, (5), 499-517.

122. Thompson, M. S.; Tsurkan, M. V.; Chwalek, K.; Bornhauser, M.; Schlierf, M.; Werner, C.; Zhang, Y. *Chemistry–A European Journal* **2015,** 21, (8), 3178-3182.

123. Dankers, P. Y.; Hermans, T. M.; Baughman, T. W.; Kamikawa, Y.; Kieltyka, R. E.; Bastings, M.; Janssen, H. M.; Sommerdijk, N. A.; Larsen, A.; Van Luyn, M. J. *Adv. Mater.* **2012,** 24, (20), 2703-2709.

124. Dai, X.; Zhang, Y.; Gao, L.; Bai, T.; Wang, W.; Cui, Y.; Liu, W. *Adv. Mater.* **2015,** 27, (23), 3566-3571.

125. Zhang, S.; Bellinger, A. M.; Glettig, D. L.; Barman, R.; Lee, Y.-A. L.; Zhu, J.; Cleveland, C.; Montgomery, V. A.; Gu, L.; Nash, L. D. *Nat. Mater.* **2015,** 14, (10), 1065-1071.

126. Cui, J.; del Campo, A. *Chem. Commun.* **2012,** 48, (74), 9302-9304.

127. Koenigs, M. M.; Pal, A.; Mortazavi, H.; Pawar, G. M.; Storm, C.; Sijbesma, R. P. *Macromolecules* **2014,** 47, (8), 2712-2717.

128. Lange, R. F.; Van Gurp, M.; Meijer, E. *J. Polym. Sci., Part A: Polym. Chem.* **1999,** 37, (19), 3657-3670.

129. Cordier, P.; Tournilhac, F.; Soulié-Ziakovic, C.; Leibler, L. *Nature* **2008,** 451, (7181), 977-980.

130. Bai, T.; Liu, S.; Sun, F.; Sinclair, A.; Zhang, L.; Shao, Q.; Jiang, S. *Biomaterials* **2014,** 35, (13), 3926-3933.

131. Wang, Q.; Mynar, J. L.; Yoshida, M.; Lee, E.; Lee, M.; Okuro, K.; Kinbara, K.; Aida, T. *Nature* **2010,** 463, (7279), 339-343.

132. Hunt, J. N.; Feldman, K. E.; Lynd, N. A.; Deek, J.; Campos, L. M.; Spruell, J. M.; Hernandez, B. M.; Kramer, E. J.; Hawker, C. J. *Adv. Mater.* **2011,** 23, (20), 2327-2331.
133. Sun, T. L.; Kurokawa, T.; Kuroda, S.; Ihsan, A. B.; Akasaki, T.; Sato, K.; Haque, M. A.; Nakajima, T.; Gong, J. P. *Nat. Mater.* **2013,** 12, (10), 932-937.
134. Varley, R. J.; van der Zwaag, S. *Acta Mater.* **2008,** 56, (19), 5737-5750.
135. Varley, R. J.; van der Zwaag, S. *Polym. Int.* **2010,** 59, (8), 1031-1038.
136. Wathier, M.; Grinstaff, M. W. *J. Am. Chem. Soc.* **2008,** 130, (30), 9648-9649.
137. Chujo, Y.; Sada, K.; Saegusa, T. *Macromolecules* **1993,** 26, (24), 6315-6319.
138. Chujo, Y.; Sada, K.; Saegusa, T. *Polym. J.* **1993,** 25, (6), 599-608.
139. Asoh, T. A.; Yoshitake, H.; Takano, Y.; Kikuchi, A. *Macromol. Chem. Phys.* **2013,** 214, (22), 2534-2539.
140. Lee, B. P.; Dalsin, J. L.; Messersmith, P. B. *Biomacromolecules* **2002,** 3, (5), 1038-1047.
141. Harrington, M. J.; Masic, A.; Holten-Andersen, N.; Waite, J. H.; Fratzl, P. *Science* **2010,** 328, (5975), 216-220.
142. Bode, S.; Zedler, L.; Schacher, F. H.; Dietzek, B.; Schmitt, M.; Popp, J.; Hager, M. D.; Schubert, U. S. *Adv. Mater.* **2013,** 25, (11), 1634-1638.
143. Burnworth, M.; Tang, L.; Kumpfer, J. R.; Duncan, A. J.; Beyer, F. L.; Fiore, G. L.; Rowan, S. J.; Weder, C. *Nature* **2011,** 472, (7343), 334-337.
144. Frisch, H.; Besenius, P. *Macromol. Rapid Commun.* **2015,** 36, (4), 346-363.
145. Qi, Z.; Schalley, C. A. *Acc. Chem. Res.* **2014,** 47, (7), 2222-2233.
146. Loh, X. J. *Mater. Horiz.* **2014,** 1, (2), 185-195.
147. Zhang, M.; Xu, D.; Yan, X.; Chen, J.; Dong, S.; Zheng, B.; Huang, F. *Angew. Chem.* **2012,** 124, (28), 7117-7121.
148. Liu, D.; Wang, D.; Wang, M.; Zheng, Y.; Koynov, K.; Auernhammer, G. n. K.; Butt, H.-J. r.; Ikeda, T. *Macromolecules* **2013,** 46, (11), 4617-4625.
149. Li, J.; Harada, A.; Kamachi, M. *Polym. J.* **1994,** 26, (9), 1019-1026.
150. Li, J.; Li, X.; Ni, X.; Wang, X.; Li, H.; Leong, K. W. *Biomaterials* **2006,** 27, (22), 4132-4140.
151. Nakahata, M.; Takashima, Y.; Yamaguchi, H.; Harada, A. *Nat. Commun.* **2011,** 2, 511.
152. Himmelein, S.; Lewe, V.; Stuart, M. C.; Ravoo, B. J. *Chem. Sci.* **2014,** 5, (3), 1054-1058.
153. Frisch, H.; Klempner, D.; Frisch, K. *J. Polym. Sci. Polym. Lett.***1969,** 7, (11), 775-779.
154. Sperling, L.; Friedman, D. *J. Polym. Sci. Polym. Phys.* **1969,** 7, (2), 425-427.

155. Sperling, L., History and development of interpenetrating polymer networks. In *High Performance Polymers: Their Origin and Development*, Springer: **1986**; pp 225-231.

156. Grates, J.; Thomas, D.; Hickey, E.; Sperling, L. *J. Appl. Polym. Sci.* **1975,** 19, (6), 1731-1743.

157. Qin, C.; Zhao, D.; Bai, X.; Zhang, X.; Zhang, B.; Jin, Z.; Niu, H. *Mater. Chem. Phys.* **2006,** 97, (2), 517-524.

158. Dillon, M. E., Silicone and Poly (tetrafluoroethylene) Interpenetrating Polymer Networks. ACS Publications: **1994**.

159. Barber, T. A.; Ho, J. E.; De Ranieri, A.; Virdi, A. S.; Sumner, D. R.; Healy, K. E. *J. Biomed. Mater. Res. Part A* **2007,** 80, (2), 306-320.

160. Lipatov, Y. S.; Karabanova, L. *J. Mater. Sci.* **1995,** 30, (10), 2475-2484.

161. Hirotsu, S. *J. Chem. Phys.* **1991,** 94, (5), 3949-3957.

162. Li, B.; Jiang, Y.; Liu, Y.; Wu, Y.; Yu, H.; Zhu, M. *J. Polym. Sci., Part B: Polym. Phys.* **2009,** 47, (1), 96-106.

163. Liu, Y.; Cui, Y. *Polym. Int.* **2011,** 60, (7), 1117-1122.

164. Chang, C.; Han, K.; Zhang, L. *Polym. Adv. Technol.* **2011,** 22, (9), 1329-1334.

165. Kim, S. J.; Park, S. J.; Chung, T. D.; An, K. H.; Kim, S. I. *J. Appl. Polym. Sci.* **2003,** 89, (8), 2041-2045.

166. Zhang, X.-Z.; Wu, D.-Q.; Chu, C.-C. *Biomaterials* **2004,** 25, (17), 3793-3805.

167. Changez, M.; Koul, V.; Krishna, B.; Dinda, A. K.; Choudhary, V. *Biomaterials* **2004,** 25, (1), 139-146.

168. Lee, W. F.; Chiang, W. H. *J. Appl. Polym. Sci.* **2004,** 91, (4), 2135-2142.

169. Ekici, S.; Saraydin, D. *Polym. Int.* **2007,** 56, (11), 1371-1377.

170. Kim, B. S.; Hrkach, J. S.; Langer, R. *Biomaterials* **2000,** 21, (3), 259-265.

171. Shiga, T.; Hirose, Y.; Okada, A.; Kurauchi, T. *J. Appl. Polym. Sci.* **1992,** 44, (2), 249-253.

172. Osada, Y.; Okuzaki, H.; Hori, H. *Nature* **1992,** 355, (6357), 242.

173. Kim, S. Y.; Shin, H. S.; Lee, Y. M.; Jeong, C. N. *J. Appl. Polym. Sci.* **1999,** 73, (9), 1675-1683.

174. Sun, S.; Mak, A. F. *J. Polym. Sci., Part B: Polym. Phys.* **2001,** 39, (2), 236-246.

175. Osada, Y.; Okuzaki, H.; Gong, J. *Trends Polymer Sci.* **1994,** 2, 61-66.

176. Kim, S. J.; Lee, K. J.; Kim, S. I.; Lee, Y. M.; Chung, T. D.; Lee, S. H. *J. Appl. Polym. Sci.* **2003,** 89, (9), 2301-2305.

177. Kie Shim, J.; Ryong Oh, S.; Bong Lee, S.; Cho, K. M. *J. Appl. Polym. Sci.* **2008,** 107, (4), 2136-2141.

178. Zhang, C.; Zhao, K.; Hu, T.; Cui, X.; Brown, N.; Boland, T. *J. Controlled Release* **2008,** 131, (2), 128-136.

179. Liu, F.; Urban, M. W. *Macromolecules* **2008,** 41, (17), 6531-6539.

180. Yin, X.; Hoffman, A. S.; Stayton, P. S. *Biomacromolecules* **2006,** 7, (5), 1381-1385.

181. Zhang, J.; Peppas, N. A. *Macromolecules* **2000,** 33, (1), 102-107.

182. Bouillot, P.; Vincent, B. *Colloid Polym. Sci.* **2000,** 278, (1), 74-79.

183. Kim, S. J.; Yoon, S. G.; Kim, S. I. *Polym. Int.* **2005,** 54, (1), 149-152.

184. Wu, W.; Li, W.; Wang, L. Q.; Tu, K.; Sun, W. *Polym. Int.* **2006,** 55, (5), 513-519.

185. Garoushi, S.; Vallittu, P. K.; Watts, D. C.; Lassila, L. V. *Dent. Mater.* **2008,** 24, (2), 211-215.

186. Lastumäki, T.; Lassila, L.; Vallittu, P. *J. Mater. Sci.: Materials in Medicine* **2003,** 14, (9), 803-809.

187. Ruyter, I. E.; Sjoevik, I. J. *Acta Odontol. Scand.* **1981,** 39, (3), 133-146.

188. Øysæd, H.; Ruyter, I. E. *J. Biomed. Mater. Res.* **1989,** 23, (7), 719-733.

189. Øysæd, H.; Ruyter, I. *J. Mater. Sci.* **1987,** 22, (9), 3373-3378.

190. Jagger, R.; Huggett, R. *Dent. Mater.* **1990,** 6, (4), 276-278.

191. Vallittu, P. K. *Acta Odontol. Scand.* **1995,** 53, (2), 99-104.

192. Pizzi, A.; Mittal, K. L., *Handbook of adhesive technology, revised and expanded*. CRC press: **2003**.

193. Pocius, A. V., *Adhesion and adhesives technology: an introduction*. Carl Hanser Verlag GmbH Co KG: **2012**.

194. Kinloch, A., *Adhesion and adhesives: science and technology*. Springer Science & Business Media: **2012**.

195. Sheets, J. L.; Wilcox, C. W.; Barkmeier, W. W.; Nunn, M. E. *Journal Prosthet Dent.* **2012,** 107, (2), 102-108.

196. Goss, C. A.; Charych, D. H.; Majda, M. *Anal. Chem.* **1991,** 63, (1), 85-88.

197. Kim, H.-J.; Lim, D.-H.; Hwang, H.-D.; Lee, B.-H., Composition of Adhesives. In *Handbook of Adhesion Technology*, da Silva, L. F. M.; Öchsner, A.; Adams, R. D., Eds. Springer Berlin Heidelberg: Berlin, Heidelberg, **2011**; pp 291-314.

198. Greff, R. J.; Tighe, P. J.; Byram, M. M.; Barley, L. V. Cyanoacrylate adhesive compositions. US Patent 5480935, **1996**.

199. Moszner, N.; Hirt, T. *J. Polym. Sci., Part A: Polym. Chem.* **2012,** 50, (21), 4369-4402.

200. Pizzi, A.; Mittal, K. L., *Wood adhesives*. CRC Press: **2011**.

201. Shaw, S., Epoxy resin adhesives. In *Chemistry and technology of epoxy resins*, Springer: **1993**; pp 206-255.

202. Lapique, F.; Redford, K. *Int. J. Adhes. Adhes.* **2002,** 22, (4), 337-346.

203. Buonocore, M. G. *J. Dent. Res.* **1955,** 34, (6), 849-853.

204. Bertolotti, R. L. *J. Esthet Restor. Dent.* **1991,** 3, (1), 1-6.

205. Pashley, D. H.; Tay, F. R.; Breschi, L.; Tjäderhane, L.; Carvalho, R. M.; Carrilho, M.; Tezvergil-Mutluay, A. *Dent. Mater.* **2011,** 27, (1), 1-16.

206. Nakabayashi, N. *Polym. Int.* **2008,** 57, (2), 159-162.

207. Derbanne, M.; Goff, S. L.; Attal, J.-P. *Biomaterials* **2014**, 199-215.

208. Rosa, W. L. d. O. d.; Piva, E.; Silva, A. F. d. *J. Dent.* **2015,** 43, (7), 765-776.

209. Yoshida, Y.; Meerbeek, B. V.; Nakayama, Y.; Yoshioka, M.; Snauwaert, J.; Abe, Y.; Lambrechts, P.; Vanherle, G.; Okazaki, M. *J. Den. Res.* **2001,** 80, (6), 1565-1569.

210. Edizer, S.; Sahin, G.; Avci, D. *J. Polym. Sci., Part A: Polym. Chem.* **2009,** 47, (21), 5737-5746.

211. Sahin, G.; Albayrak, A. Z.; Bilgici, Z. S.; Avci, D. *J. Polym. Sci., Part A: Polym. Chem.* **2009,** 47, (7), 1953-1965.

212. Moszner, N.; Pavlinec, J.; Lamparth, I.; Zeuner, F.; Angermann, J. *Macromol. Rapid Commun.* **2006,** 27, (14), 1115-1120.

213. Salz, U.; Bock, T. J. *Adhes. Dent.* **2010,** 12, 7-10.

214. Moszner, N.; Pavlinec, J.; Angermann, J. *Macromol. Chem. Phys.* **2007,** 208, (5), 529-540.

215. Zanchi, C. H.; Münchow, E. A.; Ogliari, F. A.; de Carvalho, R. V.; Chersoni, S.; Prati, C.; Demarco, F. F.; Piva, E. *J. Biomed. Mater. Res. Part B: Applied Biomaterials* **2011,** 99B, (1), 51-57.

216. Wang, Y.; Oxman, J. D.; Krepski, L. R.; Zhu, P.; Lewandowski, K. M.; Holmes, B. N. *Curable dental compositions and articles comprising polymerizable ionic liquids* WO2011087621A2, **2010**.

217. Moszner, N.; Salz, U.; Zimmermann, J. *Dent. Mater.* **2005,** 21, 895-910.

218. Moszner, N.; Zeuner, F.; Angermann, J.; Fischer, U. K.; Rheinberger, V. *Macromol. Mater. Eng.* **2003,** 288, (8), 621-628.

219. Moszner, N.; Fischer, U. K.; Angermann, J.; Rheinberger, V. *Dent. Mater.* **2006,** 22, 1157-1162.

220. Yeniad, B.; Albayrak, A. Z.; Olcum, N. C.; Avci, D. *J. Polym. Sci., Part A: Polym. Chem.* **2008,** 46, (6), 2290-2299.

221. Ikemura, K.; Endo, T. *Dent. Mater. J.* **2010,** 29, (2), 109-121.

222. Morlet-Savary, F.; Klee, J. E.; Pfefferkorn, F.; Fouassier, J. P.; Lalevée, J. *Macromol. Chem. Phys.* **2015,** 216, (22), 2161-2170.

223. Ganster, B.; Fischer, U. K.; Moszner, N.; Liska, R. *Macromol. Rapid Commun.* **2008,** 29, (1), 57-62.

224. Moszner, N.; Zeuner, F.; Lamparth, I.; Fischer, U. K. *Macromol. Mater. Eng.* **2009,** 294, (12), 877-886.

225. Durmaz, Y. Y.; Kukut, M.; Monszner, N.; Yagci, Y. *Macromolecules* **2009,** 42, (8), 2899-2902.

226. Moszner, N.; Salz, U. *Macromol. Mater. Eng.* **2007,** 292, (3), 245-271.

227. Yiu, C. K. Y.; Pashley, E. L.; Hiraishi, N.; King, N. M.; Goracci, C.; Ferrari, M.; Carvalho, R. M.; Pashley, D. H.; Tay, F. R. *Biomaterials* **2005,** 26, (34), 6863-6872.

228. Malacarne, J.; Carvalho, R. M.; de Goes, M. F.; Svizero, N.; Pashley, D. H.; Tay, F. R.; Yiu, C. K.; Carrilho, M. R. d. O. *Dent. Mater.* **2006,** 22, (10), 973-980.

229. Pavlinec, J.; Kleinová, A.; Moszner, N. *Macromol. Mater. Eng.* **2012,** 297, (10), 1005-1013.

230. Höfer, M.; Moszner, N.; Liska, R. *J. Polym. Sci., Part A: Polym. Chem.* **2008,** 46, (20), 6916-6927.

231. Langer, M.; Brandt, J.; Lederer, A.; Goldmann, A. S.; Schacher, F. H.; Barner-Kowollik, C. *Polym. Chem.* **2014,** 5, (18), 5330-5338.

232. Inglis, A. J.; Nebhani, L.; Altintas, O.; Schmidt, F. G.; Barner-Kowollik, C. *Macromolecules* **2010,** 43, (13).

233. Klán, P.; Šolomek, T.; Bochet, C. G.; Blanc, A.; Givens, R.; Rubina, M.; Popik, V.; Kostikov, A.; Wirz, J. *Chem. Rev.* **2013,** 113, (1), 119-191.

234. Themistou, E.; Patrickios, C. S. *Macromolecules* **2006,** 39, (1), 73-80.

235. Diels, O.; Alder, K. *Eur. J. Org. Chem.* **1928,** 460, (1), 98-122.

236. Diels, O.; Blom, J. H.; Koll, W. *Eur. J. Org. Chem.* **1925,** 443, (1), 242-262.

237. Diels, O.; Alder, K. *Cantharidin. Chem Bet* **1929,** 62, (3), 554-562.

238. Diels, O.; Alder, K. *Chem. Ber.* **1929,** 62, 2081-2087.

239. Diels, O.; Alder, K. *Eur. J. Org. Chem.* **1929,** 470, (1), 62-103.

240. Diels, O.; Alder, K. *Eur. J. Org. Chem.* **1931,** 490, (1), 277-294.

241. Desimoni, G.; Tacconi, G. *Chem. Rev.* **1975,** 75, (6), 651-692.

242. Middleton, W. *J. Org. Chem.* **1965,** 30, (5), 1390-1394.

243. Vedejs, E.; Eberlein, T.; Mazur, D.; McClure, C.; Perry, D.; Ruggeri, R.; Schwartz, E.; Stults, J.; Varie, D. *J. Org. Chem.* **1986,** 51, (9), 1556-1562.

244. König, B.; Martens, J.; Praefcke, K.; Schönberg, A.; Schwarz, H.; Zeisberg, R. *Chem. Ber.* **1974,** 107, (9), 2931-2937.

245. Hartke, K.; Kissel, T.; Quante, J.; Henssen, G. *Angew. Chem. Int. Edit.* **1978,** 17, (12), 953-954.

246. Sauer, J.; Sustmann, R. *Angew. Chem. Int. Edit.* **1980,** 19, (10), 779-807.

247. Sakai, S. *J. Phys. Chem. A* **2000,** 104, (5), 922-927.

248. Treptow, R. S. *J. Chem. Educ* **1980,** 57, (6), 417.

249. Glassner, M.; Blinco, J. P.; Barner-Kowollik, C. *Macromol. Rapid Commun.* **2011,** 32, (9-10), 724-728.

250. Mantovani, G.; Lecolley, F.; Tao, L.; Haddleton, D. M.; Clerx, J.; Cornelissen, J. J.; Velonia, K. *J. Am. Chem. Soc.* **2005,** 127, (9), 2966-2973.

251. Gandini, A. *Prog. Polym. Sci.* **2013,** 38, (1), 1-29.

252. Gandini, A.; Silvestre, A. J.; Coelho, D. *Polym. Chem.* **2011,** 2, (8), 1713-1719.

253. Hager, M. D.; Greil, P.; Leyens, C.; van der Zwaag, S.; Schubert, U. S. *Adv. Mater.* **2010,** 22, (47), 5424-5430.

254. McElhanon, J. R.; Zifer, T.; Kline, S. R.; Wheeler, D. R.; Loy, D. A.; Jamison, G. M.; Long, T. M.; Rahimian, K.; Simmons, B. A. *Langmuir* **2005,** 21, (8), 3259-3266.

255. Zhang, Y.; Broekhuis, A. A.; Picchioni, F. *Macromolecules* **2009,** 42, (6), 1906-1912.

256. Rulíšek, L.; Šebek, P.; Havlas, Z.; Hrabal, R.; Čapek, P.; Svatoš, A. *J. Org. Chem.* **2005,** 70, (16), 6295-6302.

257. Chen, X.; Dam, M. A.; Ono, K.; Mal, A.; Shen, H.; Nutt, S. R.; Sheran, K.; Wudl, F. *Science* **2002,** 295, (5560), 1698-1702.

258. Kennedy, J. P.; Castner, K. F. *J. Polym Sci. Polym. Chem. Edit.* **1979,** 17, (7), 2039-2054.

259. Murphy, E. B.; Bolanos, E.; Schaffner-Hamann, C.; Wudl, F.; Nutt, S. R.; Auad, M. L. *Macromolecules* **2008,** 41, (14), 5203-5209.

260. Xiong, Z.; Mi, Z.; Zhang, X. *React. Kinet. Catal. Lett.* **2005,** 85, (1), 89-97.

261. Jones, J. R.; Liotta, C. L.; Collard, D. M.; Schiraldi, D. A. *Macromolecules* **1999,** 32, (18), 5786-5792.

262. Oehlenschlaeger, K. K.; Guimard, N. K.; Brandt, J.; Mueller, J. O.; Lin, C. Y.; Hilf, S.; Lederer, A.; Coote, M. L.; Schmidt, F. G.; Barner-Kowollik, C. *Polym. Chem.* **2013,** 4, (16), 4348-4355.

263. Jiang, H.; Cruz, D. C.; Li, Y.; Lauridsen, V. H.; Jørgensen, K. A. *J. Am. Chem. Soc.* **2013,** 135, (13), 5200-5207.

264. Nebhani, L.; Sinnwell, S.; Inglis, A. J.; Stenzel, M. H.; Barner-Kowollik, C.; Barner, L. *Macromol. Rapid Commun.* **2008,** 29, (17), 1431-1437.

265. Vyas, D.; Hay, G. *J. Chem. Soc D: Chem. Commun.* **1971**, (21), 1411-1412.

266. Quemener, D.; Davis, T. P.; Barner-Kowollik, C.; Stenzel, M. H. *Chem. Commun.* **2006**, (48), 5051-5053.

267. Inglis, A. J.; Nebhani, L.; Altintas, O.; Schmidt, F. G.; Barner-Kowollik, C. *Macromolecules* **2010,** 43, (13), 5515-5520.

268. Guimard, N. K.; Ho, J.; Brandt, J.; Lin, C. Y.; Namazian, M.; Mueller, J. O.; Oehlenschlaeger, K. K.; Hilf, S.; Lederer, A.; Schmidt, F. G.; Coote, M. L.; Barner-Kowollik, C. *Chemical Science* **2013,** 4, (7), 2752-2759.

269. Pahnke, K.; Brandt, J.; Gryn'ova, G.; Lindner, P.; Schweins, R.; Schmidt, F. G.; Lederer, A.; Coote, M. L.; Barner-Kowollik, C. *Chem. Sci.* **2015,** 6, (2), 1061-1074.

270. Pahnke, K.; Altintas, O.; Schmidt, F. G.; Barner-Kowollik, C. *ACS Macro Letters* **2015,** 4, (7), 774-777.

271. Wang, F.; Rong, M. Z.; Zhang, M. Q. *J. Mater. Chem.* **2012,** 22, (26), 13076-13084.

272. Pazos, J. F. *Photopolymerizable compositions containing nitroso dimers to selectively inhibit thermal polymerization*. US Patent 4168982, **1979**.

273. Chang, J. Y.; Do, S. K.; Han, M. J. *Polymer* **2001,** 42, (18), 7589-7594.

274. Pelliccioli, A. P.; Wirz, J. *Photochem. Photobiol. Sci.* **2002,** 1, (7), 441-458.

275. Literák, J.; Dostálová, A.; Klán, P. *J. Org. Chem.* **2006,** 71, (2), 713-723.

276. Sheehan, J. C.; Umezawa, K. *J. Org. Chem.* **1973,** 38, (21), 3771-3774.

277. Barltrop, J.; Plant, P.; Schofield, P. *Chem. Commun. (London)* **1966**, (22), 822-823.

278. Schmidt, R.; Geissler, D.; Hagen, V.; Bendig, J. *J. Phys.Chem.A* **2007,** 111, (26), 5768-5774.

279. Chamberlin, J. W. *J. Org. Chem.* **1966,** 31, (5), 1658-1660.

280. Schatzschneider, U. *Eur. J. Inorg. Chem.* **2010,** 2010, (10), 1451-1467.

281. Patchornik, A.; Amit, B.; Woodward, R. *J. Am. Chem. Soc.* **1970,** 92, (21), 6333-6335.

282. Radl, S.; Kreimer, M.; Manhart, J.; Griesser, T.; Moser, A.; Pinter, G.; Kalinka, G.; Kern, W.; Schlögl, S. *Polymer* **2015,** 69, 159-168.

283. Azagarsamy, M. A.; Anseth, K. S. *Angew. Chem. Int. Ed.* **2013,** 52, (51), 13803-13807.

284. Kharkar, P. M.; Kiick, K. L.; Kloxin, A. M. *Polym. Chem.* **2015,** 6, (31), 5565-5574.

285. Givens, R. S.; Park, C.-H. *Tetrahedron Lett.* **1996,** 37, (35), 6259-6262.

286. Park, C.-H.; Givens, R. S. *J. Am. Chem. Soc.* **1997,** 119, (10), 2453-2463.

287. Givens, R. S.; Jung, A.; Park, C.-H.; Weber, J.; Bartlett, W. *J. Am. Chem. Soc.* **1997,** 119, (35), 8369-8370.

288. Givens, R. S.; Matuszewski, B. *J. Am. Chem. Soc.* **1984,** 106, (22), 6860-6861.

289. Furuta, T.; Wang, S. S.-H.; Dantzker, J. L.; Dore, T. M.; Bybee, W. J.; Callaway, E. M.; Denk, W.; Tsien, R. Y. *P. Natl. A. Sci.* **1999,** 96, (4), 1193-1200.

290. Hagen, V.; Bendig, J.; Frings, S.; Eckardt, T.; Helm, S.; Reuter, D.; Kaupp, U. B. *Angew. Chem. Int. Ed.* **2001,** 40, (6), 1045-1048.

291. Azagarsamy, M. A.; McKinnon, D. D.; Alge, D. L.; Anseth, K. S. *ACS Macro Letters* **2014,** 3, (6), 515-519.

292. Babin, J.; Pelletier, M.; Lepage, M.; Allard, J.-F.; Morris, D.; Zhao, Y. *Angew. Chem. Int. Ed.* **2009,** 48, (18), 3329-3332.

293. Kohler, E. P.; MacDonald, M. B. *American Chemical Journal* **1899,** 22, 219-226.

294. Kawasoe, Y.; Nishie, K., *Nonaqueous electrolyte secondary battery and method for producing nonaqueous electrolyte secondary battery*. US Patent 20140335426: **2014**.

295. Chen, L.; Hongmin, W.; Wu, J.; Chen, S. *A sulfone-containing epoxy resin and its preparation method*. CN 106008919, Oct 12, **2016**.

296. Sudo, S.; Shimanuki, I.; Kawasaki, D.; Ishikawa, H., *Electrolyte solution and second battery*, WO 2015037382, Mar 19, **2015**.

297. Hinsberg, O. *Chem. Ber.* **1916,** 49, 2593-2596.

298. Pearl, I. A.; Evans, T. W.; Dehn, W. M. *J. Am. Chem. Soc.* **1938,** 60, (10), 2478-2480.

299. Karrer, P.; Wehrli, W.; Biedermann, E.; Vedova, M. d. *Helv. Chim. Acta* **1928,** 11, 236-240.
300. Gebauer-Fülnegg, E.; Riesz, E.; Ilse, S. *Monatsh. Chem.* **1928,** 49, 42-46.
301. Allen, P.; Karger, L. S.; Haygood, J., D.; Shrensel, J. *J. Org. Chem.* **1951,** 16, (5), 767-770.
302. Deacon, G.; Johnson, I. *J. Organomet. Chem.* **1976,** 112, (2), 123-133.
303. Furukawa, M.; Nishikawa, M.; Inaba, Y.; Noguchi, Y.; Okawara, T.; Hitoshi, T. *Chem. Pharm. Bull.* **1981,** 29, (3), 623-628.
304. Denzer Jr, G. C.; Allen Jr, P.; Conway, P.; Veen, M. v. d. *J. Org. Chem.* **1966,** 31, (10), 3418-3419.
305. Allen Jr, P.; Brook, J. W. *J. Org. Chem.* **1962,** 27, (3), 1019-1020.
306. Oae, S.; Takata, T. *Chem. Lett.* **1981,** 10, (7), 845-848.
307. Bartmann, E. A. *Synthesis* **1993,** 1993, (05), 490-496.
308. Liu, Y.; Zhang, Y. *Tetrahedron Lett.* **2003,** 44, (22), 4291-4294.
309. Kice, J. L.; Kasperek, G. J.; Patterson, D. *J. Am. Chem. Soc.* **1969,** 91, (20), 5516-5522.
310. Kice, J. L.; Legan, E. *J. Am. Chem. Soc.* **1973,** 95, (12), 3912-3917.
311. Farng, L.-P. O.; Kice, J. L. *J. Am. Chem. Soc.* **1981,** 103, (5), 1137-1145.
312. Kice, J. L.; Kasperek, G. J. *J. Am. Chem. Soc.* **1969,** 91, (20), 5510-5516.
313. Brown, W. S.; Dewey, W. A.; Jacobs, H. R. *J. Dent. Res.* **1970,** 49, (4), 752-755.
314. Schenzel, A. M.; Klein, C.; Rist, K.; Moszner, N.; Barner-Kowollik, C. *Adv. Sci.* **2016,** 3, (3), 1500361.
315. Tischer, T.; Goldmann, A. S.; Linkert, K.; Trouillet, V.; Börner, H. G.; Barner-Kowollik, C. *Adv. Funct. Mater.* **2012,** 22, (18), 3853-3864.
316. Hiorns, R. *Polym. Int.* **2000,** 49, (7), 807-807.
317. Oehlenschlaeger, K. K.; Mueller, J. O.; Brandt, J.; Hilf, S.; Lederer, A.; Wilhelm, M.; Graf, R.; Coote, M. L.; Schmidt, F. G.; Barner-Kowollik, C. *Adv. Mater.* **2014,** 26, (21), 3561-3566.
318. Jang, B. N.; Wilkie, C. A. *Thermochim. Acta* **2005,** 426, (1–2), 73-84.
319. Schenzel, A. M.; Moszner, N.; Barner-Kowollik, C. *Polym. Chem.* **2017,** 8, (2), 414-420.
320. Griesser, T.; Hofler, T.; Jakopic, G.; Belzik, M.; Kern, W.; Trimmel, G. *J. Mater. Chem.* **2009,** 19, (26), 4557-4565.
321. Babin, J.; Lepage, M.; Zhao, Y. *Macromolecules* **2008,** 41, (4), 1246-1253.

322. Zhao, H.; Sterner, E. S.; Coughlin, E. B.; Theato, P. *Macromolecules* **2012,** 45, (4), 1723-1736.

323. Kawasoe, Y.; Nishie, K., *Nonaqueous electrolyte secondary battery with electrolyte containing cyclic disulfone and manufacture thereof*, US 20140335426, Nov 13, **2014**.

324. You, W.; Gao, J.; Xiao, S.; Zhan, C., *Novel benzo[b]thieno[3,2-b]benzo[b]thiophene disulfone monomer, its copolymer and application of the copolymer*, CN 105778061, Jul 20, **2016**.

325. Schenzel, A. M.; Moszner, N.; Barner-Kowollik, C. *ACS Macro Letters* **2017,** 6, (1), 16-20.

326. Burtscher, P.; Moszner, N.; Rheinberger, V., *Polymerizable compositions comprising germanium-derivative photoinitiator, diketone and accelerator*, US 20150080490, Mar 19, **2015**.

327. http://www.ampolymer.com/Mark-HouwinkParameters.html (10.09.),

Appendix

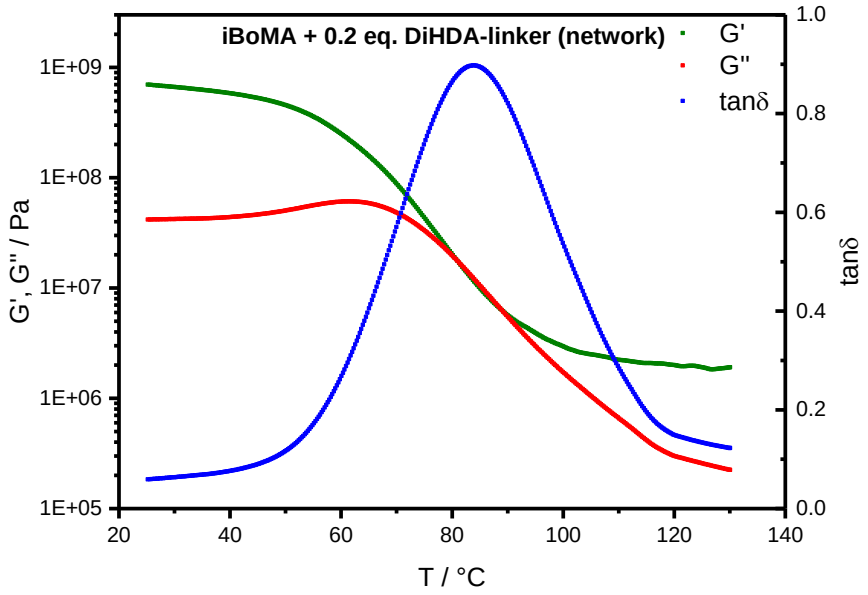

Figure 24 Rheological measurement of a polymer network of iBoMA and 0.2 eq. of the DiHDA-linker. Depicted are G', G'' and tanδ.

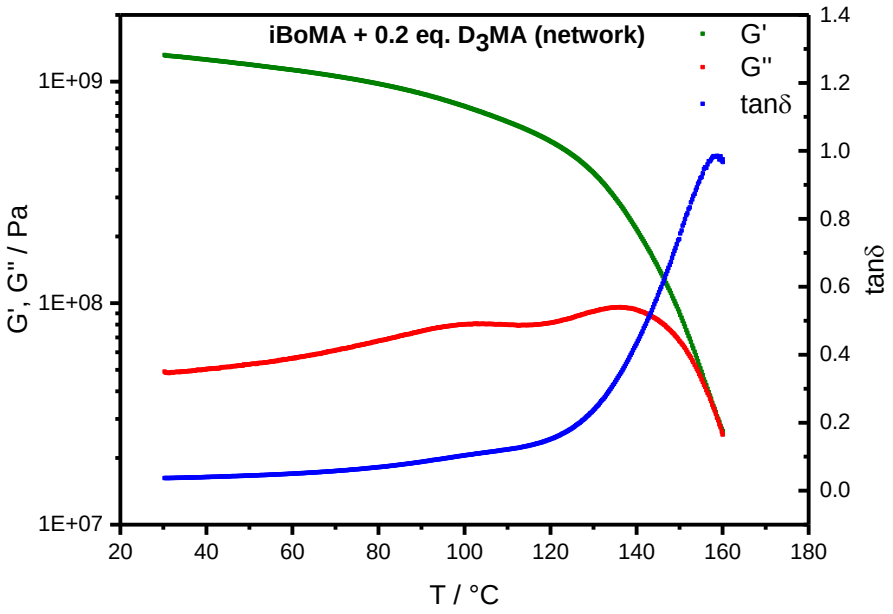

Figure 25 Rheological measurement of a polymer network of isobornyl methacrylate (iBoMA) and 0.2 eq. of a non-degradable dimethacrylate (D3MA). Depicted are G', G'' and tanδ.

Table 4 Pull-off force F determined for test specimens bound with two different self-curing two-component mixtures using nBMA and 0.2 eq. of either bisGMA (a non-degradable dimethacrylate) or the DiHDA-linker. Detailed information regarding the preparation of the test specimens are provided in section 7.2. *BP-50-FT or DABA as Initiator.

	nBMA + 0.2 eq. bisGMA*	**nBMA + 0.2 eq. DiHDA-linker***
F (23 °C)	962 N (+/- 229 N)	663 N (+/- 184 N)
F (80 °C)	553 N (+/- 171 N)	42 N (+/- 15 N)

Table 5 Sum formula, the exact masses of the obtained data *via* ESI-MS analysis, theoretical m/z values and the deviation of both values for the HDA-triol and the products of the rHDA reaction (rHDA1, rHDA2 and rHDA3).

Label	**Sum formula**	**m/z_{exp}**	**m/z_{theo}**	**Δm/z**
$[HDA\text{-}triol+Na]^+$	$[C_{78}H_{99}NaO_{24}P_3S_6]^+$	1727.4114	1727.3956	0.0158
$[rHDA1+Na]^+$	$[C_{15}H_{21}NaO_6PS_2]^+$	415.0411	415.0409	0.0002
$[rHDA2+Na]^+$	$[C_{48}H_{57}NaO_{12}PS_2]^+$	943.2940	943.2921	0.0019
$[rHDA3+Na]^+$	$[C_{63}H_{78}NaO_{18}P_2S_4]^+$	1335.3455	1335.3438	0.0017

Table 6 Sum formula, the exact masses of the obtained data *via* ESI-MS analysis, theoretical m/z values and the deviation of both values for the HDA-diol and the products of the rHDA reaction (rHDA1 and rHDA2).

Label	**Sum formula**	**m/z_{exp}**	**m/z_{theo}**	**Δm/z**
$[HDA\text{-}diol+Na]^+$	$[C_{50}H_{72}NaO_{12}P_2S_4]^+$	1077.3289	1077.3274	0.0015
$[rHDA1+Na]^+$	$[C_{15}H_{21}NaO_6PS_2]^+$	415.0414	415.0409	0.0005
$[rHDA2+Na]^+$	$[C_{35}H_{51}NaO_6PS_2]^+$	685.7277	685.7257	0.0020

Table 7 SEC analysis of the prepared linear polycarbonates P1 – P4. M_n and M_w in g mol^{-1}.

	M_n	M_w	Đ
P1	3100	4200	1.4
P2	2800	5600	2.0
P3	7500	16000	2.4
P4	7600	20000	2.7

Table 8 SEC analysis of the decomposition of P4 upon heating. Mn and Mw in g mol^{-1}.

	M_n	M_w	Đ
P4 (25 °C)	7600	20000	2.7
P4 (60 °C)	3600	12000	3.4
P4 (100 °C)	1600	3900	2.5
P4 (140 °C)	570	590	1.04

Table 9 SEC analysis of the bonding/debonding behavior of P4. M_n and M_w in g mol^{-1}. $P4_{or.}$ is the original P4 polymer, $P4_{deg.}$ the degraded polymer at 120 °C and $P4_{ref.}$ the reformed polymer upon cooling.

	M_n	M_w	Đ
$P4_{or.}$ (25 °C	7600	20000	2.7
$P4_{deg.}$ (120 °C)	1300	1700	1.4
$P4_{ref.}$ (25 °C)	9900	20000	2.0

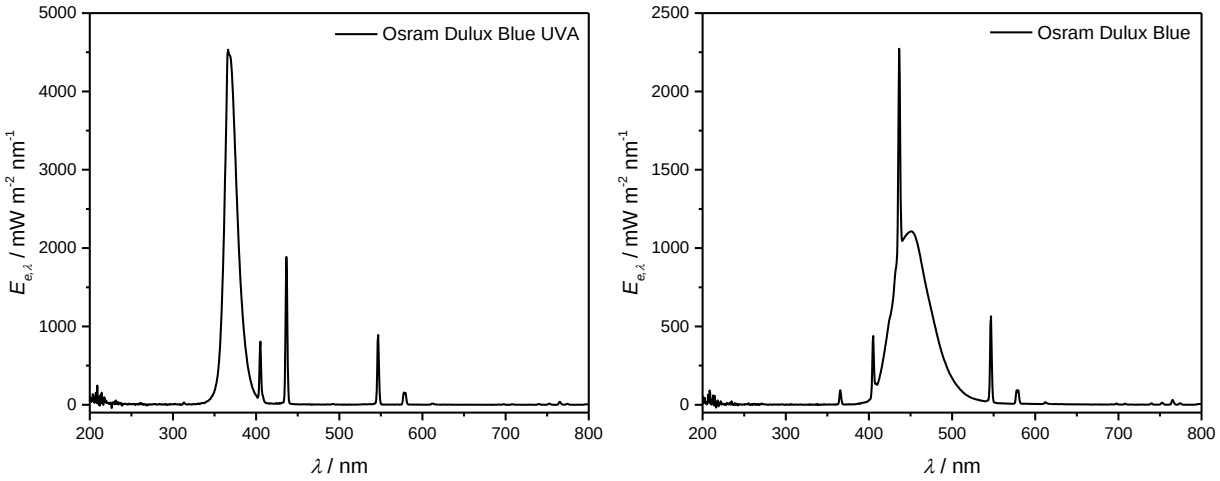

Figure 26 Emission spectrum of the employed UV light (Osram Dulux Blue UVA) and visible light (Osram Dulux Blue) source for the preparation of the disulfone containing polymer network.

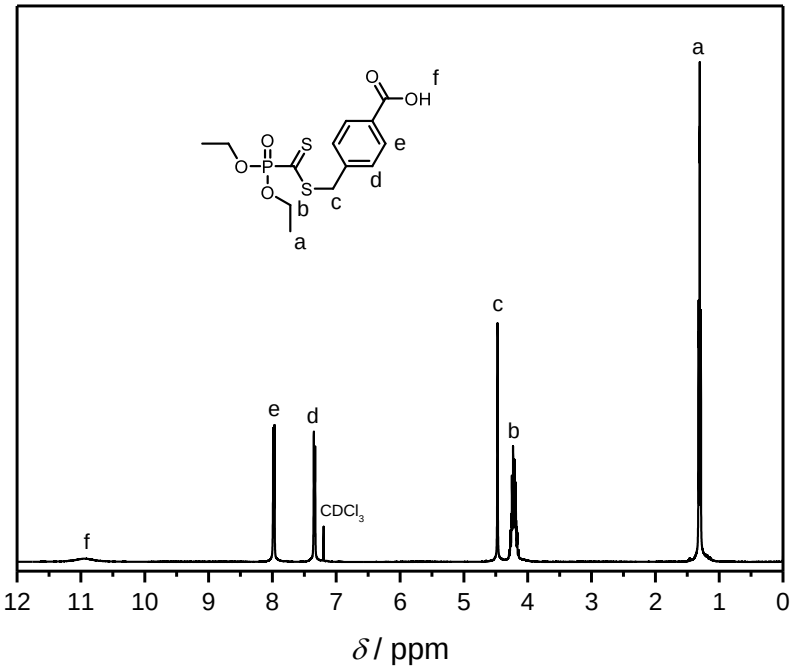

Figure 27 ^{1}H NMR spectrum of PDT in $CDCl_3$.

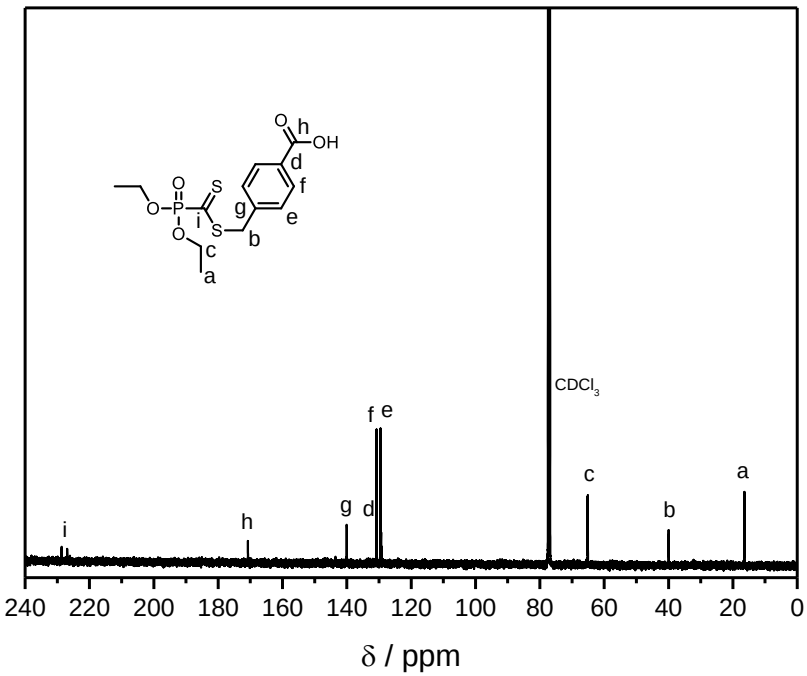

Figure 28 ^{13}C NMR spectrum of PDT in $CDCl_3$.

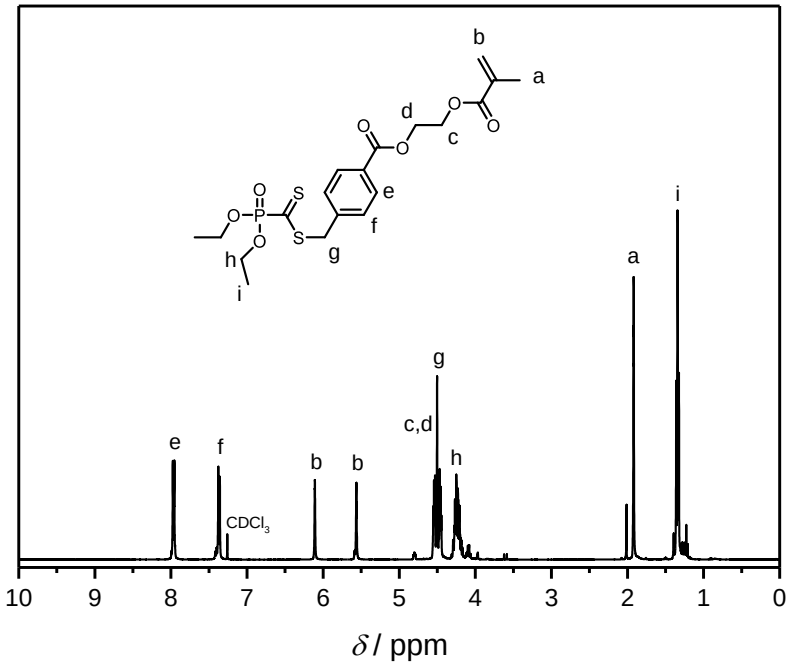

Figure 29 ^{1}H NMR spectrum of MA-PDT in $CDCl_3$.

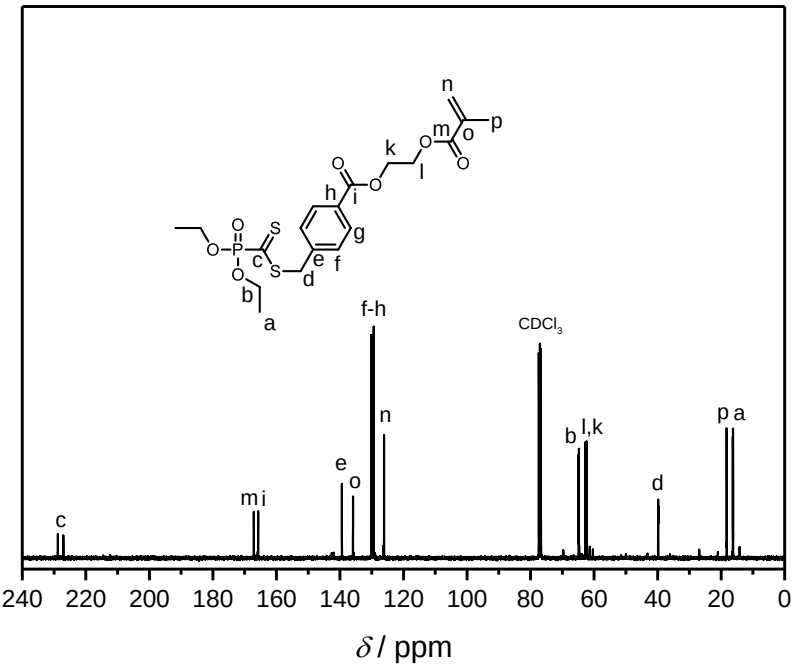

Figure 30 ^{13}C NMR spectrum of MA-PDT in $CDCl_3$

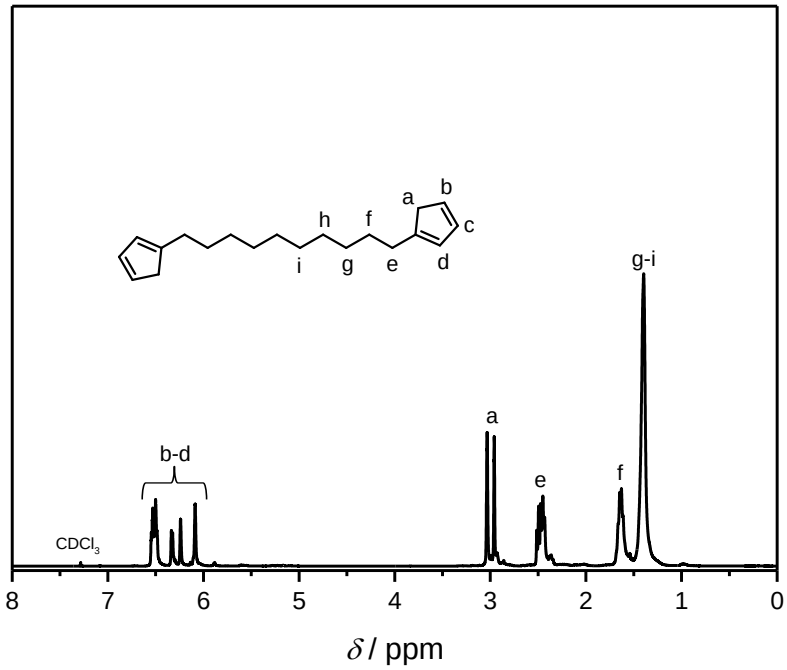

Figure 31 ^{1}H NMR spectrum of the DiCp-linker in $CDCl_3$.

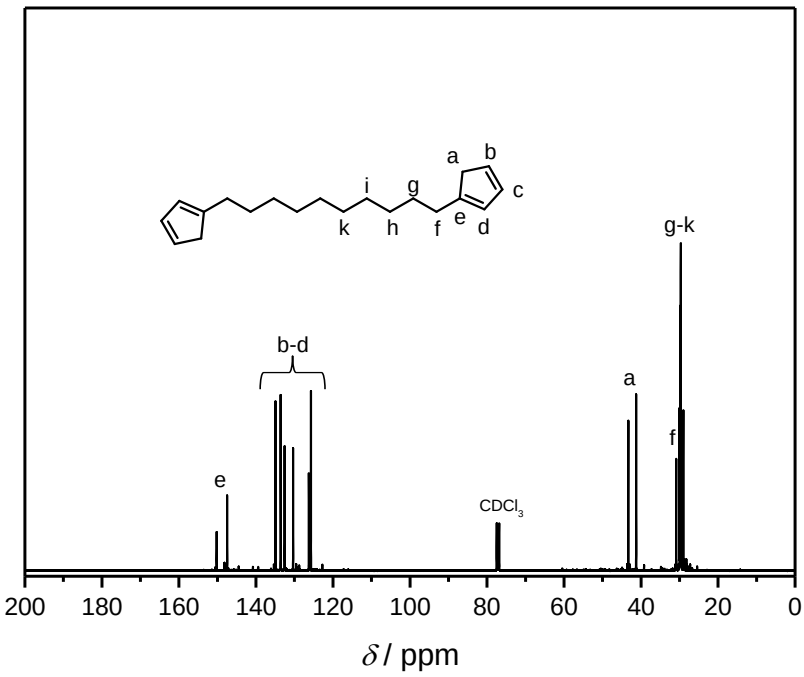

Figure 32 ^{13}C NMR spectrum of the DiCp-linker in $CDCl_3$.

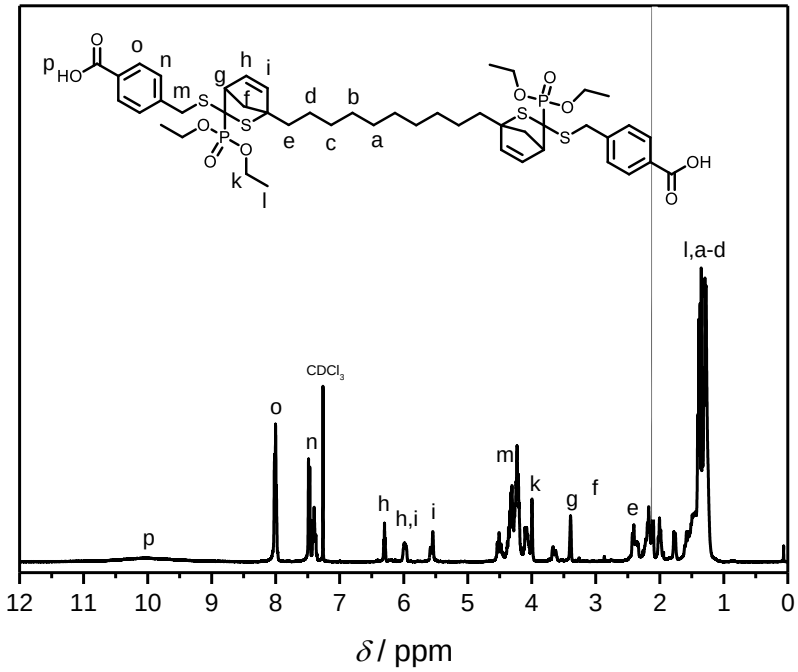

Figure 33 ^{1}H NMR spectrum DiHDA-core in $CDCl_3$.

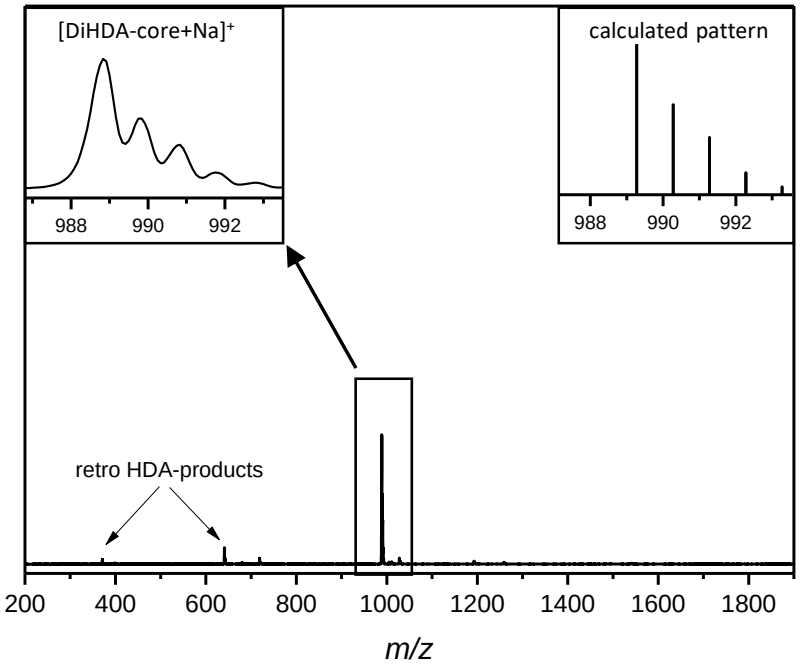

Figure 34 ESI mass spectrum of the DiHDA-core. The retro HDA products are formed during the ionization process due to the high temperatures (320 °C).

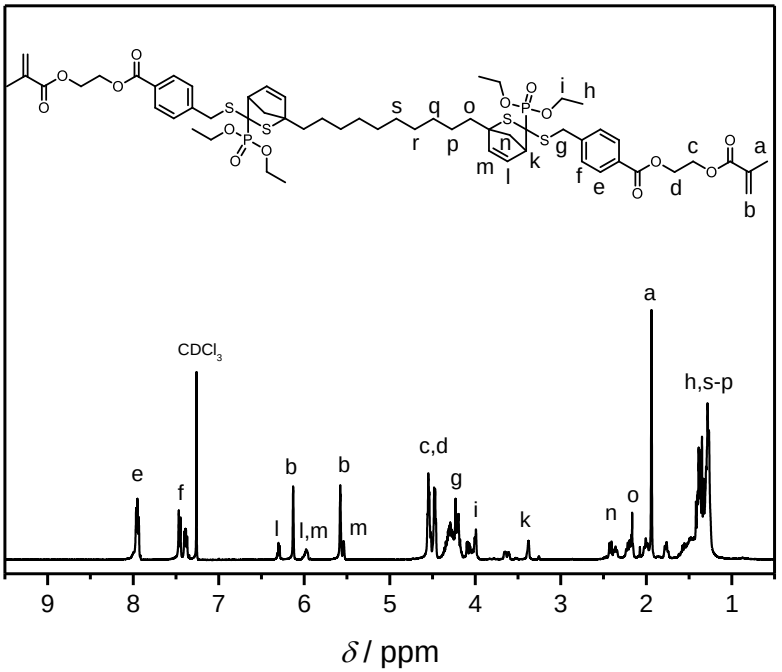

Figure 35 ^{1}H NMR spectrum DiHDA-linker in $CDCl_3$.

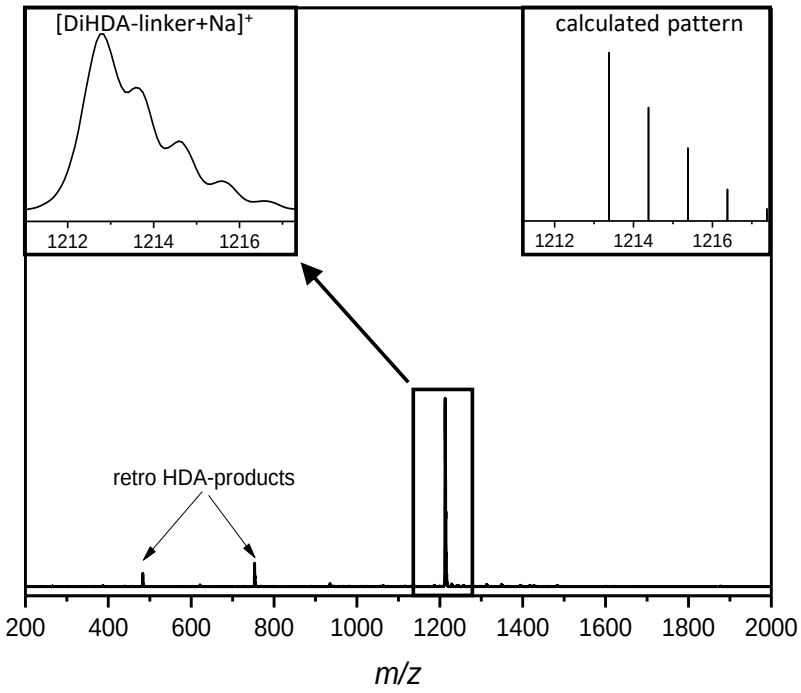

Figure 36 ESI mass spectrum of the DiHDA-linker. The retro HDA products are formed during the ionization process due to the high temperatures (320 °C).

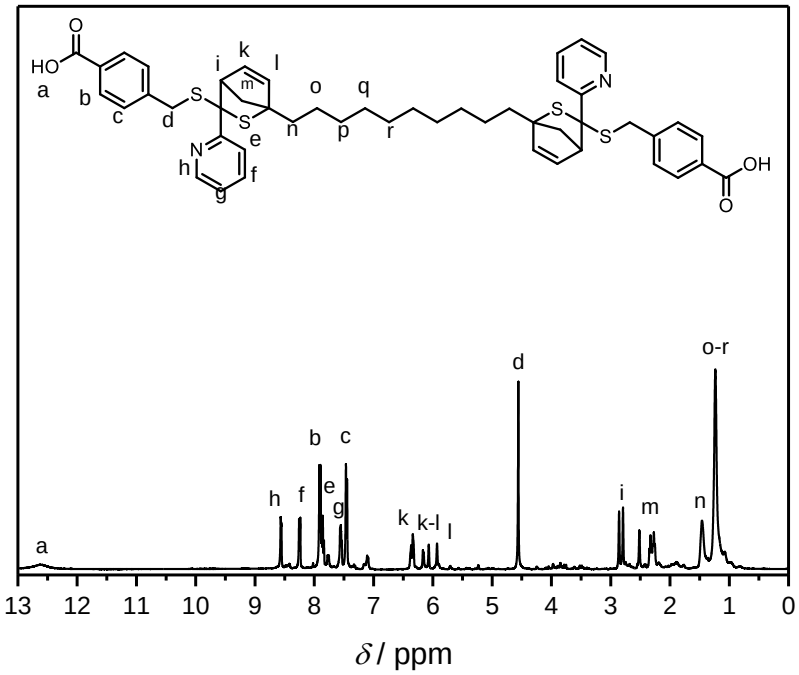

Figure 37 ^{1}H NMR spectrum of DiHDA2 in $CDCl_3$.

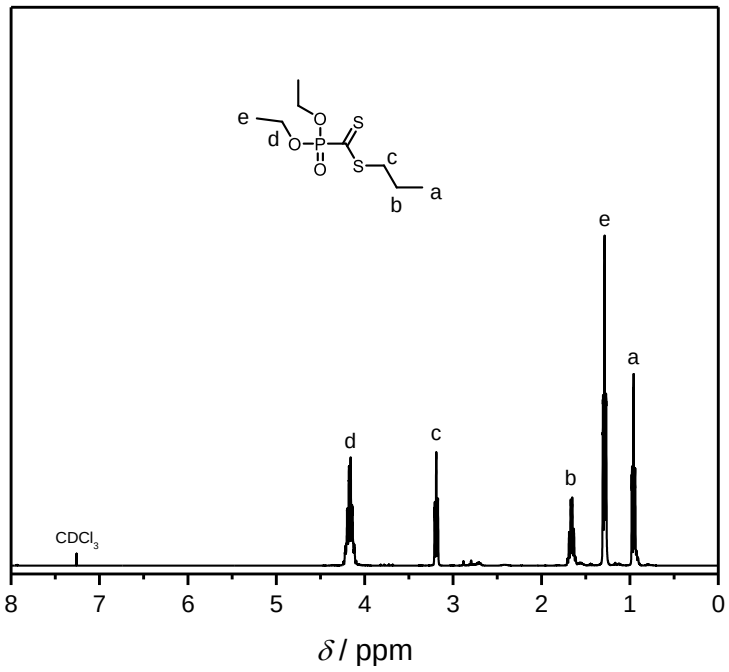

Figure 38 ^{1}H NMR spectrum of PDT2 in $CDCl_3$.

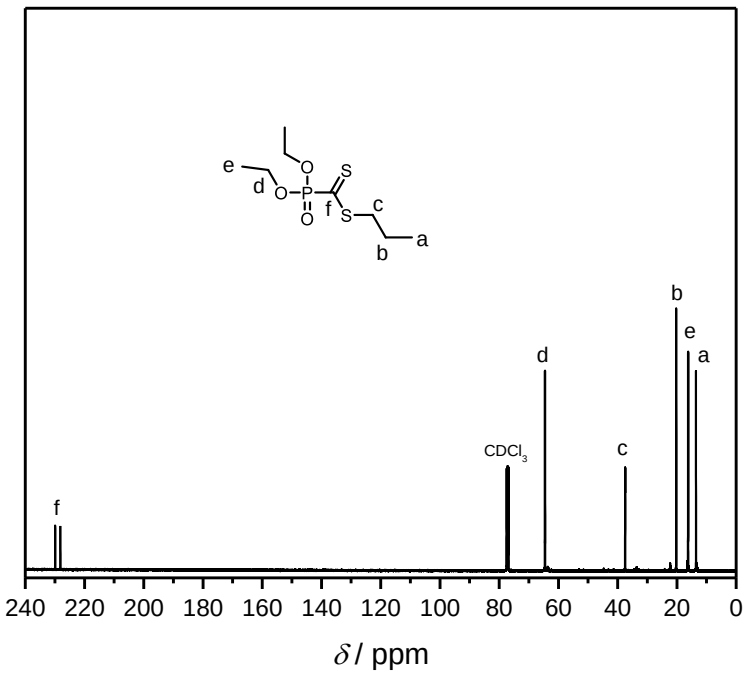

Figure 39 ^{1}H NMR spectrum of PDT2 in $CDCl_3$.

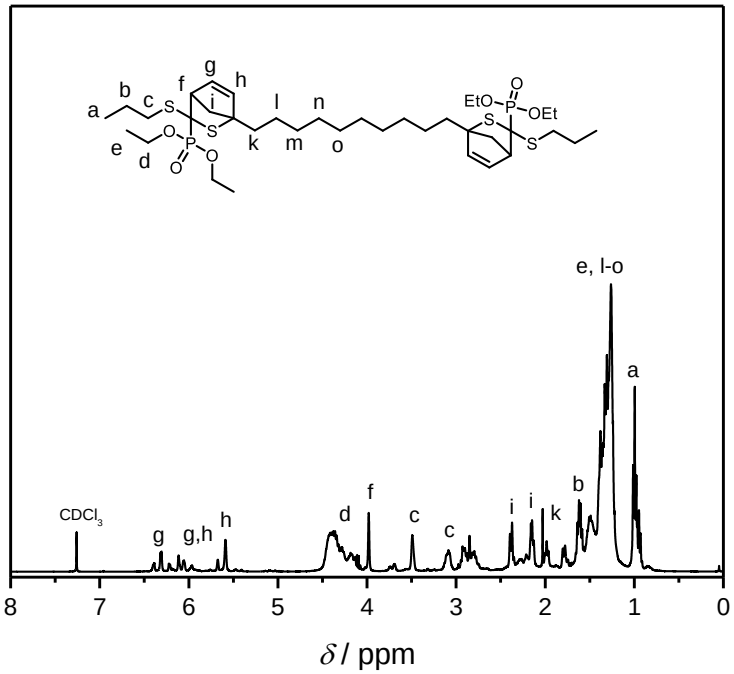

Figure 40 ^{1}H NMR spectrum of DiHDA3 in $CDCl_3$.

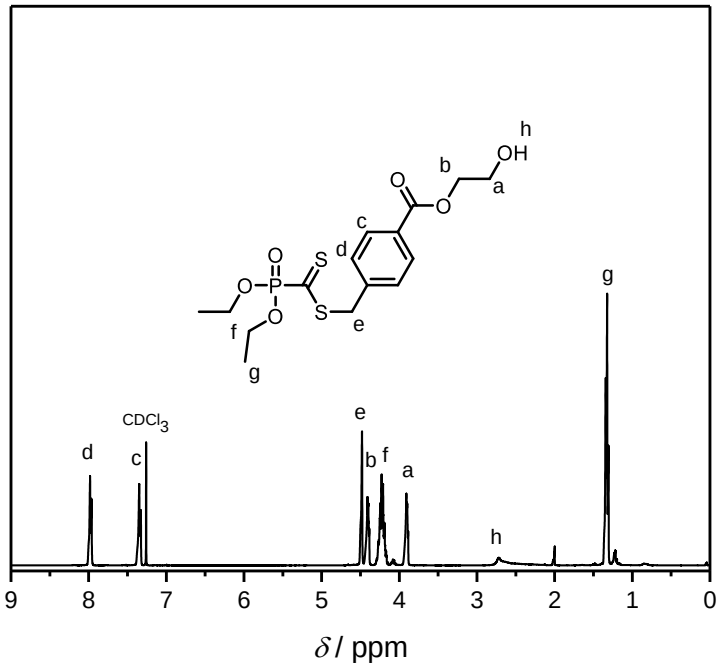

Figure 41 ^{1}H NMR spectrum of PDT-OH in $CDCl_3$.

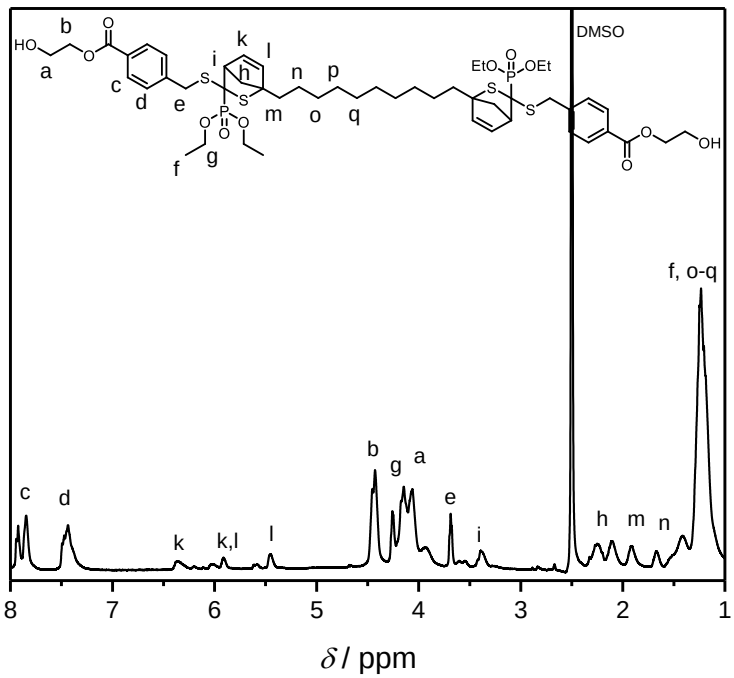

Figure 42 ^{1}H NMR spectrum of HDA-diol in DMSO-d_6.

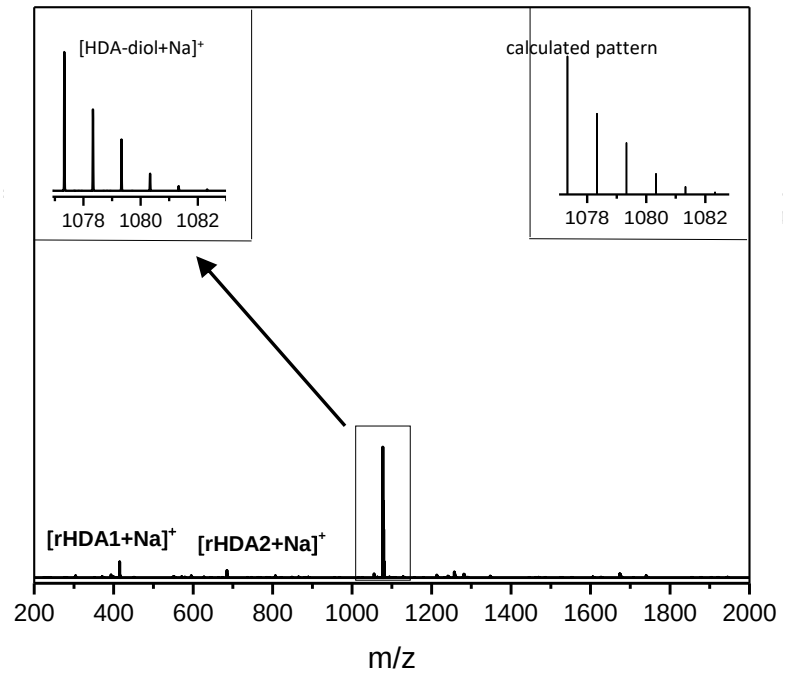

Figure 43 ESI mass spectrum of the HDA-diol. The retro HDA products are formed during the ionization process due to the high temperatures (320 °C).

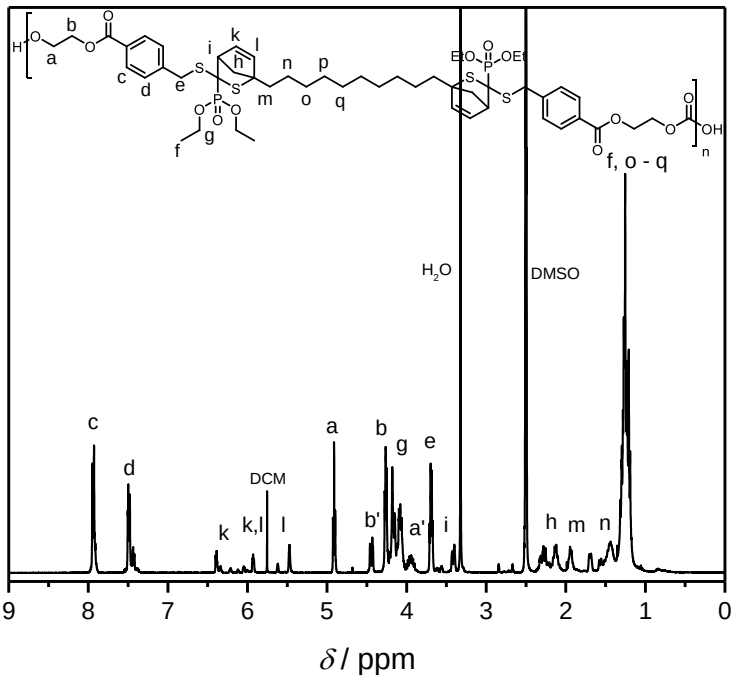

Figure 44 ^{1}H NMR spectrum of HDA-PC in DMSO-d_6.

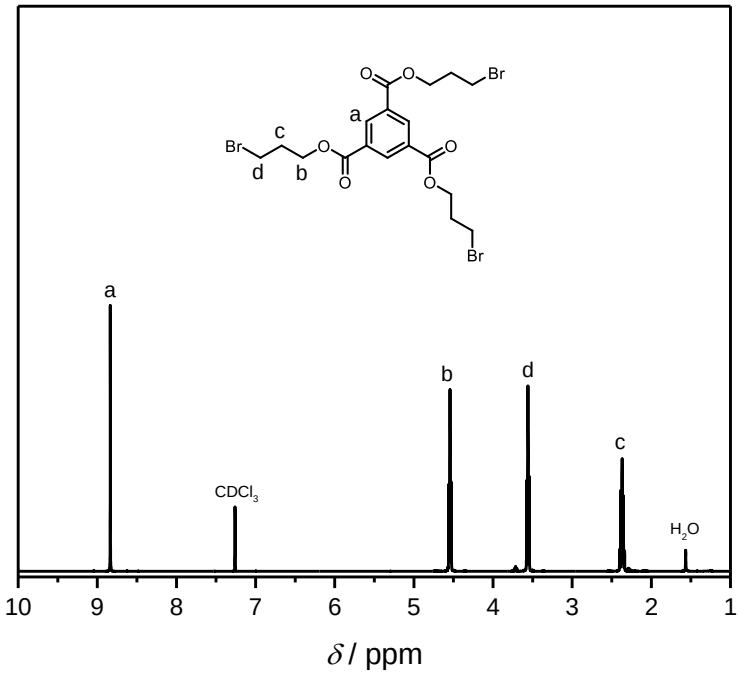

Figure 45 ^{1}H NMR spectrum of the TriBr-linker in $CDCl_3$.

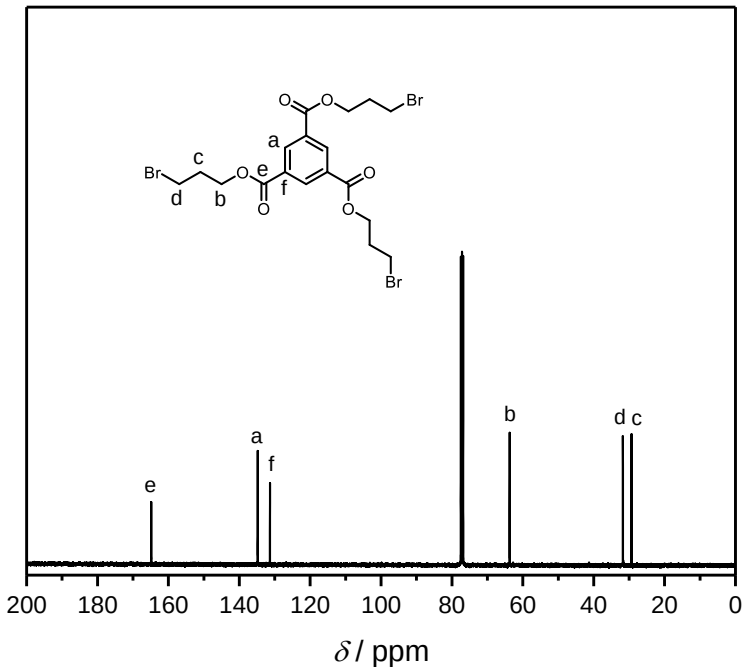

Figure 46 ^{13}C NMR spectrum of the TriBr-linker in $CDCl_3$.

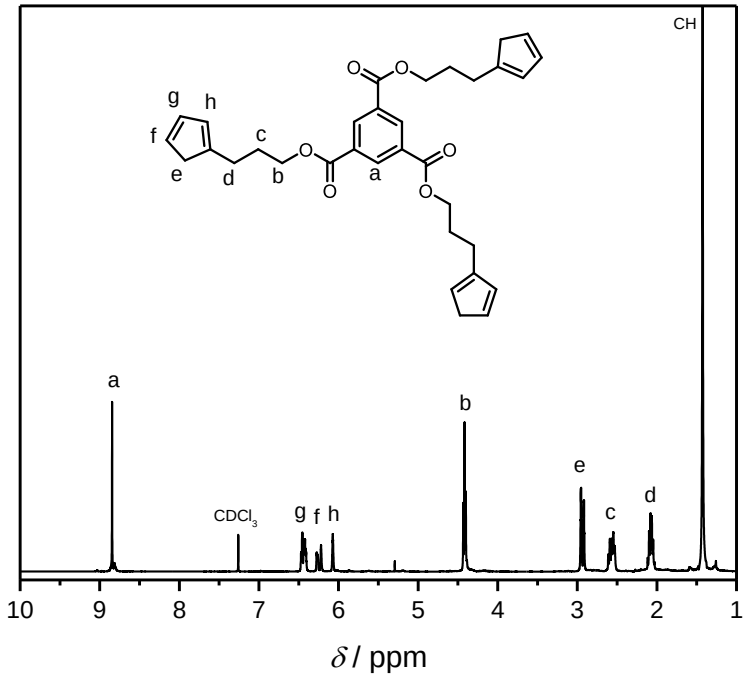

Figure 47 ^{1}H NMR spectrum of the TriCp-linker in $CDCl_3$.

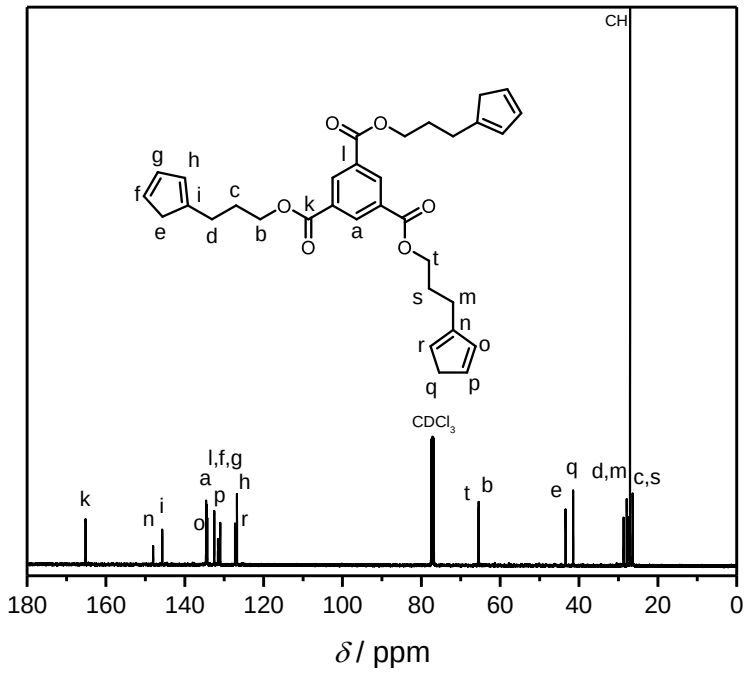

Figure 48 ^{13}C NMR spectrum of the TriCp-linker in $CDCl_3$.

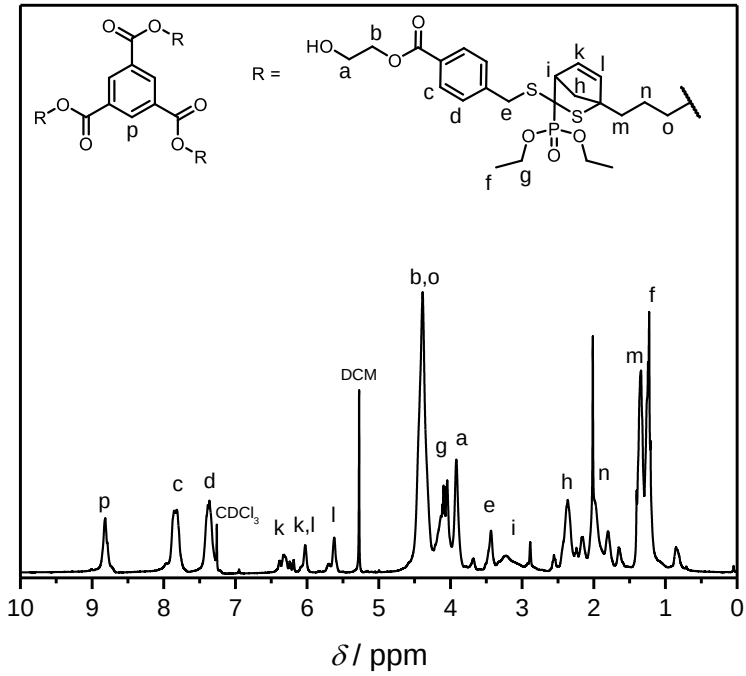

Figure 49 ^{1}H NMR spectrum of the HDA-triol in $CDCl_3$.

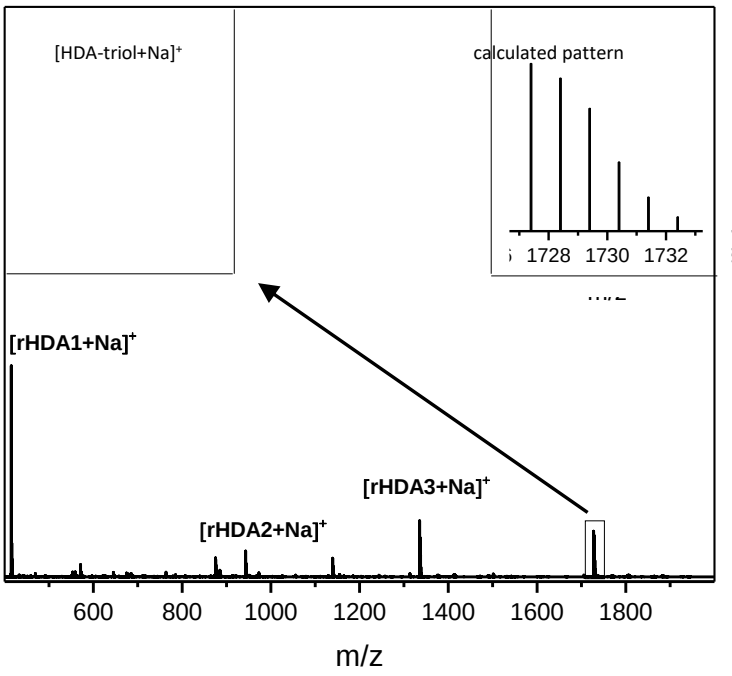

Figure 50 ESI mass spectrum of the HDA-triol. The retro HDA products are formed during the ionization process due to the high temperatures (320 °C).

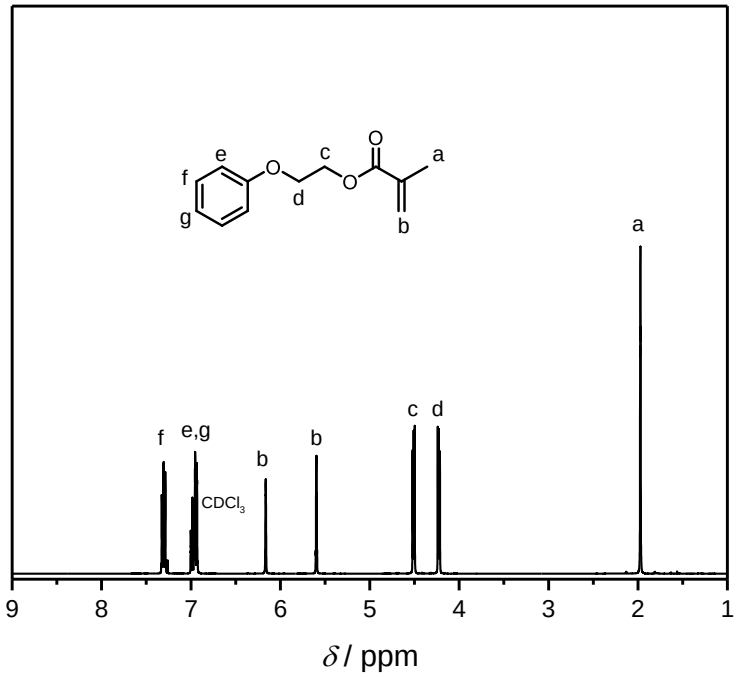

Figure 51 ^{1}H NMR spectrum of MA in $CDCl_3$.

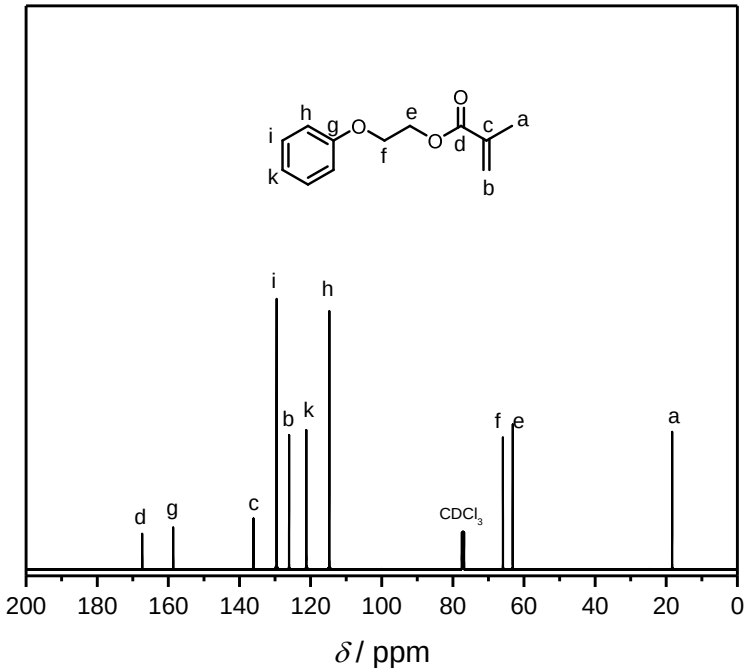

Figure 52 ^{13}C NMR spectrum of MA in $CDCl_3$.

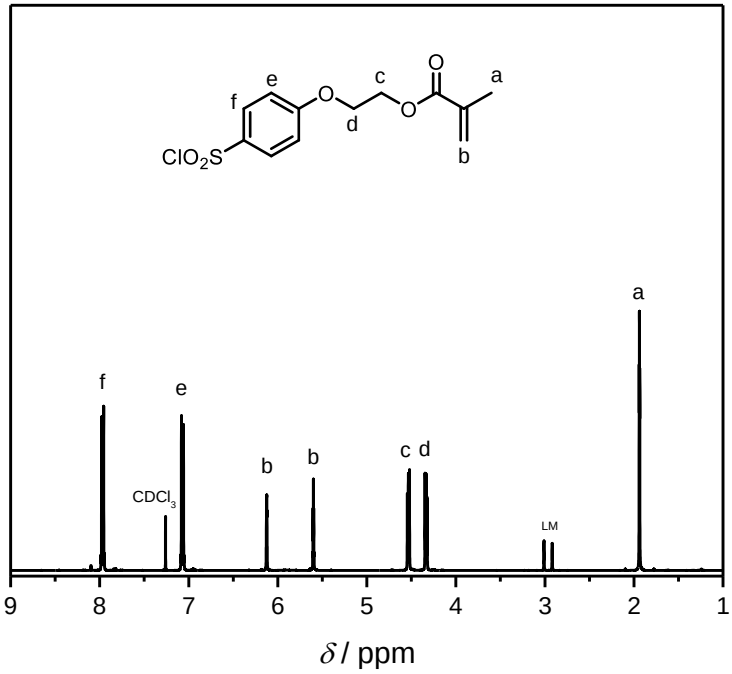

Figure 53 ^{1}H NMR spectrum of MA-$SOCl_2$ in $CDCl_3$.

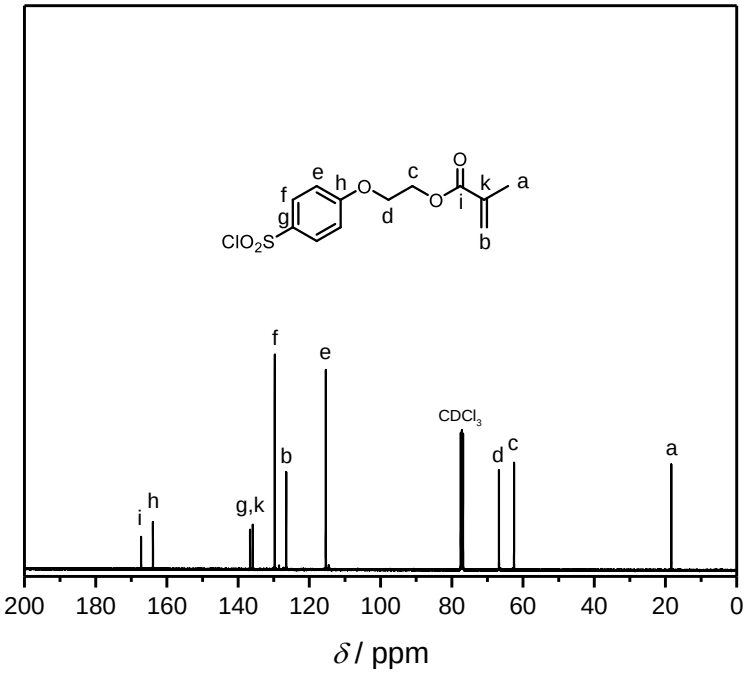

Figure 54 ^{13}C NMR spectrum of MA-$SOCl_2$ in $CDCl_3$.

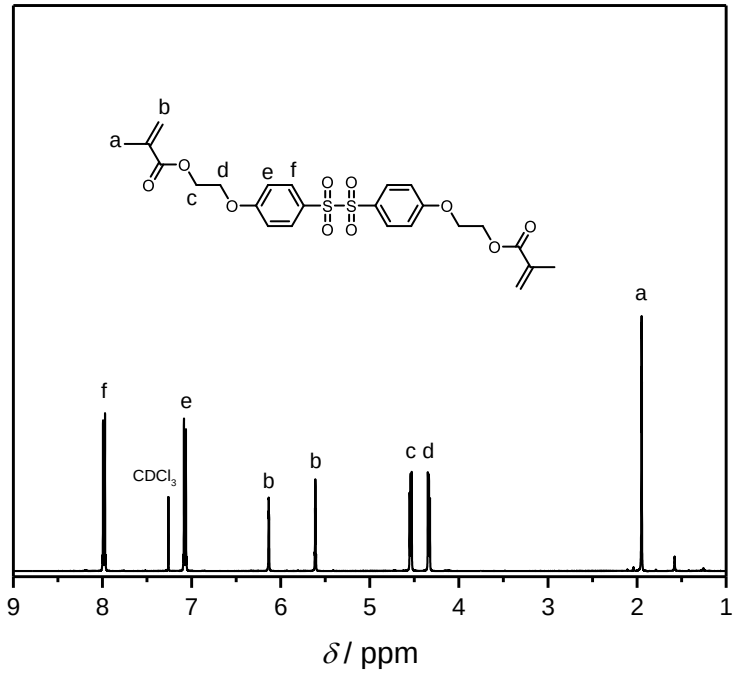

Figure 55 ^{1}H NMR spectrum of DiMA-DiSO$_2$ in CDCl$_3$.

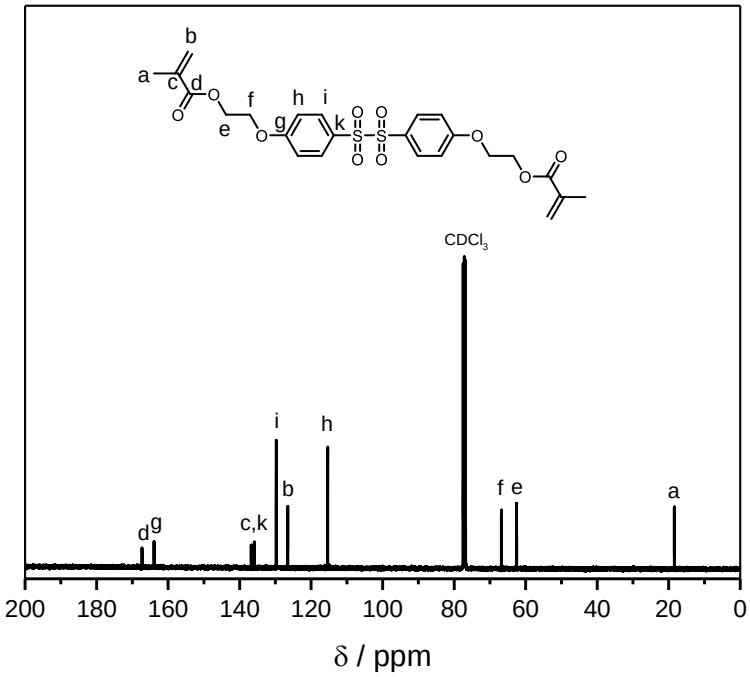

Figure 56 ^{13}C NMR spectrum of DiMA-DiSO$_2$ in CDCl$_3$.

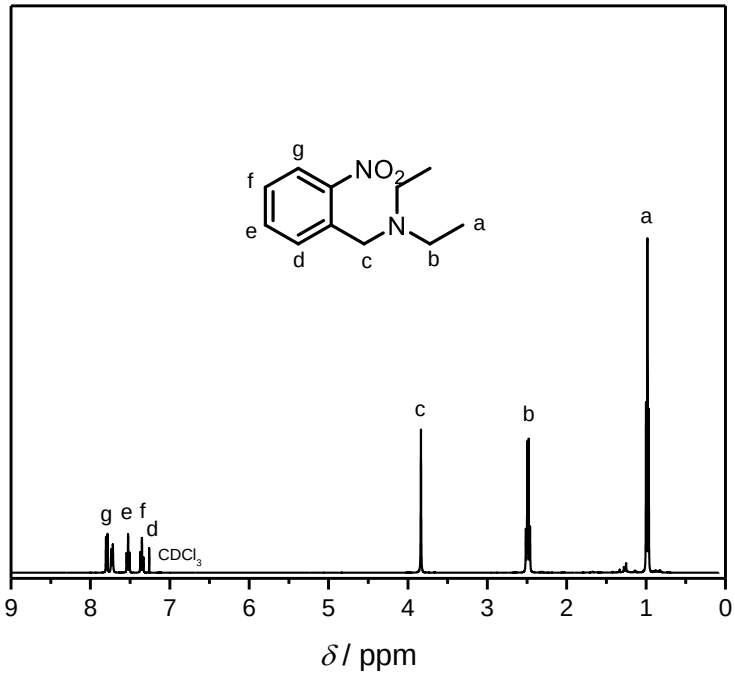

Figure 57 ^{1}H NMR spectrum of PGA1 in $CDCl_3$.

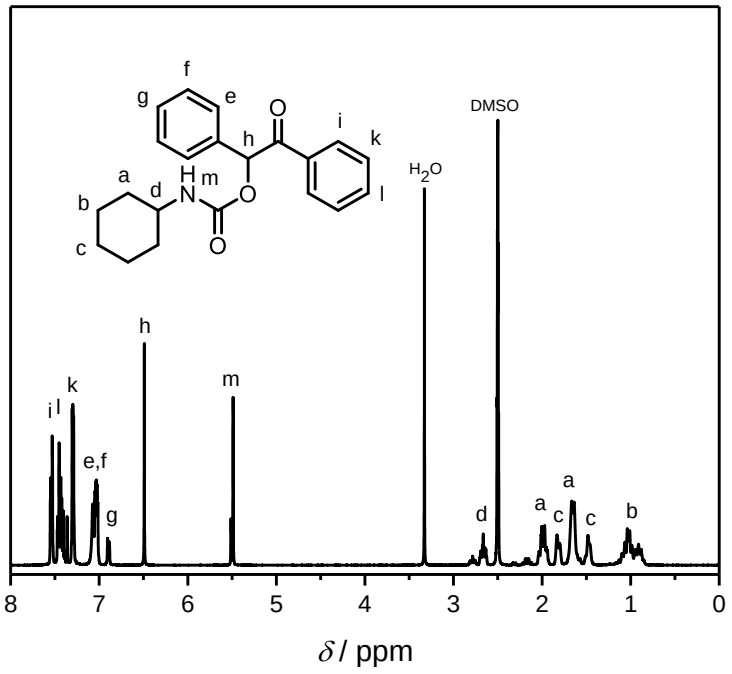

Figure 58 ^{1}H NMR spectrum of PGA2 in DMSO-d_6.

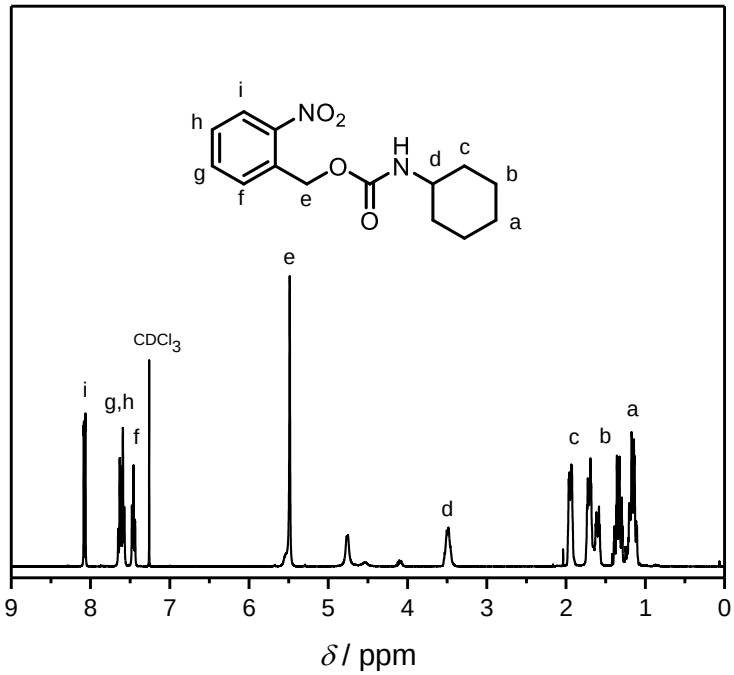

Figure 59 ^{1}H NMR spectrum of PGA3 in $CDCl_3$.

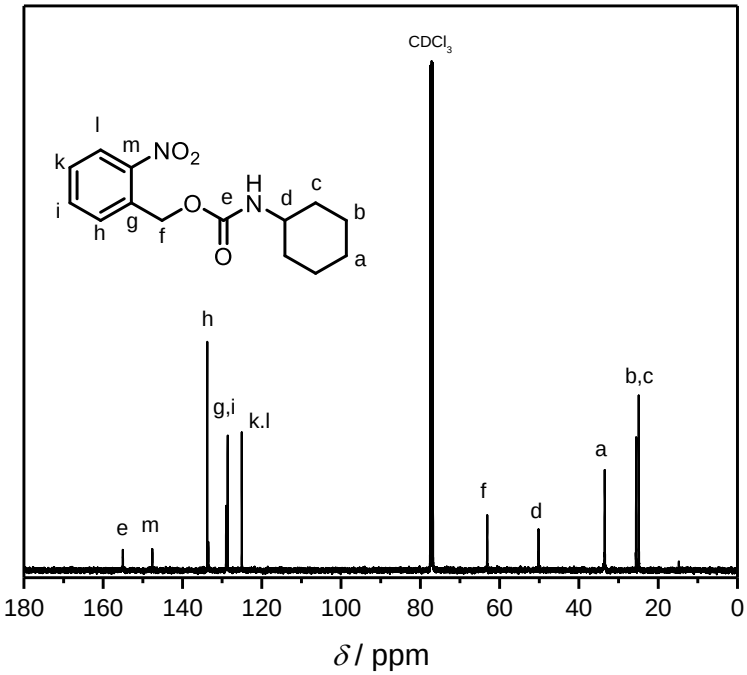

Figure 60 ^{13}C NMR spectrum of PGA3 in $CDCl_3$.

List of Figures

Figure 1 Cross section of a human tooth showing the enamel, cementum, pulp, and dentin, as well as the surrounding tissues (Author: K.D. Schroeder, graphic Human tooth diagram-en.svg from Wikimedia Commons, License: CC-BY-SA 3.0). 34

Figure 2 Required properties of the adhesive, in order to be applicable in the desired context. 56

Figure 3 ^{1}H NMR and ESI-MS analysis of the DiHDA-linker. The retro HDA products are formed during the ionization process due to high temperatures (320 °C). 59

Figure 4 ^{1}H NMR and ESI-MS analysis of the DiHDA-core. The retro HDA products are formed during the ionization process due to high temperatures (320 °C). 59

Figure 5 HT-NMR spectroscopic measurements of the DiHDA-core at 25, 700, 100, 120 °C (in toluene-d_8). At 25 °C only the proton resonances that can be assigned to the HDA moiety (H_{HDA}) are present, whereas at 120 °C only the proton resonances of the retro-HDA product (H_{Cp}) can be detected. 60

Figure 6 (a) Visible proof of the change in color upon heating to 25 (0%*), 70 (34%*), 100 (93%*) and 120 °C (99.9%*). (b) UV/Vis spectroscopic measurements of the DiHDA-core in DMSO (c = 10 mg·mL^{-1}, l = 10 mm).** (c) UV/Vis spectroscopic analysis of a cured polymer network of the DiHDA-linker (99.8 wt.% DiHDA-linker, 0.2 wt.% Ivocerin, l = 2 mm).** (d) Correlation of the intensities of the maxima at 330 nm (a) and 535 nm (b) at a given temperature to the degree of the retro HDA reaction. The absorption at 330 nm was chosen for the DiHDA-core, as the absorption at 535 nm was difficult to quantify, due to poor solubility. * Amount of retro HDA product. ** Between 25 and 140 °C. 61

Figure 7 Kinetic investigation of the debonding reaction of a cured network of the DiHDA-linker (99.8% DiHDA-linker + 0.2% Ivocerin) at 100 °C (Absorption at 535 nm, l = 2 mm). 63

Figure 8 (a) Used setup for the preparation of the bones employed in the rheological measurements. (b) Display of a cured bone of 99.8 wt.% DiHDA-linker and 0.2 wt% Ivocerin® (length: 25 mm, width: 5 mm, diameter: 1 mm). (c) Instrumental setup.

The specimen is mounted into the rheometer and an axial force is applied at temperatures between 25 and 130 °C). 64

Figure 9 (a) Rheological analysis of a pure HDA linker network. Displayed are the storage modulus (G'), the loss modulus (G'') and tanδ (G''/G'). (b) Rheological analysis of a network based on a non-degradable dimethacrylate (pure UDMA). Displayed are G', G'' and tanδ. (c) Comparison of the storage moduli (G') of (a) and (b) for the temperature range of 25 °C to 130 °C. (d) Comparison of G' and tanδ of a degradable network based on the pure DiHDA-linker with a degradable co-polymer network (iBoMA + 0.2 eq. DiHDA-linker) for the temperature range of 20 to 130 °C. A detailed rheological analysis of the co-polymer network can be found in the Appendix (Figure 24 and Figure 25) 65

Figure 10 Display of a degradable network based on 99.8 wt.% DiHDA-linker + 0.2 wt.% Ivocerin®. At 25 °C, the network is rigid and not bendable (i). At 100 °C, the network can easily be bend by using tweezers (ii) and cut into pieces (iii). 65

Figure 11 (a) Display of the test abutment and artificial dental crown employed in the pull-off tests. (b) Display of the employed tensile testing machine (Zwick-Roell Z010). A heatable water bath was used in order to ensure the temperature control. 66

Figure 12 (a) Force-elongation graphs of the performed pull-off tests of a dental model adhesive co-monomer system (*n*BMA + 0.2 eq. bisGMA*) and a mixture including the designed DiHDA-linker (*n*BMA + 0.2 eq. DiHDA-linker) at 23 °C and 80 °C. (b) Summary of the obtained values including the calculated differences between the ratios of the pull-off forces at 23 °C and 80 °C for both systems. * Bisphenol-A-glycidyl methacrylate. A table summarizing the obtained values can be found in the Appendix (Table 4). 67

Figure 13 Correlation of the intensities of the absorption maxima (535 nm) of DiHDA2 and DiHDA3 at a given temperature to the extent of debonding. 70

Figure 14 ^{1}H NMR and ESI-MS analysis of the HDA-triol. The retro HDA products are visible due to the high temperatures (320 °C) present at the ionization process. A table summarizing the exact values of the ESI-MS analysis can be found in the Appendix (Table 5). 74

Figure 15 Synthetic protocol for the preparation of the HDA-diol as well as analytical evidence (^{1}H NMR and ESI-MS analysis) for the successful synthesis. The retro HDA products

are visible due to the high temperatures (320 °C) present duringt the ionization process. A table summarizing the exact values of the ESI-MS analysis can be found in the Appendix (Table 6). 75

Figure 16 (a) Synthetic protocol for the linear polycarbonates, bearing HDA units in the backbone and the products of the retro HDA reaction upon heating (rHDA1 and rHDA2). (b) SEC analysis in THF of the polycarbonates P1 – P4 with varying degrees of polymerization. (c) SEC analysis in THF of P4 at 25, 60, 100 and 140 °C. M_w decreases due to the decomposition of the polymer based on the retro HDA reaction. Tables summarizing the obtained data of the SEC analysis can be found in the Appendix (Table 7 and Table 8). 76

Figure 17 Investigation of the reversibility of the HDA-PC P4. (a) SEC analysis in THF of the bonding/debonding of P4. $P4_{or.}$ Is the original polymer P4, the degraded polymer at 120 °C is termed $P4_{deg.}$and the reformed polymer upon cooling is $P4_{ref.}$. A table summarizing the obtained values of the SEC analysis can be found in the Appendix (Table 9). (b) UV/Vis analysis of the reversibility of P4 at 530 nm in the temperature range of 20 – 100 °C. (c) HT-NMR spectroscopy of the bonding/debonding behavior in DMSO-d_6. H_a is a resonance of the Cp moiety depicted in zoom 1 (6.5 – 6.4 ppm). H_b is a resonance associated with the HDA unit (5.85 – 5.6 ppm, zoom 2). P4 is cleaved at 110 °C, however, is reformed instantly upon cooling to 25 °C. 77

Figure 18 Polycarbonate network. (a) Synthetic protocol for the synthesis of the HDA-containing polycarbonate networks. (b) Pictures of the bonding/debonding behavior of the polymer networks (+Δ: heating to 120 °C, -Δ: cooling to 25 °C). For the heating procedure, a pre-heated oil bath was employed and a water bath was used for cooling. The red color stems from the formation of the dithioester moiety (rHDA1) upon heating. 79

Figure 19 ^{1}H and ^{13}C NMR spectra of the prepared disulfone containing dimethacrylate (DiMA-$DiSO_2$) in $CDCl_3$. 84

Figure 20 (a) Nucleophilic substitution reaction of DiMA-$DiSO_2$ with diethylamine. (b) ^{1}H NMR spectroscopic evidence of the reaction with 2 and 5 eq. of diethylamine. Resonance a and b belong to the DiMA-$DiSO_2$, whereas resonances a', b' and c' correspond to the substitution product S1. 85

Figure 21 (a) Decomposition reaction of PGA3 upon irradiation with UV light. (b) ^{1}H NMR spectra of the degradation of PGA3 during irradiation with UVA light (355 – 390 nm, 500 mW·cm^{-2}) in $CDCl_3$. The measurements were conducted after 0, 1, 2 and 4 h of irradiation. (c) Decomposition of PGA3 upon UVA and visible light irradiation, determined *via* the decreasing intensity of resonance b. No degradation can be detected under visible light irradiation (400 – 520 nm, 100 mW·cm^{-2}). The emission spectra of the employed light sources can be found in the Appendix (see Figure 26). 86

Figure 22 (a) Molecular structures of DiMA-$DiSO_2$, PGA3 and S2. (b) ^{1}H NMR spectroscopy of the reaction of DiMA-$DiSO_2$ and PGA3 in $CDCl_3$ upon irradiation with UVA light (355 – 390 nm, 500 mW·cm^{-2}) after 0, 1, 2 and 4 h. (c) Enlargement of the ^{1}H NMR spectrum between 6.7 – 7.5 ppm (1) and 5.1 – 6.0 ppm (2). Resonance a corresponds to DiMA-$DiSO_2$, resonance b to PGA3 and resonance c to S2. (d) Comparison between the decrease of PGA3 and DiMA-$DiSO_2$ with the increase of S2, by determining the equivalents used/formed during the substitution reaction calculated *via* the integrals of the specific resonance. (e) Observable color change during the reaction between 0 and 4 h. The coloration stems from the formation of 2-nitroso benzaldehyde. 88

Figure 23 Analysis of the stiffness of the polymer network before and after irradiation with UV light (400 – 520 nm, 100 mW·cm^{-2}) *via* a tube inversion test. 90

Figure 24 Rheological measurement of a polymer network of iBoMA and 0.2 eq. of the DiHDA-linker. Depicted are G', G'' and tanδ. 131

Figure 25 Rheological measurement of a polymer network of isobornyl methacrylate (iBoMA) and 0.2 eq. of a non-degradable dimethacrylate (D3MA). Depicted are G', G'' and tanδ. 131

Figure 26 Emission spectrum of the employed UV light (Osram Dulux Blue UVA) and visible light (Osram Dulux Blue) source for the preparation of the disulfone containing polymer network. 133

Figure 27 ^{1}H NMR spectrum of PDT in $CDCl_3$. 134

Figure 28 ^{13}C NMR spectrum of PDT in $CDCl_3$. 134

Figure 29 ^{1}H NMR spectrum of MA-PDT in $CDCl_3$. 135

Figure 30 ^{13}C NMR spectrum of MA-PDT in $CDCl_3$ 135

Figure 31 ^{1}H NMR spectrum of the DiCp-linker in $CDCl_3$. 136
Figure 32 ^{13}C NMR spectrum of the DiCp-linker in $CDCl_3$. 136
Figure 33 ^{1}H NMR spectrum DiHDA-core in $CDCl_3$. 137
Figure 34 ESI mass spectrum of the DiHDA-core. The retro HDA products are formed during the ionization process due to the high temperatures (320 °C). 137
Figure 35 ^{1}H NMR spectrum DiHDA-linker in $CDCl_3$. 138
Figure 36 ESI mass spectrum of the DiHDA-linker. The retro HDA products are formed during the ionization process due to the high temperatures (320 °C). 138
Figure 37 ^{1}H NMR spectrum of DiHDA2 in $CDCl_3$. 139
Figure 38 ^{1}H NMR spectrum of PDT2 in $CDCl_3$. 139
Figure 39 ^{1}H NMR spectrum of PDT2 in $CDCl_3$. 140
Figure 40 ^{1}H NMR spectrum of DiHDA3 in $CDCl_3$. 140
Figure 41 ^{1}H NMR spectrum of PDT-OH in $CDCl_3$. 141
Figure 42 ^{1}H NMR spectrum of HDA-diol in DMSO-d_6. 141
Figure 43 ESI mass spectrum of the HDA-diol. The retro HDA products are formed during the ionization process due to the high temperatures (320 °C). 142
Figure 44 ^{1}H NMR spectrum of HDA-PC in DMSO-d_6. 142
Figure 45 ^{1}H NMR spectrum of the TriBr-linker in $CDCl_3$. 143
Figure 46 ^{13}C NMR spectrum of the TriBr-linker in $CDCl_3$. 143
Figure 47 ^{1}H NMR spectrum of the TriCp-linker in $CDCl_3$. 144
Figure 48 ^{13}C NMR spectrum of the TriCp-linker in $CDCl_3$. 144
Figure 49 ^{1}H NMR spectrum of the HDA-triol in $CDCl_3$. 145
Figure 50 ESI mass spectrum of the HDA-triol. The retro HDA products are formed during the ionization process due to the high temperatures (320 °C). 145
Figure 51 ^{1}H NMR spectrum of MA in $CDCl_3$. 146
Figure 52 ^{13}C NMR spectrum of MA in $CDCl_3$. 146
Figure 53 ^{1}H NMR spectrum of MA-$SOCl_2$ in $CDCl_3$. 147
Figure 54 ^{13}C NMR spectrum of MA-$SOCl_2$ in $CDCl_3$. 147
Figure 55 ^{1}H NMR spectrum of DiMA-$DiSO_2$ in $CDCl_3$. 148
Figure 56 ^{13}C NMR spectrum of DiMA-$DiSO_2$ in $CDCl_3$. 148
Figure 57 ^{1}H NMR spectrum of PGA1 in $CDCl_3$. 149
Figure 58 ^{1}H NMR spectrum of PGA2 in DMSO-d_6. 149

Figure 59 ^{1}H NMR spectrum of PGA3 in $CDCl_3$. 150
Figure 60 ^{13}C NMR spectrum of PGA3 in $CDCl_3$. 150

List of Schemes

Scheme 1 Steps during the initiation process of a free radical polymerization. After homolytic dissociation of the initiator, a monomer is added to the radical initiation species, whereupon the reactive center is transferred to the monomer. 9

Scheme 2 Propagation reaction. A (macro-)radical reacts with monomer molecules, leading to an increase in the molecular weight of the polymer. 10

Scheme 3 Possible pathways for a termination reaction in a free radical polymerization (combination and disproportionation)..... 11

Scheme 4 Chain transfer in free radical polymerization. A macroradical can transfer the reactive center to the solvent, the initiator, the monomer, another polymer chain or a transfer agent (T). The transferred radical can potentially reinitiate the reaction *via* addition to a monomer. 12

Scheme 5 Schematic display of a step-growth polymerization, either using to different monomers (A-A and B-B), or a monomer bearing two different functional groups, which are capable of reacting with each other (A-B)..... 14

Scheme 6 Schematic display of the two procedures conducted for the preparation of Bisphenol A based polycarbonate: Schotten-Baumann reaction and transesterification. ... 17

Scheme 7 Possible pathways for the reaction of pendant double bonds. Depending on the reaction partner, the double bond can form a primary or secondary cycle or a crosslink. 22

Scheme 8 Different kinds of polymer networks. A supramolecular polymer network (SPN) is (reversibly) crosslinked by noncovalent interactions. A interpenetrating polymer network (IPN) is a combination of two polymer networks, where at least one of the networks is formed in the immediate presence of the other network. A covalent adaptable network (CAN) is reversibly crosslinked by covalent interactions. The reversible moiety can either be the crosslink itself or other motives along the polymer chains. 23

Scheme 9 (a) Ureidopyromidinone and (b) urea hydrogen bonding employed for the preparation of supramolecular polymer networks. 24

Scheme 10 Poly(ethylene-*co*-methacrylic acid) mixed with zinc stearate for the electrostatic interaction bonding of supramolecular polymer networks. 25

Scheme 11 Self-healing supramolecular polymer network based on metal coordination of Fe^{2+} and terpyridine.[142] 26

Scheme 12 Stimuli-responsive supramolecular polymer hydrogels can be prepared by employing the host-guest interaction of cyclodextrins (α-CD, β-CD) with various molecules, including poly(ethylene glycol). 27

Scheme 13 Schematic presentation of different ways to form an interpenetrating polymer network (IPN). (a) The IPN is prepared by a simultaneous, noninterfering formation of two networks (M: monomer, C: crosslinker). (b) Sequential strategy: One network is prepared first. The network is swollen in the monomer mixture for the second network formation, which is formed in a second step. (c) One polymer network is formed in the presence of a linear polymer, which is subsequently crosslinked in the following step to form the IPN. 28

Scheme 14 Classes of current dental adhesives employed for restorative composites. Adapted with permission from John Wiley and Sons.[199] Copyright 2012 Polymer Chemistry. 35

Scheme 15 AD concept, adapted from Yoshida et al.[209] The acidic monomer cleaves phosphate and hydroxyl ions from the tooth surface before it is either bonded or debonded, depending on the strength of the ionic bond. 36

Scheme 16 Examples of acidic monomers employed for adhesive formulations. 37

Scheme 17 Examples of crosslinking monomers used for dental adhesives. 38

Scheme 18 Radical formation of the camphorquinone/ethyl 4-dimethlaminobenzoate pair upon irradiation with blue light.[222] 39

Scheme 19 Selection of employed photoinitiators, as well as the decomposition mechanism of the novel germanium based initiators. Both, the germyl and the benzoyl radicals are capable of initiating a polymerization. 40

Scheme 20 Selection of commonly employed inhibitors for dental formulations. 41

Scheme 21 Possible diastereomers obtained during a Diels-Alder reaction (*exo*- and *endo*-product). 44

Scheme 22 HOMO-LUMO display of Diels-Alder reactions with common and inverse electron demand, including an example for both cases. 45

Scheme 23 The equilibrium of the Diels-Alder reaction between furan and *N*-maleimide. Below 65 °C, only the starting materials are present, whereas at temperatures above 110 °C the product dominates. 46

Scheme 24 Equilibrium of the Diels-Alder reaction of cyclopentadiene. Dimers and trimers can be formed upon the cycloaddition. Depending on the substitution, the retro-DA reaction is induced at temperatures between 120 and 170 °C. 46

Scheme 25 Equilibrium of the Hetero-Diels-Alder reaction of dithioesters with cyclopentadiene. Depending on the Z and R group, the onset of the debonding can vary between 20 and 40 °C..... 47

Scheme 26 Selection of thermodegradable moieties. (a) Alkoxyamines, (b) nitroso dimers, (c) reaction of isocyanates with imidazoles and (d) carbene dimerization. 49

Scheme 27 Mechanism of the photo-triggered decomposition of *o*-nitrobenzyl moieties. ... 50

Scheme 28 Proposed mechanism for the photocleavage of *p*-hydroxyphenacyl moieties. ... 51

Scheme 29 Mechanism of the photo-triggered decomposition of coumarin-4-yl-methyl motives. 52

Scheme 30 Preparation of asymmetrical disulfones using hydrazine and nitric acid. 53

Scheme 31 Schematic display of the selective preparation of diaryl disulfones, diaryl thiosulfonates or diaryl disulfides from sulfonyl chlorides, depending on the reaction temperature and the amount of samarium..... 54

Scheme 32 (a) Schematic display of the degradation of the cured adhesive. (b) Display of the retro HDA reaction occurring upon thermal impact, as well as the structures of the monomer (DiHDA-linker) and a monomer-free system (DiHDA-core) used for the molecular analysis in order to avoid any self-initiation. Any methacrylate can be used as co-monomer if necessary.[314] 57

Scheme 33 Synthetic protocol for the preparation of the DiHDA-linker. The prepared phosphoryl dithioester (PDT) is reacted with HEMA to yield the methacrylate containing PDT (MA-PDT). MA-PDT and a previously prepared DiCp-linker are employed to synthesize the desired crosslinker containing two HDA moieties (DiHDA-linker)..... 58

Scheme 34 Display of the additional HDA systems tested for their degradation temperatures. (a) Dithioester based on a pyridinyl moiety (DiHDA2). The HDA reaction is catalyzed by a strong acid (e.g. TFA). (b) Dithioester based on a phosphoryl moiety

bearing an alkyl chain instead of the benzoic acid functionality (DiHDA3). The HDA reaction is catalyzed using $ZnCl_2$. 69

Scheme 35 (a) Schematic display of the bonding/debonding on demand polycarbonate network. The polymer network is prepared *via* the reaction of a triol (HDA-triol) with dimethylcarbonate using catalytic amounts of triazabicyclodecene (TBD). The polycarbonate can then be debonded and rebonded multiple times within minutes depending on the applied temperature, based on the HDA units. (b) Synthetic pathway for the preparation of the HDA triol.[319] 73

Scheme 36 General concept of the polymer network, curable and degradable in a λ-orthogonal fashion. After a free radical polymerization using a visible light decomposable photoinitiator, the degradation of the network is realized *via* a UV light induced substitution reaction of the disulfone crosslinks with a photo-generated amine.[325] 83

Scheme 37 Synthetic procedure for the preparation of the dimethacrylate crosslinker containing the disulfone species (DiMA-$DiSO_2$). 84

Scheme 38 Three different PGAs, which were analyzed in terms of their degradation behavior upon irradiation with visible and UV light. 86

Scheme 39 Summary of the monomer mixture, employing *n*-butyl methacrylate, 10 mol% of DiMA-DiSO2, 50 mol% of PGA3 and 0.2 wt% Ivocerin®. 89

Scheme 40 Preparation of PDT. 99

Scheme 41 Synthesis of DiCp-linker. 100

Scheme 42 Synthesis of MA-PDTMBA. 101

Scheme 43 Synthesis of the DiHDA-core. 102

Scheme 44 Synthesis of the DiHDA-linker. 102

Scheme 45 Synthesis of DiHDA2. 103

Scheme 46 Synthesis of PDT2. 104

Scheme 47 Synthesis of DiHDA3. 104

Scheme 48 Synthesis of PDT-OH. 105

Scheme 49 Synthesis of the DiHDA-diol. 106

Scheme 50 Synthesis of the DiHDA-PCs. 106

Scheme 51 Synthesis of the TriBr-linker. 107

Scheme 52 Synthesis of the TriCp-linker. 108

Scheme 53 Synthesis of the HDA-triol. 109
Scheme 54 Synthesis of the TriHDA-PC. 110
Scheme 55 Synthesis of 2-phenoxyethyl methacrylate. 110
Scheme 56 Synthesis of 2-(4-(chlorosulfonyl)phenoxy)ethyl methacrylate. 111
Scheme 57 Synthesis of DS-DMA. 112
Scheme 58 Synthesis of PGA1. 112
Scheme 59 Synthesis of PGA2. 113
Scheme 60 Synthesis of PGA3. 113
Scheme 61 Synthesis of the disulfone and PGA3 containing polymer network. 114

List of Tables

Table 1 E_A, A and k_p values of a selection of vinylic monomers obtained *via* PLP-SEC.[66, 67] 11

Table 2 Relation between the stoichiometric ratio of the reaction partners r, the conversion p and the degree of polymerization DP_n in a step-growth polymerization. 15

Table 3 Different classifications of adhesives and their primary resins. 33

Table 4 Pull-off force F determined for test specimens bound with two different self-curing two-component mixtures using nBMA and 0.2 eq. of either bisGMA (a non-degradable dimethacrylate) or the DiHDA-linker. Detailed information regarding the preparation of the test specimens are provided in section 7.2. *BP-50-FT or DABA as Initiator. 132

Table 5 Sum formula, the exact masses of the obtained data *via* ESI-MS analysis, theoretical m/z values and the deviation of both values for the HDA-triol and the products of the rHDA reaction (rHDA1, rHDA2 and rHDA3). 132

Table 6 Sum formula, the exact masses of the obtained data *via* ESI-MS analysis, theoretical m/z values and the deviation of both values for the HDA-diol and the products of the rHDA reaction (rHDA1 and rHDA2). 132

Table 7 SEC analysis of the prepared linear polycarbonates P1 – P4. M_n and M_w in g mol^{-1}. 132

Table 8 SEC analysis of the decomposition of P4 upon heating. Mn and Mw in g mol^{-1} 133

Table 9 SEC analysis of the bonding/debonding behavior of P4. M_n and M_w in g mol^{-1}. $P4_{or.}$ is the original P4 polymer, $P4_{deg.}$ the degraded polymer at 120 °C and $P4_{ref.}$ the reformed polymer upon cooling. 133

Abbreviations

4-MET	4-methacryloyloxyethyl trimellitic acid
AD	adhesion-decalcification
AMADDP	10-(N-acryloyl-N-methoxyamino)-decyl dihydrogen phosphate
APO	2,4,6-trimethylbenzoyldiphenylphosphineoxide
BAPO	bis-(2,4,6-trimethylbenzoyl)phenylphosphine oxide
BHT	2,6-di-tert-butyl-4-methylphenol
BisGMA	Bisphenol-A-glycidyl methacrylate
BPA	Bisphenol A
c	concentration
CAN	covalent adaptable network
CD	cyclodextrins
CM	coumarin-4-yl-methyl
Cp	cyclopentadiene
CQ	camphorquinone
Đ	dispersity
$[DB_o]$	initial double bond concentration
DBA	9,10-dibutylanthracene
DBPO	dibenzoylperoxide
DCM	dichloromethane
DEBAAP	*N,N*'-diethyl-1,3-bis(acrylamido)propane
DEPT	*N,N*-diethanol-p-toluidine
DMABP-A	bisphenol-A derivative
DMC	dimethyl carbonate
DMI	dimethyl itaconate
DMF	dimethylformamide
DoD	debonding on demand
DOPA	3,4-dihydroxyphenylalanine
DP_n	degree of polymerization
DPF	2,5-diphenylfuran

E&RA	etch-and-rinse adhesive
EA	ethyl acetate
EDTA	ethylenediaminetetraacetic acid
EMBO	ethyl 4-dimethlaminobenzoate
ESI-MS	electrospray ionization mass spectrometry
FRP	free radical polymerization
GA	glutaraldehyde
Ge-1	benzoyltrimethylgermane
GDMA	glycerol dimethacrylate
HAP	hydroxyapatite crystals
HEMA	hydroxyethyl methacrylate
HDA	Hetero-Diels-Alder
HT	high temperature
iBoMA	isobornyl methacrylate
IPN	interpenetrating polymer network
k_d	rate coefficient of the initiator decomposition
k_i	rate coefficient of the initiation
k_p	rate coefficient of the propagation reaction
k_t	rate coefficient of the termination reaction
k_{tr}	rate coefficient of the transfer reaction
λ	wavelength
L	liters
LCST	lower critical solution temperature
M	molar mass
M_n	number-average molecular weight
M_w	weight-average molecular weight
$[M_{xl}]$	concentration of double bonds
$\overline{Mc}$	average molecular weight between crosslinks
$\overline{Mr}$	average molecular weight of one repeating unit on a double bond basis
MA	methyl acrylate
MMA	methyl methacrylate
MA-B-18-C-6	4-(methacryloyloxymethyl)-benzo-18-crown-6

MAC-10	11-methacryloyloxy-1,10-undecanedicarboxylic acid
MBAAm	*N,N*'-methylenebisacrylamide
MDP	methacryloyloxydecyl dihydrogen phosphate
MIAMS	1-butyl-3-methylimidazolium 2-acrylamido-2-methyl-1-propanesulfonate
MMA	methyl methacrylate
MPTC	3-(methacryloylamino)propyl-trimethylammonium chloride
MS	mass spectrometry
*n*BMA	n-butyl methacrylate
ndb	number of double bonds of a crosslinker
NMR	nuclear magnetic resonance
NTG-GMA	N-tolylglycine glycidyl methacrylate
o-NB	*o*-nitrobenzyl
p	conversion
p-HP	*p*-hydroxyphenacyl
Pa	pascal
PA	phosphonic acid
PA-1	(5-(methacryloyloxy)pentyl)phosphonic acid
PA-2	2,5-bis(methacryloyloxy)-1,4-phenylenediphosphonic acid
PAA	poly(acrylic acid)
PDMS	polydimethylsiloxane
PEG	poly(ethylene glycol)
PGA	photo-generated amine
PMMA	poly(methyl methacrylate)
PNIPAM	poly(*N*-isoproylacrylamide)
PTFE	polytetrafluoroethylene
PTZ	phenothiazine
PVA	poly(vinylic alcohol)
PVC	poly(vinyl chloride)
ρ	density
RDRP	reversible-deactivation radical polymerization
SEA	self-etching adhesive
SEC	size exclusion chromatography

SPN	supramolecular polymer networks
SRM	stimuli responsive moiety
TBD	triazabicyclodecene
TEGDMA	triethyleneglycol dimethacrylate
ν	concentration of the crosslinked chains
UDMA	1,6-bis-[2-methacryloyloxyethoxycarbonylamino]-2,4,4-trimethylhexane

Curriculum Vitae

Not available in the electronic version.

Publications and Conference Contributions

Publications

(1) *Reversing Adhesion – A Triggered Release Self-Reporting Adhesive*
A. M. Schenzel, C. Klein, K. Rist, N. Moszner and C. Barner-Kowollik, *Adv. Sci.* **2016**, *3*, 1500361.

(2) *Self-Reporting Dynamic Covalent Polycarbonate Networks*
A. M. Schenzel, N. Moszner and C. Barner-Kowollik, *Polym. Chem.* **2017**, *8*, 414-420.

(3) *Disulfone Crosslinkers for λ-Orthogonal Photo-Induced Curing and Degradation of Polymeric Networks*
A. M. Schenzel, N. Moszner and C. Barner-Kowollik, *ACS Macro Lett.* **2017**, *6*, 16–20.

(4) *Photo-Induced Tetrazole-Based Functionalization of Off-Stoichiometric Clickable Microparticles*
C. Wang, M. M. Zieger, **A. M. Schenzel**, M. Wegener, J. Willenbacher, C. Barner-Kowollik and C. N. Bowman, *Adv. Funct. Mater.* **2017**, in press.

Patents

(5) *Polymerizable compositions based on thermally splittable thermolabile compounds for use in adhesives, composites, stereolithog. materials etc. in dental materials*
A. Schenzel, C. Barner-Kowollik, M. Langer, N. Moszner, I. Lamparth, K. Rist, **WO Patent 2017064042**, 20. April 2017.

Conference Contributions

(6) Reversing Adhesion: A Triggered Release Self-Reporting Adhesive

A. M. Schenzel, C. Klein, K. Rist, N. Moszner and C. Barner-Kowollik, MacroBeGe, February 2016, Houffalize **Belgium**.

(7) Reversing Adhesion: A Triggered Release Self-Reporting Adhesive

A. M. Schenzel, C. Klein, K. Rist, N. Moszner and C. Barner-Kowollik, Makromolekulares Colloquium Freiburg, February 2015, Freiburg **Germany**.

Acknowledgments

Zu allererst gilt mein Dank selbstverständlich meinem Doktorvater Prof. Dr. Christopher Barner-Kowollik. Vielen Dank für das interessante und herausfordernde Thema, sowie die gute persönliche Betreuung und die hervorragenden Arbeitsbedingungen. Du zeigst immer vollen Einsatz und kümmerst dich gut um jeden einzelnen in der Gruppe.

Des Weiteren möchte ich mich bei meinem Kooperationspartner, der Ivoclar Vivadent AG dafür bedanken, dass sie Wissenschaft und Anwendung in einer herausfordernden Problemstellung vereinigt haben. Mich hat die direkte Nähe zur Anwendung stets sehr begeistert und motiviert. Vielen Dank dafür, dass Sie mir trotz der klaren Aufgabenstellung während der Forschung den Freiraum gegeben haben meine eigenen Ideen zu testen und zu verwirklichen. Ich sehe die Zusammenarbeit als für beide Parteien sehr ertragreich an, da neben der Lösung der gegeben Aufgabenstellung, welche in der Einreichung eines Patents mündete, auch die Veröffentlichung dreier wissenschaftlicher Publikationen gelang. Möglich war dies nur durch die vielen gemeinsamen Meetings, die in einer sehr kollegialen und angenehmen Atmosphäre stattfanden und bei denen stets viele Ideen zustande kamen und diskutiert wurden. Ein besonderer Dank gilt hierbei Dr. Norbert Moszner, Kai Rist und Dr. Iris Lamparth. Noch einmal vielen Dank für die gute Zusammenarbeit und das Vertrauen, welches Sie in mich gesetzt haben.

A big thank you goes to Prof. Dr. Martina Stenzel for inviting me to come and work with her group at the University of New South Wales in Sydney. I learned a lot and felt welcomed by the whole group. Special thanks to Dr. Robert Chapman, Janina Noy and Dr. Florent Jasinski for all the help you gave me in the lab, for the nice lunch breaks and the fun after-work activities.

Of course thank you to the whole macroarc team and all former members for the great working atmosphere and team spirit. Ein besonderer Dank gilt hierbei Dr. Anja Goldmann, Dr. Maria Schneider, Vincent Schüler und Katharina Elies die sich stets hervorragend um alle organisa-

torischen Aufgaben gekümmert haben umso bestmögliche Arbeitsbedingungen zu gewährleisten. Dann geht natürlich ein großer Dank an das Altbau Labor- und Büroteam. Neben der angenehmen Arbeitsatmosphäre kamen stets produktive wissenschaftliche Diskussionen zustande. Des Weiteren danke für all die schönen Doktorfeiern, Grill- und Doktorwagenbauabende. Danke an Nils Wedler und Dr. Bryan Tuten für das Korrekturlesen meiner Arbeit.

An letzter Stelle stehend und doch eigentlich mit am wichtigsten, geht ein großer Dank an mein soziales Umfeld. Der erste Dank geht hierbei ganz klar an meine Familie. Danke, dass ihr immer für mich da seid und mich bei allen meinen Vorhaben unterstützt. Vielen Dank auch dafür, dass ihr mir mein Studium und eine schöne Zeit in Karlsruhe ermöglicht habt. Natürlich gilt auch ein großer Dank meinen Freunden, durch die meine Zeit in Karlsruhe so sehr bereichert wurde. Last but not least, danke ich meiner Freundin Karin für die große Unterstützung und die wunderschöne Zeit die wir schon zusammen verbracht haben.

Declaration

Hiermit erkläre ich wahrheitsgemäß, dass diese Arbeit im Rahmen der Betreuung durch Prof. Dr. Christopher Barner-Kowollik selbstständig von mir verfasst wurde, keine anderen als die angegebenen Quellen und Hilfsmittel verwendet, die wörtlich oder inhaltlich übernommenen Stellen als solche kenntlich gemacht sowie die Regeln zur Sicherung guter wissenschaftlicher Praxis des Karlsruher Instituts für Technologie (KIT) beachtet wurden, die elektronische Version der Arbeit mit der schriftlichen übereinstimmt und die Abgabe und Archivierung der Primärdaten gemäß Abs. A (6) der Regeln zur Sicherung guter wissenschaftlicher Praxis des KIT beim Institut gesichert ist.

Ort, Datum Unterschrift

Schenzel out *drops mic*